

**NCAT Report 16-04**

**PHASE V (2012-2014)  
NCAT TEST TRACK FINDINGS**

**By**

**Randy West**

**David Timm**

**Buzz Powell**

**Michael Heitzman**

**Nam Tran**

**Carolina Rodezno**

**Don Watson**

**Fabricio Leiva**

**Adriana Vargas**

**Richard Willis**

**Michael Vrtis**

**Miguel Diaz**

**August 2018**



**National Center for  
Asphalt Technology**  
**NCAT**  
at AUBURN UNIVERSITY

**277 Technology Parkway ■ Auburn, AL 36830**

Phase V (2012-2014) NCAT Test Track Findings

By

Randy West, Ph.D., P.E.  
David Timm, Ph.D., P.E.  
Buzz Powell, Ph.D., P.E.  
Michael Heitzman, Ph.D., P.E.  
Nam Tran, Ph.D., P.E., LEED GA, MBA  
Carolina Rodezno, Ph.D.  
Don Watson, P.E.  
Fabricio Leiva, Ph.D.  
Adriana Vargas, Ph.D.  
Richard Willis, Ph.D., P.E. \*  
Michael Vrtis, Ph.D. \*  
Miguel Diaz\*

\*Work completed while at National Center for Asphalt Technology

Sponsored by

Alabama Department of Environmental Management  
Alabama Department of Transportation  
Federal Highway Administration  
Florida Department of Transportation  
FP<sup>2</sup> For Pavement Preservation  
Georgia Department of Transportation  
Kraton Polymers  
Mississippi Department of Transportation  
Missouri Department of Transportation  
North Carolina Department of Transportation  
Oklahoma Department of Transportation  
Seneca Petroleum  
South Carolina Department of Transportation  
Tennessee Department of Transportation  
Virginia Department of Transportation

August 2018

### **ACKNOWLEDGEMENTS**

This project was sponsored by the Alabama Department of Environmental Management, Alabama DOT, FHWA, Florida DOT, FP<sup>2</sup>, Georgia DOT, Kraton Polymers, Mississippi DOT, Missouri DOT, North Carolina DOT, Oklahoma DOT, Seneca Petroleum, South Carolina DOT, Tennessee DOT, and Virginia DOT. The authors also wish to thank Astec Industries, Blacklidge Emulsions, Ergon, Holcim, Instrotek, Martin Marietta Aggregates, Maymead, MeadWestvaco, Oldcastle Materials Group, Polycon, Roadtec, Stalite, Transtech Systems, Troxler Electronic Laboratories Vulcan Materials, and Wiregrass Construction.

### **DISCLAIMER**

The contents of this report reflect the views of the authors who are responsible for the facts and accuracy of the data presented herein. The contents do not necessarily reflect the official views or policies of Test Track sponsors, the National Center for Asphalt Technology, or Auburn University. This report does not constitute a standard, specification, or regulation. Comments contained in this paper related to specific testing equipment and materials should not be considered an endorsement of any commercial product or service; no such endorsement is intended or implied.

## TABLE OF CONTENTS

<b>1. INTRODUCTION.....</b>	<b>7</b>
<b>1.1. NCAT Test Track Background.....</b>	<b>7</b>
<b>1.2. Key Findings from Previous Cycles.....</b>	<b>9</b>
Mix Design.....	9
Aggregate Characteristics.....	10
Binder Characteristics.....	11
Structural Design and Analysis.....	12
Relationships Between Laboratory Results and Field Performance.....	13
Tire-Pavement Interaction.....	14
References.....	15
<b>1.3. Overview of the 2012 Test Track (Fifth Cycle).....</b>	<b>16</b>
Construction.....	19
Traffic.....	21
Performance Monitoring.....	22
Laboratory Testing.....	23
<b>2. STRUCTURAL EXPERIMENTS.....</b>	<b>25</b>
Overview of Structural Studies.....	25
Instrumentation.....	25
Data Collection and Processing.....	27
Falling Weight Deflectometer Testing.....	29
Performance Monitoring.....	33
References.....	33
<b>2.1. 2009 Group Experiment.....</b>	<b>35</b>
Background and Objective.....	35
Mix Design and As-Built Properties.....	36
Structural Analysis.....	39
Test Track Field Performance.....	50
Preliminary Forensic Analysis.....	52
Laboratory Testing and Results.....	54
Conclusions and Recommendations.....	64
References.....	65
<b>2.2. 2012 Green Group Experiment.....</b>	<b>67</b>
Background and Objectives.....	67
Test Section Design and Construction Summary.....	68
Laboratory Test Results.....	70
Performance and Structural Analyses.....	76
N5 – Standard RAP.....	76
S5 – High RAP.....	82
S6 – RAP/RAS.....	89
S13 – GTR.....	95
Summary.....	102
Conclusions and Lessons Learned.....	105
References.....	106
<b>2.3. Virginia Department of Transportation CCPR and Stabilized Base Experiment.....</b>	<b>107</b>
Background and Objectives.....	107
Test Sections.....	107

Performance .....	108
Backcalculated Moduli .....	110
Pavement Response .....	112
CCPR Structural Coefficient .....	117
Summary and Conclusions .....	121
References .....	122
<b>2.4. Oklahoma Department of Transportation Perpetual Pavement Study .....</b>	<b>124</b>
Introduction .....	124
Objectives and Scope .....	124
Test Sections .....	125
Performance History .....	126
Structural Response Characterization .....	129
Life-Cycle Cost Analysis .....	130
Summary .....	132
References .....	133
<b>2.5. Kraton Polymers High Polymer Test Section .....</b>	<b>134</b>
Introduction .....	134
Objective and Scope .....	135
Field Performance .....	135
Structural Capacity .....	138
References .....	140
<b>3. NON-STRUCTURAL EXPERIMENTS .....</b>	<b>141</b>
References .....	144
<b>3.1. Virginia Department of Transportation Noise Experiment .....</b>	<b>145</b>
Overview .....	145
Performance .....	145
Findings .....	149
<b>3.2. Alabama Department of Transportation OGFC Experiment .....</b>	<b>150</b>
Background .....	150
Sections E9A, E9B, and E10 .....	151
Test Sections .....	152
Findings .....	154
<b>3.3. Tennessee Department of Transportation RAS Experiment .....</b>	<b>156</b>
Comparison of OGFC from 2003 Cycle to OGFC with 3% RAS .....	156
Findings .....	158
<b>3.4. Oklahoma Department of Transportation OGFC Mix Design and Tack Method Study .....</b>	<b>159</b>
Background .....	159
Objective and Scope .....	159
Experimental Plan .....	159
Field Performance Evaluation Results .....	162
Conclusions and Recommendations .....	164
References .....	165
<b>3.5. Florida Department of Transportation Tack Coat Effect on OGFC Performance Study .....</b>	<b>166</b>
Background .....	166
Objective and Scope .....	167
Experimental Plan .....	168
Results .....	171
Conclusions and Recommendations .....	181

References.....	182
<b>3.6. Florida Department of Transportation Cracking Study.....</b>	<b>184</b>
Introduction.....	184
Objective and Scope.....	184
Mix Design and Construction.....	184
Laboratory Testing.....	185
Field Cracking Performance.....	192
Conclusions.....	193
References.....	193
<b>3.7. Georgia Department of Transportation Surface Treatment vs. OGI Reflective Crack Prevention Experiment.....</b>	<b>195</b>
Introduction.....	195
Overview.....	195
Performance.....	197
Findings.....	197
<b>3.8. Mississippi Department of Transportation Evaluation of 45% RAP Mix Performance.....</b>	<b>199</b>
Background.....	199
Objective.....	200
Test Track Performance.....	200
Conclusions.....	205
<b>3.9. Missouri Department of Transportation GTR Modified Surface Mixture Study.....</b>	<b>206</b>
Introduction.....	206
References.....	208
<b>3.10. Federal Highway Administration HFST Alternative Aggregates Study.....</b>	<b>209</b>
Introduction.....	209
Objective and Scope.....	209
Construction and Testing.....	209
Data Analysis.....	210
Findings.....	213
<b>4. EXECUTIVE SUMMARY.....</b>	<b>214</b>
<b>4.1. Structural Experiments.....</b>	<b>214</b>
2009 Group Experiment.....	214
2012 Green Group Experiment.....	215
Virginia Department of Transportation CCPR and Stabilized Base Experiment.....	217
Oklahoma Department of Transportation Perpetual Pavement Study.....	217
Kraton Polymers High Polymer Test Section.....	218
<b>4.2. Non-Structural Experiments.....</b>	<b>218</b>
Virginia Department of Transportation Noise Experiment.....	218
Alabama Department of Transportation OGFC Experiment.....	219
Tennessee Department of Transportation RAS Experiment.....	219
Oklahoma Department of Transportation OGFC Mix Design and Tack Method Study.....	219
Florida Department of Transportation Tack Coat Effect on OGFC Performance Study.....	220
Florida Department of Transportation Cracking Study.....	220
Georgia Department of Transportation Surface Treatment vs. OGI Reflective Crack Prevention Experiment .....	221
Mississippi Department of Transportation Evaluation of 45% RAP Mix Performance.....	221
Missouri Department of Transportation GTR Modified Surface Mixture Study.....	222
Federal Highway Administration HFST Alternative Aggregates Study.....	222

## 1. INTRODUCTION

### 1.1. NCAT Test Track Background

The National Center for Asphalt Technology (NCAT) Test Track has been a successful pavement proving ground for the past 15 years. The 1.7-mile oval Test Track is a unique accelerated pavement testing facility that brings together full-scale pavement construction with high-speed, heavy trafficking for detailed analysis of realistic asphalt pavements.



**Figure 1 Aerial Photograph of the NCAT Test Track**

The NCAT Test Track is funded and managed as a cooperative project. Highway agencies and industry sponsors have the opportunity to explore specific research needs that can be evaluated in one or two test sections, and broader research needs of the asphalt pavement community can be met through experiments involving several test sections. Since the results of the track's experiments are typically evident in the performance of the sections, the findings are generally easy to interpret. This gives highway agency sponsors confidence to make decisions regarding their specifications for materials, mixes, and construction practices, as well as pavement design methods that can improve the performance of their roadways. Industry sponsors can use the track to publicly and convincingly demonstrate their product or technology to the pavement engineering community.

There are 46 different test sections on the track. Each section is nominally 200 ft in length. In some cases, a test section may be divided into two subsections. Twenty-six sections are located on the two straight segments of the track, and 10 sections are located in each of the two curves. Test sections are sponsored on three-year cycles. Each cycle consists of three major parts. The first part of each cycle begins with building or replacing test sections, which normally takes about six months. The second part of each cycle involves trafficking of the test sections, collection of field performance data and pavement response data, and laboratory testing of the plant-produced materials sampled during construction. Trafficking is accomplished with a fleet of

heavily loaded tractor-trailer rigs to provide approximately 10 million 18,000-pound equivalent single-axle loads (ESALs) within a two-year period. The final part of the cycle involves forensic analyses of damaged sections to determine factors that may have contributed to the observed distresses.

The first Test Track cycle began in 2000. Experiments in the inaugural cycle focused only on surface mix performance in the 46 test sections. The pavement structure under the experimental surface mixes was built with approximately 20 in. of asphalt pavement over a granular base and a stiff subgrade to isolate damage to only the surface layers.

The second cycle, started in 2003, included 26 of the original test sections built in 2000. These were left in place to further evaluate their performance through the second cycle. Fourteen sections had new surface layers, and eight sections were entirely new pavement structures. These were the first “structural sections” designed and built to analyze the entire pavement structure, not just the surface layers. Construction of the structural sections was done by removing the original thick pavement structure down to the subgrade material, then rebuilding the subgrade, aggregate base, and asphalt layers to result in test sections with asphalt pavement thicknesses of 5, 7, and 9 inches. Strain gauges, pressure plates, and temperature probes were built into the structural sections to monitor how the sections responded to traffic and temperature changes.

The third cycle of the track started in 2006. Twenty-two new sections were built, including 15 new surface mix performance sections, five new structural study sections, and two reconstructed structural sections. Eight original sections built in 2000 remained in place and accumulated 30 million ESALs by the end of the third cycle. Sixteen sections from the second cycle remained in place and carried a total of 20 million ESALs by the end of the third cycle.

The track’s fourth cycle began in 2009 and was completed in 2012. Three of the original surface mix performance sections built in 2000 remained in place and had accumulated 40 million ESALs by the end of the fourth cycle. Nine sections from the 2003 track (seven mix performance and two structural) remained in place and had accumulated 30 million ESALs. Nine sections from the 2006 track (eight mix performance and one structural) remained in place and had accumulated 20 million ESALs. Twenty-five new sections (12 mix performance and 13 structural) were built for the 2009 research cycle. All totaled, the 2009 Track consisted of 16 structural sections, 30 surface mix performance sections, and 21 sections from previous research cycles (three from 2000, nine from 2003, and nine from 2006).

This report summarizes key findings from the previous cycles and documents the experiments, analyses, and findings from the fifth cycle of the Test Track conducted from 2012 to 2014.

## 1.2. Key Findings from Previous Cycles

Many highway agencies have used Test Track findings to improve their materials specifications, construction practices, and pavement design procedures for asphalt pavements. This section provides a summary of key track research findings that have resulted in more cost-effective mixes, refined specifications, and improved pavement designs for the sponsoring agencies. Some of the findings have already been implemented by several states and have the potential for broader implementation. These key findings are organized into six areas: (1) mix design, (2) aggregate characteristics, (3) binder characteristics, (4) structural pavement design and analysis, (5) relationships between laboratory results and field performance, and (6) tire-pavement interaction.

### *Mix Design*

**Fine-Graded vs. Coarse-Graded Mixtures.** In the early years of Superpave implementation, there was an emphasis on coarse-graded mixtures to improve rutting resistance. However, that notion was called into question when the results of Westrack showed that a coarse-graded gravel mix was less resistant to rutting and fatigue cracking than a fine-graded mix with the same aggregate. In the first cycle of the NCAT Test Track, the issue was examined more completely. Twenty-seven sections were built with a wide range of aggregate types to compare coarse-, intermediate-, and fine-graded mixtures. Results demonstrated that fine-graded Superpave mixes perform as well as coarse-graded and intermediate-graded mixes under heavy traffic and tend to be easier to compact, less prone to segregation, and less permeable. Based on these findings, many state highway agencies revised their specifications to allow the use of more fine-graded mix designs.

**Design Gyration.** A related issue dealt with the number of gyrations used to compact mixes ( $N_{design}$ ) for design and control of Superpave mixtures. The Test Track, along with data from field projects across the U.S. collected as part of NCHRP project 9-29, showed the gyratory compactive effort specified in AASHTO standards to be too high. High  $N_{design}$  numbers tend to grind aggregate particles and break them down much more than what occurs during construction or under traffic, so the lab compactive effort was not representative of what actually occurs in pavements. Mix designers typically were using coarse-graded mixes to meet the volumetric mix design criteria, but those mixes are more challenging to compact in the field and tend to be more permeable, making pavements less durable. Numerous mixes on the Test Track designed with 50 to 70 gyrations in the Superpave gyratory compactor (SGC) held up to the heavy loading with great performance. Many states significantly reduced their  $N_{design}$  levels as a result of Test Track research.

**Stone-Matrix Asphalt (SMA) Mixtures.** Through the first three cycles of the track, 19 SMA sections (eight on the 2000 track, eight on the 2003 track, and three on the 2006 track) were put to the test. Excellent performance of the SMA test sections in the first cycle prompted several states to adopt this premium mix type for heavy traffic highways. Mississippi, Missouri, and Georgia then used the Test Track to evaluate lower-cost aggregates in SMA, which have helped make the mix type more economical.

**High Reclaimed Asphalt Pavement (RAP) Content Mixtures.** Six test sections built in the third cycle and trafficked through the fourth cycle were devoted to evaluating the performance of

pavements containing moderate (20%) to high (45%) RAP contents. After carrying approximately 20 million ESALs, the sections in this experiment had practically no rutting, very little raveling, and small amounts of low severity surface cracking. The use of a softer virgin binder was shown to provide better resistance to raveling and cracking of the 45% RAP mixes. No rutting or cracking benefit was observed for using polymer-modified virgin binder in the mixes with 20% or 45% RAP. Additional test sections built in 2009 with 50% RAP in each pavement layer performed better than a companion virgin test section in all performance measures.

**Warm-Mix Asphalt (WMA).** An early version of MeadWestvaco's Evotherm WMA technology was used in the repair of two test sections that had extensive damage near the end of the 2003 research cycle. The two WMA test sections were opened to heavy loading from the track fleet immediately after construction. Both sections remained in service throughout the 2006 cycle, with rutting performance comparable to HMA for 10.5 million ESALs and no cracking. One section was left in place at the start of the 2009 cycle, enduring more than 16 million ESALs before the test section was used for a different experiment. The performance of those test sections was early evidence that WMA could hold up to extremely heavy traffic. Additional WMA test sections built in 2009 also performed very well and helped agencies gain confidence to implement WMA despite concerns of rutting raised by laboratory tests.

**4.75 mm Nominal Maximum Aggregate Size (NMAS) Mix.** Thin HMA overlays (less than 1¼-in. thick) are a common treatment for pavement preservation. Currently, about half of U.S. states utilize 4.75 mm NMAS mixtures in thin overlay applications. An advantage of the 4.75 mm mixtures is that they can be placed as thin as ½ inch, allowing the mix to cover a much larger area than thicker overlays. In the second track cycle, the Mississippi DOT sponsored a test section of 4.75 mm surface mix containing limestone screenings, fine crushed gravel, and a native sand. That 11-year old section has now carried more than 40 million ESALs with only 7 mm of rutting and no cracking. This section is proof that well-designed 4.75 mm mixes are a durable option for pavement preservation.

#### *Aggregate Characteristics*

**Polishing and Friction.** The South Carolina DOT used the Test Track to assess the polishing behavior of a new aggregate source in 2003. A surface mix containing the aggregate was designed, produced, and placed on the track. Friction tests conducted at regular intervals showed a sharp decline in friction, indicating that the aggregate was not suitable for use in surface mixes. The track enabled South Carolina to make this assessment in less than two years without putting the driving public at risk. Mississippi and Tennessee DOTs constructed sections to assess blends of limestone and gravel on mix performance and friction. Both states concluded that mixes containing crushed gravel provided satisfactory performance and revised their specifications to allow more gravel in their surface mixes. Test sections sponsored by the Florida DOT used a limestone aggregate source that was known to polish. When the sections became unsafe for the NCAT track fleet, a special surface treatment containing an epoxy binder and calcined bauxite aggregate was evaluated to restore good friction performance. That surface treatment has provided excellent friction results and has endured over 30 million ESALs.

**Elimination of the Restricted Zone.** Part of the original Superpave mix design procedure included a restricted zone within the gradation band for each nominal aggregate size. Test Track sections

with a variety of aggregate types proved that mixtures with gradations through the restricted zone were not necessarily susceptible to rutting. The restricted zone was subsequently removed from Superpave specifications.

**Flat and Elongated.** The Georgia DOT has led the way in using SMA since the early 1990s and soon after began to modify their open-graded friction course (OGFC) mixes toward a coarser, thicker porous European mix. Based on European experience, Georgia established strict aggregate shape limits for these premium mixes. However, few aggregate producers invested in the extra processing needed to make the special coarse aggregate for these mixes. As prices for the special aggregates rose to more than four times the price of conventional coarse aggregates, the Georgia DOT used the track to evaluate the effect of using aggregates with a less strict flat and elongated requirement for their OGFC mix. Test Track performance showed that the lower cost aggregates actually improved drainage characteristics.

**Toughness.** The South Carolina DOT used the track to evaluate an aggregate with an LA abrasion loss that exceeded their specification limit. Aggregate degradation was assessed through plant production, construction, and under traffic. Although the aggregate did break down more than other aggregates through the plant, the test section performed very well. Rutting performance on the track was similar to other sections, and there were no signs of raveling as indicated by texture measurements. Based on these results, the agency revised its specifications to allow the aggregate source.

#### *Binder Characteristics*

**Effect of Binder Grade on Rutting.** Superpave guidelines have recommended using a higher PG grade for high-traffic volume roadways to minimize rutting. Results from the first cycle of testing showed that permanent deformation was reduced by an average of 50% when the high-temperature grade was increased from PG 64 to PG 76. This two-grade bump is typical for heavy traffic projects. These results validated one of the key benefits of modified asphalt binders. The Alabama DOT also sponsored test sections to evaluate surface mixes designed with 0.5 percent more asphalt binder. Results of those sections showed that increasing the asphalt content of mixes containing modified binders did not adversely affect rutting resistance; however, mixes produced with neat binders were more sensitive to changes in asphalt content.

**Comparison of Different Types of Binder Modification.** Experiments with paired test sections in the first track cycle compared mixes containing PG 76-22 polymer-modified asphalt binders using styrene butadiene styrene (SBS) and styrene butadiene rubber (SBR). Test sections included dense-graded Superpave mixes, SMA mixes, and porous friction course mixes. Excellent performance was observed in all mixes produced with modified binders regardless of the type of modifier used. A similar experiment sponsored by the Missouri DOT and Seneca Petroleum compared the performance of a surface mix containing an SBS-modified binder and a binder modified with ground tire rubber (GTR). This experiment also demonstrated that a GTR-modified binder can provide the same performance as traditional polymer modification.

**Evaluation of Alternative Binders.** Increasing energy costs and the strong global demand for petroleum has spurred the research and development of alternative materials that can modify or replace petroleum-based asphalt binders. To this end, three test sections were built in 2009

to evaluate Trinidad Lake Asphalt (TLA) and Thiopave pellets for use in asphalt mixtures. TLA pellets are made from a naturally occurring asphalt binder source in Trinidad, while the Thiopave pellets are produced based on a sulfur-modified asphalt formulation. Thiopave pellets must be used in combination with a warm mix additive to lower the mixing temperature to 275°F or less to reduce hydrogen sulfide emissions to an acceptable level. Both TLA and Thiopave pellets were added through the plant's RAP collar. All three asphalt layers of the TLA section were modified with 25% TLA based on weight of total binder. For the two Thiopave sections, the base and intermediate mixes were modified with 30% and 40% Thiopave, respectively, while the surface mixes were not modified with Thiopave. The field performance of the three test sections was compared with that of a control section constructed with conventional asphalt mixtures as part of a pooled fund group experiment in 2009. The pavement response measurements indicated that all of the test sections were structurally sound. No cracking was found in any of the test sections, and rutting was below the 12.5-mm rutting failure threshold. Furthermore, ride quality in each section was deemed excellent after 10 million ESALs.

### *Structural Design and Analysis*

**Asphalt Layer Coefficient for Pavement Design.** Although many highway agencies are preparing for implementation of a mechanistic-based pavement design method, thousands of projects are still designed using the empirical pavement design method referred to as the 1993 AASHTO Pavement Design Guide, which was largely based on the AASHTO Road Test in the late 1950s. In simplified terms, the 1993 AASHTO design guide relates the pavement serviceability to the expected traffic and the structural capacity of the pavement structure. The pavement's structural capacity is calculated by summing the products of the thickness and the layer coefficient of each layer. Many states (45%) use 0.44 as the coefficient for asphalt concrete layers, while 28% of state agencies use an asphalt layer coefficient less than 0.44 (1). The value of 0.44 was established during the AASHTO Road Test, long before modern mix design methods, polymer modification, modern construction equipment and methods, and quality assurance specifications. A study funded by the Alabama DOT re-examined the asphalt layer coefficient using the performance and loading history of all structural sections from the second and third cycles. These test sections represented a broad range in asphalt thicknesses, mix types, bases, and subgrades. The analysis indicated that the asphalt layer coefficient should be increased from 0.44 to 0.54 (2). This 18% increase in the layer coefficient translates directly to an 18% reduction in the design thickness for new pavements and overlays. ALDOT implemented the new layer coefficient in its pavement design practice in 2010 and has estimated a resulting \$25 to \$50 million savings per year in construction costs (3).

**Perpetual Pavement Design Validation.** The Perpetual Pavement design concept has been validated using several Test Track sections. This pavement thickness design approach is based on engineering each layer in the pavement to withstand critical stresses so that damage never occurs in lower layers of the structure. On a life-cycle cost basis, Perpetual Pavements are more economical than traditional pavement designs and are less disruptive to traffic since roadway maintenance is minimized. Two of the original 2003 structural sections carried more than three times their "design traffic" based on the 1993 AASHTO guide with only minor surface damage evident before the sections were replaced for another experiment. In the 2006 cycle, Oklahoma

sponsored two sections to further validate the concept for pavements built on a very soft subgrade. One of the Oklahoma sections was designed using the 1993 AASHTO guide and the other section was designed using the PerRoad Perpetual Design program. The conventional design resulted in a 10-inch asphalt cross-section, whereas the perpetual design was 14 inches thick.

Results validated the concept of limiting critical strains to eliminate bottom-up fatigue cracking. Economic analysis of the two pavement design alternatives demonstrated that Perpetual Pavement is more cost-effective in a life-cycle cost comparison (4).

**Measured Performance versus MEPDG Predicted Performance.** Fifteen structural study test sections were analyzed with the MEPDG using the default national calibration coefficients. (5, 6). For virtually all sections, the MEPDG over-predicted rutting, generally with errors in the range of 70 to 100%. The rutting predictions for most sections were significantly improved after calibrating the model coefficients. MEPDG fatigue cracking predictions with the default coefficients were also poor for the majority of the sections. In about half of the cases, the MEPDG grossly under-predicted fatigue cracking, but in a few cases it over-predicted the amount of fatigue cracking. Attempts to adjust the fatigue model coefficients did not improve the overall correlation of predicted versus measured fatigue.

#### *Relationships Between Laboratory Results and Field Performance*

**Air Voids.** Air voids in laboratory-compacted specimens is one of the most common pay factors for asphalt pavements. The Indiana DOT sponsored Test Track research to identify an appropriate lower limit for this acceptance parameter. Surface mixes were intentionally produced with air voids between 1.0 and 3.5% by adjusting the aggregate gradation and increasing the asphalt content. Results showed that rutting increased significantly when the air voids were less than 2.75% (7). When test results are below that value and the roadway is to be subject to heavy traffic, removal and replacement of the surface layer is appropriate. It is important to note that the experiment used only mixes with neat (unmodified) asphalt binder. Other surface mixes on the track containing modified binders or high recycled asphalt binder ratios that were produced with air voids below 2.5% have held up very well under the extreme traffic on the track.

**Top-Down Cracking.** Florida DOT's pavement management system has shown that top-down cracking is the state's most prevalent form of pavement distress. Previous research has indicated that the energy ratio determined from properties of the surface mixture and stress conditions in the pavement structure can be used to predict top-down cracking. Florida DOT-sponsored sections in the 2006 cycle validated the energy ratio concept and showed that using a polymer-modified binder in dense-graded surface layers increases a pavement's resistance to top-down cracking (7, 8).

**Asphalt Pavement Analyzer (APA).** The APA is a popular test for assessing the rutting potential of asphalt mixes and has consistently provided reasonable correlations with Test Track performance. Based on a correlation between APA results and rutting on the track in the third cycle, an APA criteria of 5.5 mm was established for heavy traffic surface mixes for tests conducted in accordance with AASHTO T 340-10. As a result of this testing, the Oklahoma DOT implemented a specification requiring the use of the APA on new mix designs.

**Hamburg Wheel Tracking.** Popularity of the Hamburg wheel tracking test has increased in recent years, and numerous state DOTs now have Hamburg requirements for mix design approval. The test is considered to be a proof test for rutting and moisture damage susceptibility. Although there are no national criteria for Hamburg results, many highway agencies set the maximum rut depth between 4 and 10 mm at 20,000 wheel passes. NCAT conducted the Hamburg test in accordance with AASHTO T 324 at 50°C on 18 mixtures from the fourth track cycle. The Hamburg results correlated reasonably well ( $R^2 = 0.74$ ) with rutting measurements on the track (9). None of the test sections had any evidence of moisture damage.

**Flow Number.** In the last few years, the flow number (FN) test has gained popularity among researchers as a lab test to evaluate the rutting resistance of asphalt mixes. For the 2006 Test Track (third cycle), NCAT used a confined FN test with 10 psi and a repeated axial stress of 70 psi. A strong correlation was found between the results of the FN test using these conditions and rutting on the track. Using this method, a minimum FN of 800 cycles was recommended for heavy traffic pavements (7). Recently, NCHRP Report 673, *A Manual for Design of Hot Mix Asphalt with Commentary*, and NCHRP Report 691, *Mix Design Practices for Warm Mix Asphalt*, both recommended the FN test for assessing the rutting resistance of mix designs. The testing criteria and traffic level performance thresholds from these reports have been recently adopted in AASHTO TP 79-13. Flow number tests conducted on surface mixes from the 2009 track did not correlate well with the measured rutting for the test sections. However, all results met the FN criteria in AASHTO TP 79-13 for 3 to 10 million ESALs of traffic (9).

**Dynamic Modulus Prediction.** In mechanistic-based pavement design methods, dynamic modulus ( $E^*$ ) is a primary input for asphalt pavement layers since this property characterizes the rate of loading and temperature dependency of asphalt concrete. Three predictive dynamic modulus models and laboratory-measured  $E^*$  values were compared to determine which model most accurately reflected  $E^*$  values determined in laboratory testing. The Hirsch model proved to be the most reliable  $E^*$  model for predicting the dynamic modulus of an HMA mixture (7, 10).

**Lab Testing of Friction and Texture Changes.** NCAT used Test Track data to validate a method for determining texture and friction changes of any asphalt surface layer subjected to traffic. The procedure involves making slabs of the pavement layer in the laboratory and subjecting the slabs to simulated trafficking in the three-wheel polishing device developed at NCAT. The slabs are periodically tested for friction and texture using the ASTM standards for the Dynamic Friction Tester and the Circular Track Meter, respectively. Excellent correlations were established between the friction results in the lab and the field.

#### *Tire-Pavement Interaction*

**Tire-Pavement Noise and Pavement Surface Characteristics.** Noise generated from tire-pavement interaction is substantially influenced by the macrotexture and porosity of the surface layer. Tire-pavement noise testing on the track indicated that the degree to which these factors influence noise levels is related to the weight of the vehicle and tire pressure. For lighter passenger vehicles, the porosity of the surface, which relates to the degree of noise attenuation, is the dominant factor. For heavier vehicles (with higher tire pressure), the macrotexture of the surface and the positive texture presented at the tire-pavement interface has a greater influence.

**New Generation Open-Graded Friction Course Mixes.** Each of the previous cycles of the Test Track included new-generation open-graded friction course (OGFC) mixtures featuring a variety of aggregate types. Testing has shown that OGFC surfaces, also known as porous friction courses (PFCs), eliminate water spray and provide excellent skid resistance.

**High-Precision Diamond Grinding.** Smoothness is the most important pavement characteristic from the perspective of users. Occasionally, pavement maintenance or rehabilitation results in a bump in the roadway surface that needs to be removed. Precision diamond grinding has been used on the track in each cycle to smooth out transitions between some test sections. None of the areas leveled with the grinding equipment have exhibited any performance issues. Some of the leveled areas were in service for up to 10 years with no performance problems. No sealing was applied to these treated surfaces.

### *References*

1. Timm, D., M. Robbins, N. Tran, and C. Rodezno. *Flexible Pavement Design – State of the Practice*. NCAT Report 14-04, National Center for Asphalt Technology at Auburn University, Auburn, Ala., 2014.
2. Peters-Davis, K., and D. Timm. *Recalibration of the Asphalt Layer Coefficient*. NCAT Report 09-03, National Center for Asphalt Technology at Auburn University, Auburn, Ala., 2009.
3. Timm, D., and K. Davis. *Are We Underestimating the Strength of Asphalt?* Hot Mix Asphalt Technology, Vol. 15, No. 1, National Asphalt Pavement Association, January/February 2010.
4. Sakhaeifar, M., R. Brown, N. Tran, and J. Dean. Evaluation of Long-Lasting Perpetual Asphalt Pavement with Life-Cycle Cost Analysis. *Transportation Research Record: Journal of the Transportation Research Board*, No. 2368, Transportation Research Board of the National Academies, Washington, D.C., 2013, pp. 3-11.
5. Guo, X. *Local Calibration of the MEPDG Using Test Track Data*. MS thesis. Auburn University, Auburn, Ala., 2013.
6. Guo, X., and D. Timm. Local Calibration of MEPDG Using National Center for Asphalt Technology Test Track Data. *TRB 94th Annual Meeting Compendium of Papers*, Paper 15-1032, Transportation Research Board 94th Annual Meeting, Washington, D.C., 2015.
7. Willis, R., D. Timm, R. West, B. Powell, M. Robbins, A. Taylor, A. Smit, N. Tran, M. Heitzman, and A. Bianchini. *Phase III NCAT Test Track Findings*. NCAT Report 09-08, National Center for Asphalt Technology at Auburn University, Auburn, Ala., 2009.
8. Timm, D., G. Sholar, J. Kim, and R. Willis. Forensic Investigation and Validation of Energy Ratio Concept. *Transportation Research Record: Journal of the Transportation Research Board*, No. 2127, Transportation Research Board of the National Academies, Washington, D.C., 2009, pp. 43-51.
9. West, R., D. Timm, R. Willis, B. Powell, N. Tran, M. Sakhaeifar, R. Brown, M. Robbins, A. Vargas-Nordbeck, F. Leiva Villacorta, X. Guo, and J. Nelson. *Phase IV NCAT Pavement Test Track Findings*. NCAT Report 12-10, National Center for Asphalt Technology at Auburn University, Auburn, Ala., 2012.
10. Robbins, M. *An Investigation into Dynamic Modulus of Hot-Mix Asphalt and Its Contributing Factors*. MS thesis. Auburn University, Auburn, Ala., 2009.

### **1.3. Overview of the 2012 Test Track (Fifth Cycle)**

As with the previous four cycles, the 2012 Test Track included new sections as well as continued evaluation of existing sections. Of the 46 total sections, 22 were new experimental pavements, 14 were left in place from the 2009 cycle, six were left in place from the 2006 cycle, three sections remained from 2003, and two sections remained from the original construction.

The 2012 track featured a more complex range of experiments than any of the previous cycles. Many of the experiments focused on the use of recycled materials in pavements. This included the continued evaluation of the 2009 Group Experiment, the new Green Group Experiment, new test sections using 100% stabilized RAP, several sections containing GTR, as well as sections containing recycled asphalt shingles (RAS). A second major focus of the 2012 cycle was on PFC mixes. Eight new PFC test sections and one section with a PFC surface built in the previous cycle were analyzed. The third major focus of the 2012 cycle was on pavement preservation.

The 2009 Group Experiment was built to assess the performance and structural response of pavements constructed using WMA technologies, high RAP contents, the combination of high RAP contents and WMA, and a porous friction course containing 15% RAP. This experiment included six test sections constructed on the same base and subgrade. The Group Experiment test sections were expected to have a range of fatigue cracking due to different mixes used in the sections. Since none the sections in this experiment had any signs of damage after one cycle, it was decided to continue traffic and monitor them into the fifth cycle.

The 2012 Green Group experiment was conceived as a follow-up to the 2009 Group Experiment. The objective of this experiment was to compare the performance and structural responses of a control section to three other test sections using recycled materials in ways that would enhance the design characteristics of each layer. Each section included three asphalt layers. The control section used RAP contents typical of current specifications—20% in the surface layer and 35% in the intermediate and base layers. The second section had an SMA surface layer containing 25% RAP, a high-modulus intermediate layer with 50% RAP, and a strain-tolerant base layer containing 35% RAP and a highly modified binder. The third section had an SMA with 5% post-consumer RAS and no added fibers. The intentionally stiff intermediate layer contained RAP and RAS to have a recycled binder ratio of approximately 0.5. The strain-tolerant base layer for this section contained 25% RAP and a PG 76-22 binder. The fourth section was designed to optimize the use of GTR. The surface layer was an SMA with GTR and no added fibers. The high-modulus intermediate layer had 35% RAP and a GTR-modified binder. The strain-tolerant base layer was a gap-graded asphalt-rubber mix with 20% GTR by weight of asphalt. All the mixes used in the Green Group were produced using WMA technologies.

A new feature of the 2012 cycle was a large pavement preservation study. In recent years, state DOTs have faced the pressures of preserving aging infrastructure with diminishing resources. In response, agencies recognized the need to use preservation treatments at the right time in a pavement's life. The performance of a preservation treatment is dependent on the existing condition of the pavement, so while a treatment may perform well when placed on a road in relatively good condition, the same treatment placed on a deteriorated surface may perform poorly. Thus, an experiment was conceived to develop realistic estimates of life-extension by linking pretreatment condition with pavement performance. This information will be useful to

reliably identify which treatment is the best investment based on the existing distresses. In the experiment, a local county route, Lee Road 159, was selected to be the test bed for 23 pavement preservation treatment sections, each 100-ft long. These treatment sections and two untreated control sections are monitored to assess deterioration relative to the pre-existing condition, time, and traffic. After reaching a preselected cracking threshold, preservation treatments were applied to the 2009 Test Track Group Experiment sections.

**2012 Test Track Sponsors.** Sponsors of the 2012 Test Track are identified below in alphabetical order. Table 1 lists all of the test sections on the track starting at Section E2 and moving around the track in a clockwise direction.

*Alabama Department of Environmental Management (ADEM)* - ADEM was a funding partner in the Green Group experiment, with its primary interest being the economic use of GTR in asphalt pavements.

*Alabama Department of Transportation (ALDOT)* - ALDOT sponsored the Green Group experiment, the Preservation Group study, and two new OGFC test sections.

*Florida Department of Transportation (FDOT)* - FDOT sponsored two sections to evaluate alternative tack coat materials for OGFC and two sections to evaluate the cracking resistance of surface mixes containing RAS and a GTR-hybrid binder.

*Federal Highway Administration (FHWA)* - FHWA provided funding to evaluate high friction surface treatments and to conduct research and deployment of the Safety Edge<sub>SM</sub> using various Test Track sections. Safety Edge<sub>SM</sub> is a simply constructed beveled pavement edge to reduce accidents resulting from overcorrected steering when a vehicle wheel drops off the pavement.

*For Pavement Preservation (FP<sup>2</sup>)* - FP<sup>2</sup> was an equal funding partner and was instrumental in the development, marketing, and construction of the Preservation Group experiment.

*Georgia Department of Transportation (GDOT)* - GDOT sponsored two sections to compare the effectiveness of two alternative treatments for mitigating reflective cracking. Deep saw cuts were made in existing sections to simulate a cracked pavement. One section used a stress absorbing interlayer consisting of a triple surface treatment application with a sand seal surface. The second section used what is referred to as an open-graded interlayer (OGI), which is similar to a PFC mix without fiber stabilizer and has a lower asphalt content.

*Kraton Polymers* - Kraton sponsored continued trafficking and evaluation of the 2009 structural section using a highly modified asphalt binder. The section was built as a companion to the control section in the Group Experiment but at a reduced thickness.

*Mississippi Department of Transportation (MSDOT)* - MSDOT sponsored the continuation of traffic on their section containing 45% RAP, a new low-cost thin overlay test section, and the Preservation Group study.

*Missouri Department of Transportation (MODOT)* - MODOT was a sponsor of the Preservation Group experiment.

*North Carolina Department of Transportation (NCDOT)* - NCDOT was a sponsor of the Green Group and Preservation Group experiments.

*Oklahoma Department of Transportation (OKDOT)* - OKDOT was a sponsor of the Preservation Group experiment, a new PFC section to assess alternative tack coat materials, and the continuation of traffic and performance monitoring of its Perpetual Pavement test section built in 2006.

*Seneca Petroleum* - Seneca sponsored continued traffic and evaluation of the GTR-modified surface mix section that was funded in the previous cycle by Missouri DOT.

*South Carolina Department of Transportation (SCDOT)* - SCDOT was a sponsor of the Green Group and Preservation Group experiments.

*Tennessee Department of Transportation (TNDOT)* - TNDOT was a sponsor of the Green Group, the Preservation Group, and the evaluation of a new PFC section containing RAS.

*Virginia Department of Transportation (VDOT)* - VDOT joined the Test Track pooled-fund project for the first time in 2012 by sponsoring two surface performance sections and three structural performance sections. The surface performance sections were built to primarily evaluate tire-pavement noise of OGFC mixes using GTR-modified binder and a conventional SBS-modified binder. The three structural sections were built with foamed asphalt stabilized RAP using a cold central-plant recycling (CCPR) process. The primary objective of the structural sections was to determine the structural contribution of the stabilized RAP base layer.

Numerous companies provide generous donations of equipment, materials, and human resources to help build test sections. This support helps to minimize costs and ensures that the highest quality research is achieved. As before, Astec Industries provided personnel and equipment to assist in production of the experimental mixes and construction of test sections. Roadtec provided placement equipment. Construction materials were donated by Blacklidge Emulsions, Ergon, Holcim, Martin Marietta Aggregates, Maymead, MeadWestvaco, Oldcastle Materials Group, Polycon, Stalite, Vulcan Materials, and Wiregrass Construction. Other material suppliers donated materials directly to state DOT sponsors. Instrotek, Transtech Systems, and Troxler Electronic Laboratories provided equipment for mix and pavement quality testing.

**Table 1 List of Test Sections on the 2012 NCAT Test Track**

Test Sec	Study Mix (in)	Surface Mix Stockpile Materials	Year of Completion	Design Methodology	Specified Binder	Total Mix (in)	Base Material	Sub-Grade	Research Objective(s)
E2	4	Granite Micro Surface	2014	Micro	CSS-1HP	24	Granite	Stiff	Restore Friction on Worn High Friction Epoxy Surface
E3	4	Granite Micro Surface	2014	Micro	CSS-1HP	24	Granite	Stiff	Restore Friction on Worn High Friction Epoxy Surface
E4A	4	Granite	2000	Superpave	PG76-22	24	Granite	Stiff	Performance of Coarse Gradation
E4B	4	Granite	2000	Superpave	PG76-22	24	Granite	Stiff	Performance of Coarse Gradation with Rejuvenating Fog Seal
E5A	2	Grm/Lms/Snd (45% RAP)	2006	Superpave	PG67-22	24	Granite	Stiff	RAP Mix Design/Construction/Performance w/ Rej. Fog Seal
E5B	2	Grm/Lms/Snd (45% RAP)	2006	Superpave	PG67-22	24	Granite	Stiff	RAP Mix Design/Construction/Performance
E6	2	Grm/Lms/Snd (45% RAP)	2006	Superpave	PG76-22	24	Granite	Stiff	RAP Mix Design/Construction/Performance
E7A	1.5	Granite/Limestone	2012	Superpave	PG76-22	24	Granite	Stiff	SBS-Modified Control Mix from 2006 Research Cycle
E7B	1.5	Granite/Limestone	2012	Superpave	StAR	24	Granite	Stiff	GTR-Modified Research Mix Variant of E7A-1 Control
E8A	1.5	Granite (25% RAP)	2012	Superpave	PG76-22	24	Granite	Stiff	25% RAP Research Mix Variant of E7A-1 Control
E8B	1.5	Granite (20% RAP, 5% RAS)	2012	Superpave	PG76-22	24	Granite	Stiff	20% RAP + 5% RAS Research Mix Variant of E7A-1 Control
E9A	0.75	Granite	2012	PFC	PG76-22	24	Granite	Stiff	9.5 NMAS Mix with Cellulose Fibers
E9B	0.75	Granite	2012	PFC	ARB12	24	Granite	Stiff	12.5 NMAS with Forta-Fi and No Cellulose Fibers
E10	0.75	Granite	2012	PFC	ARB12	24	Granite	Stiff	12.5 NMAS with ARB12 and No Cellulose Fibers
N1A	0.75	Granite (15% RAP)	2012	PFC	PG76-22	7.75	Limerock	Stiff	Surface Cracks in PFC Tacked with eTac
N1B	0.75	Granite (15% RAP)	2012	PFC	PG76-22	7.75	Limerock	Stiff	Surface Cracks in PFC Tacked with UltraFuse
N2	0.75	Granite (15% RAP)	2012	PFC	PG76-22	7.75	Limerock	Stiff	Surface Cracks in PFC Tacked with Trackless
N3	6	Traprock (11% RAP)	2012	SMA	PG76-22	11	Granite	Stiff	Thicker Overlay for 100% Recycle Mix
N4	4	Traprock (11% RAP)	2012	SMA	PG76-22	9	Granite	Stiff	Thinner Overlay for 100% Recycle Mix
N5A	6	Grm/Lms (15% RAP, 5% RAS)	2014	SMA	PG76-22	6	Granite	Stiff	Maint for GG Control M-E Design Validation/Calibration
N5B	6	Lms/Gm/Snd (15% RAP, 5% RAS)	2014	Superpave	PG76-22	6	Granite	Stiff	Maint for GG Control M-E Design Validation/Calibration
N6	7	Granite/Sand/Limestone	2009	Superpave	PG76-22	7	Granite	Stiff	GE+ Standard Shell Thiopave & M-E Design
N7	5.75	Granite/Sand/Limestone	2009	Superpave	PG88-22	5.75	Granite	Stiff	GE+ Thin Kraton High Polymer & M-E Design
N8	5.75	Granite/Sand/Limestone	2009	Superpave	PG88-22	10	Stiff Sub	Soft	Kraton High Polymer for Extreme Rehabilitation
N9	14	Oklahoma Granite	2006	SMA	PG76-28	14	Stiff Sub	Soft	Perpetual Pavement & M-E Design
N10	7	Sand/Granite (50% RAP)	2009	Superpave	PG67-22	7	Granite	Stiff	GE 50% RAP Hot Mix Asphalt & M-E Design
N11	7	Sand/Granite (50% RAP)	2009	Superpave	PG67-22	7	Granite	Stiff	GE 50% RAP Foamed Warm Mix Asphalt & M-E Design
N12	2	Georgia Granite	2012	Superpave	PG67-22	24	Granite	Stiff	Reflective Crack Prevention with Triple Chip
N13	2.75	Georgia Granite	2012	Superpave	PG67-22	24	Granite	Stiff	Reflective Crack Prevention with Open Graded Interlayer
W1	4	Georgia Granite	2000	SMA	PG76-22	24	Granite	Stiff	Columbus Granite SMA
W2	0.38	Lightweight Aggregate	2012	Chip Seal	PG67-22	24	Granite	Stiff	Pavement Preservation
W3	2	Grm/Lms/Snd (20% RAP)	2006	Superpave	PG76-22	24	Granite	Stiff	RAP Mix Design/Construction/Performance
W4	2	Grm/Lms/Snd (20% RAP)	2006	Superpave	PG67-22	24	Granite	Stiff	RAP Mix Design/Construction/Performance
W5	2	Grm/Lms/Snd (45% RAP)	2006	Superpave	PG52-28	24	Granite	Stiff	RAP Mix Design/Construction/Performance
W6	1	Lms Screenings/Sand	2003	Superpave	PG76-22	24	Granite	Stiff	Low Volume Road Preservation
W7	1.5	Granite	2010	Superpave	PG67-22	24	Granite	Stiff	Shell Thiopave with Latex 5/11/10
W8A	0	Granite	2011	Research	Epoxy	24	Granite	Stiff	Granite Epoxy Surface Treatment
W8B	1	Granite	2003	NovaChip	PG70-28	24	Granite	Stiff	Low Volume Road Preservation Epoxy Surface Control
W8C	0	Calcined Bauxite	2011	Research	Epoxy	24	Granite	Stiff	Bauxite Epoxy Surface Treatment
W9	0	Chert	2011	Research	Epoxy	24	Granite	Stiff	Chert Epoxy Surface Treatment
W10	2	Traprock (10% RAP)	2012	PFC	PG76-22	24	Granite	Stiff	Conventional PFC
S1	2	Traprock (10% RAP)	2012	PFC	ARB12	24	Granite	Stiff	Quiet PFC
S2	4	Gravel/Sand (45% RAP)	2009	Superpave	PG67-22	24	Granite	Stiff	High RAP Content Gravel Superpave
S3	1	Gravel/Sand (25% RAP)	2012	Superpave	PG67-22	24	Granite	Stiff	Low Cost Mix for Low Volume Roads
S4	1.25	Limestone (3% RAS)	2012	PFC	PG76-22	24	Granite	Stiff	PFC Construction/Performance without Cellulose Fibers
S5	6	Granite/Flyash (25% CFRAP)	2013	SMA	PG67-22	6	Granite	Stiff	GG Buildup with RAP Focus & M-E Design
S6	6	Lms/Gm/Snd (15% RAP, 5% RAS)	2014	SMA	PG76-28E	6	Granite	Stiff	Maint for GG Buildup with RAP+RAS & M-E Design
S7	1.75	Limestone/Porphyr	2009	Superpave	PG76-22R	24	Granite	Stiff	GTR-Modified Superpave Mix
S8A	7	Lms/Gm/Snd (15% RAP, 5% RAS)	2014	Superpave	PG76-28E	7	Granite	Stiff	PG Micro Mill / Thin Overlay in GE Buildup with PFC Surface
S8B	7	Granite (15% RAP)	2009	PFC	PG76-22	7	Granite	Stiff	PG S8A Control (GE Buildup with PFC Surface w/ Rej. Fog)
S9A	7	Lms Screenings/Sand	2014	Superpave	PG76-22	7	Granite	Stiff	PG Thin Overlay on GE Control Virgin HMA
S9B	7	Calera Limestone	2014	Micro	CSS-1HP	7	Granite	Stiff	PG Micro Surface on GE Control Virgin HMA
S10A	7	Calera Lms / 89 Columbus Grm	2014	Micro / Scrub	CSS-1HP / CMS-1P(CR)	7	Granite	Stiff	PG Scrub Cape on GE Foamed Virgin WMA
S10B	7	89 Columbus Granite	2014	Scrub	CMS-1P(CR)	7	Granite	Stiff	PG Scrub Seal on GE Foamed Virgin WMA
S11A	7	89 Columbus Granite	2014	Chip	CRS-2HP	7	Granite	Stiff	PG Chip Seal on GE Additized Virgin WMA
S11B	7	Granite/Sand/Limestone	2009	Superpave	PG76-22	7	Granite	Stiff	PG Virgin DGA Control (GE Additized Virgin WMA)
S12	4	Traprock (11% RAP)	2012	SMA	PG76-22	9	FDR	Stiff	Thinner Overlay for 100% Recycle Mix on FDR Foundation
S13	6	Granite/Flyash	2012	SMA	ARB12	6	Granite	Stiff	Maint for GG Buildup with Recycled Tire Rubber & M-E Design
E1A	0.75	Granite	2012	PFC	PG76-28	24	Granite	Stiff	PFC Design/Construction/Performance Tacked with UltraFuse
E1B	0.75	Granite	2012	PFC	PG76-28	24	Granite	Stiff	PFC Design/Construction/Performance Tacked with Trackless

**Construction**

New test sections were prepared by milling to the appropriate depth for each section. Roadtec Inc. generously provided milling machines and highly skilled operators at no cost to the track’s budget. The Test Track manager coordinated milling locations and depths. NCAT personnel operated dump trucks to collect and haul millings.

**Instrumentation for Structural Test Sections**

The instrumentation system developed and improved through previous cycles of the NCAT Test Track was again used to measure pavement response in all structural test sections. The instrumentation plan and analysis routines have proven to be robust and effective in gathering data for mechanistic pavement analysis. This system and methodology is thoroughly detailed in NCAT Report 09-01.



**Figure 2 Installation of a Pressure Plate Before Placing the Aggregate Base**

East Alabama Paving Company was awarded contracts to produce the asphalt mixtures and construct the test sections through a competitive bidding process through Auburn University. Due to space limitations on the contractor's yard, it was necessary to stage some materials at paved storage locations on the track property before they were needed for mix production.

A special production sequence was used to produce each mix. The plant's cold feed bins were calibrated for each unique stockpile. Production began with running the aggregate through the drier and mixer without the addition of asphalt binder to ensure a uniform gradation and temperature. This uncoated material was discharged and wasted. Liquid asphalt was then turned on and the mix was discharged at the slat conveyor bypass chute until the aggregates were well coated. The bypass chute was then closed and the mixture was conveyed into the storage silo until the plant controls indicated that approximately one truckload had accumulated. This mix was loaded into a truck and then dumped into a stockpile for future recycling. At this point, the plant was assumed to have reached steady state conditions and that subsequent mix run into the silo would be uniform in terms of aggregate gradation, asphalt content, and temperature. After the desired quantity of mix had been produced, the aggregate and asphalt flows were stopped, the remaining materials in the drier and mixer were discharged at the bypass chute, and the plant was shut down. The cold feed bins were unloaded, and the plant was readied for the next test mix.

Prior to placement of mixes on each test section, a trial mix was produced to evaluate the quality control requirements of the sponsor. The trial mixes were hauled to the track and sampled by NCAT personnel for laboratory testing and evaluation. Test results of the trial mixes were presented to each sponsor to determine appropriate adjustments in plant settings for the subsequent production of mix for placement on the track.

Mix produced for placement on the test sections followed the same production sequence described above. Mix production continued until a sufficient quantity of material was available for placement. The contractor was responsible for hauling mixes to the track, and the paving equipment and crew were staged at the track.



**Figure 3 Paving the Base Layer of a Test Section on the 2012 NCAT Test Track**

Before placing mixtures on the test sections, the contractor tacked the underlying asphalt pavement with a PG 67-22 binder, NTSS-1HM emulsion, or other tack material depending on the sponsor's preference. The target application rates were generally between 0.04 to 0.07 gallons per square yard (residual for emulsion), unless otherwise directed.

Mixtures were dumped from end-dump haul trucks into a Roadtec SB2500 material-transfer machine operated from the track inside lane so that only the paving machine operated on the actual test sections. Compaction was accomplished by at least three passes of a steel-wheeled roller. The roller was capable of vibrating during compaction; however, this technique was not used on every test section. After the steel-wheeled roller was removed from the pavement mat, the contractor continued compacting the mat with a rubber tire roller until the desired density was achieved.

#### *Traffic*

Trafficking for the 2012 Test Track was applied in the same manner as with previous cycles. Two shifts of professional drivers operated four trucks pulling triple flatbed trailers (Figure 4) and one truck pulling a triple box trailer from 5 a.m. until approximately 10:40 p.m. Tuesday through

Saturday. Trafficking began on October 23<sup>rd</sup>, 2012 and ended October 18<sup>th</sup>, 2014. The total traffic applied to the sections during this cycle was 10,045,790 ESALs.



**Figure 4 Heavily Loaded Triple-Trailer used for Accelerated Loading on the Test Track**

Axle weights for each of the five trucks are shown in Table 2. On some occasions, either due to a specialized study or mechanical malfunction, trailers were removed from the operation. This left the truck pulling either a single flatbed trailer or a combination of double flatbeds.

**Table 2 Axle Weights (lbs.) for the 2012 Truck Fleet**

Truck ID	Steer	Tandem		Single				
	Axle 1	Axle 2	Axle 3	Axle 4	Axle 5	Axle 6	Axle 7	Axle 8
1	10,150	19,200	18,550	21,650	20,300	21,850	21,100	19,966
2	11,000	20,950	20,400	20,950	21,200	21,000	20,900	20,900
3	10,550	20,550	21,050	21,000	21,150	21,150	21,350	20,850
4	10,550	21,050	20,700	21,100	21,050	21,050	20,900	21,050
5	11,200	19,850	20,750	20,350	20,100	21,500	19,500	20300
Avg.	10,680	20,320	20,290	20,760	20,760	21,310	20,550	20,613
COV, %	3.9	3.9	4.9	2.2	2.5	1.7	3.6	2.2

*Performance Monitoring*

Performance of the test sections was evaluated with a comprehensive range of surface measurements. Additionally, the structural health and response of the structural sections were routinely evaluated using embedded stress and strain gauges and falling-weight deflectometer (FWD) testing. Table 3 summarizes the performance monitoring plan. Rut depths, International Roughness Index (IRI), mean texture depth, and cracking results were reported on the Test Track website.

**Table 3 NCAT Test Track Performance Monitoring Plan**

Activity	Sections	Frequency	Method
Rut depth	all	weekly	ARAN van
Mean texture depth	all	weekly	ARAN van, ASTM E1845
Mean texture depth	select	quarterly	CTM, ASTM E2157-09
International Roughness Index	all	weekly	ASTM E950, AASHTO R 43
Crack mapping	sponsored	weekly	Jason 3000
FWD	structural	3 times/mo.	AASHTO T 256-01
Stress/Strain response to live traffic	structural	weekly	NCAT method
Pavement temperature at four depths	all	hourly	Campbell Sci. 108 thermistors
Pavement reflectivity/albedo	sponsored	quarterly	ASTM E 1918-06
Field permeability	OGFC/PFCs	quarterly	NCAT method
Core density	sponsored	quarterly	ASTM D979, AASHTO T 166
Friction	all	monthly	ASTM E274, AASHTO T 242
Friction	select	quarterly	DFT, ASTM E1911
Tire-pavement noise	all	quarterly	OBSI, AASHTO TP 76-11 CPX, ISO 11819-2 Absorption, ASTM E1050-10

**Laboratory Testing**

Mixture samples for quality assurance (QA) testing were obtained from the beds of the haul trucks using a sampling stand located at the track. Typical quality assurance tests were conducted immediately on the hot samples. Table 4 lists the test methods used for the quality assurance testing. The results of these tests were reviewed by the respective test section sponsor for acceptance. In cases where the QA results did not meet the sponsor's approval, the mixture placed on the section was removed, adjustments were made at the plant, and another production run was made until the mix properties were satisfactory. Results of the quality assurance tests and the mix designs for each layer for all test sections were reported on the Test Track website.

**Table 4 Tests Used for Quality Assurance of Mixes**

Test Description	Test Method	Replicates
Splitting samples	AASHTO T 328-05	as needed
Asphalt content	AASHTO T 308-10	2
Gradation of recovered aggregate	AASHTO T 30-10	2
Laboratory compaction of samples	AASHTO T 312-12	2
Maximum theoretical specific gravity	AASHTO T 209-12	2
Bulk specific gravity of compacted specimens	AASHTO T 166-12	2

NCAT staff obtained large representative samples of each unique mixture placed on the Test Track for additional testing by diverting mix from the conveyor of the material transfer machine going into the paver into the bucket of a front-end loader. The front-end loader then brought the mix to the rear of the track laboratory where the mix was then shoveled into 5-gallon buckets and labeled. In total, over 900 buckets of mix were sampled for additional testing. Samples of the asphalt binders were also obtained at the plant for characterization.

A testing plan for advanced characterization of the 24 unique mixtures was established to meet section-specific and general Test Track research objectives. Table 5 summarizes the tests and which materials or layers were typically evaluated. Results of these tests are maintained in a database at NCAT.

**Table 5 Summary of Testing for Advanced Materials Characterization**

<b>Test Description</b>	<b>Test Method</b>	<b>Material or Layer</b>
PG grade	AASHTO R 29-08	Tank binders and recovered binders from mixes containing RAP, RAS and/or WMA (No GTR modified binders were recovered)
Multiple stress creep recovery	AASHTO TP 70-09	Same as above
Cantabro	ASTM D7064-08	OGFC surface mixes
Moisture susceptibility	AASHTO T 283-07	All Green Group mixes and HMA mixes from VA CCPR sections
Hamburg wheel tracking	AASHTO T 324-11	FL surface cracking study
Asphalt Pavement Analyzer	AASHTO T 340-10	Surface mixes from Green Group, FL surface cracking study, MS low-volume road mix, HMA from VA CCPR sections
Dynamic modulus	AASHTO TP 79-13	All mixes from Green Group, FL surface cracking study, HMA from VA CCPR sections
Flow number	AASHTO TP 79-13	Surface mixes from Green Group mixes and HMA mixes from VA CCPR sections
Bending beam fatigue	AASHTO T 321-07	Intermediate and base mixes from Green Group
AMPT fatigue (SVECD)	AASHTO TP 107-14	Base mixes from Green Group
Energy ratio	Univ. of Florida	Surface mixes from Green Group and FL surface cracking study

## 2. STRUCTURAL EXPERIMENTS

### *Overview of Structural Studies*

Structural studies have been conducted at the NCAT Test Track since 2003. These studies feature test sections that include embedded instrumentation to support mechanistic pavement response testing and analysis while evaluating the performance of new or innovative technologies under live traffic and real-world environmental conditions. The sections also support the evaluation, calibration, and validation of mechanistic-empirical pavement design methodologies. Frequent pavement response measurements, pavement distress surveys, and falling weight deflectometer (FWD) testing are the main components of the structural studies.

### *Instrumentation*

The subsurface instrumentation and data acquisition systems used in all of the track's structural studies have been relatively consistent since the first structural sections were built in 2003. Figure 1 illustrates the typical gauge array used in these investigations. Within each section, an array of twelve asphalt strain gauges was used to capture strain at the bottom of the asphalt concrete. The gauges, manufactured by CTL, were installed such that longitudinal (parallel to traffic) and transverse (perpendicular to traffic) strains could be measured. Within the Virginia DOT (VDOT) test sections described later, the transverse gauges were substituted with vertical asphalt strain gauges. Further details are provided in that portion of the report. Two earth pressure cells, manufactured by Geokon, were installed to measure vertical stress at the asphalt concrete/aggregate base interface. Temperature probes, manufactured by Campbell Scientific, were installed just outside the edge stripe to measure temperature at the top, middle, and bottom of the asphalt concrete, in addition to 3 inches deep within the aggregate base. Again, the VDOT sections featured a slightly different temperature gauge arrangement (described later in the report). Figure 2 shows the typical strain gauge arrangement ready for paving. Full explanation regarding the sensors and installation procedures has been previously documented (1).

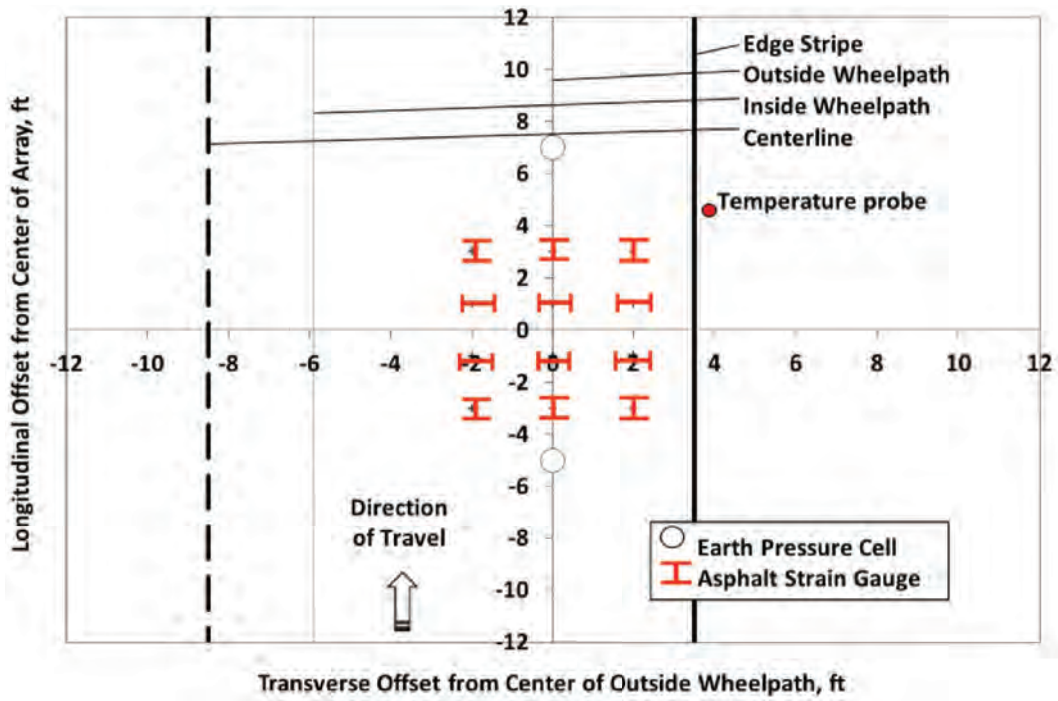


Figure 1 Subsurface Instrumentation



Figure 2 Typical Gauge Array Ready for Paving

### Data Collection and Processing

During the two-year research cycle, strain and pressure data were collected once per week. For each day's data collection, three passes of each truck were obtained from each section. The strain and pressure measurements were then evaluated to determine the 95<sup>th</sup> percentile measurements under steer, single, and tandem axles, respectively. The 95<sup>th</sup> percentile was taken to represent the best hit on a particular date and is consistent with previous data collection and processing procedures used at the track (2). Temperatures were also recorded at the time of testing and archived with the strain and pressure measurements in an Access database for further analysis and evaluation as described in the subsequent sections.

The analyses of pertinent strain and pressure data were tailored to the experimental objectives of the various structural experiments within the research cycle. However, there were some common techniques used throughout the analyses, as explained below.

**Response vs. Time.** As mentioned, strain and pressure data were collected on a weekly basis over the two-year cycle. Figure 3 shows an example data set from Section N3 (sponsored by VDOT) that includes horizontal tensile strain and mid-depth pavement temperature at the time of testing. As expected, the seasonal trends are clearly evident with strain closely following pavement temperature. The more frequent oscillations in both the temperature and strain data sets resulted from alternating between morning and afternoon data collection on a weekly basis.

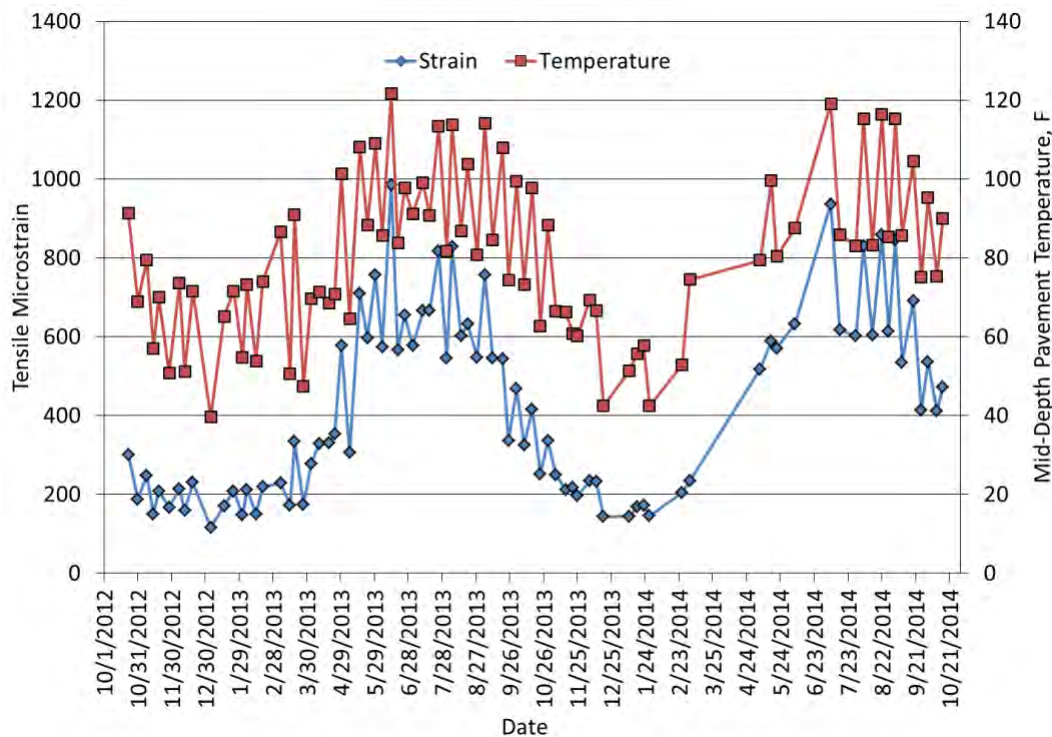


**Figure 3 Strain and Pressure vs. Time**

**Response vs. Temperature.** Since pavement temperature was monitored but not controlled during the research cycle, it is very difficult to discern any changes in the pavement response due to other factors such as aging or pavement damage. It also makes it difficult to directly compare

between sections since the temperatures may differ. Therefore, it was important to develop response-temperature relationships to normalize the data to a reference temperature. For example, Figure 4 illustrates this process whereby the strain and temperature from Figure 3 are plotted against each other. The exponential function fit to the non-normalized strain data in Figure 5 indicates a strong relationship between strain and temperature (i.e., high  $R^2$ ). The exponential regression equation was then used to normalize all the data to a reference temperature of 68°F and is shown by the temperature-normalized strain series. A linear trendline was fit to this series and clearly shows that the strong reliance on temperature was effectively eliminated (i.e., nearly zero slope and extremely low  $R^2$ ). The normalized data set can be plotted against time or compared against other sections' data at the same reference temperature. Full details of the temperature normalization process have been previously documented (3, 4, 5).

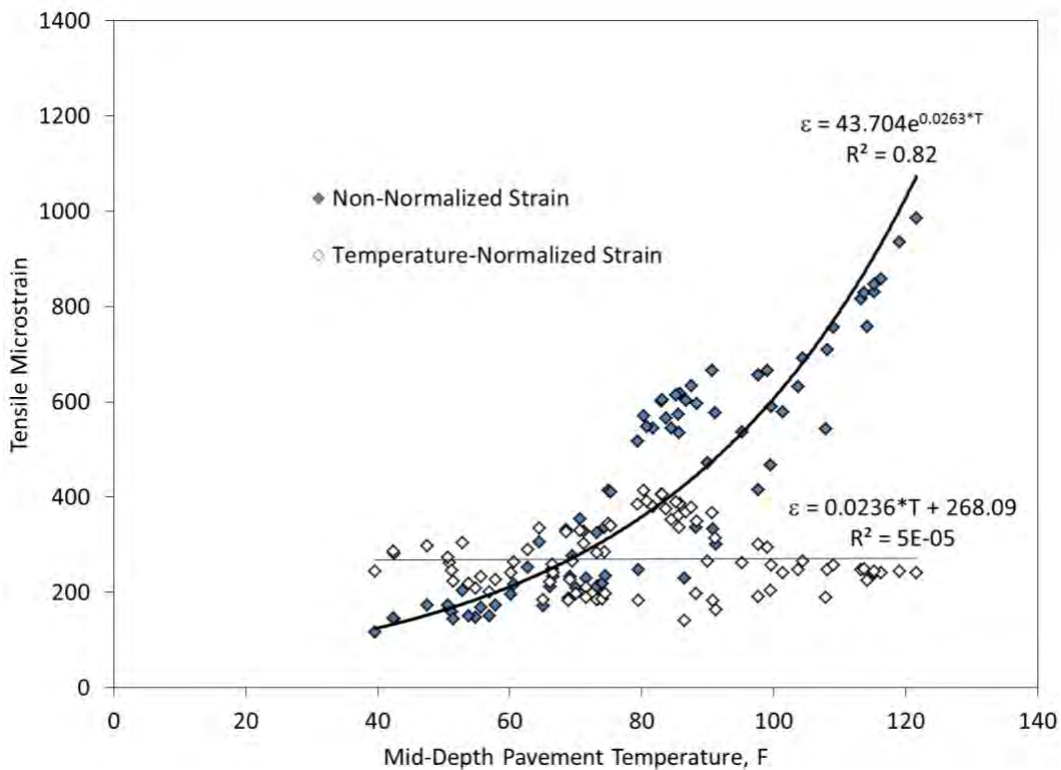


**Figure 4 Strain vs. Temperature**

**Normalized Response vs. Time.** Tracking pavement response over time to identify damage or aging of the pavement sections relied on heavily temperature-normalized data. Figure 5 illustrates the strain data set from Figure 3, which was normalized in Figure 4, plotted against date. In this case, a very slight upward trend was noted (relatively small slope and low  $R^2$ ). Full analysis of this data set in the context of the VDOT experiment is provided in the VDOT section of this report.

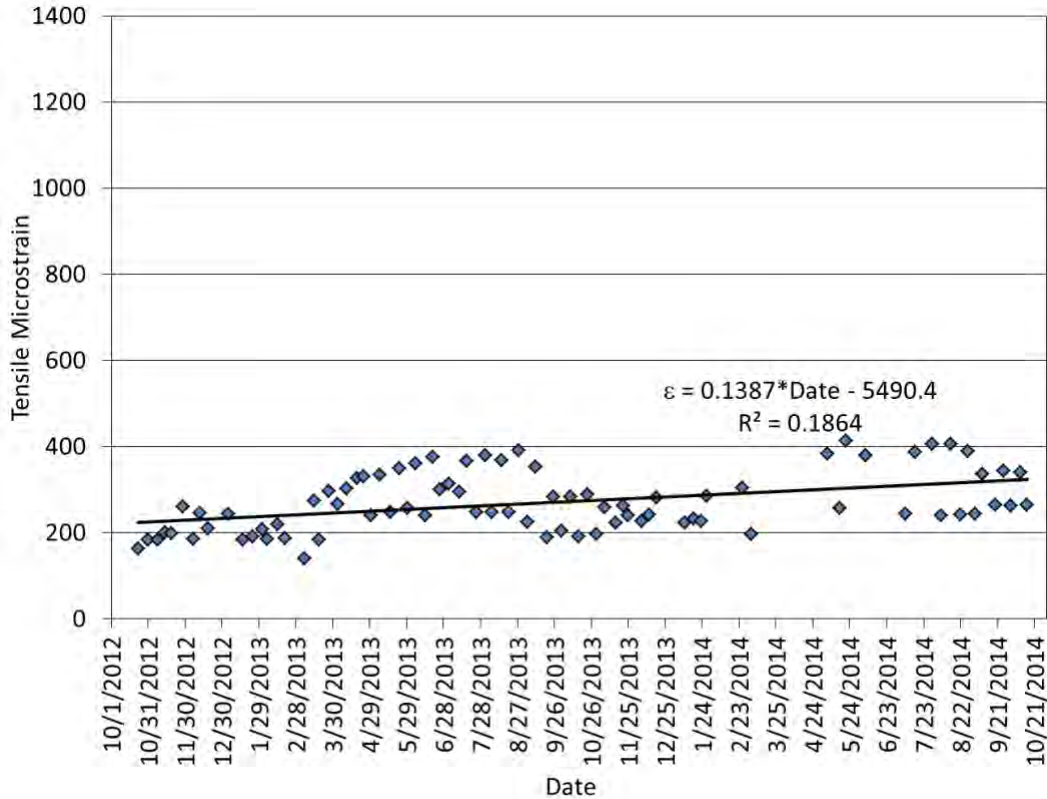


**Figure 5 Temperature-Normalized Strain vs. Time**

*Falling Weight Deflectometer Testing*

FWD testing was conducted several times per month on each section. On each testing date, four longitudinal stations in each section were tested inside the wheel paths (IWP), outside the wheel paths (OWP), and between the wheel paths (BWP). Figure 6 illustrates how a 200-ft test section was subdivided into three 50-ft subsections with 25-ft non-tested transition areas at both ends. Within each 50-ft subsection, a random location (RL1, RL2, RL3) was determined at the start of the research cycle and maintained through the two-year period. An additional location (RL4) was located in the middle of the gauge array. Figure 6 also shows the transverse offsets tested at each RL with a total of 12 stations tested within each section. Testing was conducted with a Dynatest Model 8000 FWD (Figure 7) using a 5.91-inch radius split plate with three replicates of four drop heights ranging from 6,000 to 16,000 lb. Only data obtained at the second drop height (approximately 9,000 lb) are presented in this report. Nine sensors were spaced from the load center to 72 inches from the load center and were subjected to monthly relative calibration and annual reference calibration according to the AASHTO R 32 methodology. Temperatures were recorded from FWD-mounted devices (air temperature and pavement surface temperature) in addition to the probes embedded in each section.

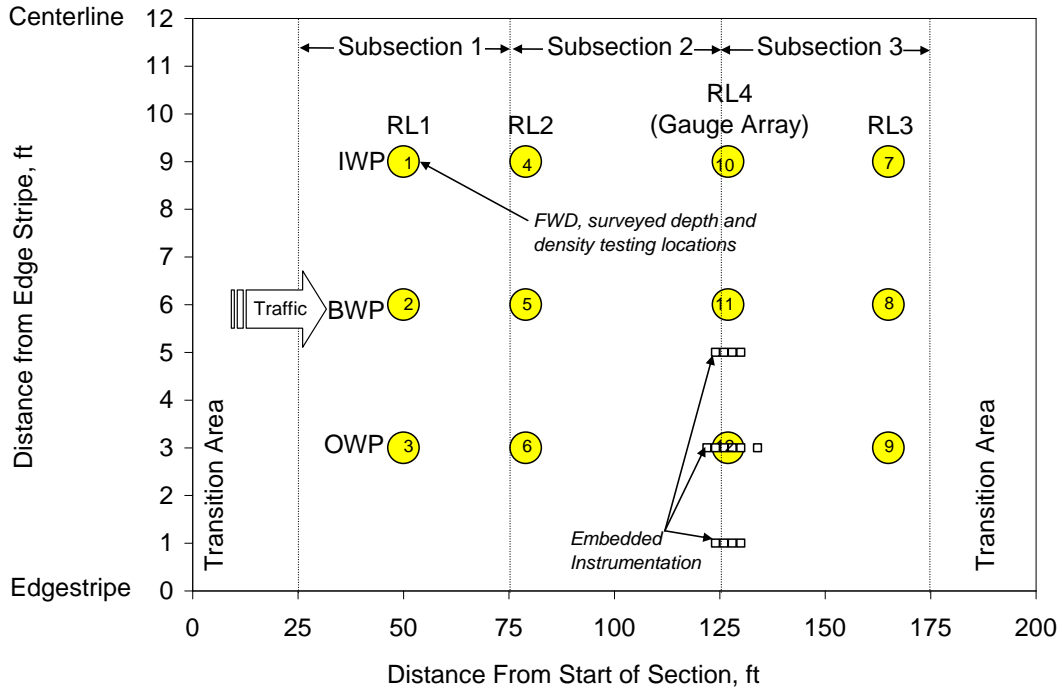


**Figure 6 Random Location and Instrumentation Schematic**



**Figure 7 Dynatest Model 8000 Falling Weight Deflectometer on the Test Track**

**Backcalculation.** Backcalculation of the FWD testing data was executed with EVERCALC 5.0. Each section was analyzed as a three-layer pavement structure consisting of asphalt concrete over aggregate base over the subgrade soil. To maintain quality data, only backcalculated results yielding a root-mean-square-error below 3% are presented in this report. The following three subsections mirror the discussion of pavement response data presented above but focus on backcalculated asphalt concrete (AC) modulus and temperature.

**Modulus vs. Time.** Deflection data collected through FWD testing were used to determine the in situ layer properties. Figure 8 shows measured temperature and backcalculated AC moduli versus time for one of the VDOT sections (N3). As expected, the inverse relationship between temperature and modulus is clearly evident. The scatter of the data on any given testing date represents the nature of the FWD testing. There are three temperatures on each test date corresponding to each offset tested (IWP, BWP, and OWP) as previously described. Testing was also conducted at four RL's in the section, so the scatter amongst the AC moduli on a given date represents both RL spatial variability and offset temperature effects.

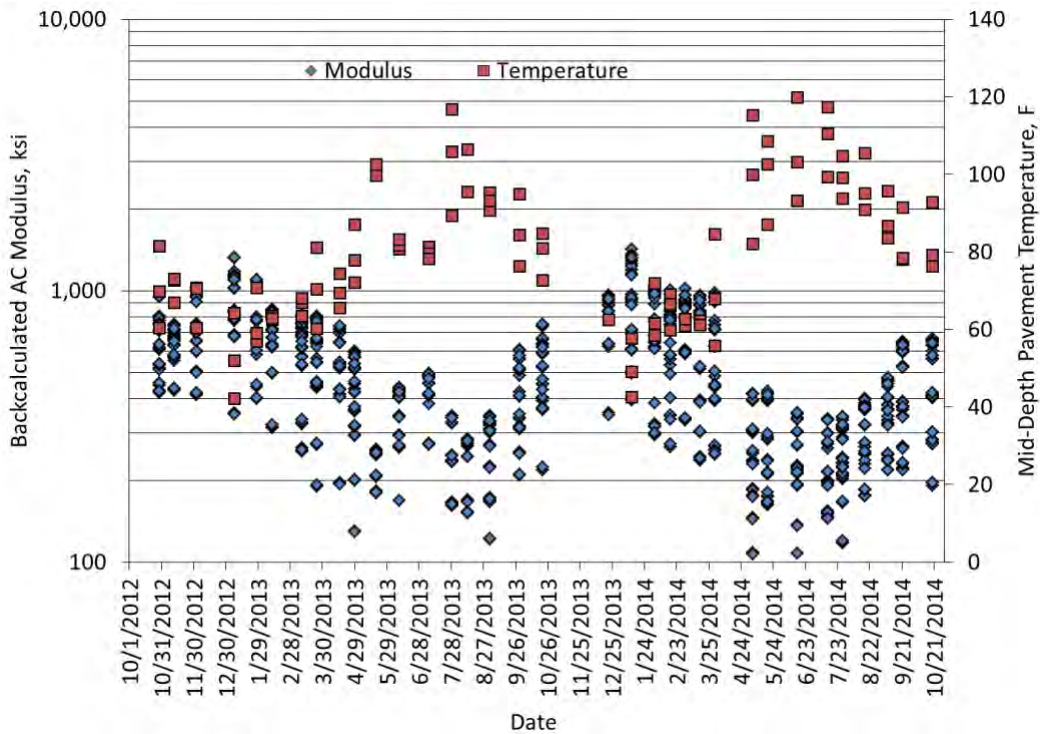


**Figure 8 AC Modulus and Temperature vs. Time**

**Modulus vs. Temperature.** As was done with the strain/temperature data presented above, the moduli and temperature data in Figure 8 were plotted in Figure 9 from which exponential and linear trendlines were fit to the data. The exponential function shown in Figure 9 was used to normalize the AC moduli to a reference temperature of 68°F. The trendline on the normalized data demonstrates that the normalization process was effective at eliminating temperature as a factor. Again, eliminating temperature allows for plotting the data over time to detect changes due to damage or aging and also allows for direct comparisons between test sections evaluated at different temperatures.

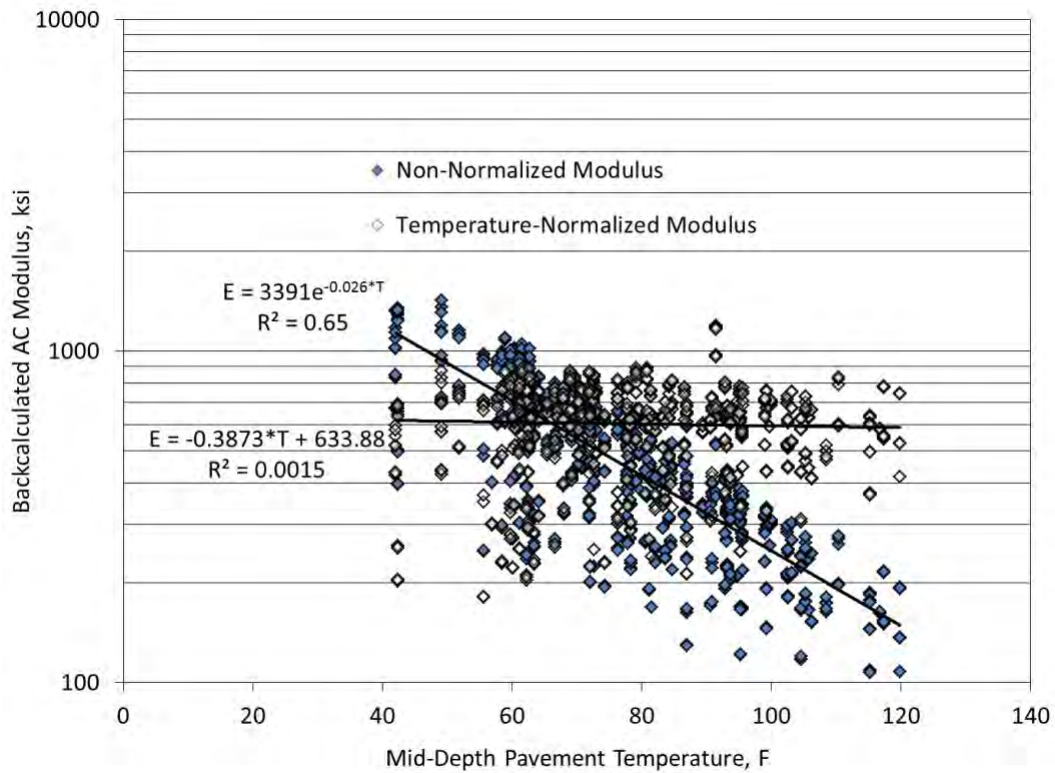


**Figure 9 AC Modulus vs. Temperature**

**Normalized Modulus vs. Time.** Tracking temperature-normalized modulus over time provides an independent data set to further evaluate the possible impact of damage or aging on the pavement structure. Figure 10 illustrates this idea by plotting temperature-normalized AC moduli against corresponding test dates. The linear trendline shows a very slight negative slope with extremely low  $R^2$ , which is consistent with the strain data presented in Figure 5. Full analyses of these data sets are presented in the VDOT section of this report.

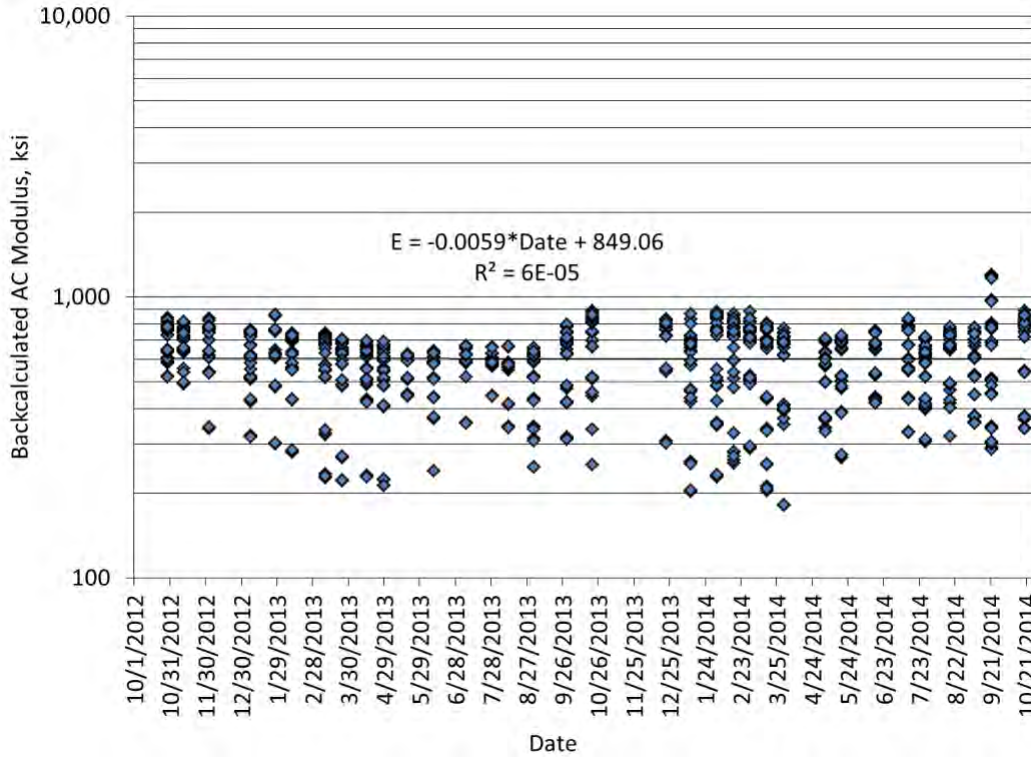


**Figure 10 Temperature-Normalized AC Modulus vs. Time**

### *Performance Monitoring*

Rutting progression and ride quality (International Roughness Index (IRI)) were measured weekly with an ARAN van. Cracking development and progression were determined through weekly visual inspection and marking of cracks followed by digital imaging in order to develop crack maps. These crack maps were then used to establish areas of cracking percentages. For this research, rutting failure was set at 0.5 in., cracking failure was set at 25% of lane area (50% of wheel path area), and ride quality failure was set at 170 in./mile.

### *References*

1. Timm, D. H. *Design, Construction, and Instrumentation of the 2006 Test Track Structural Study*. NCAT Report 09-01. National Center for Asphalt Technology at Auburn University, Auburn, Ala., 2009.
2. Willis, J. R. and D. H. Timm. *Field-Based Strain Thresholds for Flexible Perpetual Pavement Design*. NCAT Report 09-09. National Center for Asphalt Technology at Auburn University, Auburn, Ala., 2009.
3. West, R., D. Timm, R. Willis, B. Powell, N. Tran, D. Watson, M. Sakhaeifar, R. Brown, M. Robbins, A. Vargas-Nordbeck, F. Leiva-Villacorta, X. Guo, and J. Nelson. *Phase IV NCAT Test Track Findings*. NCAT Report 12-10. National Center for Asphalt Technology at Auburn University, Auburn, Ala., 2012.

4. Timm, D. H., M. M. Robbins, J. R. Willis and A. J. Taylor. *Field and Laboratory Study of High-Polymer Mixtures at the NCAT Test Track: Final Report*. NCAT Report 13-03. National Center for Asphalt Technology at Auburn University, Auburn, Ala., 2013.
5. Vargas-Nordcbeck, A. and D. Timm. *Physical and Structural Characterization of Sustainable Asphalt Pavement Sections at the NCAT Test Track*. NCAT Report 13-02, National Center for Asphalt Technology at Auburn University, Auburn, Ala., 2013.

## 2.1. 2009 Group Experiment

### *Background and Objective*

In 2009, the following six structural test sections were built as part of the Group Experiment (GE) to compare the structural pavement responses and field performance under heavy trafficking. The mixtures used in these test sections were also evaluated using several performance-related laboratory tests.

- OGFC Surface (S8)
- Virgin Control (S9)
- WMA-Foam (S10)
- WMA-Additive (S11)
- 50% RAP HMA (N10)
- 50% RAP WMA (N11)

The GE cross-sections are illustrated in Figure 1. Each section was targeted to have a total asphalt cross-section of 7 inches and was comprised of a 1.25-inch surface, a 2.75-inch intermediate layer, and a 3-inch asphalt base layer. These test sections were built on a graded aggregate base commonly used at the track and a stiff subgrade (approximately 30 ksi). The experiment was sponsored by the Alabama, North Carolina, South Carolina, and Tennessee Departments of Transportation.

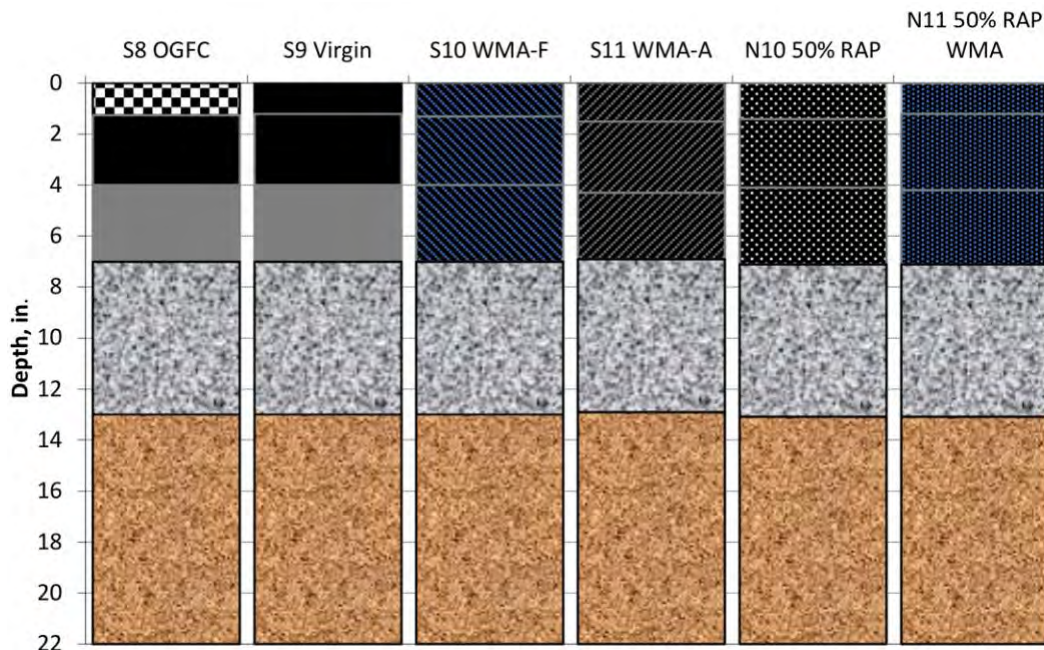


**Figure 1 2009 Group Experiment Sections**

While these test sections were targeted to have the same thicknesses, the asphalt mixtures used in these sections were different as briefly described below.

- The GE control test section in S9 was built with virgin hot-mix asphalt and provided the benchmark for comparison with the other sections.

- Section S8 was built with an open-graded friction course as the surface layer rather than the dense-graded Superpave mix used in the control section. The lower layers of S8 were identical to S9.
- Sections S10 and S11 were built with two WMA technologies: Astec’s Double Barrel Green water injection asphalt-foaming system and MeadWestvaco’s Evotherm DAT chemical additive, identified as WMA-F and WMA-A, respectively. These two WMA technologies were selected by the GE sponsors as they were the most popular WMA technologies at the time. Unlike most WMA experimental sections built around the country over the past 10 years, the WMA sections in the GE used the warm-mix technology in every lift of the asphalt pavement.
- Sections N10 and N11 were built with 50% RAP in the each of the three layers of the asphalt cross-section. The only difference between these two sections was that N10 was built at normal hot mix temperatures, whereas the mixes in N11 were produced at approximately 50°F lower temperatures using the Astec Double Barrel Green WMA asphalt foaming system. Both sections used a PG 67-22 as the virgin binder in all layers.

*Mix Design and As-Built Properties*

Mix design information is shown in Table 1. The OGFC surface in Section 8 was designed using the recommendations from NCAT Report 00-01. The other mixtures were designed by NCAT in accordance with the Superpave mix design procedure AASHTO R35 and criteria M323 using 80 gyrations in a Superpave Gyratory Compactor. The surface mixtures were fine-graded 9.5 mm nominal maximum-aggregate size (NMAS) gradations; the intermediate and base mixtures were all fine-graded 19.0 mm NMAS gradations. The mixes used in the Control section (S9) and WMA-Foam (S10) and WMA-Additive (S11) sections contained all virgin materials. The “drop-in approach” was used for the mix designs using a WMA technology—that is, the existing HMA mix design was used for setting the optimum asphalt content for the corresponding WMA mixes.

**Table 1 Mix Design Information**

Layer	Surface		Intermediate		Base		
	12.5 mm	9.5 mm	19.0 mm		19.0 mm		
NMAS							
	S8	S9, S10, S11	N10 & N11	S8, S9, S10, S11	N10, N11	S8, S9, S10, S11	N10, N11
Virgin Binder	PG 76-22	PG 76-22	PG 67-22	PG 76-22	PG 67-22	PG 67-22	PG 67-22
Total Binder %	5.5%	5.8%	6.2%	4.7%	4.8%	4.6%	4.8%
RAP Binder Ratio			0.37		0.50		0.50
No. 78 LaGrange granite	85%						
No.78 Opelika limestone		30%		30%	15%	30%	15%
No.57 Opelika limestone		18%		18%	15%	18%	15%
M10 Columbus granite		25%		25%		25%	
No.89 Columbus granite			24%	27%		27%	
Shorter Sand		27%	20%		20%		20%
Fine RAP			15%		20%		20%
Coarse RAP	15%		35%		30%		30%

As-built quality control results for the test sections are shown in Table 2. Gradations, asphalt contents, and volumetric properties were reasonably consistent among the GE mixes. These

results show that tight control standards were achieved to assure valid comparisons among the mixtures.

**Table 2 Quality Control Results for the GE Mixes**

Sieve	Surface						Intermediate					Base				
	S8	S9	S10	S11	N10	N11	S9	S10	S11	N10	N11	S9	S10	S11	N10	N11
	OGFC	Control	WMA-F	WMA-A	50% RAP HMA	50% RAP WMA	Control	WMA-F	WMA-A	50% RAP HMA	50% RAP WMA	Control	WMA-F	WMA-A	50% RAP HMA	50% RAP WMA
25.0mm	100	100	100	100	100	100	99	99	98	98	99	99	99	99	99	97
19.0 mm	100	100	100	100	100	100	92	96	94	93	93	95	94	95	95	89
12.5 mm	97	100	100	100	100	99	84	89	87	86	86	87	85	87	89	83
9.5 mm	71	100	100	100	95	95	76	80	80	79	79	77	76	80	82	75
4.75 mm	21	81	81	83	67	69	57	60	60	56	58	56	57	61	58	54
2.36 mm	11	59	60	61	48	51	47	48	48	46	47	46	47	50	47	44
1.18 mm	9	46	47	47	39	41	38	39	38	37	39	37	38	40	39	37
0.60 mm	7	31	32	31	27	27	26	27	25	26	27	26	21	28	27	25
0.30 mm	6	16	17	16	12	12	15	14	13	13	14	15	12	16	14	13
0.15 mm	4	9	10	9	7	7	9	9	8	8	8	9	9	9	9	8
0.075 mm	3.1	6.0	6.7	6.1	4.7	4.8	5.3	5.3	4.9	5.6	5.7	5.1	5.7	5.3	5.8	5.3
AC (%)	5.1	6.1	6.1	6.4	6.0	6.1	4.4	4.7	4.6	4.4	4.7	4.7	4.7	5.0	4.7	4.6
Pbe (%)		5.4	5.5	5.7	5.2	5.3	3.9	4.1	4.0	3.8	4.1	4.2	4.1	4.5	4.1	4.0
Lab Va (%)		4.0	3.3	3.4	3.8	3.2	4.4	4.3	4.9	4.5	3.7	4.0	4.1	3.0	4.2	4.1
VMA (%)		16.5	16.0	16.7	15.8	15.5	13.5	14.3	14.5	13.6	13.6	13.9	14.0	13.7	13.8	13.7
VFA (%)		76	80	80	76	79	68	68	66	67	72	71	71	78	70	70
P200/Pbe		1.1	1.2	1.1	0.9	0.9	1.4	1.3	1.2	1.5	1.4	1.2	1.2	1.2	1.4	1.3
Plant Discharge Temp. (°F)	335	335	275	250	325	275	335	275	250	325	275	325	275	250	325	275
In-Place Density (% of Gmm)	75.0	93.1	92.3	93.7	92.6	92.1	92.8	92.9	92.9	92.9	93.1	92.6	92.3	93.9	95.0	94.2

Except for the OGFC in Section S8, the average in-place density results for the test sections were similar and above the acceptable limit of 92.0%.

The asphalt binders from the plant-produced GE mixtures were extracted, recovered, and graded following AASHTO T 164, ASTM D5404, and AASHTO R 29, respectively. The solvent used in this testing was reagent-grade trichloroethylene. Results are shown in Table 3. It can be seen that critical high temperatures for the binders recovered from WMA-F surface and intermediate mixtures were similar to those of the respective control section layers despite being produced at 50-60°F lower temperatures. The true grades for the WMA-A mixtures were generally one to two degrees lower than the respective control section mixtures at the high and low critical temperatures. The slightly lower recovered true grades for the WMA binders was due to a little less aging of the binder resulting from lower plant mixing temperatures.

**Table 3 PG Grade of Binders Recovered from Control, WMA, and 50% RAP Mixes**

Layer	Section	True Grade	PG
Surface	Control	81.7-24.7	76-22
	WMA-F	82.0-25.7	82-22
	WMA-A	80.3-25.7	76-22
	50% RAP HMA	87.8-15.4	82-10
	50% RAP WMA	83.8-17.7	82-16
Intermediate	Control	85.1-25.1	82-22
	WMA-F	86.6-23.9	82-22
	WMA-A	82.5-25.1	82-22
Base	Control	77.1-24.1	76-22
	WMA-F	75.6-25.1	70-22
	WMA-A	73.7-25.4	70-22
	50% RAP HMA	95.0-12.8	88-10
	50% RAP WMA	88.7-14.1	88-10

Note: Binders for the 50% RAP intermediate layers were not recovered and tested. They were the same mix used in the corresponding base layers.

### *Structural Analysis*

The structural analysis presented in this section is the same as reported at the end of the 2009 Test Track cycle (1). It is reproduced here with minor editing for consistency with the organization of this report.

**Backcalculation of Pavement Layer Moduli.** Falling weight deflectometer (FWD) testing was performed to quantify the seasonal behavior of the pavement structure. The data presented in this report correspond to the measurements taken in the outside wheelpath with the 9 kip load. The pavement layer moduli were backcalculated from deflection data using EVERCALC 5.0 for a three-layer cross-section (asphalt concrete, aggregate base, and subgrade soil). Since the same aggregate base and subgrade were used throughout the test track, this study focuses only on the asphalt concrete layer moduli. Data were filtered to eliminate results with root-mean-square error (RMSE) exceeding 3%.

**Stress and Strain Data Collection Under Traffic.** Horizontal strains were measured at the bottom of the AC layer in the longitudinal and transverse directions, while vertical pressures were

measured at the top of the granular base and at the top of the subgrade. This analysis focused only on longitudinal tensile strain and vertical subgrade pressure. Longitudinal strain was selected since previous studies at the test track had shown that longitudinal strains were about 36% higher than transverse strain measurements (2, 3). Vertical subgrade pressure was used since classic pavement design procedures are based on limiting the vertical response at the top of the subgrade to prevent rutting (4). Data were subdivided by axle type (i.e., steer, single and tandem). Only the single-axle data are presented in this study because they represent the majority of axle passes on each section. Additionally, the values shown correspond to the “best hit” on each section for each test date, which was defined as the 95<sup>th</sup> percentile of the readings obtained on a given test date.

**OGFC Structural Contribution.** Two key adjustments to the raw deflection data were needed to properly use the AASHTO 1993 approach to find the structural number. First, the deflection data were normalized to the standard loading of 9,000 lb. For each set of deflection data at a given location on a given date, a best fit linear regression equation was determined for the center (D1) and outer (D9) deflection measurements. The best-fit equation was then used to compute deflection at exactly 9,000 lb. The second deflection data adjustment was to account for varying temperatures across the numerous test dates included in this investigation. The AASHTO method requires deflections corrected to 68°F (5). The previous correction provided deflections at 9,000 lb. but varied as a function of temperature. The 1993 AASHTO Guide provides generic correction factors for temperature, but it was decided to develop section- and location-specific corrections using measured deflection versus temperature. Further details regarding load and temperature normalization have been documented elsewhere (6).

After all the data was normalized for load (9,000 lb) and temperature (68°F), the AASHTO 1993 equations were utilized to determine the effective structural number,  $SN_{eff}$ . The equations first used the outermost deflection to determine soil modulus ( $M_r$ ). The soil modulus is then used to determine composite pavement modulus ( $E_p$ ) from which  $SN_{eff}$  is calculated. A total of 358 effective structural numbers were computed for S8 while 619 were computed for S9. The difference in number of observations stems from more frequent testing on S9 as noted above. The average and standard deviations of  $SN_{eff}$  are summarized in Figure 2. S9 was more variable than S8, though both were deemed within acceptable limits of natural construction and performance variation, with coefficients of variation less than 20%. Two-tailed statistical  $t$ -tests ( $\alpha=0.05$ ) assuming unequal variance indicated statistical differences in mean values between S8 and S9 ( $p$ -value<0.0000). Therefore, the average difference of 0.45 between sections can be viewed as statistically significant.

Figure 2 also shows the computation of the OGFC structural coefficient ( $a_{OGFC}$ ). The computation assumed that everything beneath the surface lifts was the same so that the structural contributions canceled out between the two sections. Therefore, attributing the entire difference ( $\Delta SN=0.45$ ) in  $SN_{eff}$  to the OGFC using the current structural coefficient ( $a_{control}=0.54$ ) for dense-graded mixtures in Alabama (7) and surveyed average depths of each surface layer ( $D_{OGFC}$  and  $D_{control\ surface}$ ) produces a computed  $a_{OGFC}$  equal to 0.15. This value is comparable to that often used for aggregate base materials.

Using 0.15 to represent the OGFC and 0.54 to represent the other asphalt materials, an equivalent thickness was determined to achieve the same total structural number. Assuming a 7-inch control section, a section with OGFC would require 6.6 inches of control material topped with 1.25 inches of OGFC to have an equivalent structural number. This assumes the pavement designer would select 1.25 inches for the depth of OGFC, which was used at the test track. Increases or decreases in selected OGFC thickness would alter the final cross section. In the context of this example, however, an OGFC section would require 7.85 inches total AC depth to equal a 7-inch cross section consisting of dense-graded mixes. This is a 12% increase in thickness, which was in the 10-20% range found through mechanistic analysis (8). Note that this total thickness is 0.4 inches thinner than what would be recommended in a state where no structural value is currently attributed to OGFC. In such a state, if the structural design called for 7 inches, there would be 7 inches of dense-graded material topped with the OGFC surface.

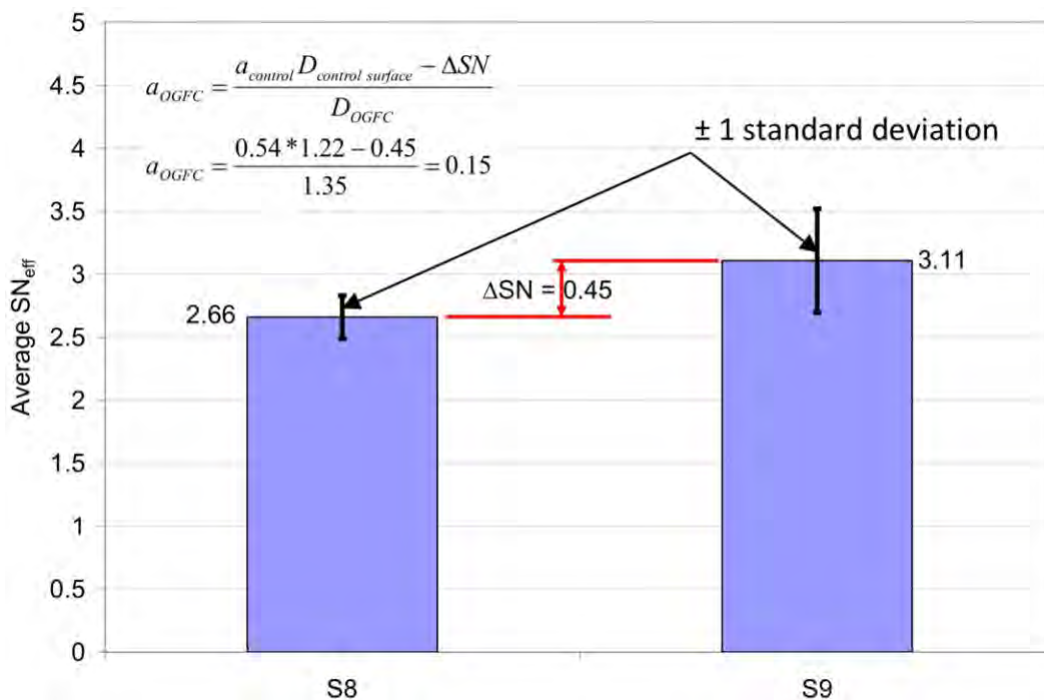


**Figure 2 Computed SNeff and Computed OGFC Structural Coefficient**

The above computations were based purely on deflection testing and empirical correlation to SNeff using the AASHTO approach. To validate the resulting structural coefficient, it was warranted to utilize embedded strain gauges in the pavement to determine an equivalent thickness of the OGFC section relative to the control section that would produce an equivalent strain between sections. This was done using strain measurements under live traffic conditions.

Tensile microstrain under single axles versus temperature is plotted in Figure 3. These data represent weekly measurements obtained from the start of traffic through April 2011. Data from both sections follow an exponential trend with reasonably high R<sup>2</sup>. It is interesting to note that the control section had lower strain up to about 95°F, at which point it crossed over and was generally higher than the OGFC section. While the reason for this behavior was not immediately

clear, it also appeared in backcalculated AC modulus from FWD testing. Figure 4 shows the backcalculated AC modulus for each section versus temperature. At cooler temperatures, S9 had higher modulus, but became softer at higher temps (above 105°F). Though this doesn't correspond directly with the temperature from the strain data, it is in a similar range. In both the strain and backcalculated data sets, the regression coefficients of the exponent were higher for the control section. This indicates a greater sensitivity to the temperature of this section. Further investigation of this behavior in the context of mechanistic-empirical pavement design is warranted. For the purposes of this investigation related to the structural coefficient, however, the main interest is in the behavior at the AASHTO reference temperature of 68°F, marked by the vertical line in both Figures 3 and 4.

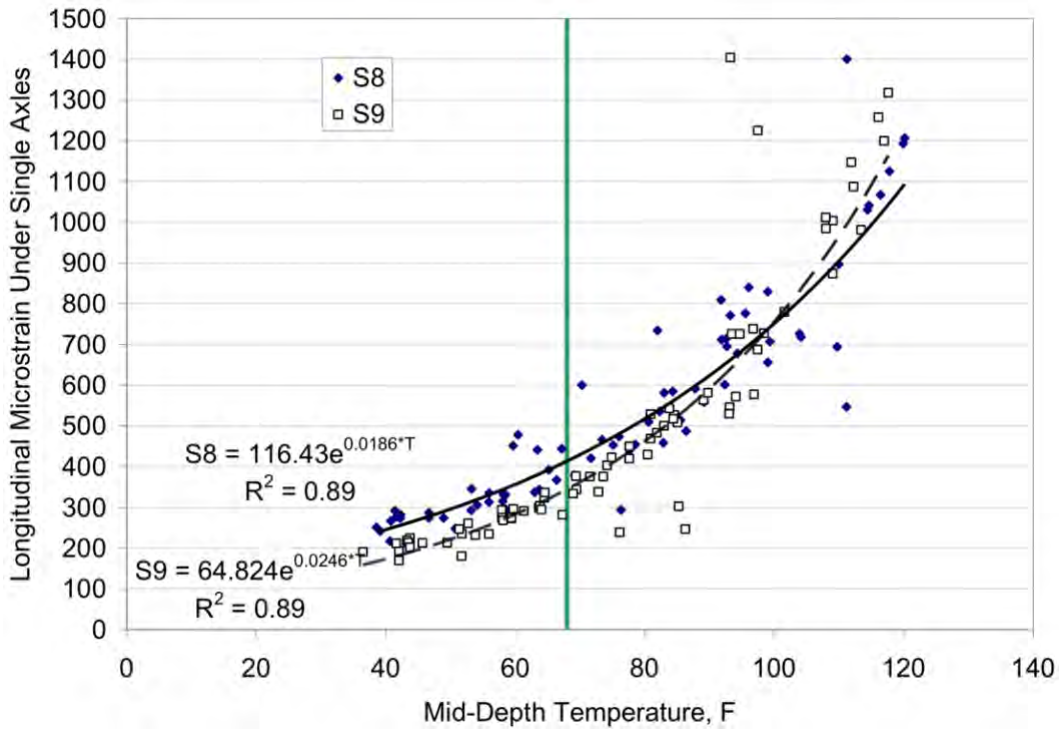


**Figure 3 Strain Response of S8 (OGFC) and S9 (Control) Sections**

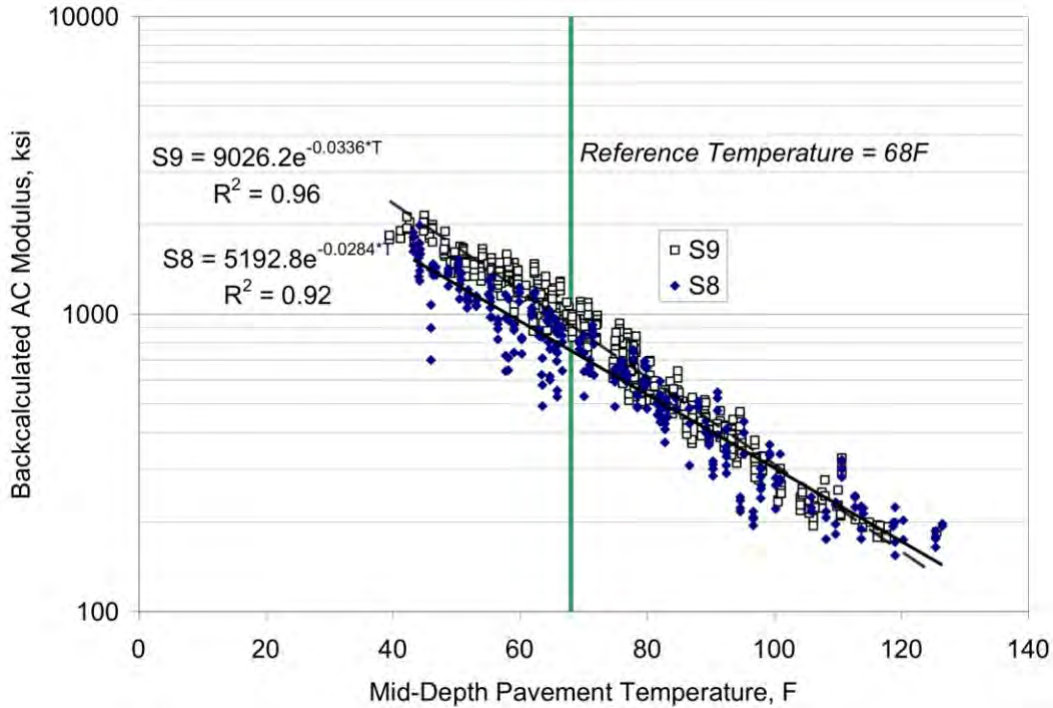


**Figure 4 Backcalculated AC Modulus of S8 (OGFC) and S9 (Control)**

Following a similar procedure as described for normalizing deflections to 68°F (6), the strain responses were also normalized to this temperature. Figure 5 summarizes the average strain and standard deviation for each section. The differences were found to be statistically significant using a two-tailed  $t$ -test ( $\alpha=0.05$ ). Given that the 80 microstrain difference was found to be statistically significant, the primary issue was determining the amount of additional thickness of OGFC required to obtain an equivalent strain. This was determined by using the approximate inverse squared relationship ( $\epsilon \approx 1/h^2$ ) between strain and thickness for a given set of materials in a cross-section (9).

Figure 6 plots the strain-thickness relationship for the OGFC section. The plot has been normalized such that 7 inches yields the field-measured strain of 413  $\mu\epsilon$ . Reducing strain at  $1/h^2$  yields a thickness of 7.8 inches to achieve 333  $\mu\epsilon$ , the field-measured strain level in the control section. Recall that using  $a_{OGFC}$  required a thickness of 7.85 inches to achieve an equivalent structural number. The strain-determined thickness was thus considered a validation of the AASHTO-derived structural coefficient.

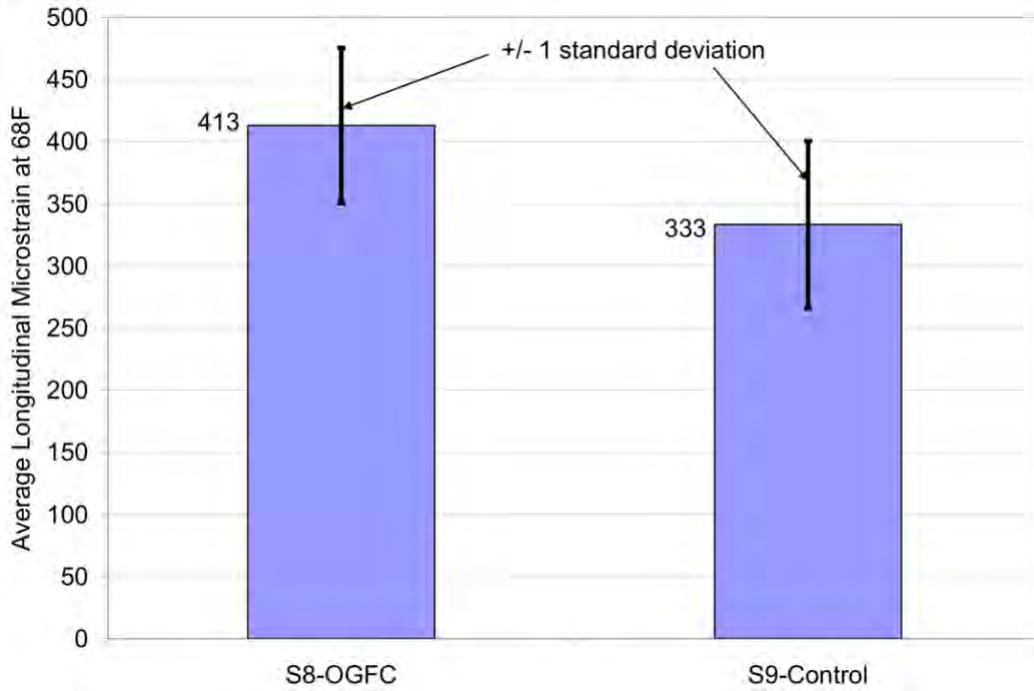


**Figure 5 Strain Response Normalized to 68°F**

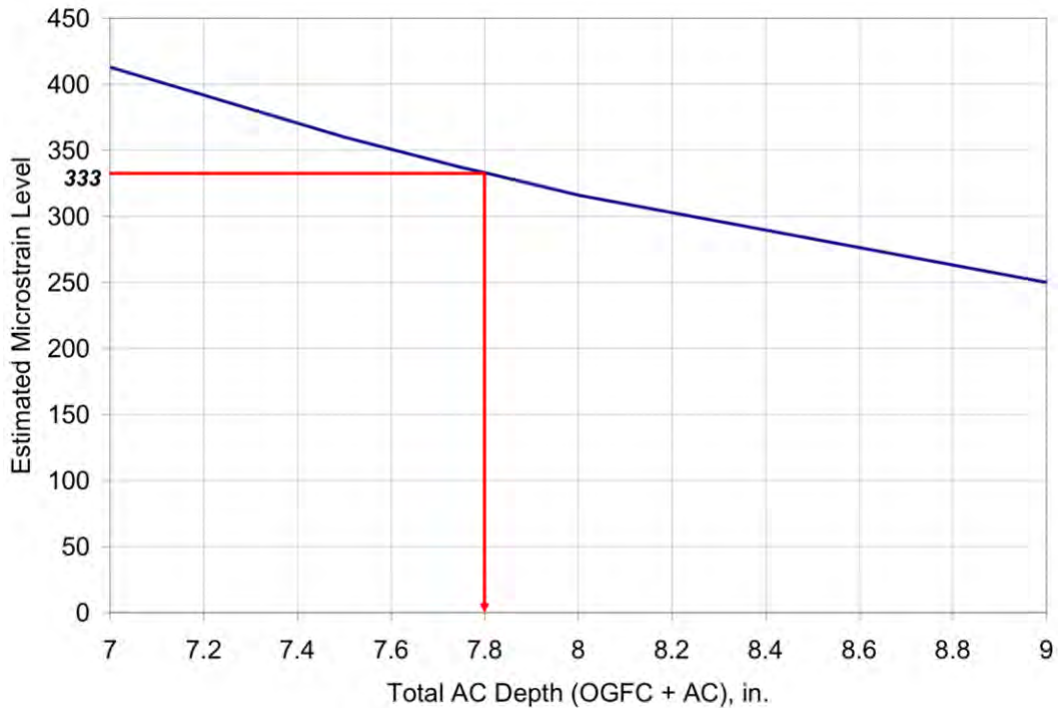


**Figure 6 Approximate Relationship Between Strain and Thickness**

**WMA and 50% RAP Structural Response.** The mid-depth pavement temperature was used to correlate the measured responses (strain and pressure) to temperature. Previous studies at the test track have shown the effectiveness of using mid-depth temperature for these correlations

(2, 10). The relationship between these parameters follows an exponential function, as shown in Equation 1.

$$response = k_1 e^{k_2 T} \tag{1}$$

where

- response* = pavement response (microstrain or subgrade pressure (psi));
- T* = mid-depth AC temperature (°F); and
- k<sub>1</sub>, k<sub>2</sub>* = section-specific regression coefficients.

Figures 7 and 8 show the longitudinal strain and vertical subgrade pressure versus mid-depth temperature for the WMA sections and the control sections. Figures 9 and 10 show the same kind of plots for the 50% RAP test sections and the control section. For the plots showing the measured stress and strain responses of the WMA sections compared to the control section it does not appear that either WMA technology appeared to be different than the Control section. However, the strain and pressure data for the 50% RAP-WMA and 50% RAP-HMA sections shown in Figures 9 and 10 appear to indicate that the high RAP content sections were less influenced by temperature presumably due to increased stiffness of the high RAP content mixes.

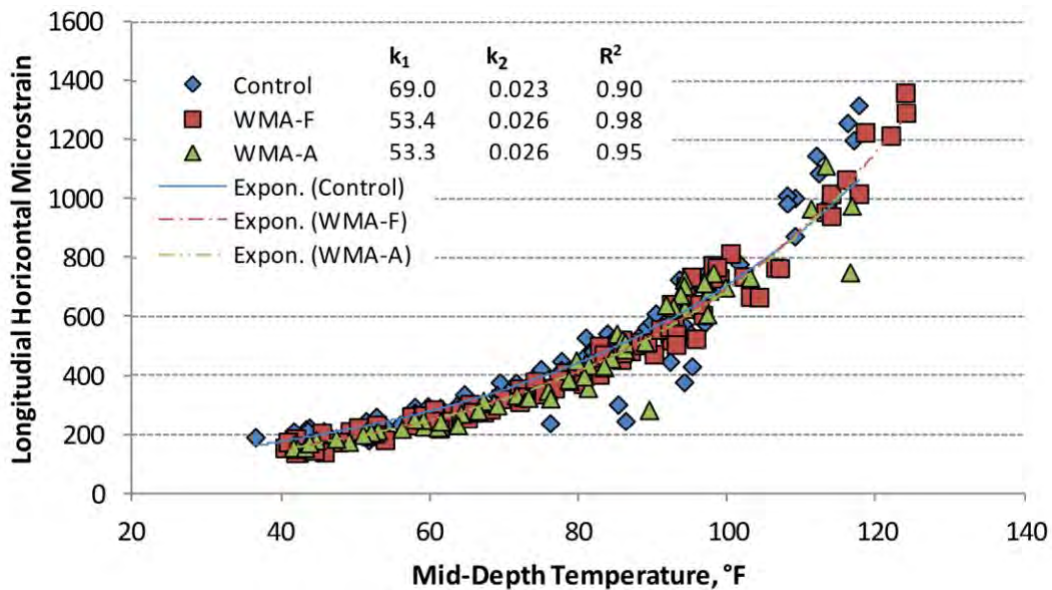


Figure 7 Longitudinal Strain Versus Temperature for WMA Sections and Control Section

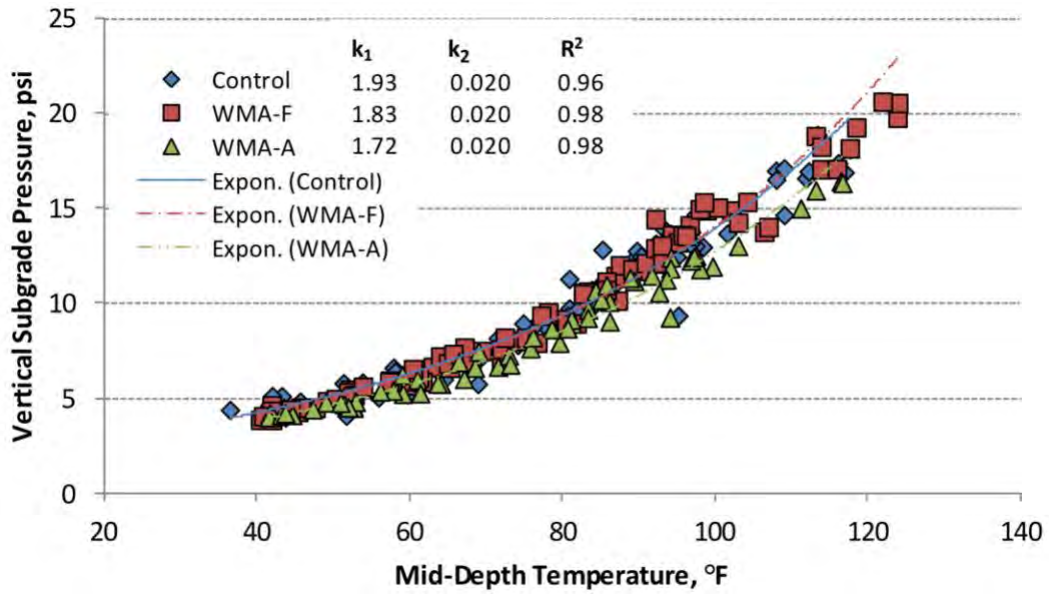


Figure 8 Subgrade Pressure Versus Temperature for WMA Sections and Control Section

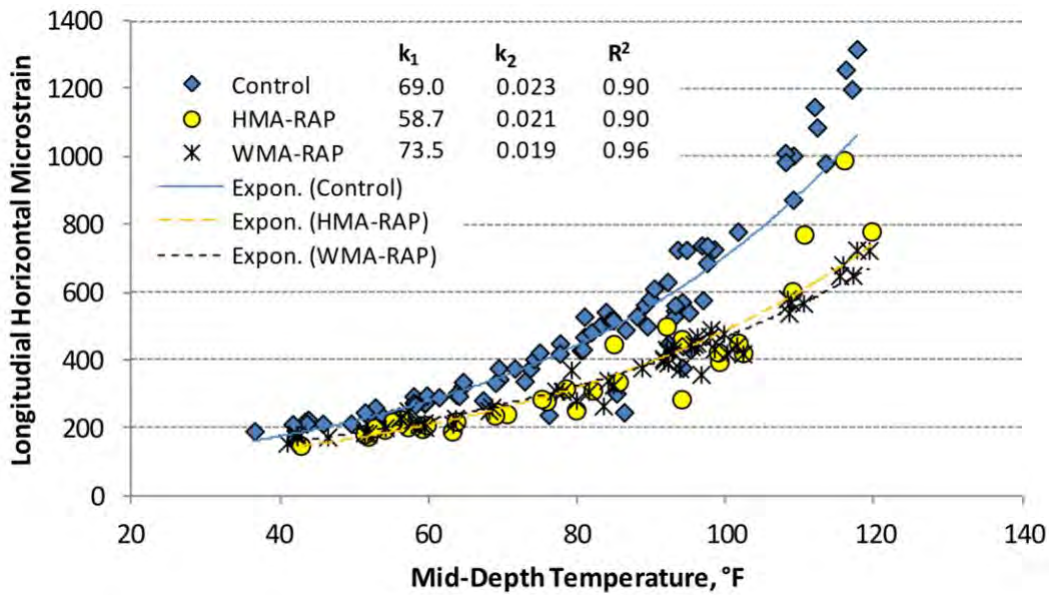
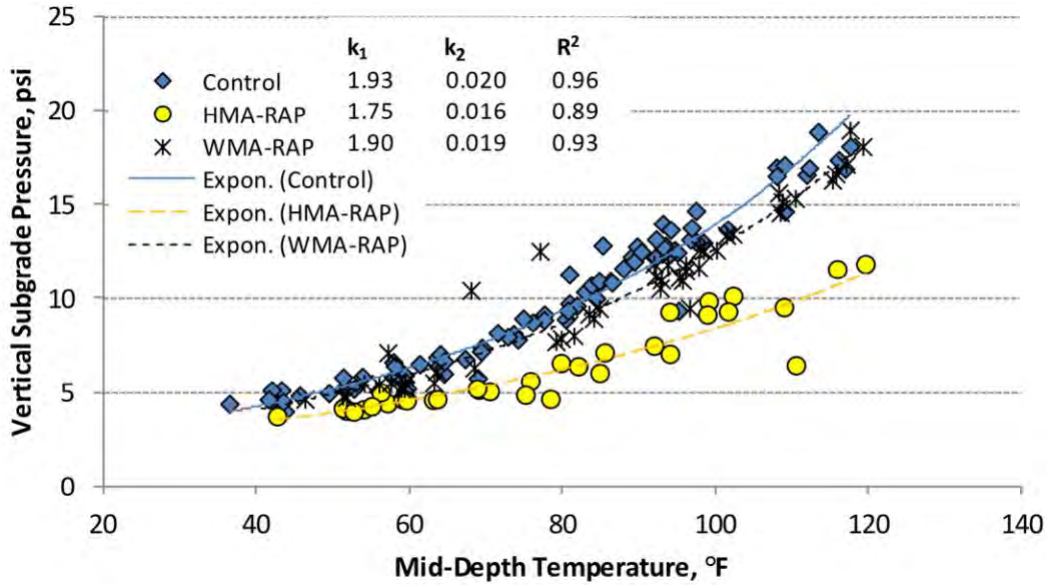


Figure 9 Longitudinal Strain Versus Temperature for 50% RAP Sections and Control Section



**Figure 10 Subgrade Pressure Versus Temperature**

To fairly compare the different test sections, it was necessary to normalize the responses to a reference temperature. Three temperatures (50, 68 and 110°F) were used to include the range of temperatures at which testing was conducted. This was accomplished by dividing Equation 1 with reference temperature ( $T_{ref}$ ) by the same equation with measured temperature ( $T_{meas}$ ) and solving for temperature-normalized response ( $response_{T_{ref}}$ ), as shown in Equation 2.

$$response_{T_{ref}} = [response_{T_{meas}}] [e^{k_2(T_{ref}-T_{meas})}] \quad (2)$$

where

$response_{T_{ref}}$  = normalized response (microstrain or subgrade pressure (psi)) at reference temperature  $T_{ref}$ ;

$response_{T_{meas}}$  = measured response (microstrain or subgrade pressure (psi)) at temperature  $T_{meas}$ ;

$T_{ref}$  = mid-depth reference temperature (°F);

$T_{meas}$  = measured mid-depth temperature at time of test (°F); and

$k_2$  = section-specific regression coefficient from Figures 8 and 9.

Because measured responses are dependent on pavement layer thickness, it was necessary to apply a correction to account for slight differences in as-built pavement thickness. The correction factors were obtained based on theoretical relationships between layer thickness and longitudinal strain or vertical pressure from layered elastic analysis. Although differences during construction were subtle, this correction allowed for a fairer comparison of the test sections.

Figures 11 and 12 illustrate the average temperature-normalized and thickness-corrected longitudinal strain and subgrade pressure, respectively. A Tukey's post-ANOVA test was performed to compare the different sections. At 95% confidence level, the results indicated that there were no statistical differences among all sections. The measured strain and pressure

responses of the high RAP sections were significantly lower than those of the control. Strains ranged from 7 to 31% lower, while pressures were between 14 and 55% lower than the control, with the largest differences observed at the highest reference temperature.

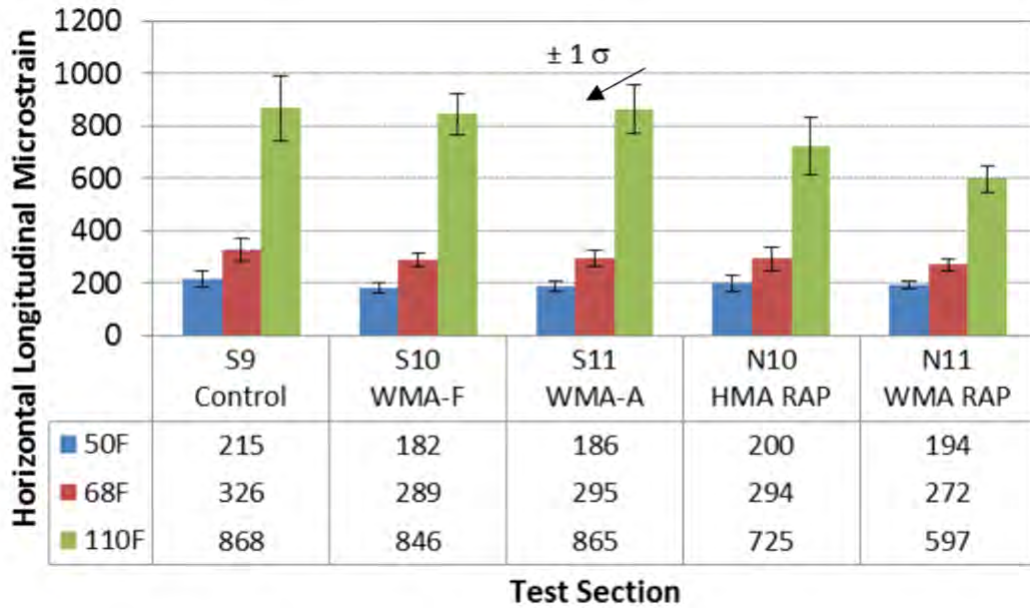


Figure 11 Average Longitudinal Strains at Reference Temperatures

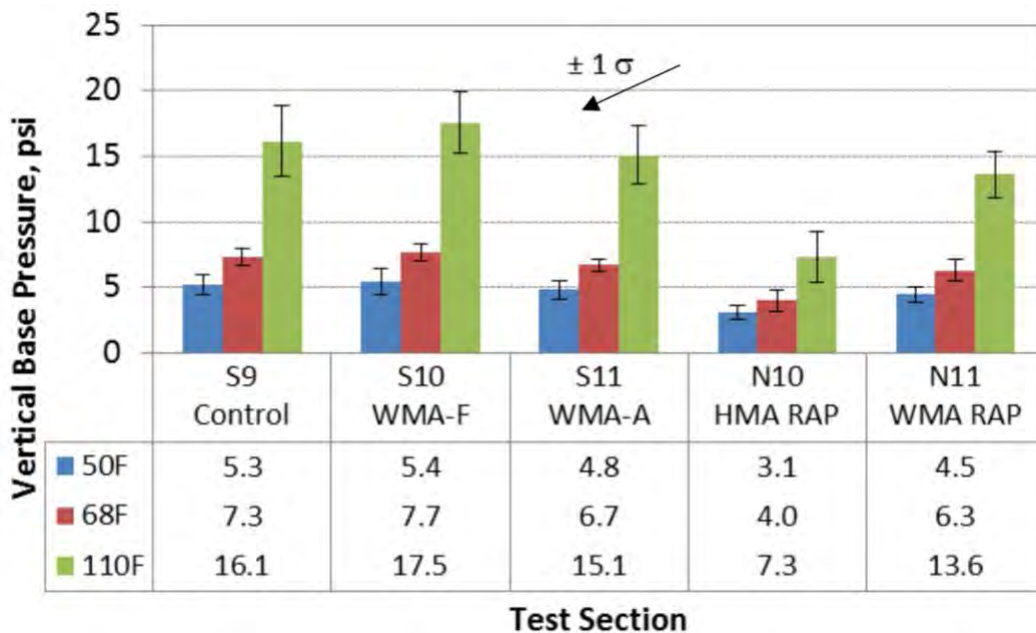


Figure 12 Average Vertical Pressures at Reference Temperatures

**Backcalculated AC Modulus.** The backcalculated AC modulus obtained from FWD testing was also dependent on pavement mid-depth temperature and followed a function similar to the one shown in Equation 1. The moduli of the WMA sections and the Control section and their

regression coefficients are shown in Figure 13. Likewise, the moduli of the 50% RAP sections and the Control section and their regression coefficients are shown in Figure 14. Hypothesis tests performed on the intercepts ( $k_1$ ) and slopes ( $k_2$ ) indicated that in general the WMA sections had lower intercepts than the control and similar slopes. This means that the WMA sections had lower moduli at all temperatures, likely due to the reduced binder-aging within these sections. The high RAP sections had similar intercepts but lower slopes than the control. This means that the high RAP sections had higher moduli at all temperatures due to the presence of stiffer aged binder and that the moduli of these sections were less susceptible to changes in temperature than the Control, a trend also observed for strain and pressure measurements.

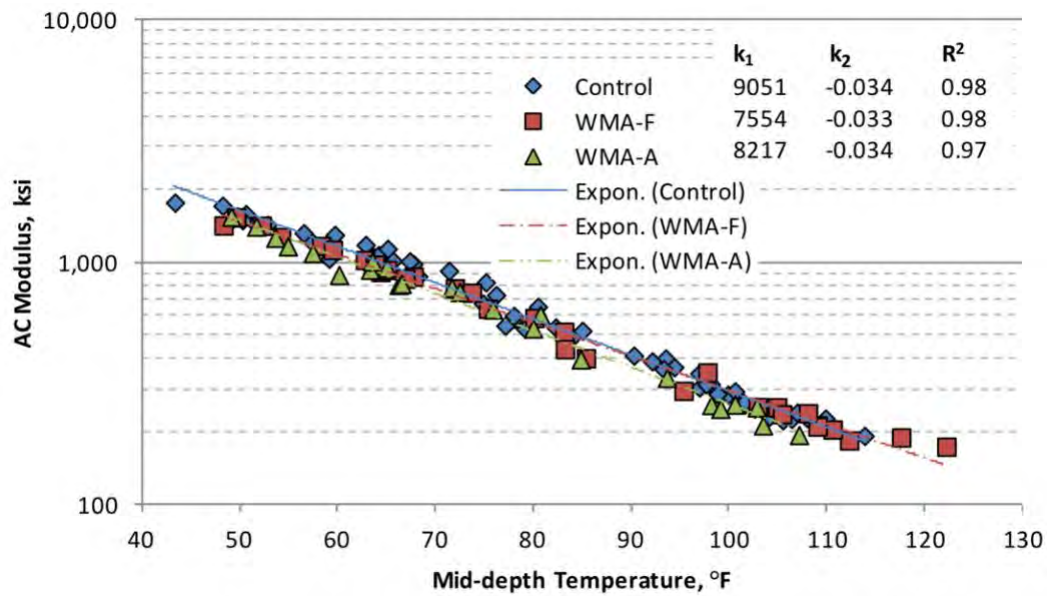


Figure 13 Backcalculated AC Modulus Versus Temperature

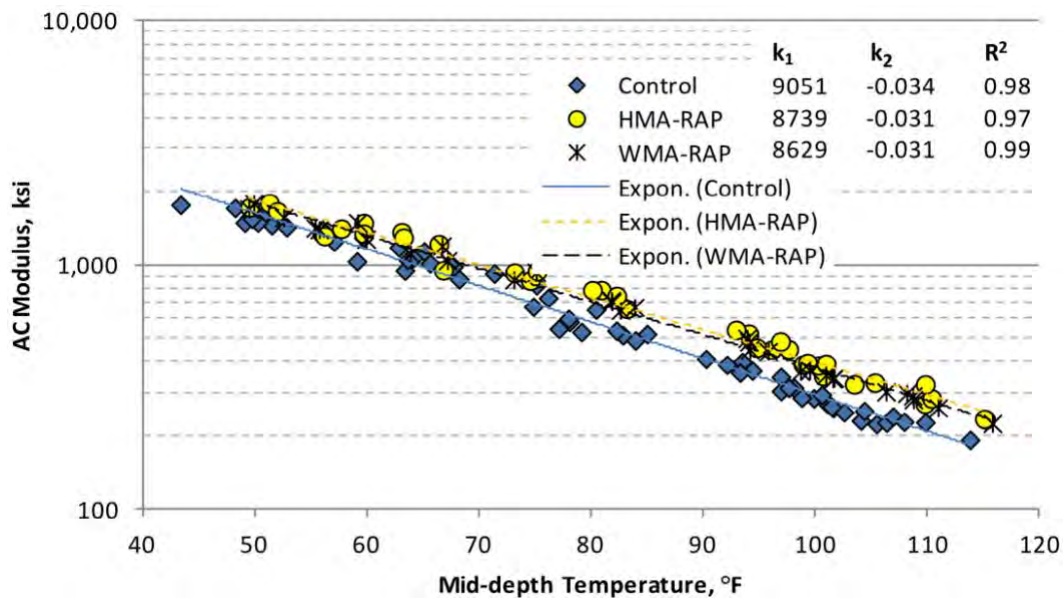
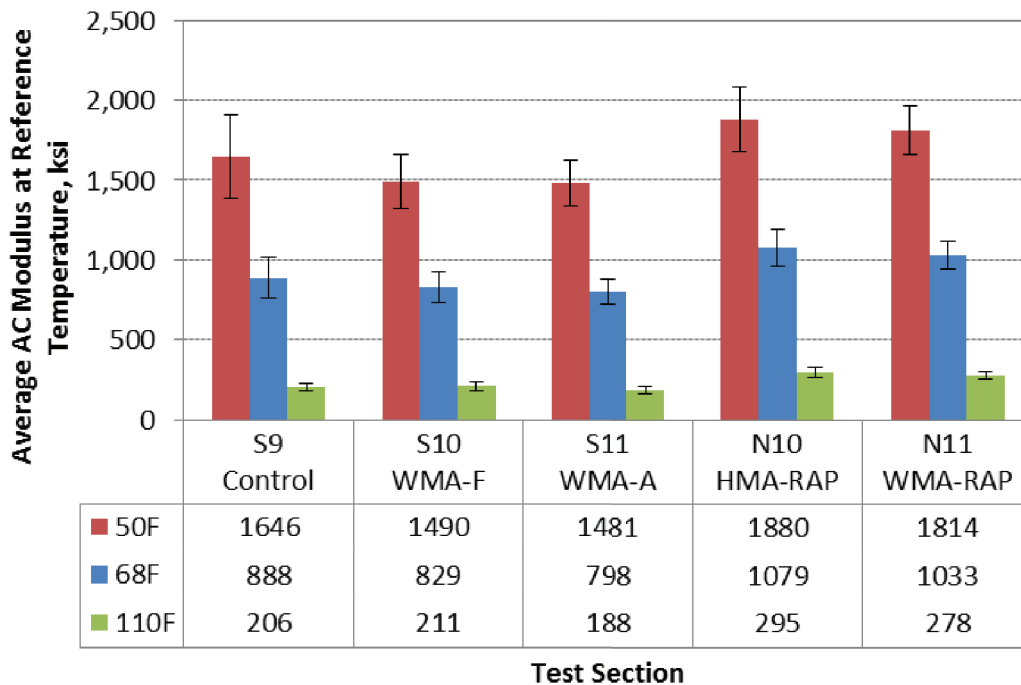


Figure 14 Backcalculated AC Modulus Versus Temperature

Figure 15 shows the average temperature-normalized moduli. Results were normalized to three reference temperatures using the same procedure applied for strain and pressure. Statistical testing indicated that there were significant differences between the WMA sections and the Control section. Overall, WMA sections had lower moduli than the control; however, these differences were only 7 to 10% lower and may not have practical significance. However, both of the 50% RAP sections had higher moduli than the Control (between 16 and 43% higher), with the largest differences observed at the higher reference temperatures.



**Figure 15 Average AC Modulus at Reference Temperature**

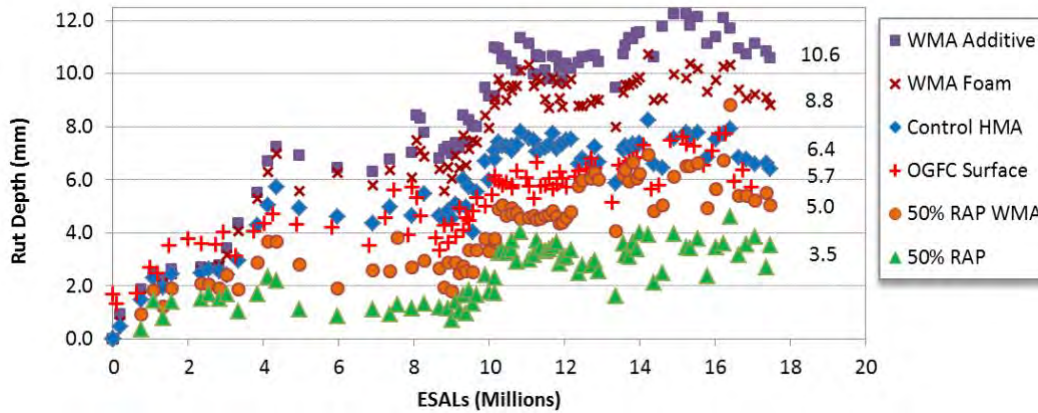
### *Test Track Field Performance*

All of the GE test sections performed better than expected based on the 1993 AASHTO Design Guide using the traditional asphalt layer coefficient of 0.44, which further supports the recommendation to increase the asphalt layer coefficient to 0.54 (7). The seven-inch test sections were expected to fail due to fatigue cracking before 10 million ESALs. An MEPDG analysis using the control mix E\* data, test traffic loading, and default transfer functions also predicted the control section would fail in rutting (0.65 in.) and fatigue cracking (40% of lane area) by 10 million ESALs.

However, after the completion of the 2009 cycle, none of the GE test sections had any cracking and rutting was generally minor. Therefore, traffic was continued on the sections into the 2012 cycle to better evaluate their relative performance and to gather data for establishing relationships between field performance and lab test results. Test Track performance of the GE sections continued through mid-April 2014 at which time they had carried over 17 million ESALs. At that point, several of the sections had reached predetermined distress thresholds and were

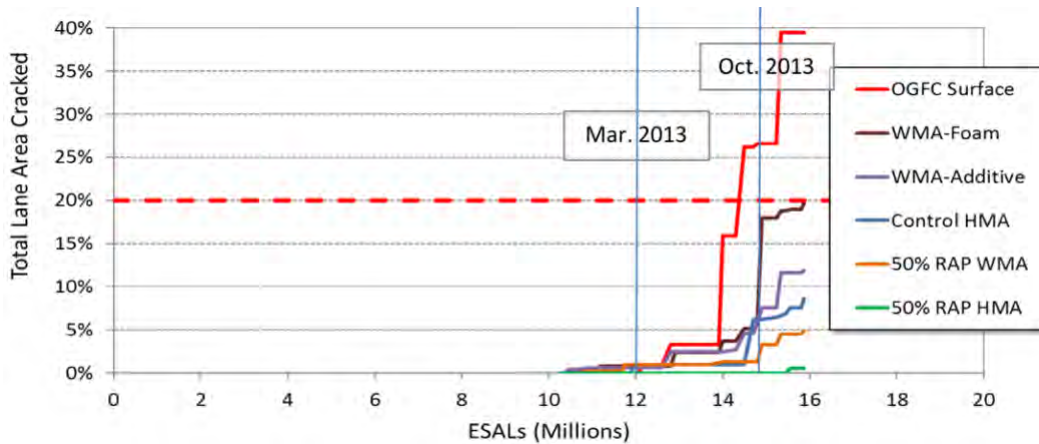
converted to the Track Pavement Preservation Experiment. However, it is important to point out that the test sections still had not “failed” at the end of the experiment.

Figure 16 shows the rutting data for the GE sections through the life of the experiment. Each of the sections performed well with regard to rutting under the heavy traffic applied on the Test Track. The WMA-A and the WMA-F sections had the highest and second highest measured rutting, respectively. The 50%RAP-HMA section had the least amount of rutting, followed by the 50%RAP-WMA section. The OGFC section performed similar to the Control section with rutting results in the middle of the range.



**Figure 16 Rutting Performance of Group Experiment Test Sections**

Cracking results for the GE sections are shown in Figure 17. It can be seen cracking began to appear on the surfaces of most sections in the early spring of 2013. Cracking increased significantly in most of the sections in the fall of 2013. During these seasons, pavements at the Test Track often experience significant temperature fluctuations. The section with the greatest amount of cracking was Section S8 with the OGFC surface. This cracking performance corroborates the analysis that the OGFC layer has a significantly lower structural value. The WMA-F section had the second most cracking, followed by the WMA-A section. This is somewhat surprising since the stress and pressure responses for both of the WMA sections were not statistically different from those of the Control section. Furthermore, the 50% RAP WMA section and the Control section had similar field performance with regard to cracking despite the sections having very different structural responses. This simply illustrates that structural responses (i.e. stresses and strains) alone are not adequate to predict cracking. It is also necessary to assess a mixture’s resistance to cracking at strain levels that will be encountered in the pavement.



**Figure 17 Cracking Performance of Group Experiment Test Sections**

Crack maps for the GE sections are shown in Figure 18 on the following page. These maps were generated from very close visual inspections of the section surfaces on December 16, 2013. These types of crack maps were the basis of the percentage of lane cracking shown in Figure 17. It can be seen that a higher percentage of the cracks in the wheelpaths were transverse or area (alligator) cracks, which are indicated on the maps as polygons. Table 4 provides a summary of the cracking at 15.9 million ESALs.

**Table 4 Summary of Cracking for GE Sections at 15.9 Million ESALs**

Test Section	Mix Type	Percent of Wheelpaths		Percent of Lane
		Longitudinal	Transverse & Area	
S9	Control	7	9	8.6
S10	WMA-F	15	21	19.7
S11	WMA-A	7	15	11.9
N10	50% RAP HMA	0.3	0.7	0.5
N11	50% RAP WMA	2	6	4.5

*Preliminary Forensic Analysis*

A series of cores were cut in each of the GE test sections in December 2013 to determine if the observed cracking was full-depth fatigue cracking, near surface (i.e. top-down) cracking, or if there were other issues in the pavement structure that contributed to the distresses. Figure 19 shows a photograph of the Control section where a transverse and a longitudinal crack were cored. Figure 20 shows those cores. It can be seen that the crack on the core from the transverse crack extended the full depth of the core, whereas the crack on the core from the longitudinal crack only extended through the surface layer. This link was confirmed with all of the cores taken in the investigation. Therefore, the research team concluded that all of the transverse cracks and cracked areas enclosed by the polygons in the crack maps were bottom-up fatigue cracks and that all longitudinal cracks were only top-down cracks. No weakly bonded or debonded cores were obtained in this preliminary forensic work.

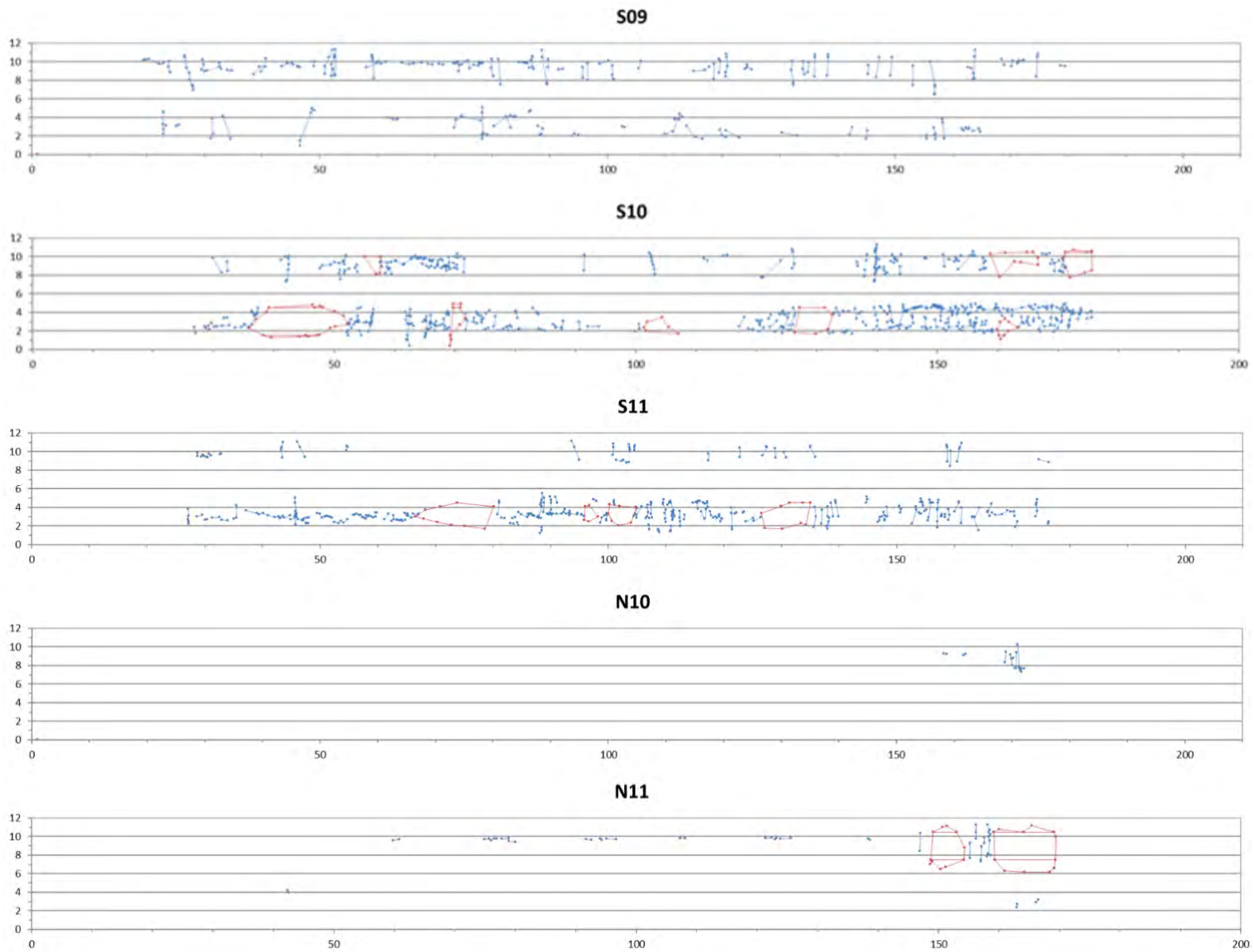


Figure 18 Crack Maps for GE Sections as of December 16, 2013



Figure 19 Photo of Typical Cracking Observed in GE Section on December 9, 2013

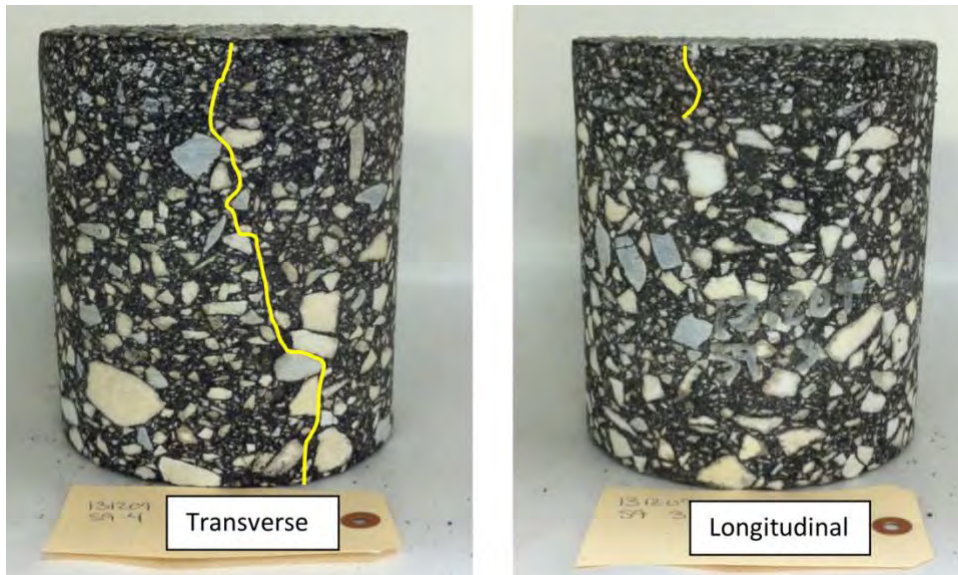


Figure 20 Cores Taken from GE Section on December 9, 2013

### *Laboratory Testing and Results*

This section focuses on the laboratory tests that characterize the resistance of the GE plant-produced mixtures to rutting and fatigue cracking (the primary distresses observed for the GE test sections) and their correlations to field performance measurements.

**Rutting.** The dense-graded mixtures used in the GE surface layers were tested for rutting susceptibility using the Asphalt Pavement Analyzer (APA) and Flow Number (FN) tests. APA tests

were conducted on laboratory-molded cylinders and tested at 64°C in accordance with AASHTO T 340-10. Flow number tests were conducted on unconfined specimens at 59.5°C in accordance with AASHTO TP 79-09. Results of the APA and FN tests are shown in Table 5. A discussion of these test results follows.

- The APA results for each of the GE surface mixes except the 50% RAP-WMA were below the maximum 5.5 mm criterion for heavy duty pavements recommended in previous test track research (West et al, 2012). The average APA rut depth for the 50% RAP-WMA surface mix was just above the criterion at 5.7 mm.
- Flow Number criteria for HMA mixes were provided in NCHRP Report 673 (11). The minimum FN criterion is 53 for mixes designed for between 3 and 10 million ESALs. The average flow number for the Control section surface mix was 164 and the average FN for the 50% RAP HMA surface mix was 73. Therefore, the two HMA mixes met the recommended FN criterion. According to NCHRP Report 691, the recommended FN criteria for WMA mix designs are considerably lower (12). For WMA mixes designed for 3 to 10 million ESALs, the minimum FN is 30. Each of the GE surface mixes that used a WMA technology met that criterion. WMA-A was close to the criterion and it had the most rutting of the test sections.
- Given the small dataset and the fact that all sections performed well, correlations between the lab results and field performance were poor.

**Table 5 Field Rut Depths and Laboratory Rutting Test Results for GE Surface Mixtures**

Test Section	Mix Type	Rut Depth (mm) at 17 million ESALs	APA Results		Flow Number Results	
			Rut Depth (mm)	COV, %	Flow Number (cycles)	COV, %
S9	Control	6.4	3.1	19.0	164	9.7
S10	WMA-F	8.8	4.3	20.9	51	37.3
S11	WMA-A	10.6	3.7	18.9	36	16.7
N10	50% RAP HMA	3.5	4.6	19.1	73	5.5
N11	50% RAP WMA	5.0	5.7	24.5	47	8.5

**Fatigue Cracking.** Fatigue-cracking resistance of the GE base asphalt layers was evaluated using three tests: the bending beam fatigue (BBF) test, the Overlay Test (OT), and the Simplified Visco-Elastic Continuum Damage (SVECD) test.

Bending beam fatigue tests were conducted in accordance with AASHTO T 321-07 at three strain levels: 200, 400, and 800 microstrain ( $\mu\epsilon$ ). The results of the beam fatigue tests for the base layer GE mixes are charted in Figure 21. This chart shows that both of the 50% RAP mixes in Sections N10 and N11 had lower BBF lives at 400 and 800  $\mu\epsilon$ , but higher BBF lives at 200  $\mu\epsilon$ . The results are also graphed in Figure 22 to show the least-squares regressions (i.e. transfer functions) between microstrain and number of cycles to failure.

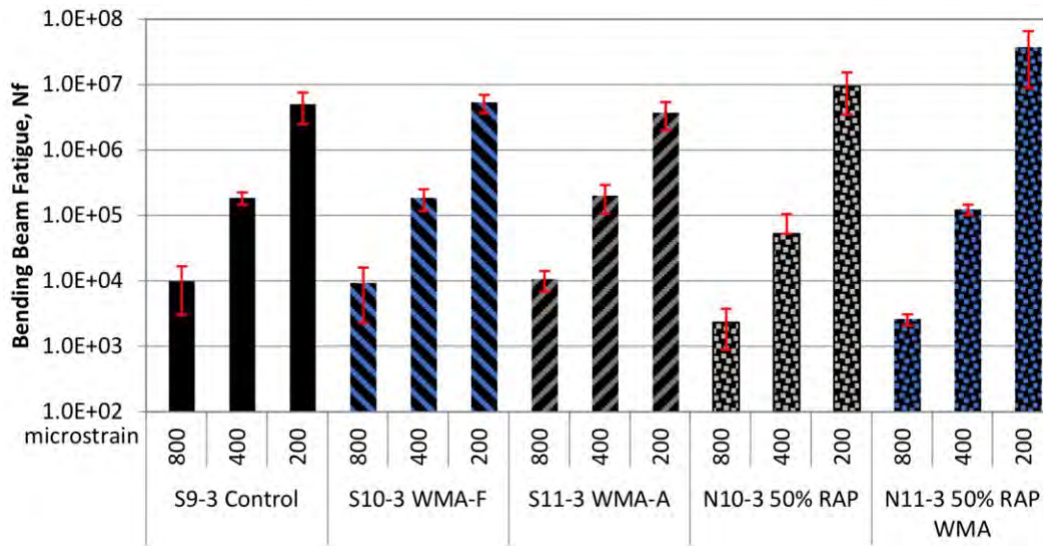


**Figure 21 Bending Beam Fatigue Results for GE Base Layer Mixes**

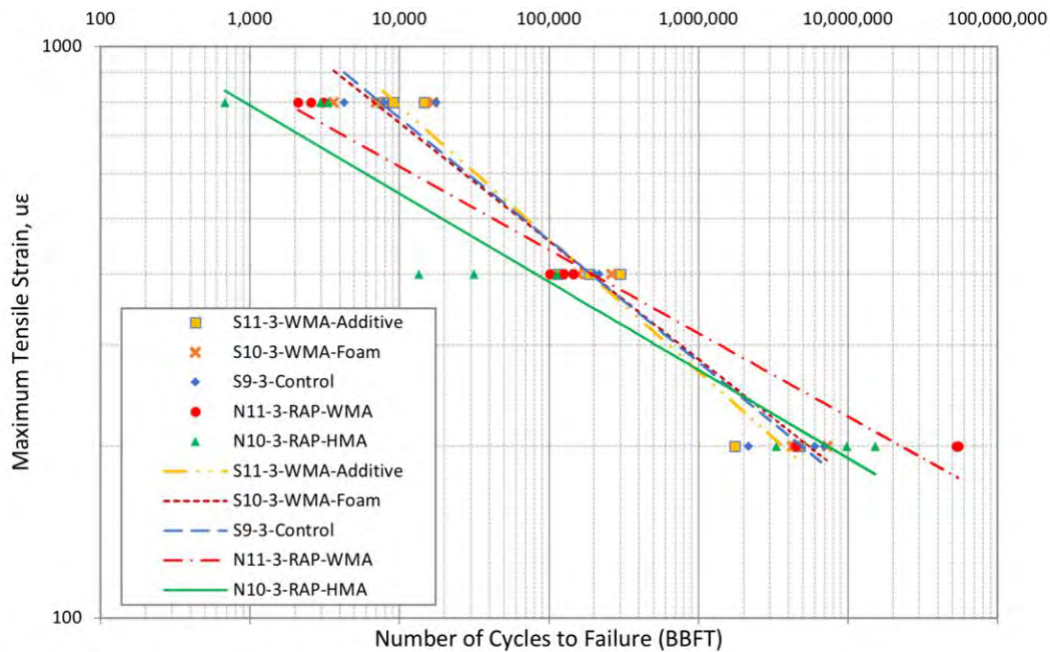


**Figure 22 Bending Beam Fatigue Results for GE Base Layer Mixes**

The least-squares regressions between BBF cycles to failure and BBF strain magnitude for each of the bottom layer mixes were used to estimate the number of cycles until failure at the field measured strain corresponding to the BBF test temperature of 68°F using Equation 3.

$$N_f = \alpha_1 \left[ \frac{1}{\epsilon_{68}} \right]^{\alpha_2} \quad (3)$$

where

$N_f$  = cycles until failure;

$\epsilon_{68}$  = estimated field strain at 68°F from Figure 7 or 9; and  
 $\alpha_1, \alpha_2$  = section-specific regression constants.

Table 6 lists the fatigue transfer function coefficients, the field strain at 68°F (from Figures 7 and 9), and the estimated BBF cycles to failure at the field strain for each bottom layer mix. The predicted BBF lives at the measured field strains corresponding to 68°F were compared to the actual field cracking measurements in Figure 23. The field cracking in this graph is only the amount of transverse and area cracking in the wheelpaths that was confirmed to be bottom-up cracking and therefore related to the fatigue resistance of the bottom asphalt layer. This plot shows the general trend of the relationship between the BBF results and field performance is correct. However, the correlation, as indicated by  $R^2$ , is weak. Although the quality of the data here is high, it also important to keep in mind that only five points were used to make the correlation.

**Table 6 Fatigue Transfer Functions and Predicted Cycles to Failure at 68°F**

Mixture	$\alpha_1$	$\alpha_2$	$R^2$	$\epsilon_{68}$	$N_f @ \epsilon_{68}$
S9 – Control	1.18E+17	4.532	0.97	330	455,349
S10 – WMA-F	7.09E+17	4.109	0.98	313	394,982
S11 – WMA-A	1.50E+16	4.192	0.97	312	524,826
N10 – HMA RAP	3.18E+20	6.022	0.93	245	1,560,870
N11 – WMA RAP	2.73E+22	6.590	0.96	268	2,717,175

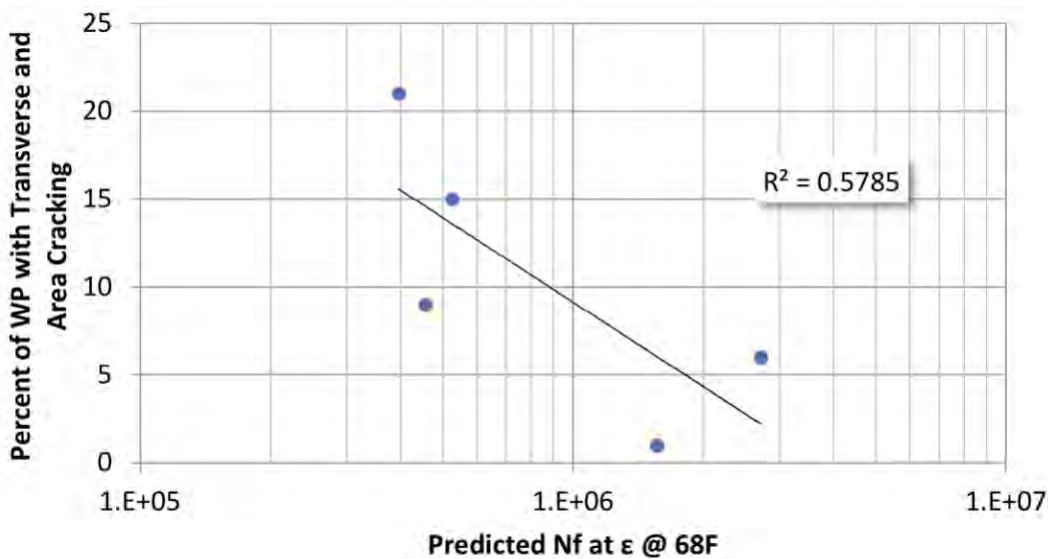


**Figure 23 Relationship between Predicted BBF  $N_f$  at  $\epsilon_{68}$  and the Percent of Wheelpath with Transverse and Area Cracking for GE**

Overlay Tests on the GE base layer mixes were conducted in an Asphalt Mix Performance Tester (AMPT) at 77°F in accordance with Tex-248 with a few important differences. The Texas standard uses a Maximum Opening Displacement (MOD) of 0.635 mm to simulate reflection cracking of an asphalt overlay on a concrete pavement. Since this study was aimed at fatigue cracking of base-layer asphalt mixtures, the Overlay Tests were conducted using three lower MOD levels

(0.381, 0.318, and 0.254 mm) to explore relationships between MOD and the number of cycles to failure. At lower MOD levels, the Overlay Test takes considerably longer to perform (especially at the MOD of 0.254 mm). Therefore, the Overlay Test was conducted at a higher frequency (i.e., 1 Hz) to reduce the testing time. The last modification to the method was a different way of determining the number of cycles to failure. The modifications to the Overlay Test procedure for characterizing fatigue cracking resistance of asphalt mixtures are described in full detail in another publication (13).

Results of the modified Overlay Test on the GE base layer mixes are charted in Figure 24. It can be seen that at each MOD level that both of the 50% RAP mixes in Section N10 and N11 had lower OT cycles to failure than the other three mixes. The virgin WMA mixes also had lower cycles to failure than the Control mix at the lowest MOD, but results were similar to the Control mix at the two higher MOD levels.

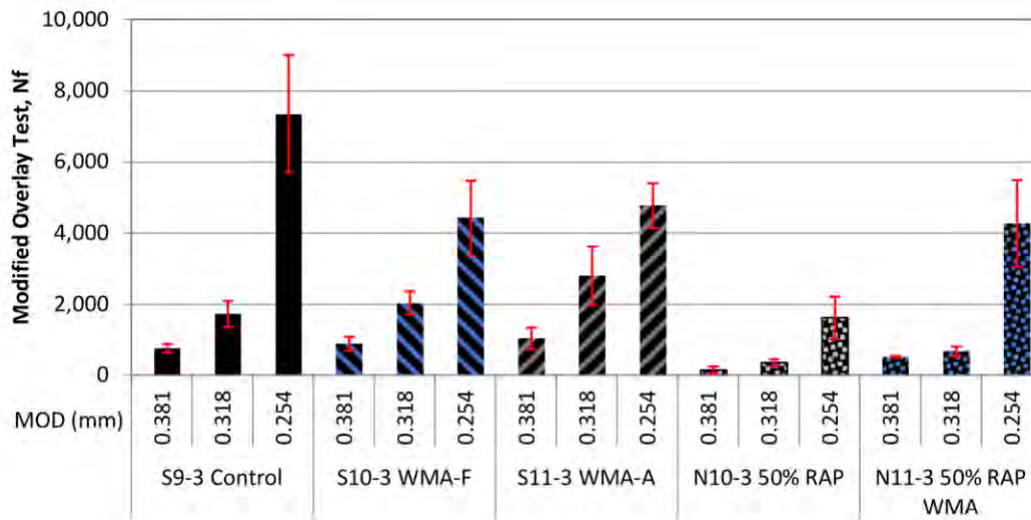


**Figure 24 Results of Modified Overlay Test on GE Base Layer Mixes**

The OT results were also plotted to establish the least-squares regressions (i.e. transfer functions) between MOD and number of cycles to failure. This plot is shown in Figure 25. As with the lab to field relationship for BBF results, the field cracking in this graph only includes the transverse and area cracking in the wheelpaths confirmed to be bottom-up cracking and therefore related to the fatigue resistance of the bottom layer. The least-squares regressions between MOD and cycles to failure for each of the GE mixes were used to estimate the number of cycles to failure at the field measured strain corresponding to the OT test temperature of 77°F using Equation 4.

$$N_f = \beta_1 \left[ \frac{1}{\epsilon_{77}} \right]^{\beta_2} \quad (4)$$

where

- $N_f$  = cycles until failure;
- $\epsilon_{77}$  = estimated field strain at 77°F from Figure 7 or 9; and
- $\beta_1, \beta_2$  = section-specific regression constants.

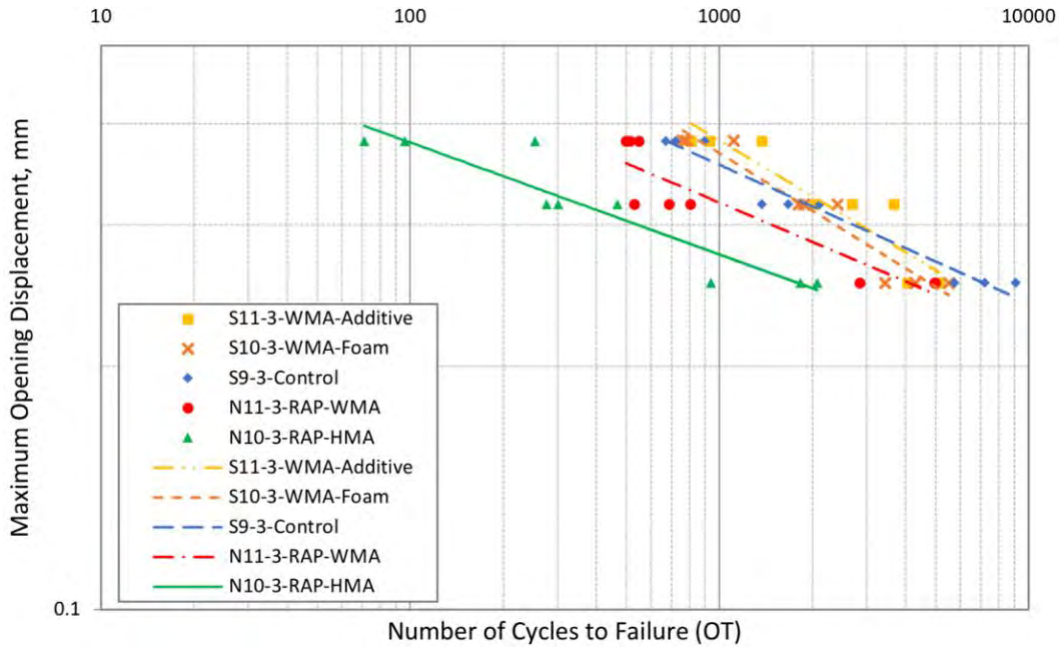


**Figure 25 OT Results at Three MOD Levels for GE Base Layer Mixes**

Table 7 lists the coefficients for each transfer function, the field strain and corresponding MOD at 77°F (from Figures 7 and 9), and the estimated OT cycles to failure at the field measured strain. At the substantially lower strain levels measured for the 50% RAP sections compared to the control and WMA sections, the predicted OT cycles to failure for the high RAP mixtures were higher than for the virgin mixtures. Those predicted OT cycles to failure at the MOD corresponding to 77°F were compared to the actual field cracking in Figure 26. As with the BBF test results, the field cracking used in this plot excludes the longitudinal cracking that was shown to be limited to the surface layer. A linear regression was also used to be consistent with the previous analysis. This plot shows a reasonably strong relationship with the predicted OT cycles to failure increasing as the percent cracking in the field decreases.

**Table 7 MOD Transfer Functions and Predicted Cycles to Failure at 77°F**

Mixture	$\beta_1$	$\beta_2$	$\epsilon_{77}$	MOD@ $\epsilon_{77}$	Predicted $N_f$ @ $\epsilon_{77}$
S9 – Control	3.158	5.601	405	0.00247	1.28E15
S10 – WMA-F	20.478	3.934	395	0.00241	4.11E11
S11 – WMA-A	29.956	3.760	395	0.00241	2.10E11
N10 – HMA RAP	0.269	6.286	296	0.00180	4.78E16
N11 – WMA RAP	2.595	5.233	317	0.00193	4.15E14

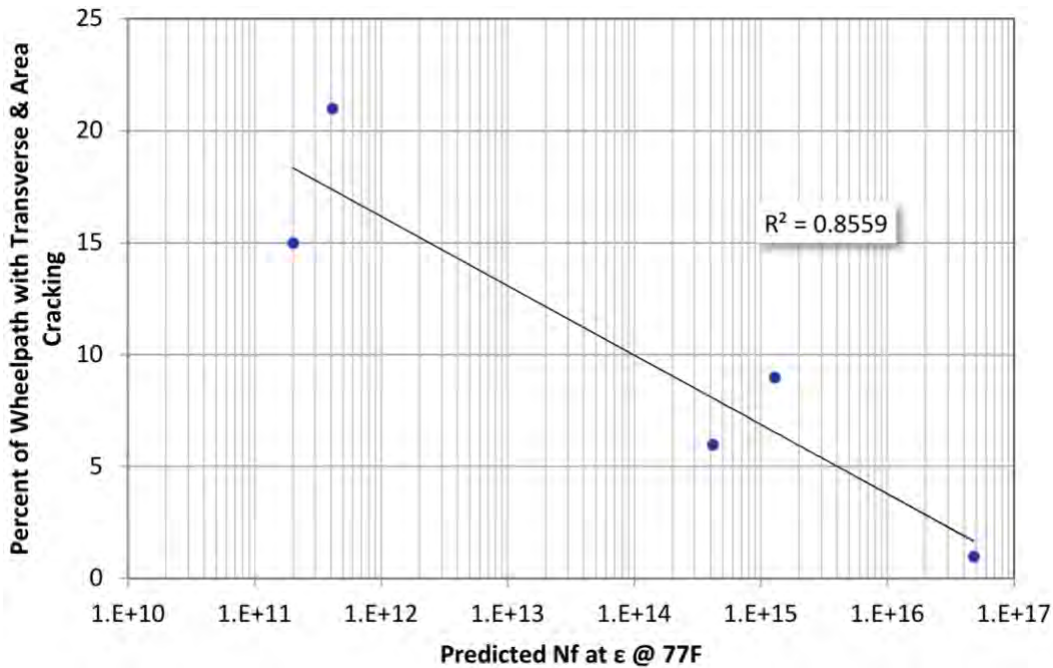


**Figure 26 Relationship Between Predicted OT  $N_f$  at  $\epsilon_{77}$  and Percent of Wheelpath with Transverse and Area Cracking for GE**

Simplified Visco-elastic Continuum Damage (SVECD) testing was completed on the GE base mixtures using an AMPT. Testing was performed using a draft procedure developed by North Carolina State University, which has recently been modified and adopted as AASHTO TP 107-14. At least four fatigue tests (two at a relatively high strain input level and two at a relatively low level) were performed at a single temperature (19°C/66°F) and at a frequency of 10 Hz. An analysis was conducted using version ALPHA-F v3.1.3 of the software developed at North Carolina State University. This analysis uses a new approach that is independent of mode of loading and temperature and is based on the energy release rate,  $G^R$ , which embodies the rate of damage accumulation during the test (14). The software outputs  $G^R$  and predicted cycles to failure for each specimen tested, allowing for the development of a relationship between the two outputs. The relationships for each of the GE mixes are plotted in Figure 27. Correspondence with Dr. Y. Richard Kim at NC State regarding recent research supports that the number of cycles to failure at  $G^R = 10$  correlates well with measured cracking in thick or thin pavements. The  $G^R$  to cycles to failure relationships in Figure 27 indicates that the 50% RAP-WMA mix has the best fatigue life throughout the range of  $G^R$ . It also interesting to note that all of the mixes have better fatigue resistance than the virgin HMA control mix when the energy release rate is above 100. Many of the relationships converge between a  $G^R$  of 50 to 70 and below this range the rankings change. At lower  $G^R$  values, the 50% RAP HMA mix had lower predicted cycles to failure compared to the other mixes. Results with this version of the software differ significantly from the results using a previous software version as reported in the previous Test Track conference report (1).

The predicted SVECD results at  $G^R=10$  were compared to the actual field cracking (wheelpath transverse and area cracking) in Figure 28. This plot shows that the correlation between the SVECD results and field performance is contrary the anticipated trend—that is, higher SVECD

cycles to failure corresponds to poorer field performance. This trend is influenced by the one data point with the predicted SVECD  $N_f$  of about 44,000 cycles. This point is for the 50% RAP HMA, which performed the best of all sections in terms of field cracking.

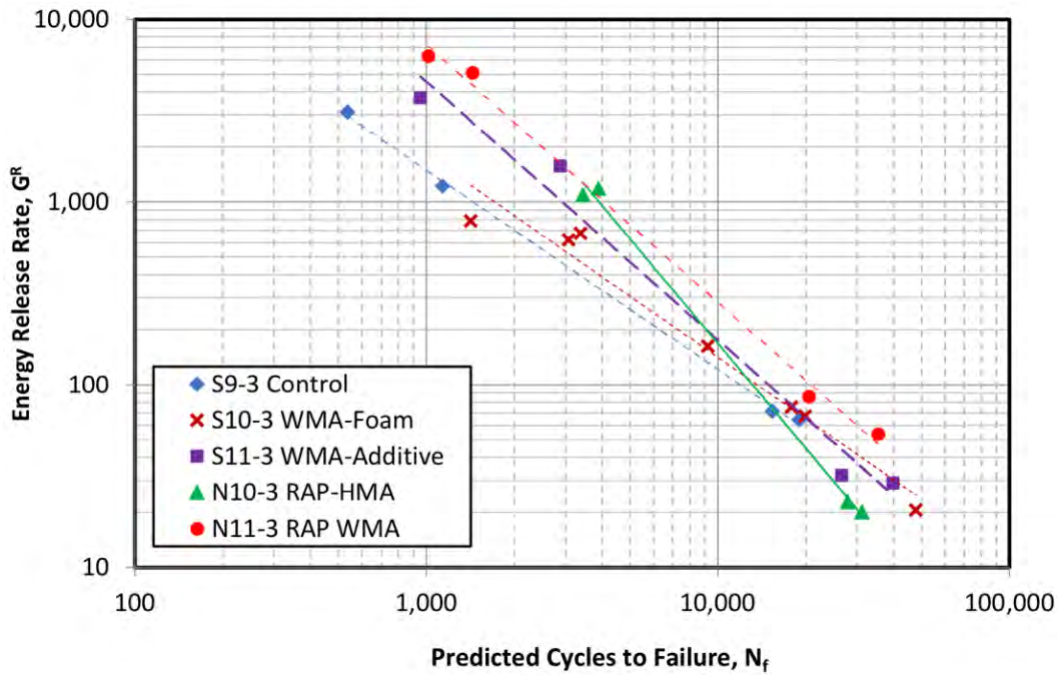


Figure 27 Predicted SVECD Cycles to Failure for GE Base Layer Mixes

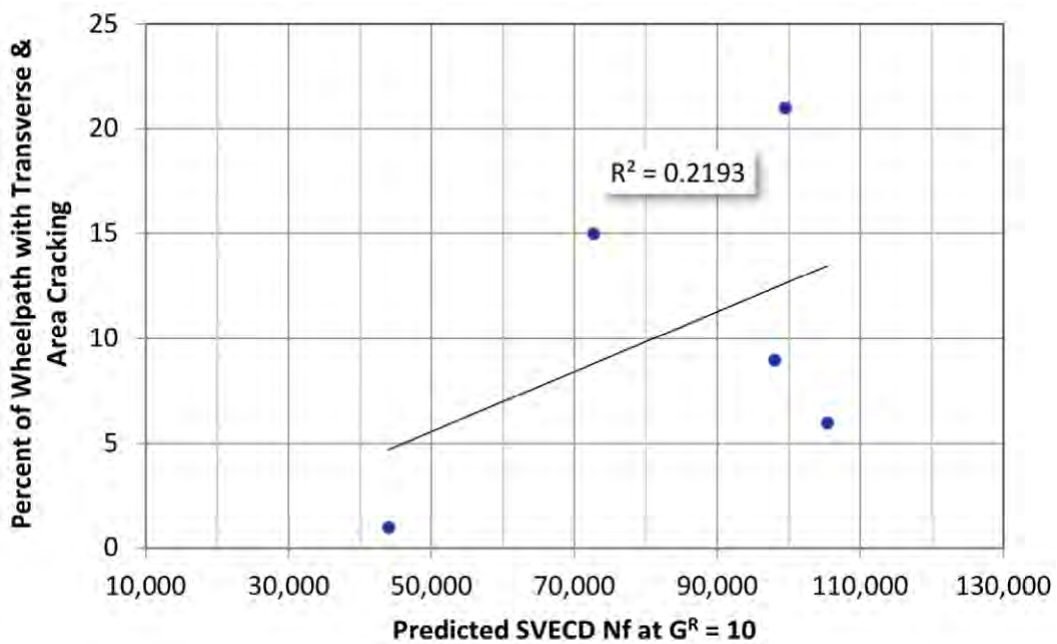


Figure 28 Relationship Between Predicted SVECD at  $G^R=10$  and Percent of Wheelpaths with Transverse and Area Cracking for GE

Discussions about these results with Dr. Richard Kim and his associates at NC State were helpful in identifying some concerns with some of the test data. In particular, the dynamic modulus ratio (DMR) for some fatigue test samples were outside of the range of 0.9 to 1.1, which they have recommended as a data quality check. The DMR is calculated from the ratio of  $E^*$  conducted on separate specimens in accordance with AASHTO TP 79-15 to  $E^*$  calculated from the cyclic tension fatigue test specimens of the same mix.

Sufficient mix was available for retesting of all GE mixes in accordance with the current SVECD procedure (AASHTO TP 107-14). For the retested samples, 16 of the 19 had DMR values within the range of 0.9 to 1.1. The three specimens that were outside of that range had borderline DMR values of 1.14, 0.88 and 0.86. These data were then analyzed with the most recent version of the ALPHA-F software, v3.1.5. Figure 29 shows the graph of  $G^R$  versus predicted cycles to failure for the retested set of samples. Table 8 provides a summary of the  $G^R$  vs  $N_f$  coefficients and predicted  $N_f$  at  $G^R = 10$  from the original and retested samples. The results were substantially different for the retested set, but the ranking of the predicted  $N_f$  at  $G^R=10$  was the same for three of the five mixes. N11-3 (50% RAP-WMA) was the best, N10-3 (50% RAP-HMA) was the worst, and S9-3 (Control) was in the middle.

**Table 8 Comparison of SVEVD Results for Original and Retested Samples**

Mix ID	Original Samples			Retested Samples		
	a coefficient	b coefficient	$N_f @ G^R = 10$	a coefficient	b coefficient	$N_f @ G^R = 10$
S9-3	807,523	-0.916	97,984	258,040	-0.624	61,332
S10-3	738,600	-0.871	99,405	135,649	-0.516	41,344
S11-3	358,935	-0.694	72,613	326,450	-0.708	63,946
N10-3	146,941	-0.524	43,969	143,286	-0.658	31,492
N11-3	535,223	-0.706	105,326	380,924	-0.737	69,797

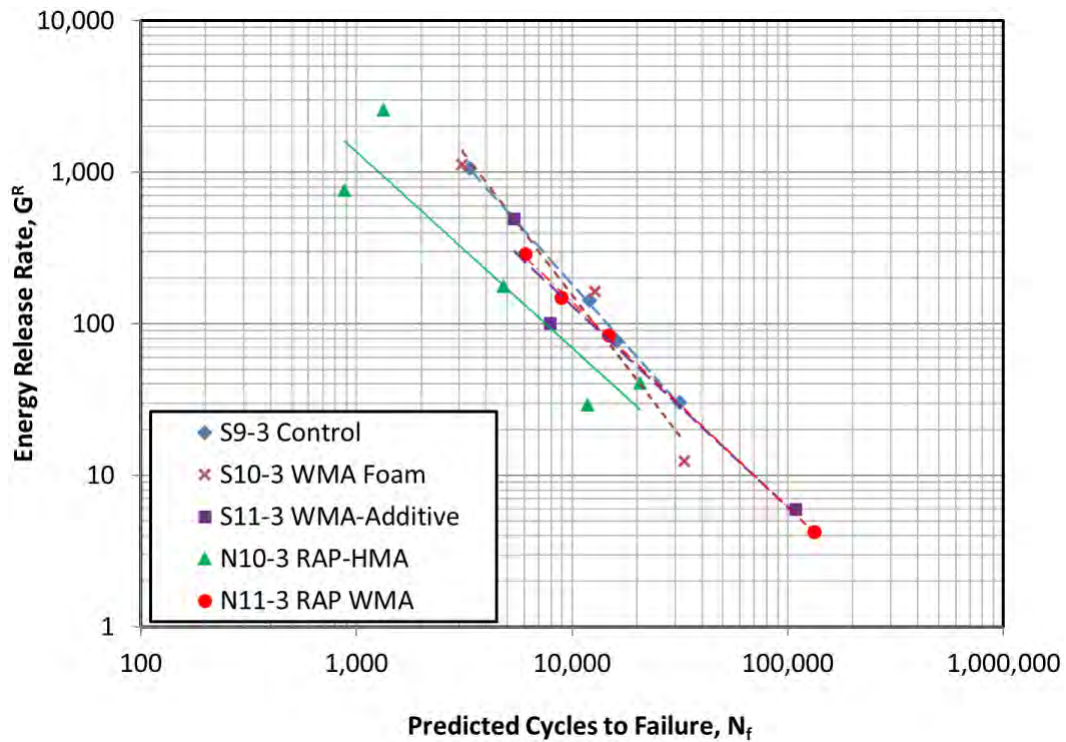


**Figure 29 Predicted SVECD Cycles to Failure for Retested GE Base Layer Mixes**

Figure 30 shows the retested SVECD results plotted versus the actual fatigue cracking. The blue dashed line is the correlation trend line including results for all mixes. This poor correlation is strongly influenced by the point for the 50% RAP HMA, which performed the best in the field but had the lowest cycles to failure in the SVECD test. If that mix is excluded from the data, the correlation improves considerably and follows the expected trend for the lab to field correlation.

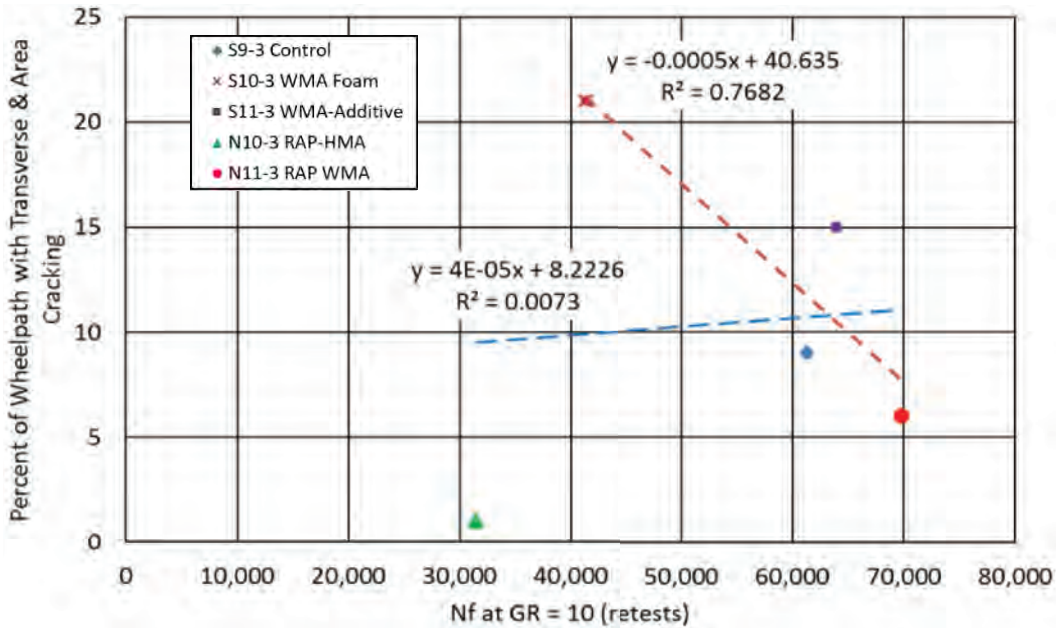


**Figure 30 Relationship between Retested SVECD  $N_f$  at  $G^R=10$  and Percent of Wheelpaths with Transverse and Area Cracking**

#### *Conclusions and Recommendations*

Analyses of the performance and structural responses of 2009 Group Experiment test sections that carried 15.9 million ESALs over five years lead to the following conclusions and recommendations:

- Performance of each of the test sections under heavy loading was substantially better than expected based on the 1993 AASHTO pavement design guide using that traditional asphalt layer coefficient of 0.44. These results further support the NCAT recommendation to increase the asphalt layer coefficient to 0.54. The MEPDG also under-predicted the performance of the test sections. An MEPDG analysis using the control mix E\* data, Test Track traffic loading, and default transfer functions also predicted the control section would fail in rutting (0.65 in.) and fatigue cracking (40% of lane area) by 10 million ESALs.
- A structural coefficient of 0.15 is recommended for OGFC layers based on backcalculated effective structural numbers from FWD testing of comparison sections with an OGFC surface and a dense-graded surface mix. Comparisons of measured strain responses and an analysis of pavement thickness further validated this coefficient.
- Although all of the rut depths were satisfactory, the WMA sections had a little more rutting than the Control section, presumably due to slightly reduced binder aging associated with WMA production. The test sections containing 50% RAP had the least amount of rutting of all of the mixtures.
- Results of APA and Flow Number tests on the surface mixes indicated the mixes would have adequate resistance to rutting based on criteria established in NCHRP studies. The field performance of the test sections validated the APA and FN criteria.
- Although the backcalculated asphalt concrete moduli of WMA sections were 7 to 10% lower than corresponding HMA sections, the critical pavement responses (strain and

stress) were similar. Thus, WMA should be considered equal to HMA from a structural point of view.

- Test sections containing 50% RAP mixtures outperformed test sections with all virgin mixes in all performance measures.
  - Fatigue cracking was the primary distress for the test sections. The test sections had a range of fatigue cracking after 15.9 million ESALs. Fatigue cracking was consistent with the high strain levels measured in the bottom asphalt layers. Limited coring of the test sections confirmed that most of the cracking was full-depth and that there was no debonding between layers. The small percentage of longitudinal cracking in the wheelpaths mapped in several of the test sections was confirmed to be limited to the surface layer. The section with the least amount of cracking was the 50% RAP section with less than 1% of the lane area cracked. The section with the second lowest amount of cracking was the 50% RAP-WMA section with only 6% of the lane area cracked.
  - The use of mixes containing 50% RAP in each pavement layer reduced pavement responses to loads and environmental changes, resulting in 7 to 31% lower critical tensile strains and 14 to 55% lower subgrade pressures than the Control section using all virgin mixes.
  - Backcalculated moduli of the 50% RAP sections were 16 to 43% higher than the all virgin mix Control section. The plots of modulus-versus-time for each section was consistent with the trends observed for strain and pressure versus time.
  - Thus, the notion that high RAP content mixtures are inherently inferior to virgin mixes should be rejected. With appropriate consideration given to the potential impact of reduced compliance of high RAP content mixtures in cold climates, the increased stiffness of high RAP content mixes can be used as an advantage as high modulus structural layers for perpetual pavement designs.
- Laboratory fatigue testing of the bottom layer mixtures of the test sections included the Bending-Beam Fatigue test, the Simplified Viscoelastic Continuum Damage test, and a modified version of the Overlay Test. Field-measured temperature-strain relationships were used with the BBF and OT fatigue test results to predict cycles to failure in the three fatigue tests. The predicted cycles to failure for SVECD testing was based on the new Energy Release Rate parameter. Only the predicted fatigue life from modified Overlay Test results and measured tensile strains correlated well with the observed fatigue cracking in the test sections. High RAP content mixes can have excellent performance when realistic strain levels are used in the analysis.

### *References*

1. West, R., D. Timm, R. Willis, B. Powell, N. Tran, D. Watson, M. Sakhaeifar, R. Brown, M. Robbins, A. Vargas-Nordbeck, F. Leiva Villacorta, and J. Nelson. *Phase IV NCAT Pavement Test Track Findings, Final Report*. NCAT Report 12-10. National Center for Asphalt Technology at Auburn University, Auburn, Ala., 2012.

2. Priest, A. L., and D. H. Timm. *Methodology and Calibration of Fatigue Transfer Functions for Mechanistic-Empirical Flexible Pavement Design*. NCAT Report 06-03. National Center for Asphalt Technology at Auburn University, Auburn, Ala., 2006.
3. Timm, D. H., and A. L. Priest. *Flexible Pavement Fatigue Cracking and Measured Strain Response at the NCAT Test Track, Paper No. 08-0256*. Presented at the 87th Annual Meeting of the Transportation Research Board, Washington, D.C., 2008.
4. Haddock, J. E., A. J. Hand, and H. Fang. *NCHRP Report 468: Contributions of Pavement Structural Layers to Rutting of Hot Mix Asphalt Pavements*. Transportation Research Board of the National Academies, Washington, D.C., 2002.
5. *AASHTO Guide for Design of Pavement Structures*. AASHTO, Washington, D.C., 1993.
6. Timm, D. H., and A. Vargas-Nordcbeck. Structural Coefficient of Open Graded Friction Course. *Transportation Research Record: Journal of the Transportation Research Board, No. 2305*, Transportation Research Board of the National Academies, Washington, D.C., 2012, pp. 102-110.
7. Peters, K., and D. Timm. Recalibration of the Asphalt Layer Coefficient. *ASCE Journal of Transportation Engineering*, Vol. 137, No. 1, 2011, pp. 22-27.
8. Van Der Zwan, J. T., T. Goeman, H. J. A. J. Gruis, J. H. Swart, and R. H. Oldenburger. Porous Asphalt Wearing Courses in the Netherlands: State of the Art Review. *Transportation Research Record: Journal of the Transportation Research Board, No. 1265*, Transportation Research Board of the National Academies, Washington, D.C., 1990, pp. 95-110.
9. Yoder, E. J., and M. W. Witczak. *Principles of Pavement Design*. Second Edition. John Wiley and Sons, Inc., New York, N.Y., 1975.
10. Willis, J. R., and D. H. Timm. *Field-Based Strain Thresholds for Flexible Perpetual Pavement Design*. NCAT Report 09-09. National Center for Asphalt Technology at Auburn University, Auburn, Ala., 2009.
11. Advanced Asphalt Technologies, LLC. *NCHRP Report 673: A Manual for Design of Hot Mix Asphalt with Commentary*. Transportation Research Board of the National Academies, Washington, D.C., 2011.
12. Bonaquist, R. *NCHRP Report 691: Mix Design Practices for Warm Mix Asphalt*. Transportation Research Board of the National Academies, Washington, D.C., 2011.
13. Ma, W., N. H. Tran, A. J. Taylor, and X. Li. *Proposed Improvements to Overlay Test for Determining Cracking Resistance of Asphalt Mixtures, Paper No. 14-3183*. Presented at 93rd Annual Meeting of the Transportation Research Board, Washington, D.C., 2014.
14. Sabouri, M. *Development of a Unified Fatigue Failure Criterion for Asphalt Mixtures and Its Applications to Reclaimed Asphalt Pavement (RAP) Mixtures*. PhD dissertation. North Carolina State University, Raleigh, 2014.

## **2.2. 2012 Green Group Experiment**

### *Background and Objectives*

A new structural experiment began in 2012 that utilized recycled materials in ways that would enhance the properties of each layer in the pavement structure. These sections featured the use of reclaimed asphalt shingles (RAS), ground-tire rubber (GTR), and reclaimed asphalt pavement (RAP). Since the Group Experiment sections built in 2009 had not experienced any significant deterioration over the previous cycle, it was decided to reduce the design thickness of the Green Experiment sections by one inch so that differences in performance would be evident within one cycle. The goal of the experiment was to demonstrate how recycled materials could be used in pavement structures such that the overall performance of the pavements would exceed what can be achieved with current practices.

Four test sections, illustrated in Figure 1, comprised this Green Group (GG) experiment. Section N5 was meant to represent the current standard practices for mix designs, while the other sections used a wider array of recycled materials and increased RAP contents. Although these test sections were not designed as perpetual pavements from the thickness perspective, the mixtures selected for each layer were designed with that philosophy in mind: a rut resistant surface layer (e.g. SMA), a high-stiffness (i.e. high-modulus) intermediate layer to reduce deflections in the pavement, and a more fatigue resistant lower layer to resist high tensile strains. A design thickness of 6 in. of asphalt concrete (AC) was selected because 6 in. has been found in previous Test Track studies to be sufficiently thick to avoid rapid failure but thin enough to develop distresses within the two-year research cycle. The sections included the standard array of asphalt strain gauges, earth pressure cells and temperature probes previously described and shown in Figure 1.

The GG sections were sponsored by the Alabama Department of Transportation, Alabama Department of Environmental Management, North Carolina Department of Transportation and South Carolina Department of Transportation.

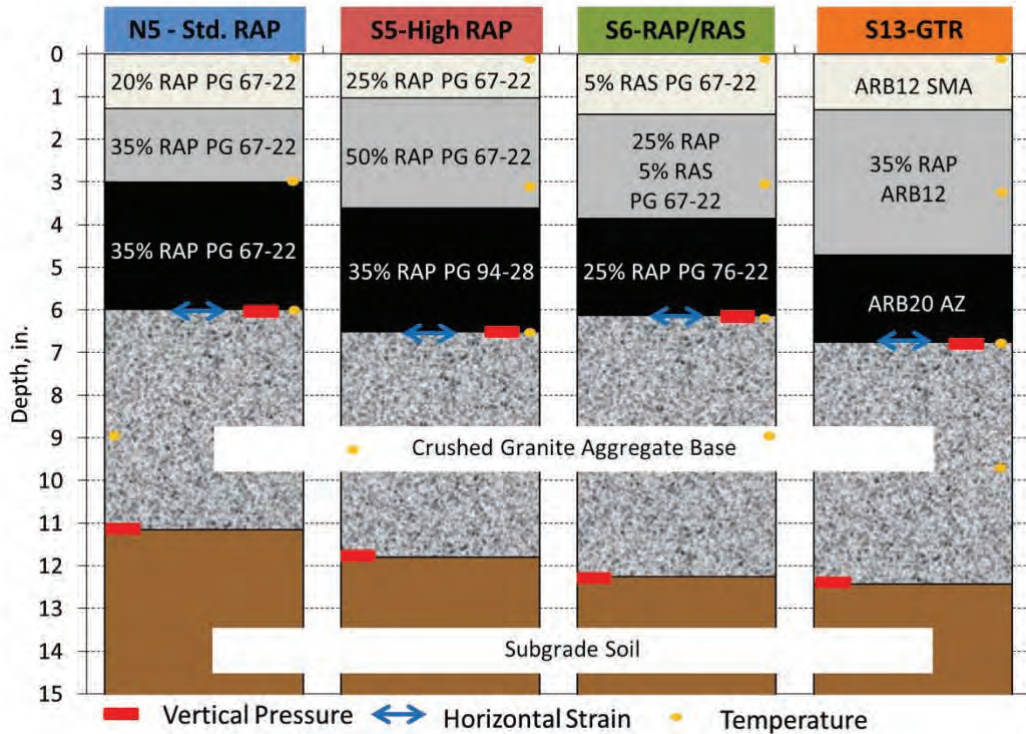


**Figure 1 2012 Green Group Experiment Sections (1)**

*Test Section Design and Construction Summary*

Table 1 provides a summary of key as-constructed mix information for the layers in each test section in the Green Group Experiment.

Section N5 (standard RAP) was designed to be consistent with current maximum RAP contents permitted by many highway agencies with higher RAP contents allowed in lower layers. In essence, this section serves as the control section in the experiment. The surface layer for this section was a Superpave mix containing 20% RAP. The intermediate and base layers used the same mix design with 35% RAP.

Section S5 (High RAP) utilized an SMA surface layer containing cellulose fibers and 25% RAP by weight of mix, an intermediate Superpave layer containing 50% RAP (30% coarse fractionated RAP and 20% fine fractionated RAP) and having a RAP binder ratio of 0.44. The bottom layer in S5 was the same mix as in N5 except a highly polymer-modified binder (PG 94-28) was used in the S5 layer.

Section S6 (RAP/RAS) incorporated 5% RAS into the SMA surface mix. It is worth noting that no cellulose fibers were added to the SMA mix containing RAS since the RAS fibers and stiffer binder prevented drain down. The intentionally stiff intermediate layer mix contained a combination of 25% RAP and 5% RAS. The bottom lift in S6 contained 25% RAP and a PG 76-22 polymer modified binder. This mix had a design target of 2.0% air voids to follow the rich-bottom approach to make the layer more fatigue resistant.

Section S13 (GTR) featured two GTR modified binders. The SMA surface and dense-graded intermediate lifts of S13 contained 12% #30-mesh GTR added to a PG 67-22. This is abbreviated as ARB12 (asphalt-rubber binder with 12% GTR). No fibers were added to the GTR modified SMA; the GTR provided excellent resistance to drain down. The dense-graded intermediate layer mix also contained the 12% #30 mesh GTR binder as well as 35% RAP. The bottom lift of S13 was designed using the Arizona method for a gap-graded asphalt-rubber asphalt concrete mix and contained 20% #16-mesh GTR. In this report, this mix is abbreviated as ARB20 AZ (asphalt-rubber binder with 20% GTR, Arizona-style gap-graded mix).

**Table 1 Design and In-Place Properties**

Section	Lift <sup>a</sup>	NMAS, mm / Mix Type	Air Voids, Design / QC, %	QC VMA, % / In-Place Density, %	Pb / Pbe, % weight	Recycled Binder Ratios, % total binder	Plant Temp. °F / WMA Type
N5 Std. RAP	1	9.5	4.0	14.2	5.2	0.17 RAP	270
		SP <sup>b</sup>	3.2	91.6	4.7		Foam
	2	19	4.0	13.0	4.6	0.35 RAP	285
		SP	3.6	93.1	4.0		Foam
	3	19	4.0	14.4	4.7	0.35 RAP	280
		SP	4.5	93.5	4.1		Foam
S5 High RAP	1	9.5	4.0	16.7	5.8	0.16 RAP	275
		SMA <sup>c</sup>	4.6	93.1	5.3		Foam
	2	19	4.0	13.9	5.0	0.44 RAP	280
		SP	3.8	95.0	4.3		Foam
	3	19	4.0	12.5	4.5	0.35 RAP	285
		SP	3.0	93.7	3.9		Evotherm
S6 RAP/RAS	1	9.5	4.0	15.6	5.5	0.20 RAS	275
		SMA	3.6	92.1	5.1		Foam
	2	19	4.0	13.5	4.9	0.20 RAS	280
		SP	3.1	94.0	4.3	0.23 RAP	Evotherm
	3	19	2.0	13.2	5.3	0.21 RAP	285
		SP	1.7	96.5	4.8		Foam
S13 GTR	1	9.5	4.0	15.3	5.7	NA	275
		SMA	3.3	92.9	5.2		Evotherm
	2	19	4.0	13.8	4.8	0.33 RAP	280
		SP	3.6	94.4	4.3		Foam
	3	12.5	5.5	19.4	7.2	NA	300
		AZ <sup>d</sup>	4.2	92.3	6.5		Evotherm

Note: <sup>a</sup>Lift (1=surface, 2=intermediate, 3=base); <sup>b</sup>SP Superpave, <sup>c</sup>SMA Stone Matrix Asphalt; <sup>d</sup>AZ Arizona Gap-Graded

Each mix was produced using the warm-mix technology listed in Table 1. The asphalt foaming technology used the Astec Double Barrel Green system with two percent water. The Evotherm product was Evotherm Q1 added at a dosage rate of 0.5% of the total binder.

A non-tracking tack (NTSS-1HM) was applied between pavement lifts at an undiluted application rate of 0.05 gal/yd<sup>2</sup> (0.028 gal/yd<sup>2</sup> residual). Tack material and application rate were selected based on previous Test Track experience. The tack coat applications were calibrated and monitored; no construction issues with the tack coat were observed.

### Laboratory Test Results

Plant mix samples for each layer were obtained during construction and tested at NCAT's main laboratory. Surface mixes were evaluated for rutting resistance using the Asphalt Pavement Analyzer (APA) in accordance with AASHTO T 340-10 and the Flow Number (FN) Test in accordance with AASHTO TP 79-13. Resistance of the surface layers to top-down cracking was assessed using the Energy Ratio procedure developed by Roque et al. (3). Moisture damage resistance was assessed in accordance with AASHTO T 283-07. The intermediate layers were tested for dynamic modulus ( $E^*$ ) in accordance with AASHTO TP 79-13 and resistance to moisture damage in accordance with AASHTO T 283-07. The mixes used as bottom layers were evaluated for fatigue resistance with the bending beam fatigue test in accordance with AASHTO T 321-07 and the simplified viscoelastic continuum damage (SVECD) test performed using a draft procedure developed by North Carolina State University. Moisture damage susceptibility of the bottom layers was also evaluated using AASHTO T 283-07.

**Surface Layers.** Results of APA testing are shown in Figure 2. The figure shows rut depths from manual and automated rut depth measurements with the APA as either are permitted in the test method. All of the mixtures had APA results well below the NCAT Test Track criteria of 5.5 mm indicating that they have good resistance to rutting under heavy traffic.

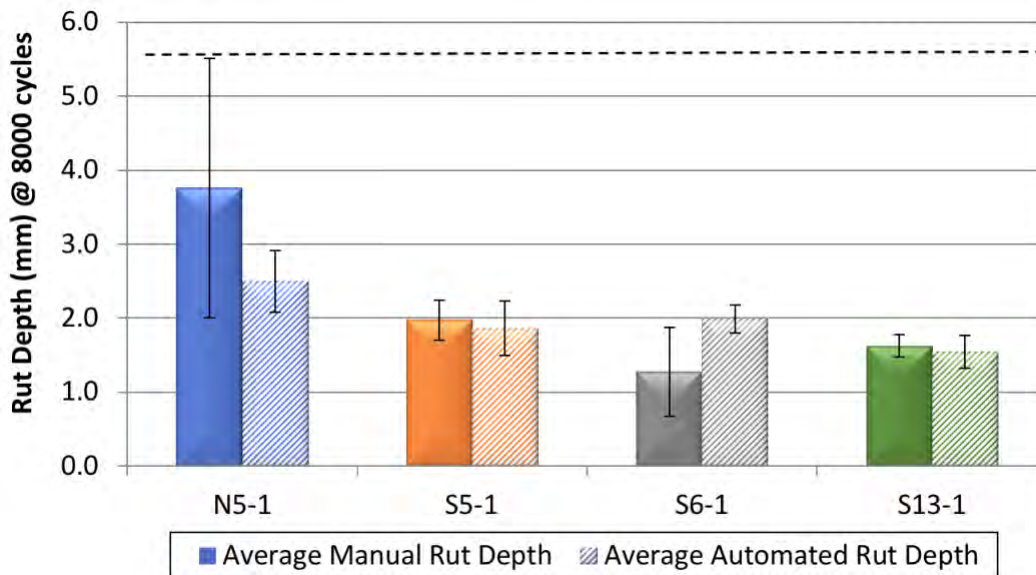


**Figure 2 Asphalt Pavement Analyzer Test Results for Green Group Surface Layers**

Flow Number (FN) test results are shown in Figure 3. The dashed lines in the chart represent minimum Flow Number criteria for different traffic levels as recommended in NCHRP Report 691 for warm mix asphalt mixtures (4). The lowest line at 30 is for traffic levels between 3 and 10 million ESALs. All of the mixtures meet that criteria. The next highest FN criteria is at 105, which applies to design traffic between 10 and 30 million ESALs. The surface mix in the conventional pavement Section N5 had a FN of 71, which does not meet that criterion. All of the other surface mixes do meet that criterion. Only the SMA containing RAS used in S6 meets the minimum criterion of 415 for the highest traffic range for design traffic greater than 30 million ESALs.

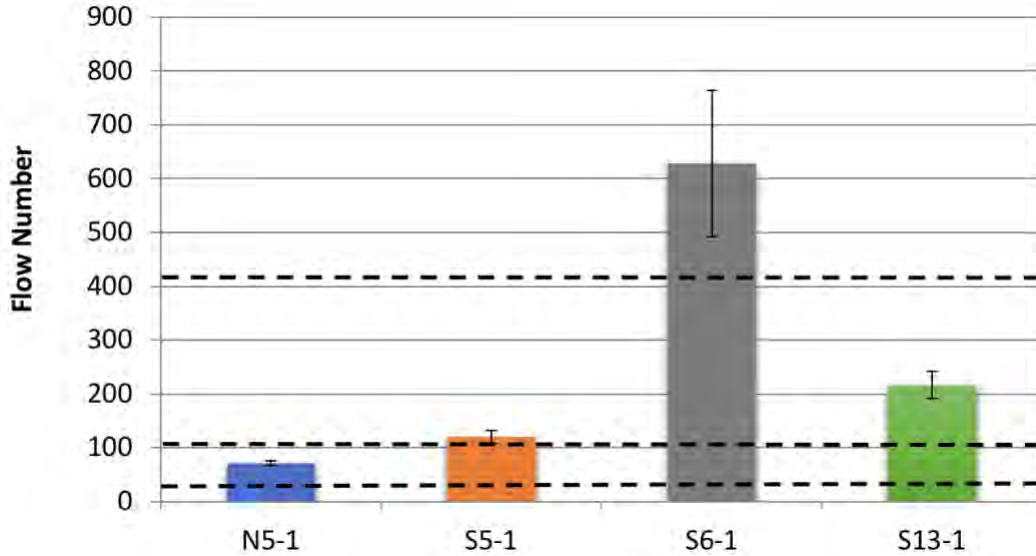


**Figure 3 Flow Number Test Results for Green Group Surface Layers**

Resistance of the surface mixes to top-down cracking was evaluated using the Energy Ratio method. Results are summarized in Figure 4. Developers of the test recommended two criteria: the Energy Ratio should be above 1.95 for traffic loadings above 1 million ESALs per year and the mixture Dissipated Creep Strain Energy ( $DCSE_{HMA}$ ) should be above  $0.75 \text{ kJ/m}^3$  to guard against brittle mixtures regardless of the pavement structure. From the figure it can be seen that all of the mixes satisfy the minimum Energy Ratio, although the GTR-modified SMA from S13 was lowest with an ER of 2.1. The reason that this mix has a low ER result is because it has a relatively high creep compliance, which is in the denominator of the ER calculation. All of the surface mixes easily passed the DCSE criterion. The ER results indicate that the only surface mix marginally susceptible to top-down cracking is the GTR-modified SMA in S13.

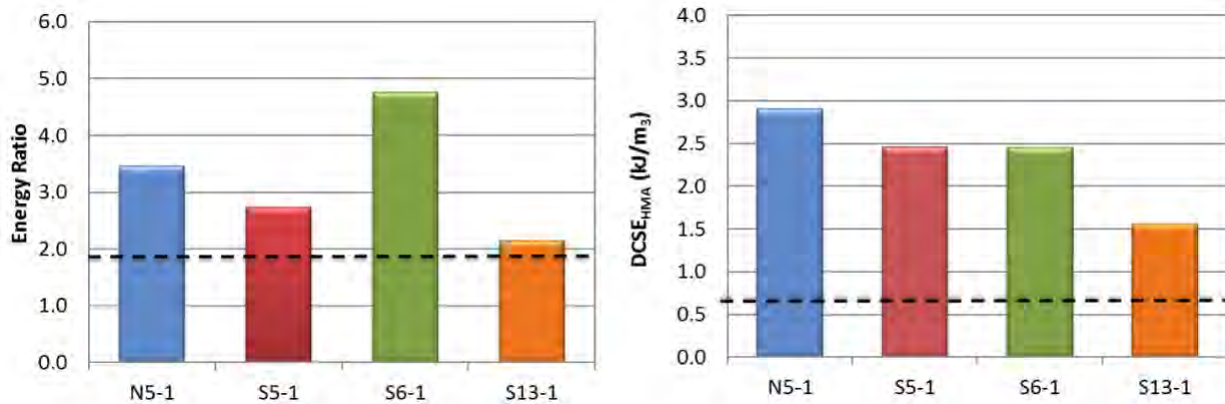


**Figure 4 Energy Ratio Test Results for Green Group Surface Layers**

**Intermediate Layers.** The intermediate lifts were designed to be a stiff strain-reducing layer in the pavement structure. Laboratory dynamic modulus testing was conducted on all mixes according to AASHTO TP-79. The  $E^*$  values presented in Figure 5 are from testing at  $68^\circ\text{F}$  and 10 Hz. As intended, it can be seen that the intermediate lift was the stiffest layer in each section.

Comparison of E\* values at 68°F and 10 Hz for the different test sections in the experiment indicates that the intermediate layers for N5 and S6 are similar. E\* for the intermediate layer in S5 was slightly lower than N5 and S6. E\* for S13 was significantly lower than the other intermediate layers. This reduction can be attributed to the GTR-modified binder used in S13-2 since that was the only significant difference between the intermediate layer in this section and N5.

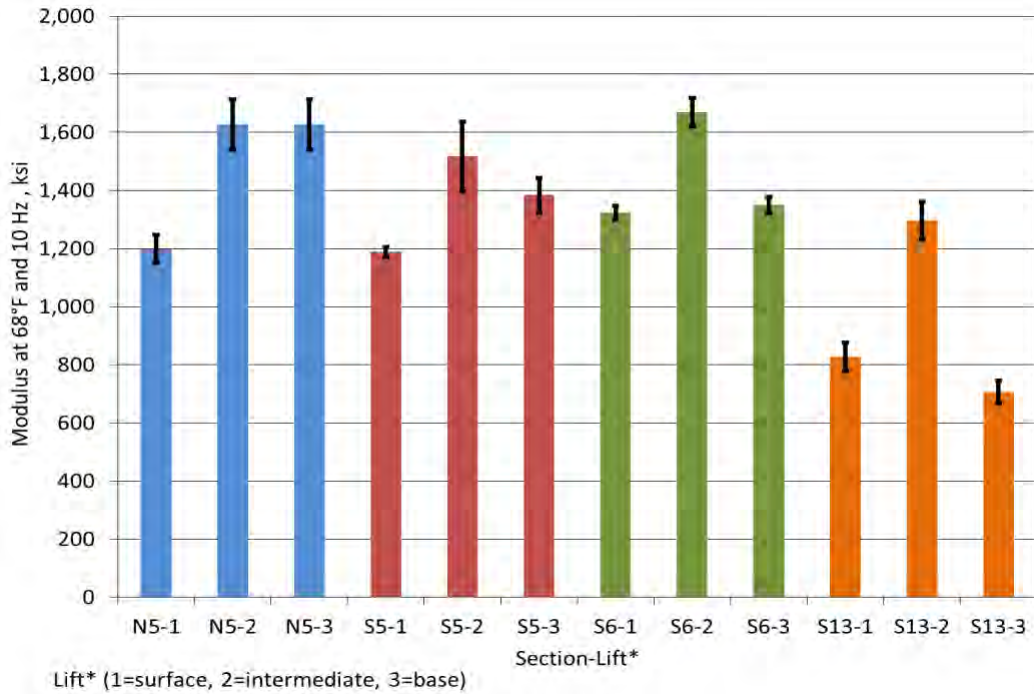


**Figure 5 Dynamic Modulus Comparison at 68°F and 10 Hz**

The full E\* master curves for the intermediate layers are plotted in Figure 6. This plot shows that the mix from S6 containing RAP and RAS was much stiffer than the other mixes at the higher temperatures and lower frequencies. The GTR modified intermediate layer from S13 had a lower stiffness at lower and intermediate temperatures but was stiffer than the conventional mix from N5 and the 50% RAP mix from S5 at high temperatures and low frequencies.

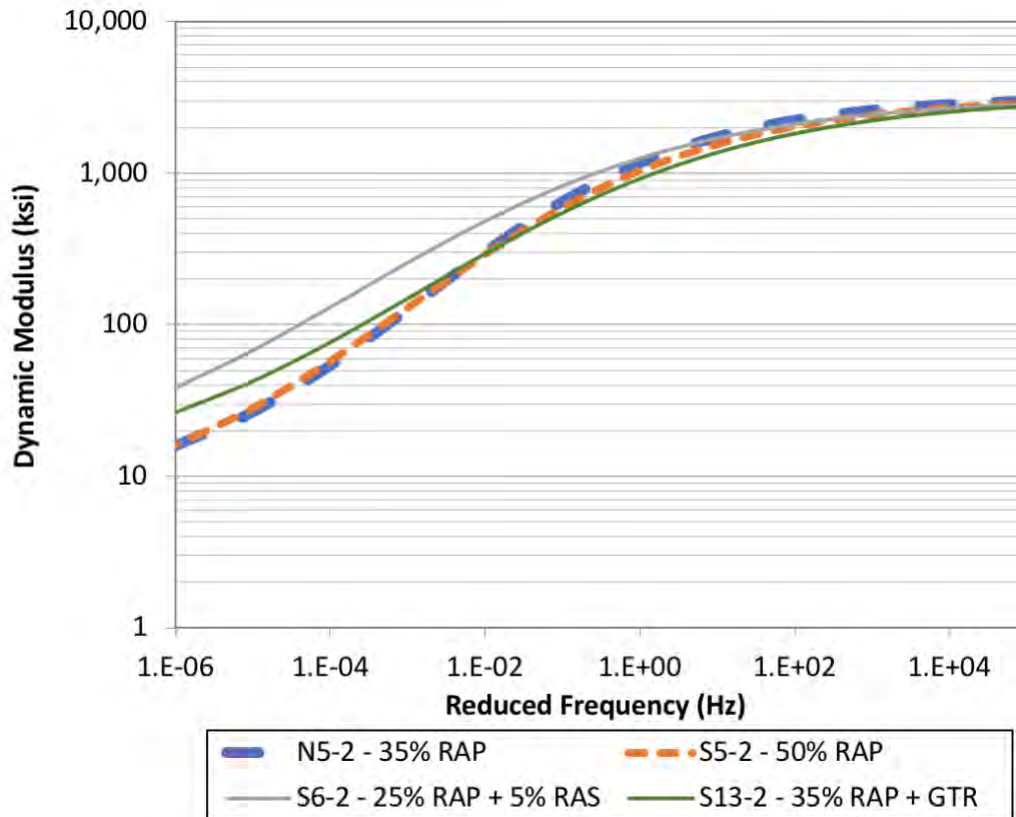


**Figure 6 Dynamic Modulus Master Curves for Intermediate Layers**

**Bottom Asphalt Layers.** The highest load-related tensile stresses in any well-bonded pavement cross-section occur at the bottom of the pavement’s lowest asphalt layer. Therefore, for this experiment, the bottom asphalt layers in sections S5, S6, and S13 were designed to have greater resistance to fatigue compared to the conventional asphalt base mix used in N5. Two laboratory tests were used to evaluate the fatigue resistance of these mixtures: the bending beam fatigue test and the simplified viscoelastic continuum damage (SVECD) test. Results of the bending beam fatigue tests on the bottom layers is shown in Figure 7. These results indicate that the bottom layers for S5 and S6 are very similar. These mixes have similar fatigue lives to the conventional mix in N5 at high strain levels (e.g. 800 microstrain) but have fatigue lives that are at least two orders of magnitude higher at relatively low strain levels (e.g. 200 microstrain). The Arizona-style gap-graded asphalt-rubber mix in S13 has a higher fatigue life at high and intermediate strain levels compared to the other bottom layer mixes. This mix was not tested at 200 microstrain, but it would appear that if the results were extrapolated that the mix in S13 would have a lower fatigue life than the corresponding mixes in S5 and S6 at that low strain level.

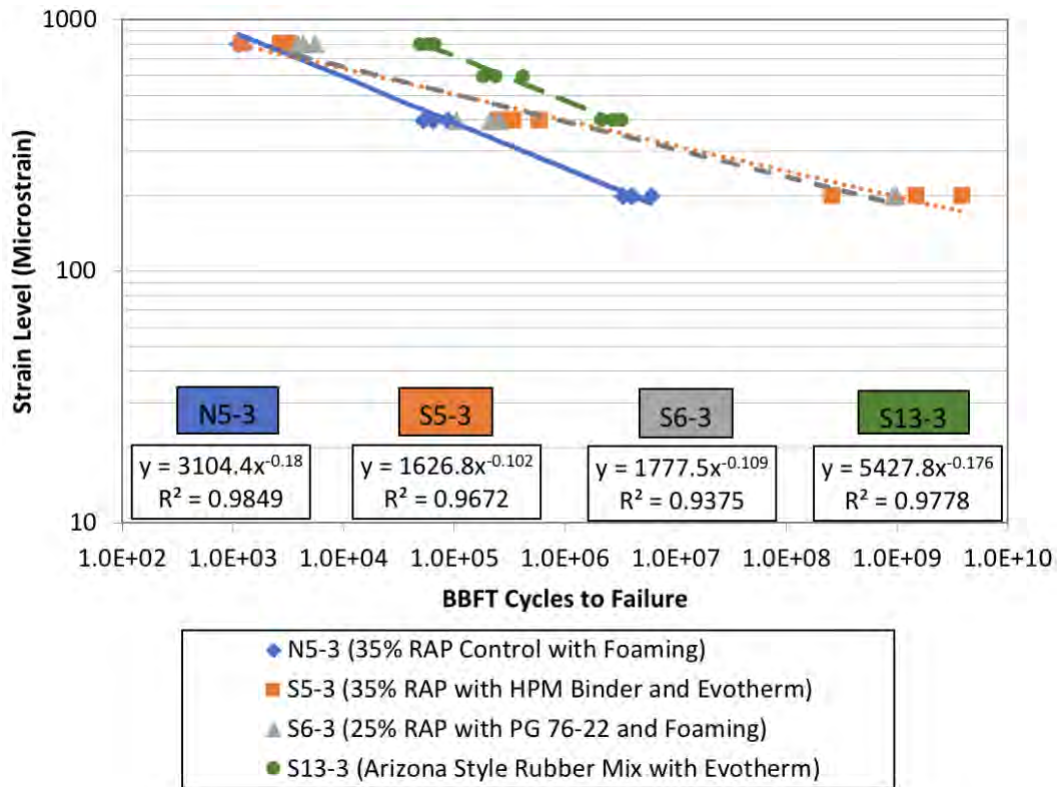


**Figure 7 Bending Beam Fatigue Results for Bottom Layers**

SVECD testing was performed on the bottom layer mixes following the draft procedure developed at North Carolina State University. In this method, at least four fatigue tests (two tests at a relatively high strain input level and two at a relatively low strain input level) were performed at 19°C and at a frequency of 10 Hz. Pseudo stiffness and damage characteristic curves were generated according to the SVECD model. The damage curves combined with the mixture's modulus were used in the ALPHA-F v3.1.3 analysis software to predict the fatigue behavior at other conditions. Results of the SVECD testing and analysis are illustrated in Figure 8. The SVECD results differ from the BBF results in several ways. For this method, the high polymer modified mix from S5 has essentially the same fatigue life as the conventional mix from N5 across all of the simulated strain levels. The SVECD results also indicate that the rich bottom mix from S6 is substantially better than the conventional mix, but the Arizona-style gap-graded asphalt-rubber mix is far superior.

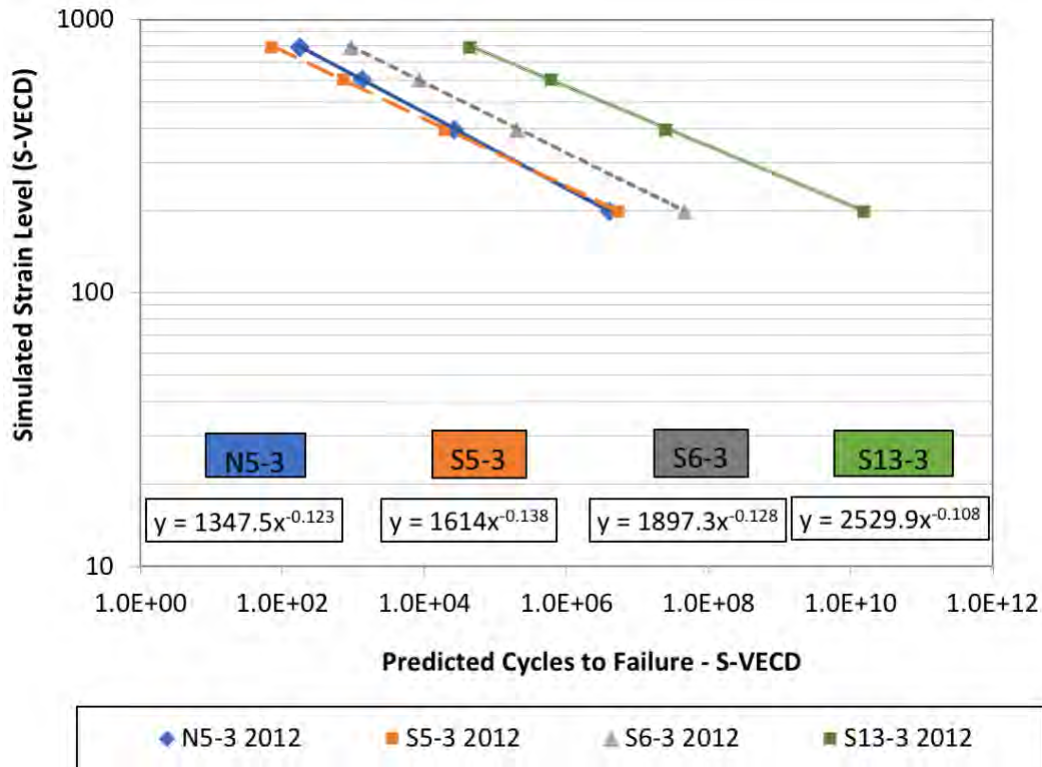


**Figure 8 Fatigue Lives of Bottom Layer Mixes from SVECD Testing and Analysis**

Moisture damage susceptibility results for each mix in the Green Group experiment are summarized in Table 2. The five mixtures produced with the Evotherm WMA technology are identified with an E superscript; the other mixtures were produced with an asphalt foaming WMA technology. The Evotherm additive also served as the antistripping additive for those mixtures. Gripper X was added to the asphalt binder for the mixtures produced with the asphalt foaming WMA technology. The dosage rates for the Gripper X and the Evotherm was 0.5% by weight of total binder. Both products were metered into the asphalt binder at the asphalt plant during production.

From Table 2 it can be seen that the surface mix from N5 was just below the standard minimum TSR criterion of 0.80, as were three of the intermediate layers (S5, S6, and S13) and the bottom layer from S5. However, none of the sections had any visual evidence of stripping as observed from cores taken for forensic testing described later in this report. It is interesting to note that the GTR modified SMA mix and the Arizona-style asphalt-rubber mix from S13 had lower tensile strengths than the corresponding mixes in the other sections. Those two mixtures did not contain any RAP or RAS.

**Table 2 Results of Moisture Damage Susceptibility Tests**

Layer	Section	Unconditioned		Conditioned		Tensile Strength Ratio
		Air Voids (%)	Tensile Strength (psi)	Air Voids (%)	Tensile Strength (psi)	
Surface	N5	6.7	208.9	6.7	164.9	0.79
	S5	6.9	173.4	7.0	155.1	0.89
	S6	7.0	172.4	7.2	151.9	0.88
	S13 <sup>E</sup>	6.9	107.3	7.0	94.9	0.88
Intermediate	N5	7.2	267.3	7.2	212.2	0.80
	S5	6.7	236.4	6.8	174.8	0.74
	S6 <sup>E</sup>	7.3	254.6	7.2	171.1	0.67
	S13 <sup>E</sup>	7.4	226.2	7.4	152.8	0.68
Bottom	N5	7.2	263.7	7.2	212.2	0.80
	S5 <sup>E</sup>	6.8	227.9	6.9	167.5	0.74
	S6	7.0	203.2	7.0	175.7	0.86
	S13 <sup>E</sup>	7.2	108.8	7.1	94.8	0.87

*Performance and Structural Analyses*

The original intention of the GG experiment was to provide direct comparisons between the conventional mixtures test section (N5) and the other sections in terms of pavement response, structural characterization and performance under the accelerated loading conditions of the Test Track. However, as described in the following subsections, the sections exhibited a variety of distress development, not necessarily resulting directly from the materials themselves, which confounded direct comparisons. Each section is presented below as a unique case study followed by a comparison of all the sections.

*N5 – Standard RAP*

**Performance.** The first crack in Section N5 (Standard RAP) was observed on April 23, 2013 after almost 2.5 million ESALs were applied since traffic began on October 22, 2012. The cracking performance is summarized in Figure 9. It can be seen that the critical dates in Figure 9 correlate well with changes in the rutting and roughness, shown in Figures 10 and 11, respectively. For example, both the rut depth and IRI began to increase around the same time as the first crack was observed in April 2013. The cracking threshold, reached in August 2013, was defined as cracking in 25% of the total lane area. In mid-August 2013, a minor patch was applied and on October 15 2013, a larger patch was applied in the right wheel path. In early April 2014, the top two inches were milled and replaced. After this rehabilitation, the average rut depth and IRI rapidly increased through the last 6 months of the research cycle.

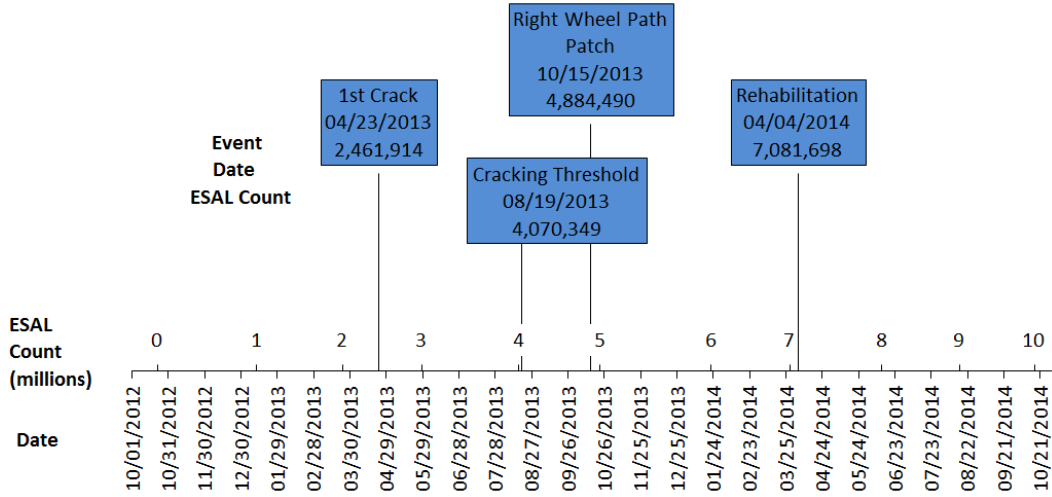


**Figure 9 Section N5 (Standard RAP) Performance Timeline**

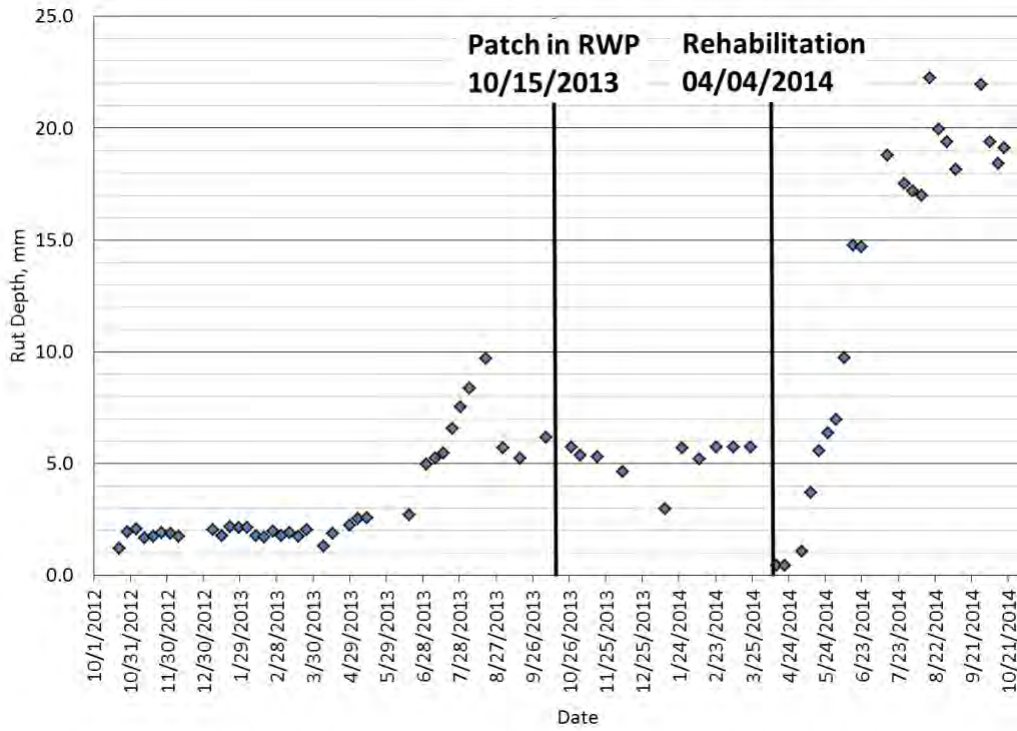


**Figure 10 Section N5 (Standard RAP) Rutting Performance**

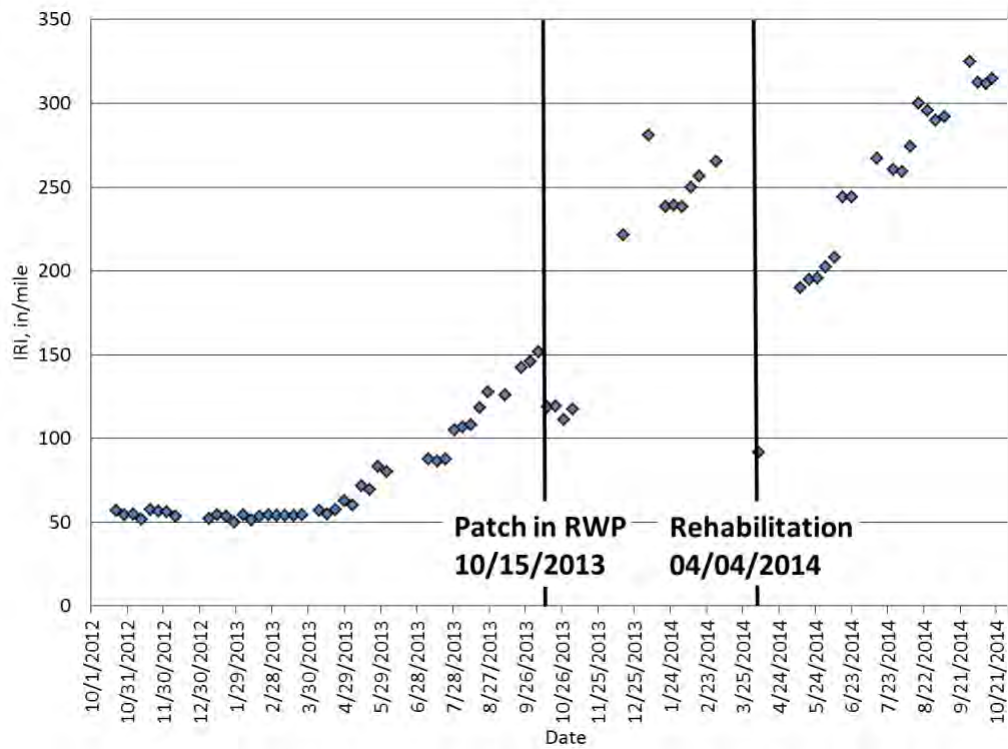


**Figure 11 Section N5 (Standard RAP) Surface Performance**

**Strain/Pressure Measurements.** The temperature-corrected vertical pressures at the top of the base and subgrade are shown in Figure 12. As expected, since the base pressure plate was higher in the pavement structure, it was therefore subjected to greater stress levels. It can be seen that the pressures were fairly consistent before the first crack appeared on April 23, 2013. After the first crack was observed, the base pressure doubled over the next year. There was also a greater amount of scatter in both data sets after the first crack appeared. After rehabilitation on April 4, 2014, the scatter reduced and the pressures were more stable. However, there was a larger difference between the base and subgrade pressures after rehabilitation indicating that despite the temporary rehabilitation restoring the pavement’s surface functionality, the pavement structure was still damaged.

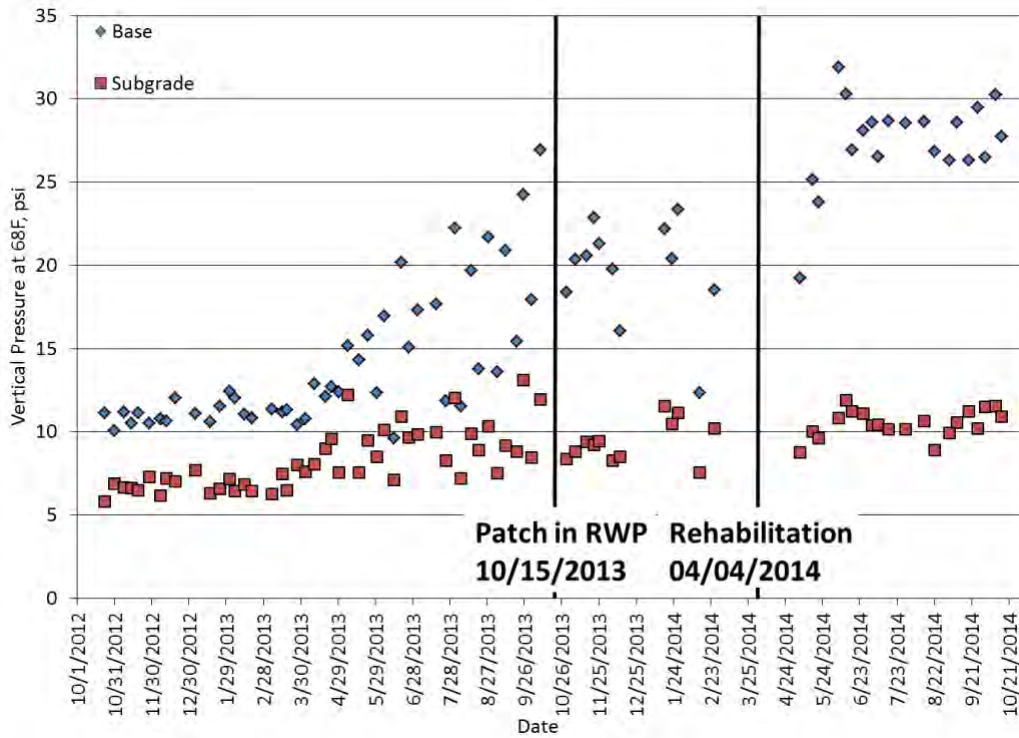


**Figure 12 Section N5 (Standard RAP) Vertical Pressure**

The horizontal strain corrected to a reference temperature of 68°F is presented in Figure 13. As observed in previous Test Track research, the longitudinal strain is greater than the transverse strain throughout the research cycle (6). Longitudinal strain results from bending in the direction of travel while transverse strains are perpendicular to the direction of travel. Both are measured in tension in the horizontal plane at the bottom of the asphalt concrete. It can be seen that the longitudinal strain level steadily increased from October 2012 through September 2013. The longitudinal strain was reduced after the patch was applied in October 2013. In February 2014, strain levels sharply increased until the rehabilitation on April 4, 2014. After rehabilitation, the strain levels became more consistent.

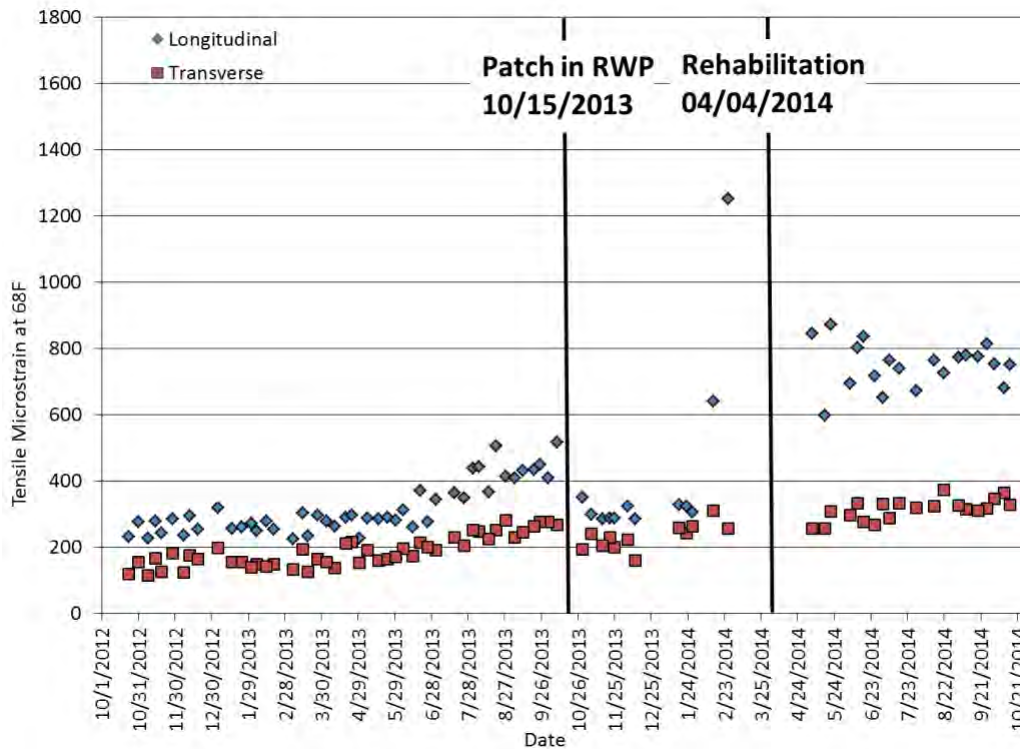


**Figure 13 Section N5 (Standard RAP) Horizontal Strain**

**Backcalculated Moduli.** As noted in the introduction to the structural experiments section, FWD testing was conducted at 12 locations within each section on a given testing date. Therefore, on a given testing date there are 12 backcalculated modulus values for each section. The root-mean-squared error (RMSE) was used to evaluate the match between the backcalculated and measured deflection basins. An RMSE cutoff value of 3% was used to maintain data quality.

The backcalculated composite AC modulus (at a reference temperature of 68°F) versus time is presented in Figure 14. Modulus values are presented with and without the 3% RMSE cutoff to show when the section was no longer behaving like a homogenous, linear-elastic material. It can be seen that from October 2012 through February 2013 the modulus was fairly stable and there were no moduli values that had an RMSE above 3%. Beginning in March 2013, there were backcalculated moduli values with an RMSE above 3% (shown as red boxes without a blue diamond marker on top). As traffic continued and the pavement accrued damage, there were fewer and fewer data points with an RMSE less than 3% until February 2014 when there were no data points below 3%. Even after rehabilitation, there were no data points with an RMSE below 3%, indicating that although the surface functionality had been temporarily restored, the pavement structure was still damaged. The variation on a given testing date is also worth noting. In the beginning of the cycle the moduli values had a relatively tight distribution on a given date. As the section became more damaged the variation on a given testing date also increased. Prior to the first crack appearing in April 2013, the modulus was only slightly decreasing with time and traffic. After that point in time, the effect of cracking on modulus degradation was much more pronounced.

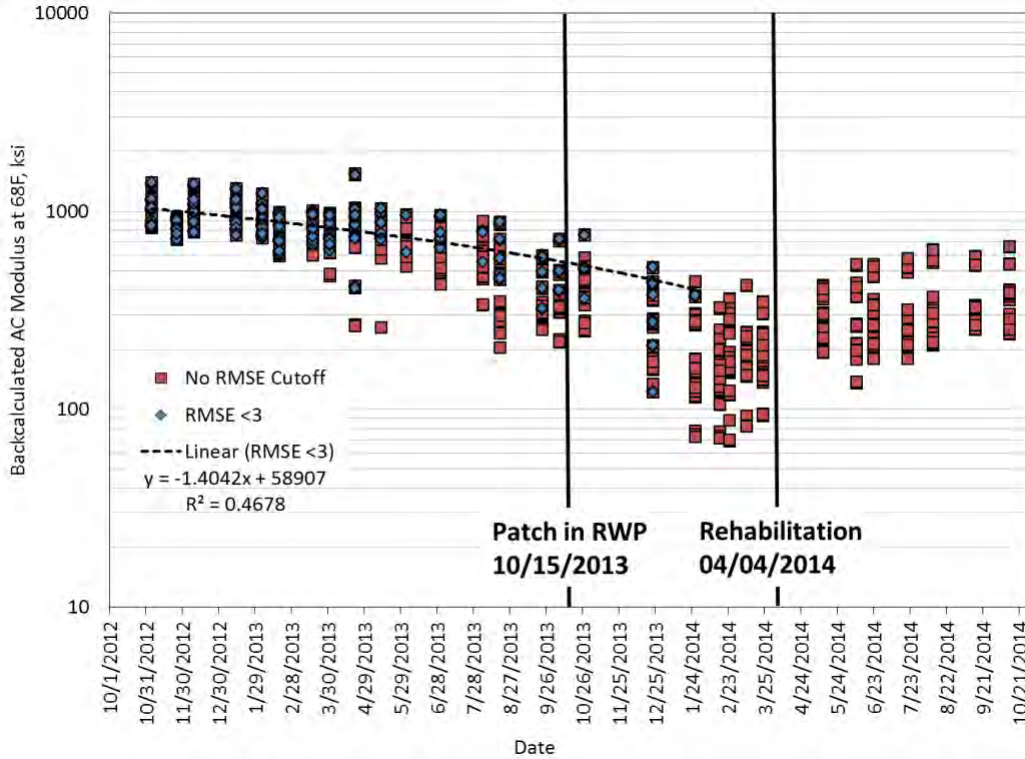


**Figure 14 Section N5 (Standard RAP) Backcalculated FWD Results**

**Forensic Investigation.** Cores were taken at locations within the section with various levels of surface cracking to capture the cracking distribution throughout the section. Cores were taken in September, 2013 and no evidence of interface debonding was found. Cores were taken again in July 2014. It can be seen in Figure 15, that the cracks are wide at the bottom of the core, which is taken to infer that the cracks initiated at the bottom of the asphalt pavement. Thus, bottom-up fatigue cracking was identified as the primary distress mechanism that led to failure in Section N5. Although this was the expected mode of failure given the thin cross-section used in the experiment, the pavement design was expected to carry more ESALs than it did. The estimated Structural Number for this section was 4.08, which translates to approximately 12 million ESALs at 90% reliability.



**Figure 15 Section N5 (Standard RAP) Cores Showing Bottom-up Cracking**

#### *S5 – High RAP*

**Performance.** As seen in the performance timeline, Figure 16, Section S5 (High RAP) rapidly deteriorated after the first crack was observed on April 6, 2013. Layer interface debonding between the intermediate and base lifts was identified as the failure mechanism. Further details regarding the initial failure and reconstruction has been documented elsewhere (1). The section was completely reconstructed on May 22, 2013.

Reconstruction included duplicating the base mix with 35% RAP and the highly polymer modified binder. The non-tracking tack coat rate was doubled to 0.10 gal/yd<sup>2</sup> (0.056 gal/yd<sup>2</sup> residual). The asphalt content of the 50% RAP intermediate layer was increased by 0.2% and the mixture was produced with foamed asphalt at 325°F rather than 280°F in the original production. The surface SMA mix with 25% RAP was redesigned with using a 50-blow Marshall hammer compaction rather than 80 gyrations with a Superpave Gyratory Compactor. This resulted in a 0.5% higher asphalt content for the SMA.

After reconstruction, the test section carried over 4.2 million ESALs before the first crack was observed. Rut depths and roughness measurements (IRI), shown in Figures 17 and 18, respectively, were fairly stable throughout and were below thresholds of 12.5 mm and 170 in/mile.

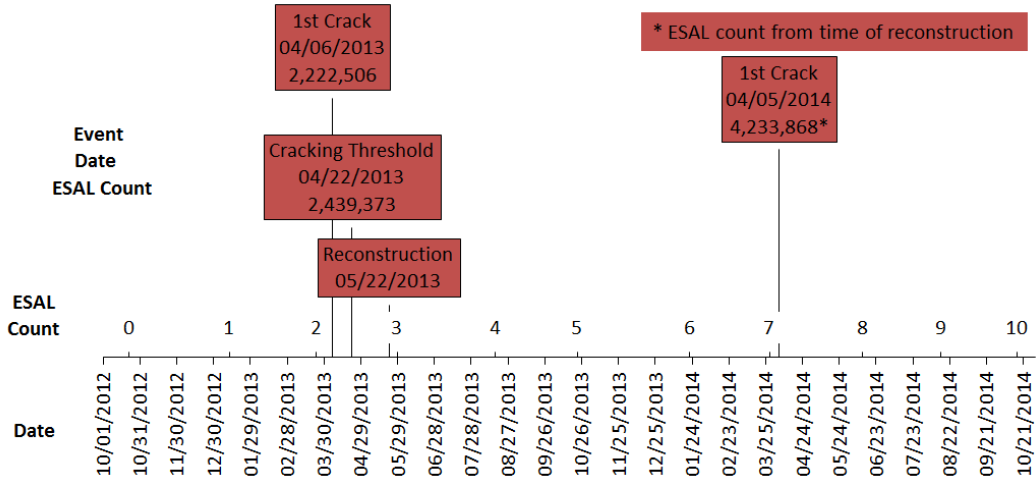


Figure 16 Section S5 (High RAP) Performance Timeline

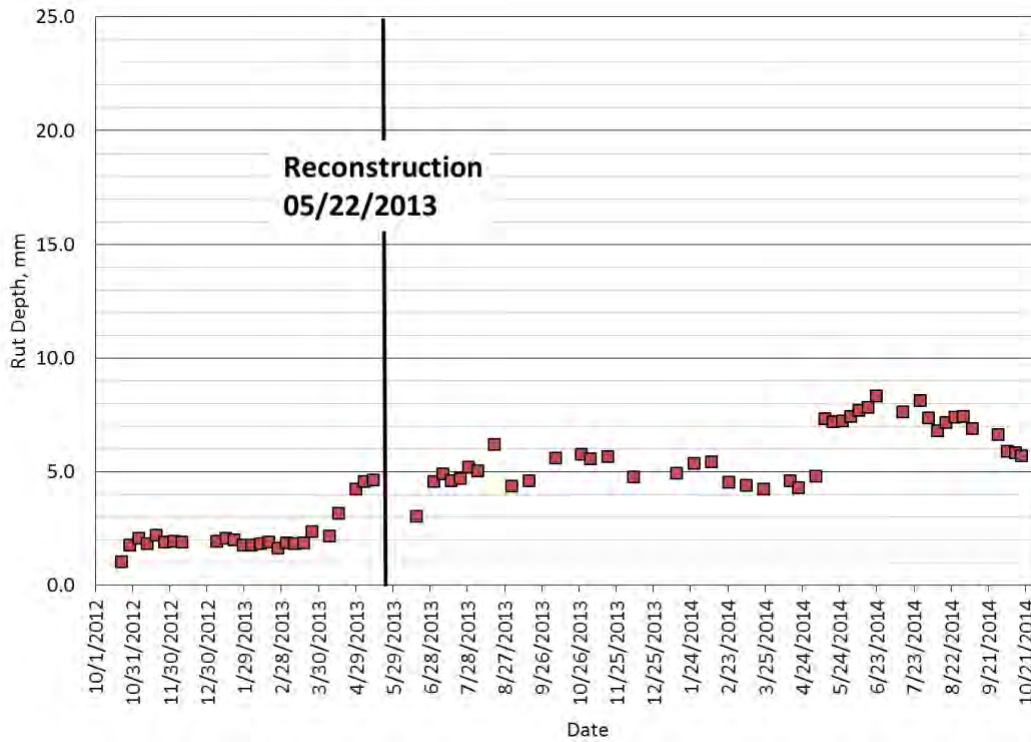
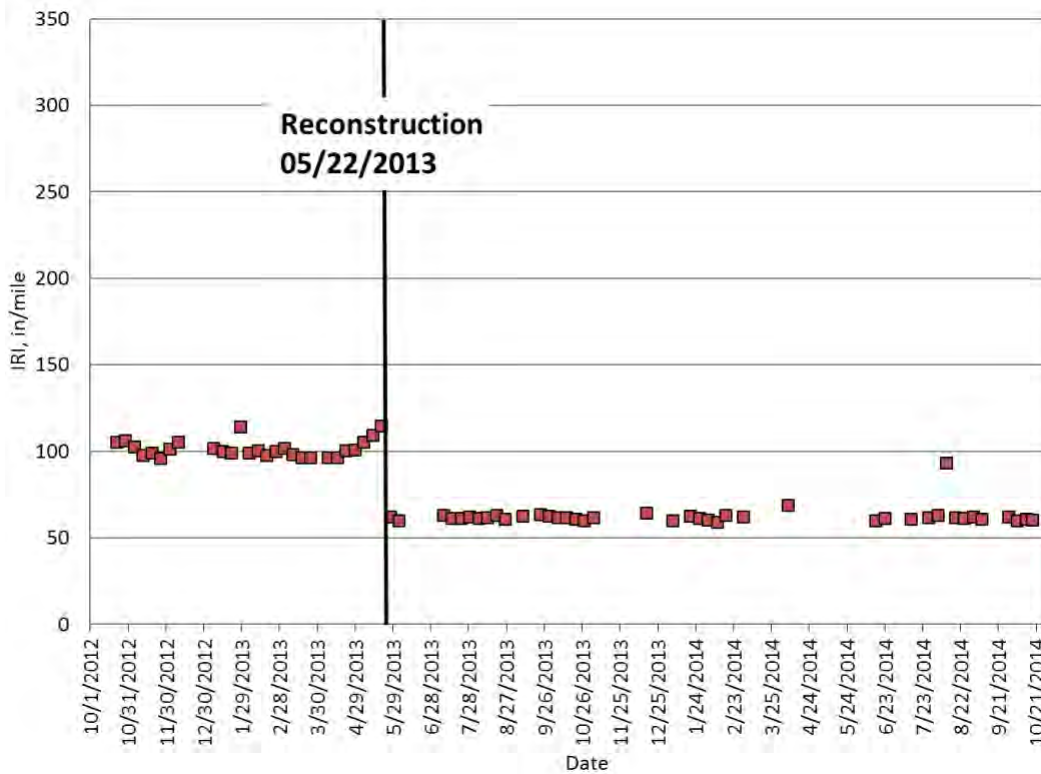


Figure 17 Section S5 (High RAP) Rutting Performance



**Figure 18 Section S5 (High RAP) Surface Performance**

**Strain/Pressure Measurements.** The vertical pressures at a reference temperature of 68°F are presented in Figure 19. An increase in pressure is apparent in April 2013 as cracking rapidly progressed throughout the section. After reconstruction, both the base and subgrade pressure were fairly stable throughout the remainder of the research cycle.

The horizontal strain, at a reference temperature of 68°F, at the bottom of the AC is shown in Figure 20. Prior to April 2013, the strain levels were drifting up slightly. After reconstruction, the transverse strain level stayed fairly constant over time. The longitudinal strain data were erratic after reconstruction indicating gauge damage during reconstruction. It should also be noted that there were no working transverse gauges past March 25, 2014 and no working longitudinal gauges past July 2014.

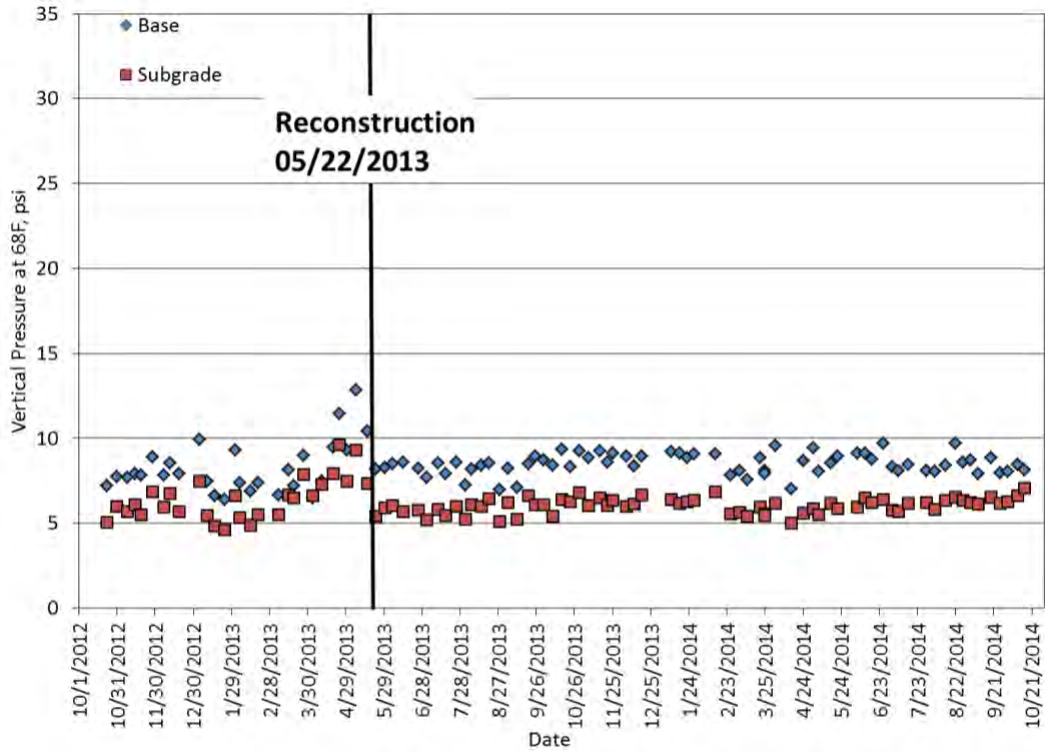


Figure 19 Section S5 (High RAP) Vertical Pressure

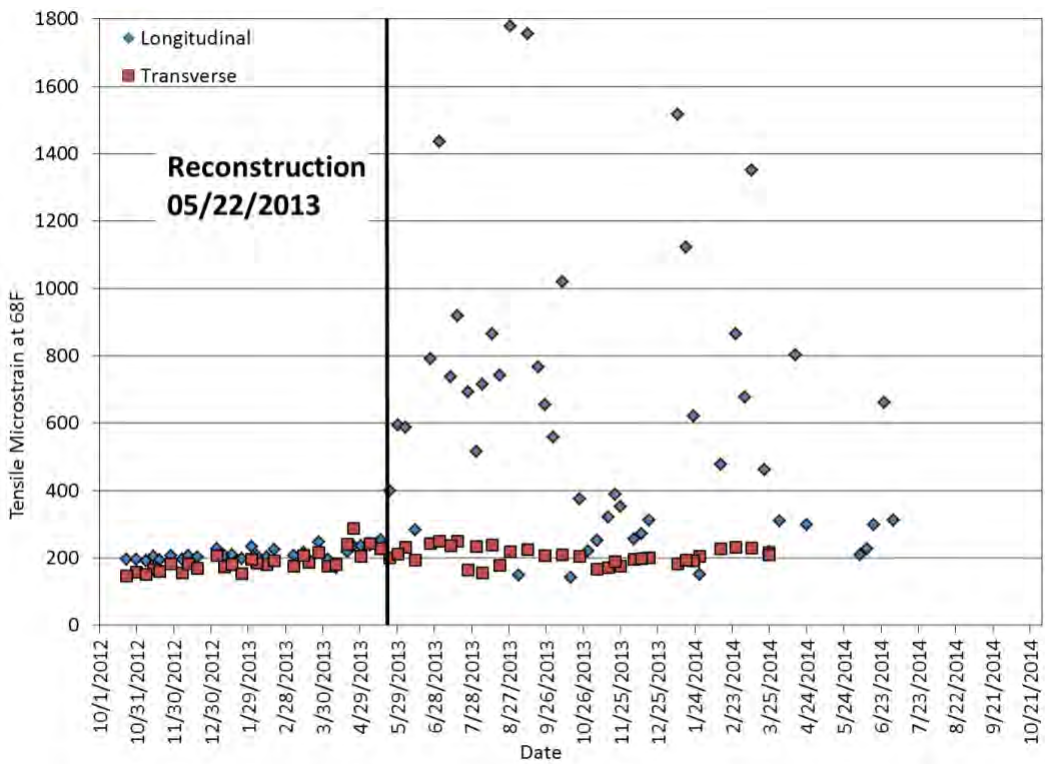
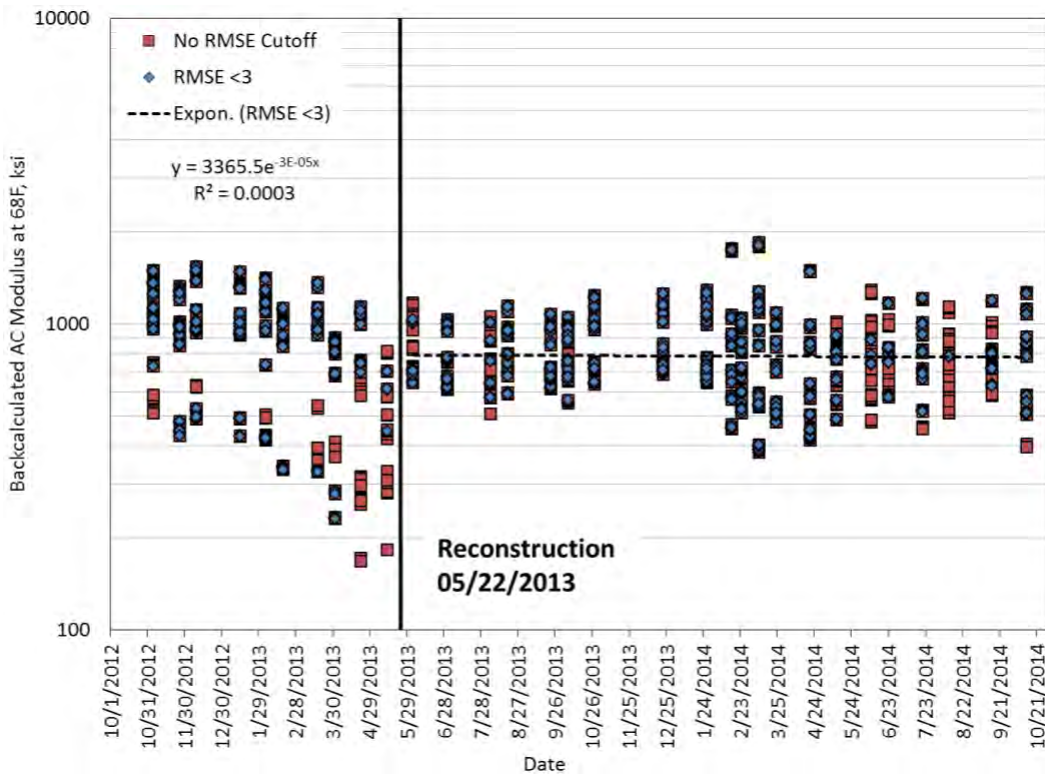


Figure 20 Section S5 (High RAP) Horizontal Strain

**Backcalculated Moduli.** It can be seen in the temperature-corrected backcalculated asphalt moduli versus time plot, presented in Figure 21, that the asphalt pavement stiffness was decreasing with traffic from the beginning of traffic until reconstruction, indicating accumulated damage to the pavement structure. The backcalculated moduli also had greater variability prior to reconstruction. After reconstruction, the modulus stayed relatively constant as shown by the low  $R^2$ .



**Figure 21 Section S5 (High RAP) Backcalculated FWD Results**

**Forensic Investigation.** Cores were taken from Section S5 (High RAP) in early April 2013 to help identify the cause of the observed cracking in the original construction. The cores shown in Figures 22, (a) and (b), were taken at locations with various levels of surface cracking to capture the crack progression. Figure 22 (b) is provided to highlight the cracking discussed in this section. Beginning at the left side of Figure 22, in core A the interface between the intermediate and base lift is visible, but intact. In core B, debonding along the same interface can be seen. In core C, a middle-up crack has originated and is propagating towards the surface. The crack has reached the surface in core D and in core E there are cracks throughout the entire core.



Figure 22 (a) Cores Taken from Section S5 (High RAP) in April 2013



Figure 22 (b) Cores Taken from Section S5 (High RAP) in April 2013 (Cracks and Debonding Highlighted)

The cause of debonding between the intermediate and base lift was investigated, but no specific factor was identified. As previously mentioned, the same non-tracking tack was applied between all pavement lifts at a calibrated application rate of 0.05 gal/yd<sup>2</sup>. Videos of the construction did not indicate any issues.

**Simulations.** To further investigate the observed debonding and the impact it had on pavement response, the pavement structure was modelled using the linear elastic analysis program, WESLEA. This approach allowed analysis at different points in the pavement structure with various interface bonding conditions. A 21,000 lb. single axle with dual tires on each side of the axle was used in all simulations to represent the Test Track truck single axles. This weight represented the average single axle weight rounded to the nearest 1,000 lb. The resulting shear stress and horizontal strain were examined under each wheel, at the edge of the wheel, and between wheels on the same side of the axle. The results presented in this section are from between the wheels because at this location the peak shear stress coincides with the interface between the intermediate and base lift. Backcalculated values for the base and subgrade moduli were used in the model. The modulus of each asphalt layer was obtained from dynamic modulus testing (AASHTO TP-79) and was used as the input for each asphalt layer.

Figure 23 (a) and 23 (b) show the WESLEA simulation results. In Figure 23 (a), it can be seen that the location of maximum shear stress (approximately 12 psi) is at the same depth as the interface between the intermediate and base lift. Figure 23 (b) depicts the section after this interface has slipped or lost its bond. In the fully bonded condition, the maximum horizontal microstrain occurs at the bottom of the base lift and has a magnitude below 150  $\mu\epsilon$ . The base lift utilized a PG 94-28 polymer modified asphalt binder because it was intended to be a strain tolerant lift. Once the lower interface is slipped, the location of the maximum horizontal microstrain moves to the bottom of the intermediate lift and the magnitude increases to around 200  $\mu\epsilon$ . The intermediate

lift was designed to be a stiff strain-reducing lift and was not intended to be subjected to the high strains seen after debonding between the intermediate and base lifts.

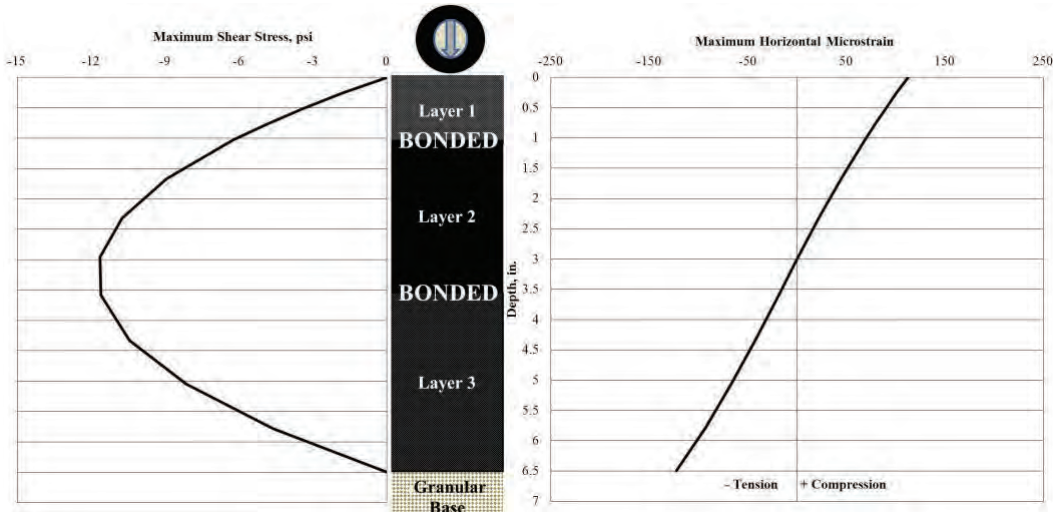


Figure 23 (a) WESLEA Simulation of Section S5 (High RAP) in Fully Bonded Condition (1)

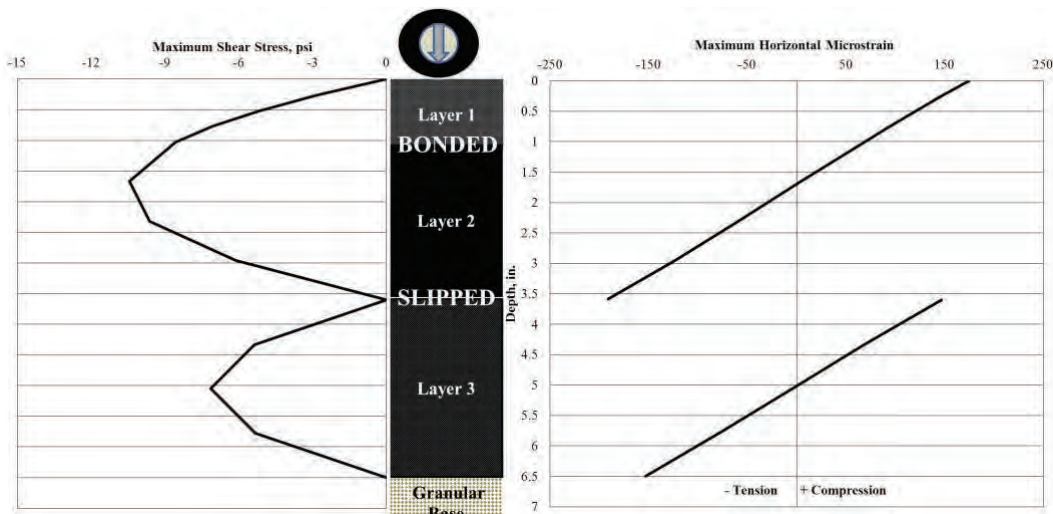


Figure 23 (b) WESLEA Simulation of Section S5 (High RAP) in Partial-Slip Condition (1)

**Bending Beam Fatigue.** The fatigue properties of the intermediate and base lifts were investigated to further validate that after the lower interface began to debond the less strain tolerant intermediate lift was subjected to high strain levels, resulting in rapid failure. Bending beam fatigue testing (BBFT) was conducted on loose mix samples collected during construction, reheated in the laboratory, and compacted into beams for testing according to AASHTO T 321-07. It can be seen in the results displayed in Figure 24 that the base lift has a less steep slope indicating better fatigue performance. The intermediate lift was only tested at 200 and 400  $\mu\epsilon$  based on the expectation in the planning phase of the experiment that the intermediate lift would not be subjected to high strains, thus strains beyond 400 would be unrealistic.

Useful insight into the rapid failure progression was gained by inputting the expected strain levels in each bonding condition from the linear elastic analysis into the fatigue equations generated from BBFT. Equation 1 was used to estimate the number of cycles to failure ( $N_f$ ) at a given strain level ( $\varepsilon$ ) using the coefficients ( $\alpha_1$  and  $\alpha_2$ ). In the fully bonded condition, the maximum strain was around 125  $\mu\varepsilon$  located at the bottom of the base lift. At this strain level, the base lift is expected to withstand  $8.43 \times 10^{10}$  cycles before fatigue failure. The intermediate lift is expected to withstand  $9.69 \times 10^{10}$  cycles before fatigue failure at the strain level from the fully bonded condition, 25  $\mu\varepsilon$  (strain at the bottom of the intermediate lift in Figure 23 (a)). In the slipped condition, the intermediate lift is subject to 200  $\mu\varepsilon$  and is then only expected to withstand  $3.63 \times 10^6$  cycles. Although this method is an approximation, it clearly shows that there are significant, multiple orders of magnitude, differences in the fatigue properties of each lift. The rapid progression of cracking after the first crack was observed was likely due to the low strain tolerance of the intermediate lift and the high strain levels it was subjected to after debonding occurred.

$$N_f = \alpha_1 \left[ \frac{1}{\varepsilon} \right]^{\alpha_2} \quad (1)$$

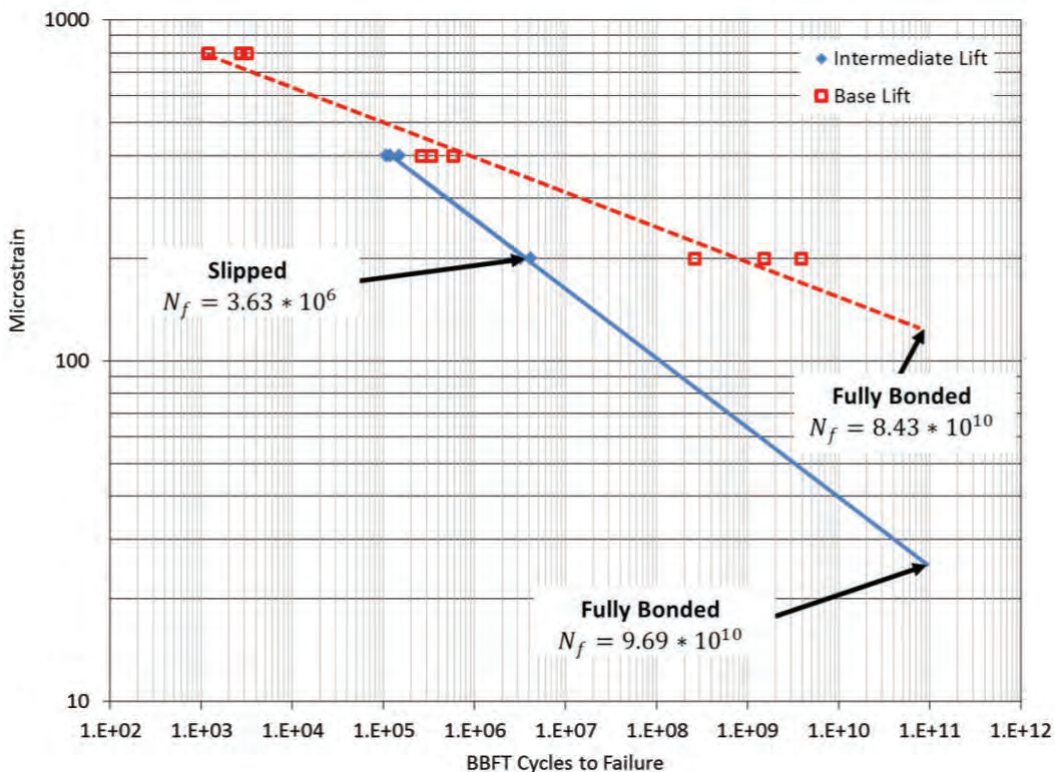


Figure 24 BBFT Results for Section S5 (High RAP) (1)

#### S6 – RAP/RAS

**Performance.** The performance timeline for Section S6 (RAP/RAS) is provided in Figure 25. The first crack in this section was observed in late June 2013. It can be seen in Figures 26 and 27 that the rut depth and IRI, respectively, begin to increase at this time. On October 15, 2013 the right

wheel path was patched in the last half of the section as well as an area over the instrumentation array. In early April 2014, the top 1.75 inches were removed and replaced with a high polymer modified binder mix. The impact of the patch and rehabilitation can be seen in the rutting and IRI plots. Although surface conditions were initially improved by maintenance and rehabilitation, the section reached and surpassed the pre-maintenance distress levels more quickly than after original construction. The effect of the maintenance and rehabilitation activities on the pavement's structural responses is discussed more in the following section.

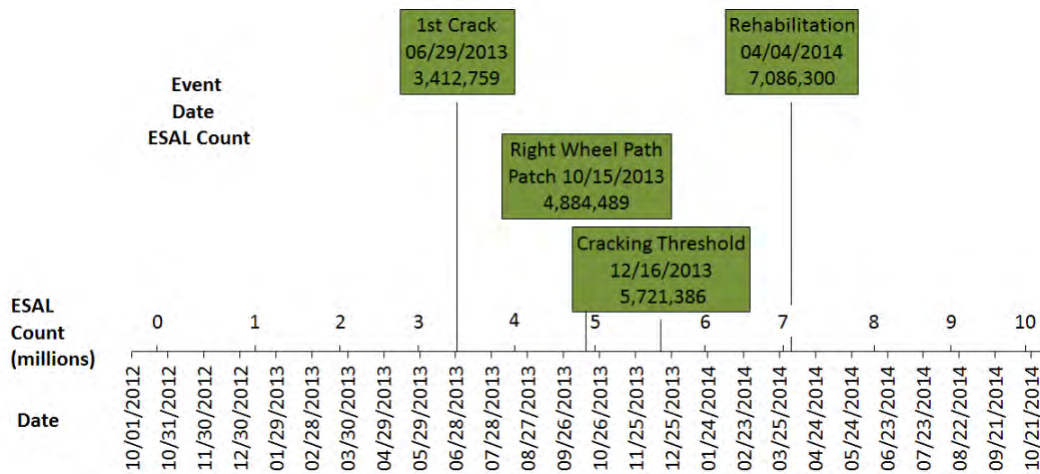


Figure 25 Section S6 (RAP/RAS) Performance Timeline

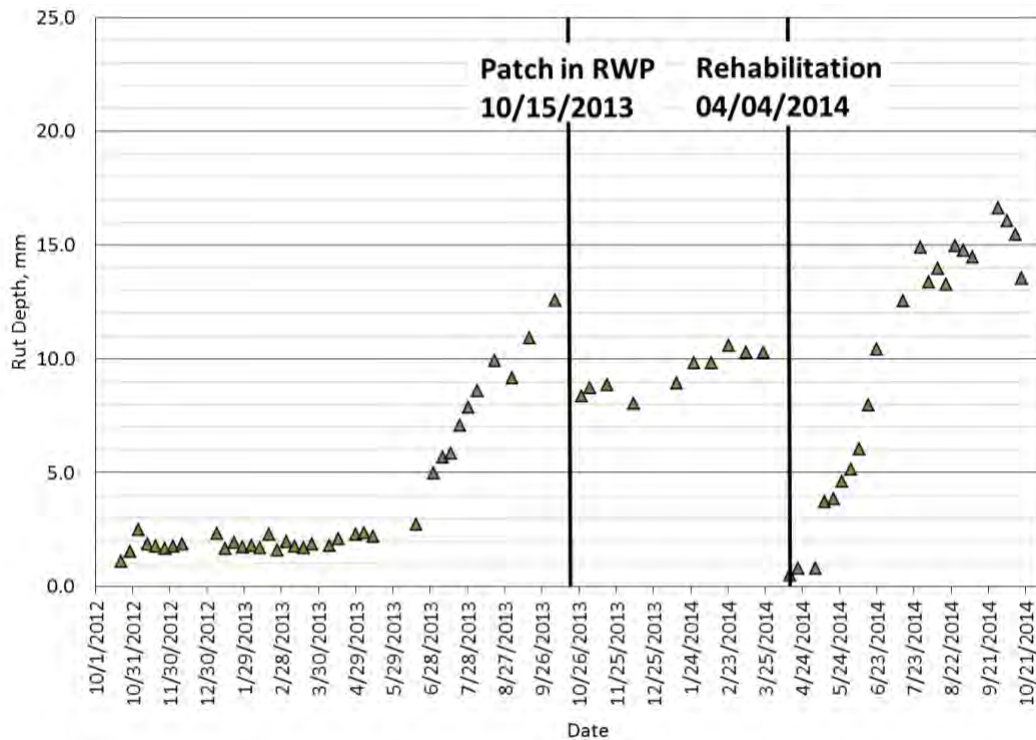
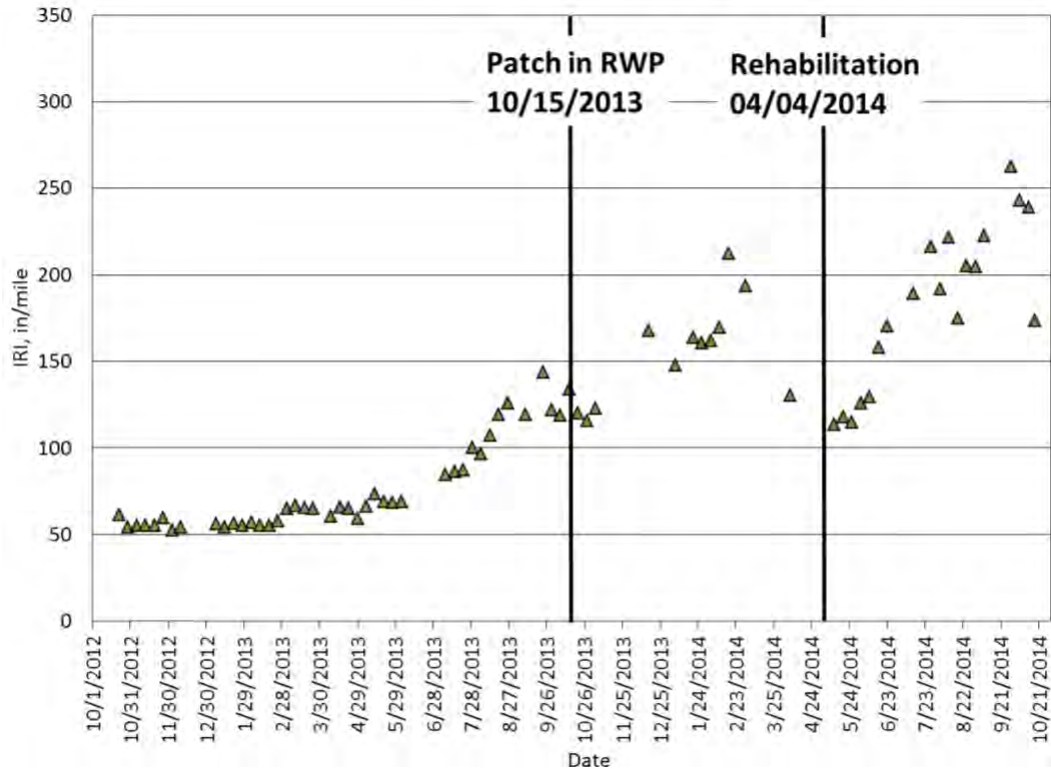


Figure 26 Section S6 (RAP/RAS) Rutting Performance



**Figure 27 Section S6 (RAP/RAS) Surface Performance**

**Strain/Pressure Measurements.** The measured temperature-corrected vertical pressures and horizontal strains are presented in Figures 28 and 29, respectively. In Figure 28, both the base and subgrade pressures were stable from the beginning of traffic through April 2013. From April 2013 through September 2013 the pressure levels steadily increased until patching was completed in October 2013. The pressures were fairly stable after patching, through March 2014. After rehabilitation on April 4, 2014 the measured subgrade pressure was greater than the base pressure. This unexpected behavior (subgrade pressure being greater than the base pressure) may be attributed to different distress levels in the asphalt above each pressure plate, spaced 12 feet apart, or possibly damage to the instrumentation itself.

In Figure 29, the longitudinal and transverse strains both steadily increased prior to rehabilitation as illustrated by the trend line. Initially there was some separation between the strain levels for longitudinal and transverse gauges however as traffic continued and damage accrued in the section there were times when the longitudinal strain was less than the transverse. After rehabilitation, all of the longitudinal strains were less than the transverse strains. This is an indication that damage has occurred in the pavement because the section is behaving differently than it did in the initial, undamaged condition.

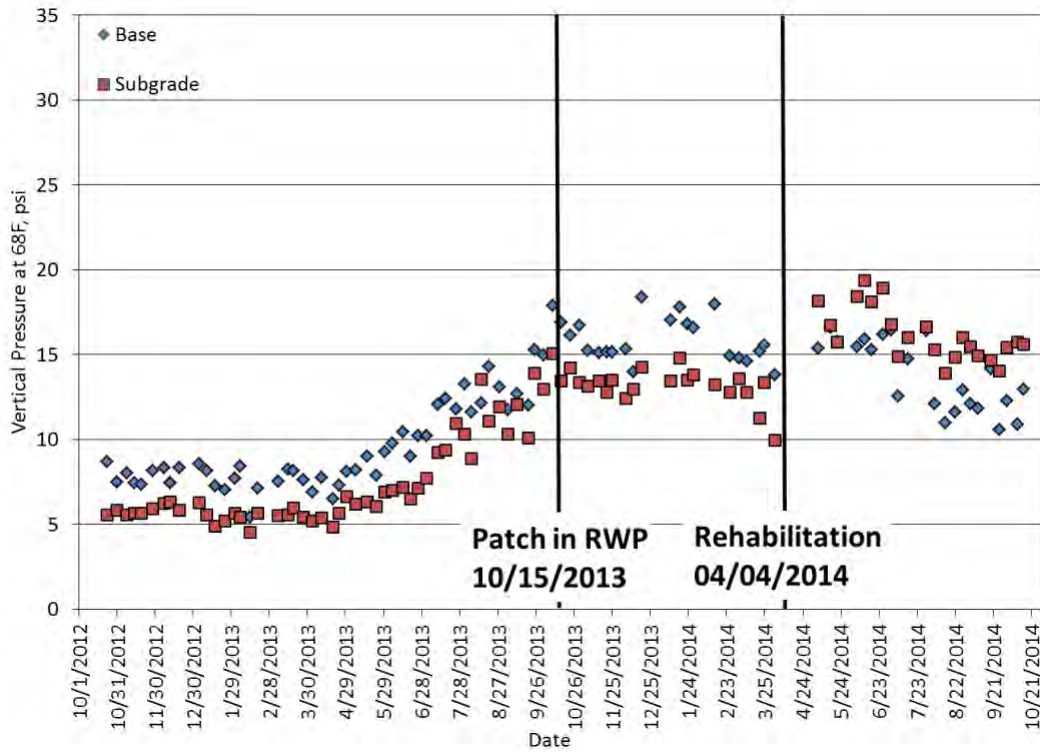


Figure 28 Section S6 (RAP/RAS) Vertical Pressure

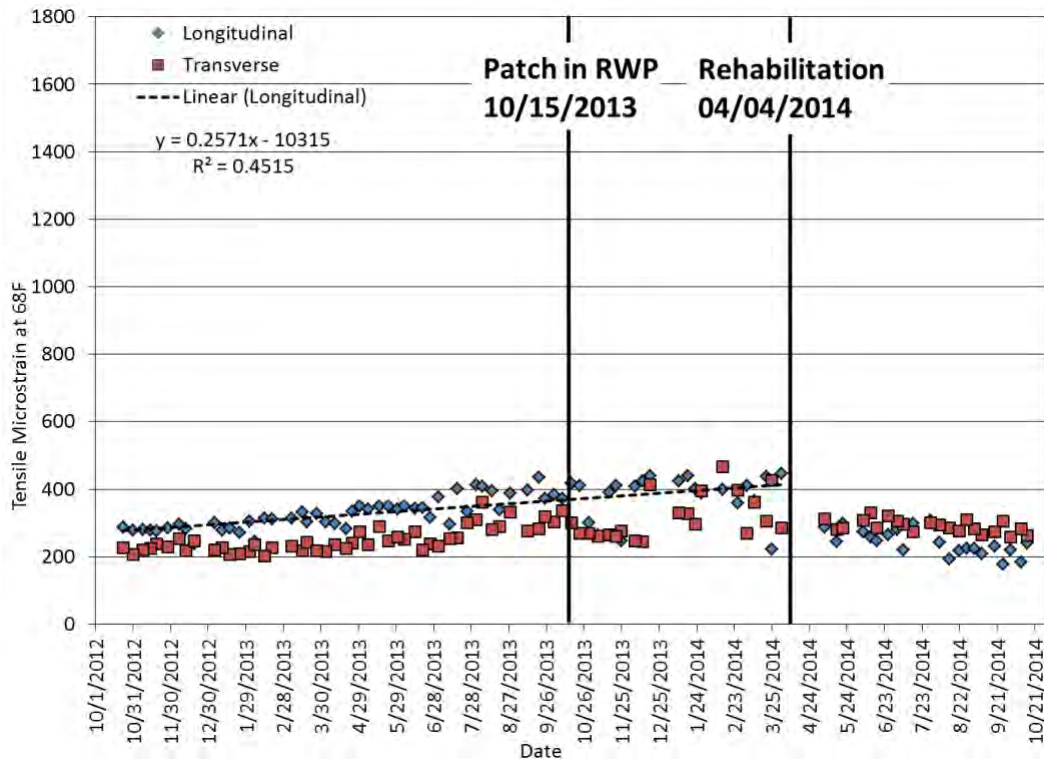
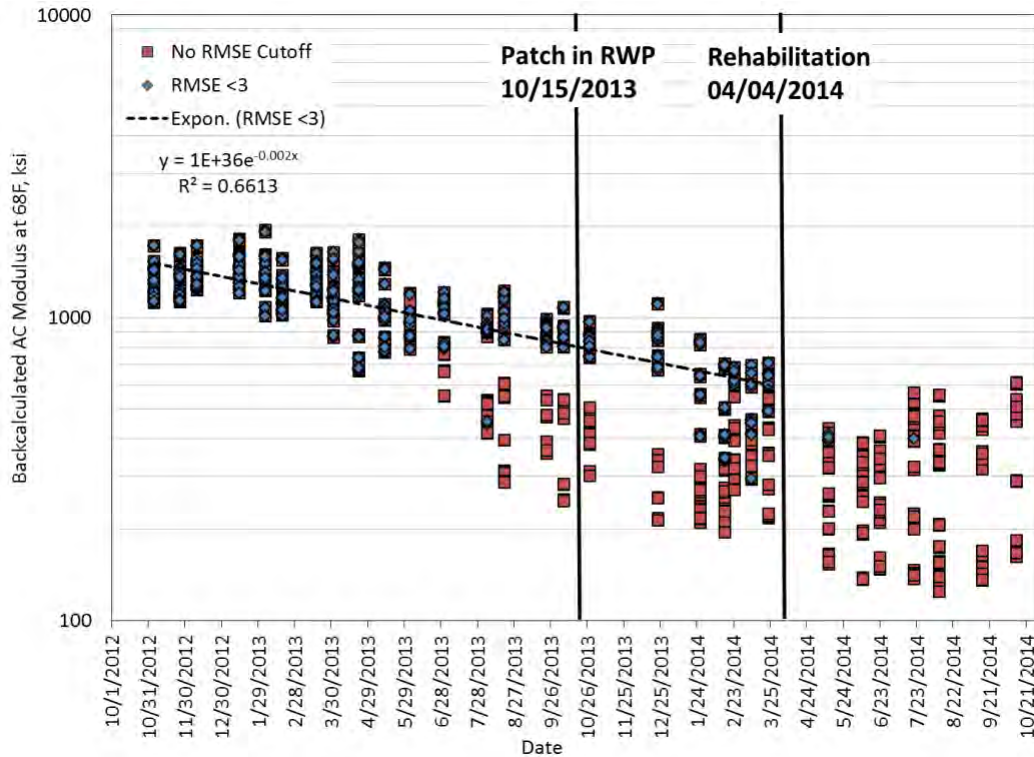


Figure 29 Section S6 (RAP/RAS) Horizontal Strain

**Backcalculated Moduli.** It can be seen in the temperature-corrected backcalculated modulus plot (Figure 30) for Section S6 (RAP/RAS) that the moduli values were relatively stable until around the time the first crack was observed in June 2013. After June 2013, the number of data points with an RMSE above 3% increased. After rehabilitation on April 4, 2014, only two data points had an RMSE below 3%. Again, this is a strong indication that the rehabilitation did not fully improve the entire structure.



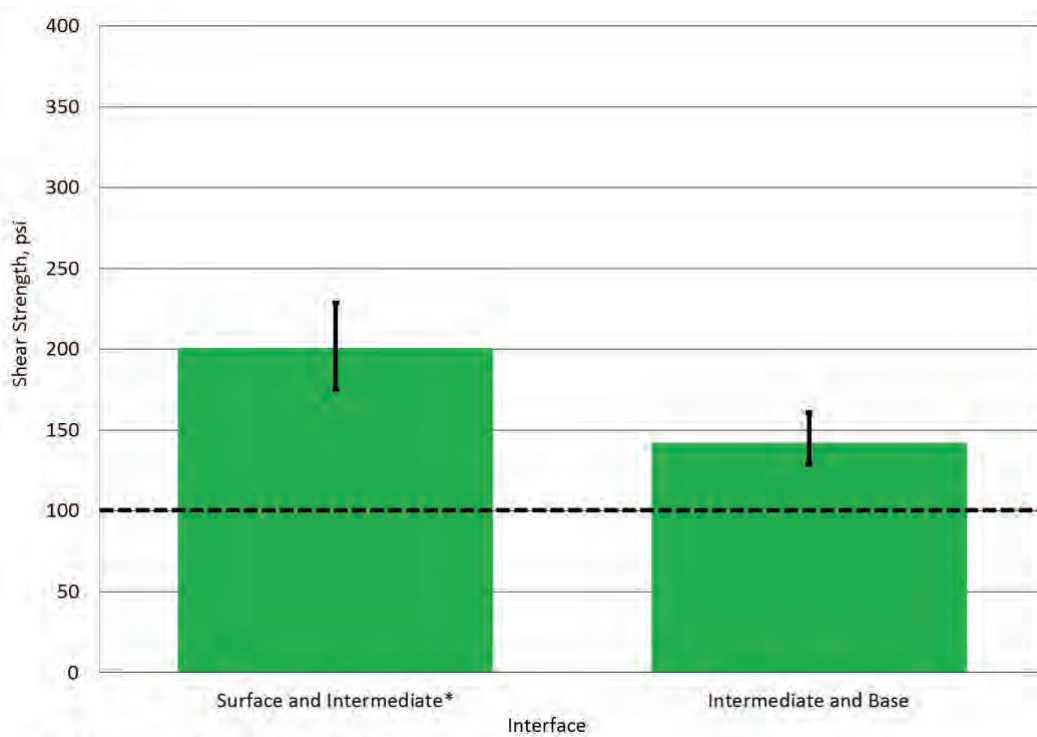
**Figure 30 Section S6 (RAP/RAS) Backcalculated FWD Results**

**Forensic Investigation.** Cores were taken from Section S6 (RAP/RAS) on September 9, 2013. Again, cores were taken from locations within the section with various levels of surface distress to capture the cracking progression/distribution within the section. One of the cores was debonded at the interface between the intermediate and base lift, as seen in middle core shown in Figure 31. It is unknown whether the debonding occurred prior to the coring or during the coring process (torque from drill rig). Other cores were obtained intact but the interface between the intermediate and base lift showed signs of cracking and flushing.



**Figure 31 Cores Taken from Section S6 (RAP/RAS) in September 2013 (1)**

Additional cores were taken from between the wheelpaths for interface bond strength testing. Bond strength testing was done following the procedure developed at NCAT for the Alabama Department of Transportation (ALDOT) (5). As shown in Figure 32, the shear strength at both interfaces was above the threshold of 100 psi. The interface between the intermediate and base lift had lower bond strength and was the interface that showed debonding during coring.



\*3 of 5 breaks had small pieces of mix stuck to interface

**Figure 32 Bond Strength Testing Results for Section S6 (RAP/RAS)**

**Simulations.** The same linear elastic analysis discussed previously for Section S5 (High RAP) was applied to the structure of Section S6 (RAS/RAP). Figure 33 shows the shear stress and horizontal strain distribution with depth between the wheel loads on one side of a 21,000 lb. single axle. It can be seen in Figure 33 (a) that in the fully bonded condition, the peak shear stress is located just above the lower interface (the interface between the base and intermediate lifts). In this condition, the maximum strain is less than 150  $\mu\epsilon$  and is located at the bottom of Layer 3. When the lower interface is slipped, as shown in Figure 33 (b), the location of maximum strain moves to bottom of layer two and increases to over 250  $\mu\epsilon$ .

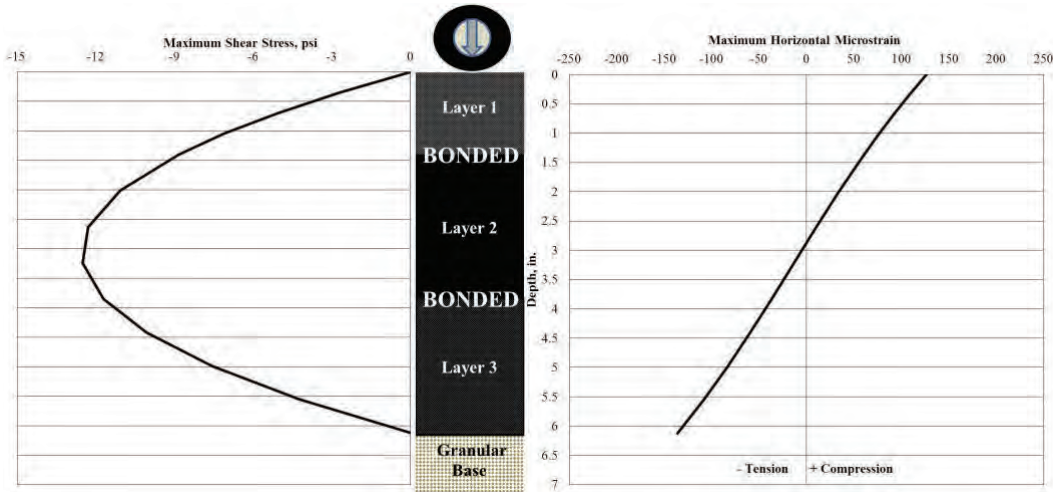


Figure 33 (a) WESLEA Simulation of Section S6 (RAP/RAS) in Fully Bonded Condition (1)

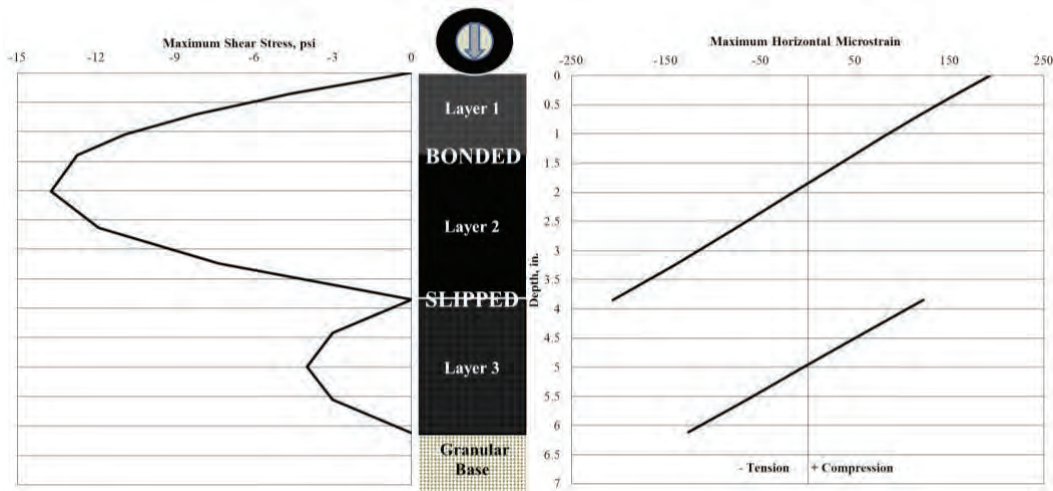


Figure 33 (b) WESLEA Simulation of Section S6 (RAP/RAS) in Fully Bonded Condition (1)

*S13 – GTR*

**Performance.** As shown in the performance timeline in Figure 34, Section S13 (GTR) did not crack until the end of July 2013. The cracking threshold (cracking in greater than 25% of the lane area) was reached in October 2013. The top 1.75 inches were removed and replaced on April 24, 2014.

The temporary benefit of the rehabilitation can be seen by the improvement in rut depths and IRI shown in Figures 34 and 35, respectively. In Figures 35 and 36, data points from April 2014 prior to the rehabilitation line, were recorded on a temporary overlay and not the final rehabilitated surface. The rehabilitation date listed, April 24, 2014, is the date of the final maintenance work.

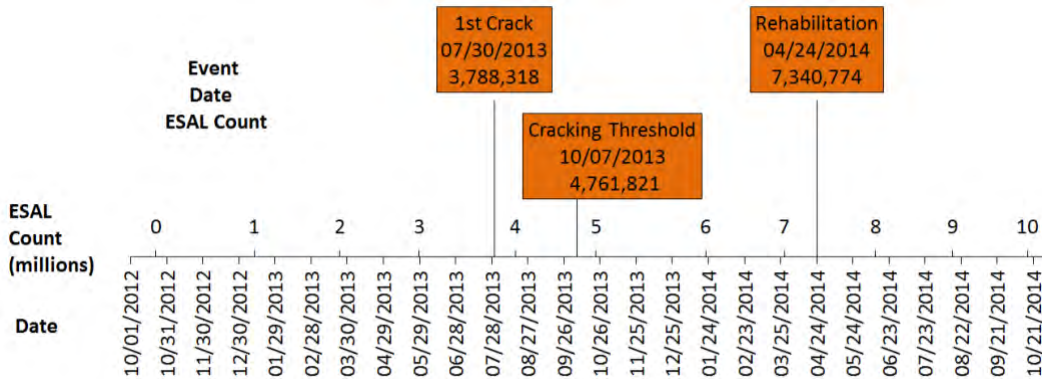


Figure 34 Section S13 (GTR) Performance Timeline

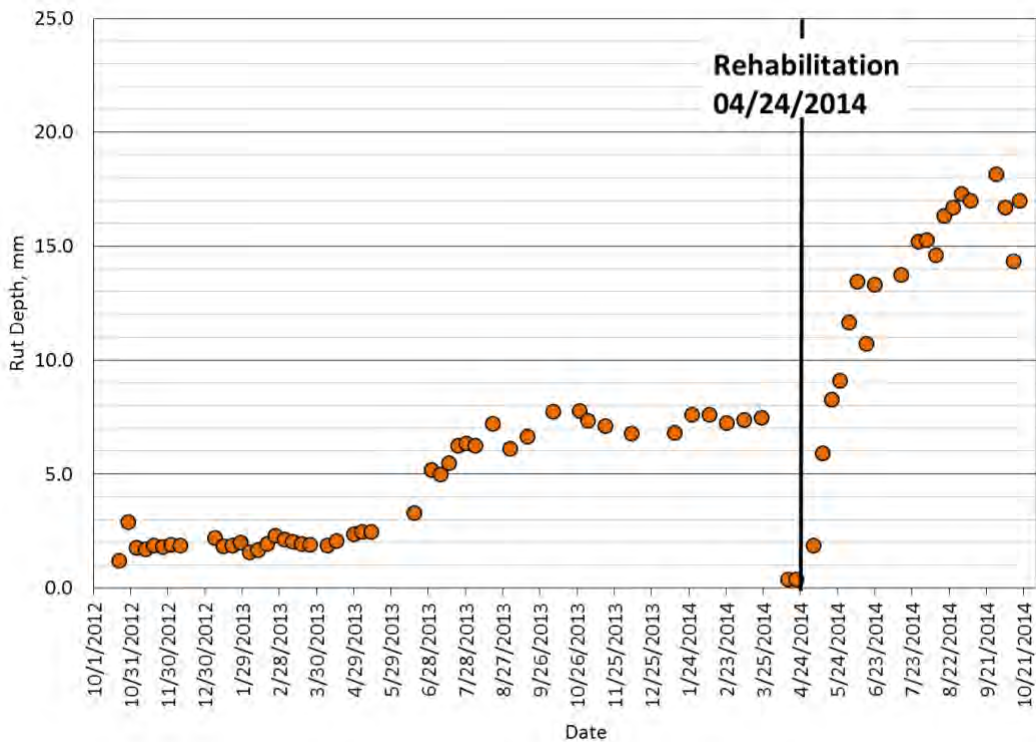
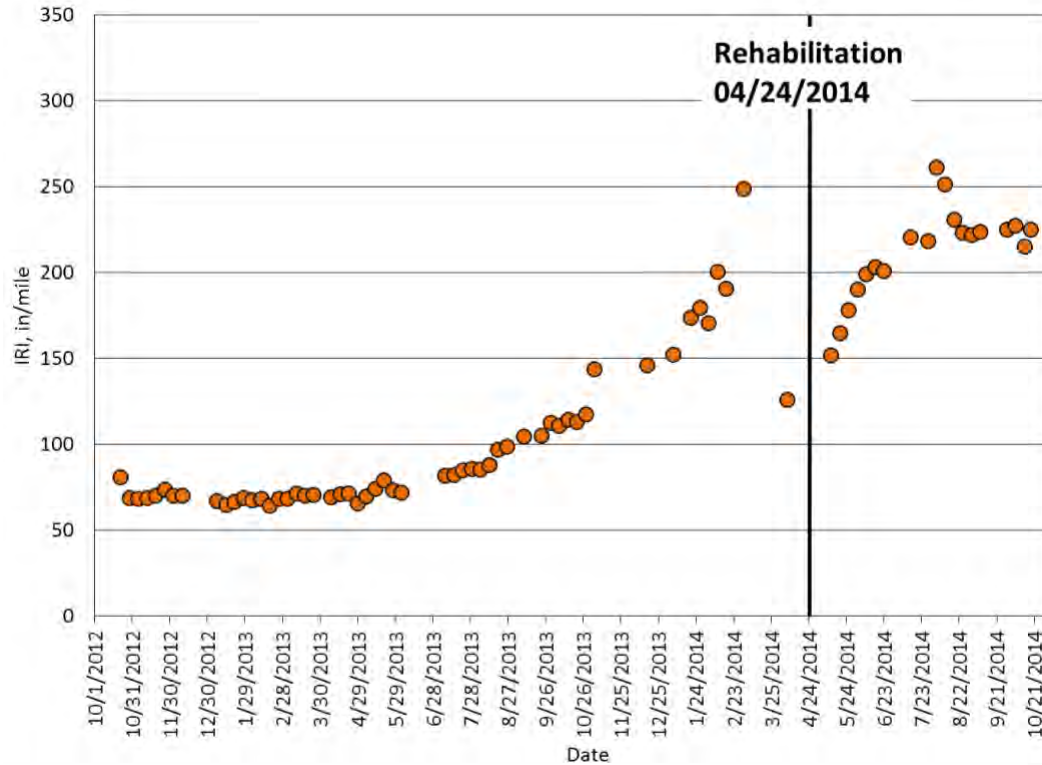
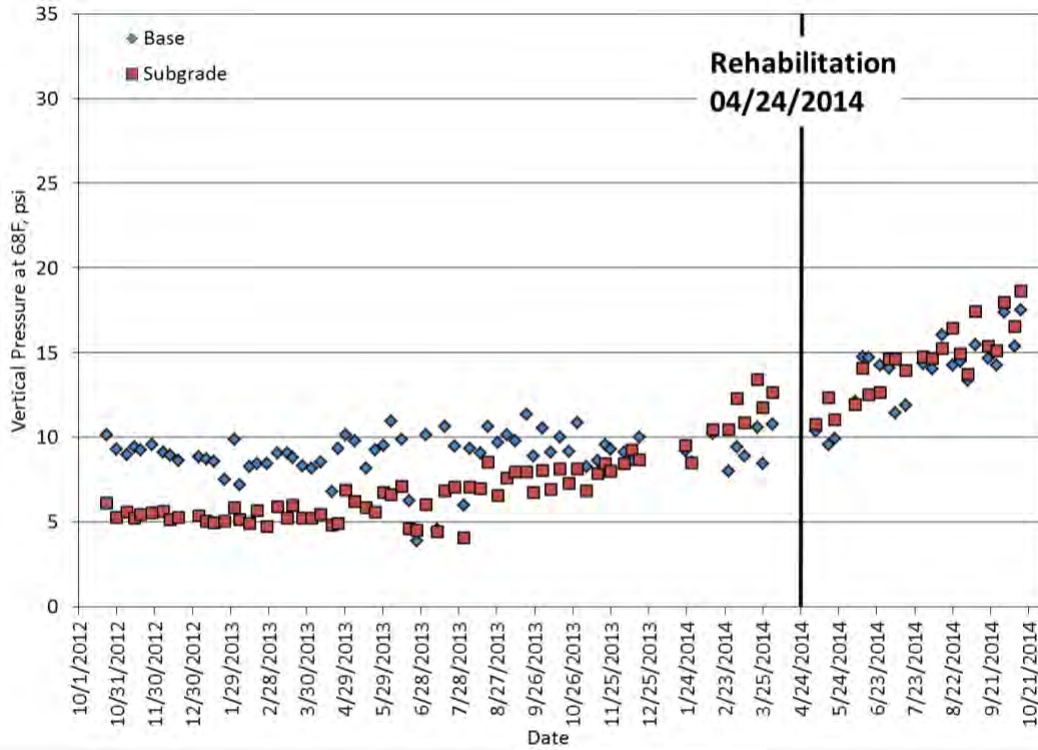


Figure 35 Section S13 (GTR) Rutting Performance



**Figure 36 Section S13 (GTR) Surface Performance**

**Strain/Pressure Measurements.** It can be seen in Figure 37 that the temperature-corrected vertical pressures were fairly constant early in the research cycle. The subgrade pressure steadily increased beginning in summer 2013. By January 2014, the subgrade pressure was higher than the base pressure. After rehabilitation, the base and subgrade pressures both showed an increasing trend. These observations are consistent with the performance data presented above in that distress began to initially accrue and was not fully rectified by the rehabilitation.



**Figure 37 Section S13 (GTR) Vertical Pressure**

The transverse and longitudinal strains at a reference temperature of 68°F are provided in Figure 38. The longitudinal started below 300  $\mu\epsilon$  in October 2012 and steadily increased to almost 500  $\mu\epsilon$  by the end of the research cycle. The transverse strain followed a similar trend; it began the research cycle around 200  $\mu\epsilon$  and ended around 400  $\mu\epsilon$ . The strain responses increased consistently throughout the research cycle despite the rehabilitation. Again, this is indicative of pavement damage development not fully being rectified by the 1.75-inch rehabilitation.

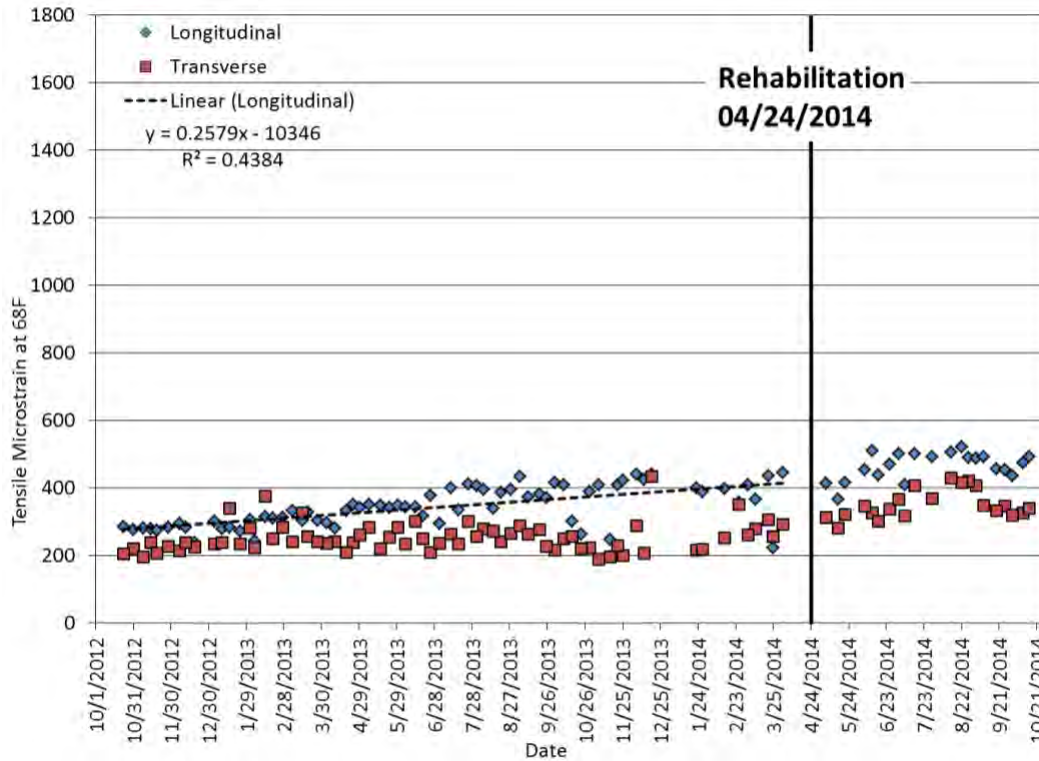


**Figure 38 Section S13 (GTR) Horizontal Strain**

**Backcalculated Moduli.** The backcalculated AC moduli at 68°F are presented versus time in Figure 39. It can be seen that prior to rehabilitation, the modulus was decreasing with time and traffic, as illustrated by the trend line. There were no data points with an RMSE less than 3% during June, July or August, indicating that the rubber-modified mixtures used in this section is causing the pavement to not behave in a linear elastic fashion under the high summer temperatures. After rehabilitation, there were no data points with an RMSE less than 3% even during the cooler fall months. Therefore, the lack of data points with an RMSE below 3% is likely a combination of damage in the structure and the unique material response at high temperatures.

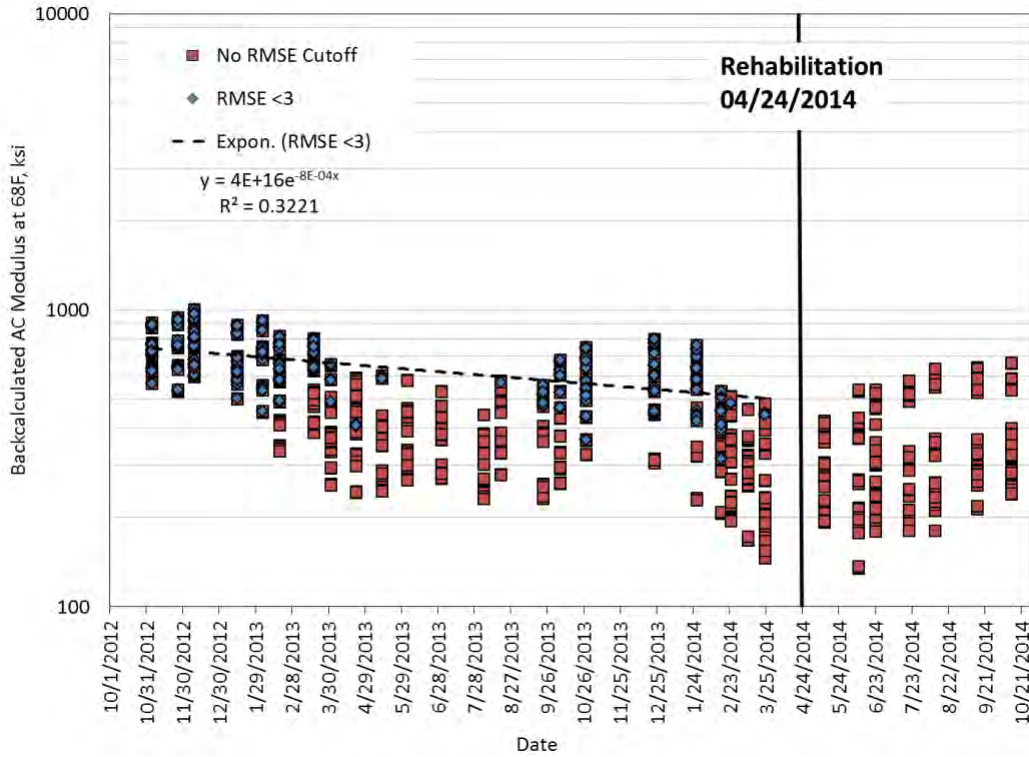


**Figure 39 Section S13 (GTR) Backcalculated FWD Results**

**Forensic Investigation.** Cores were removed from Section S13 (GTR) for visual inspection and bond strength testing on September 9, 2013. One of the cores was removed in two pieces, as shown in Figure 40. Rather than debonding occurring at one of the interfaces, the break was within the intermediate layer and nearly horizontal.



**Figure 40 Core Taken from Section S13 (GTR) in September 2013 (1)**

**Bond Strength Testing.** Bond strength testing was conducted on each of the interfaces of cores taken from between the wheelpaths. The results are provided in Figure 41. All of the intermediate and base lift specimens did not break cleanly, indicating that the interface was stronger than the mix surrounding it. The surface and intermediate lift specimens did not break cleanly either. One of the samples sheared entirely in the middle lift instead of the surface and intermediate lift interface. These observations support the idea that, for some reason, the intermediate mixture was susceptible to shearing and cracking.

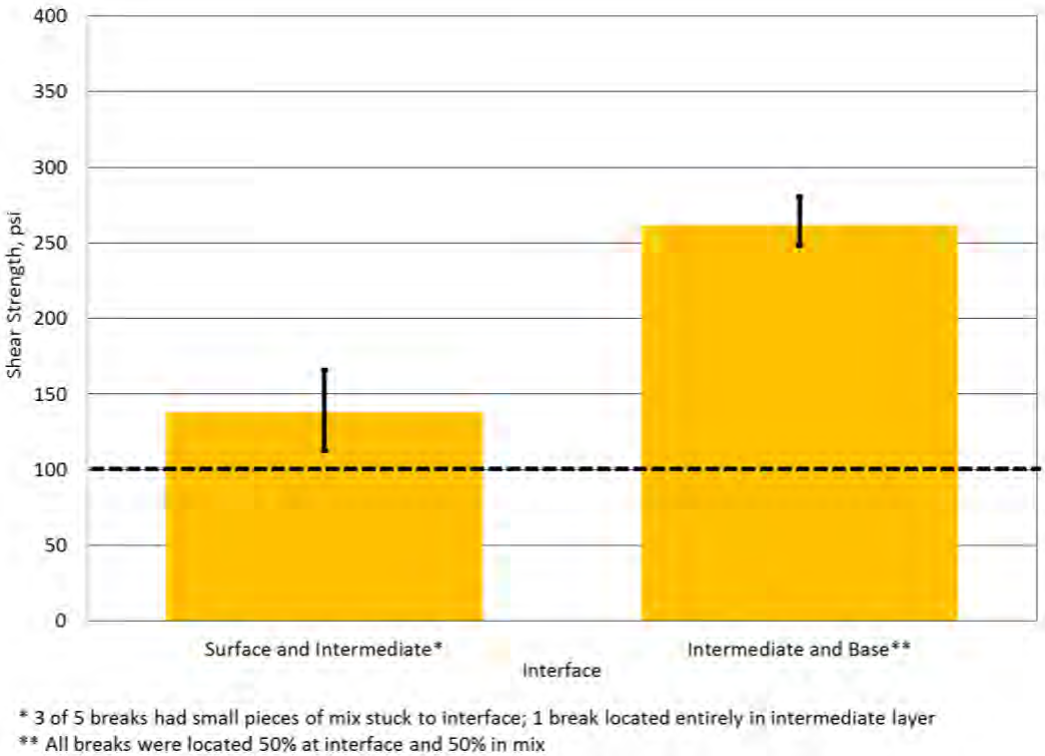


**Figure 41 Bond Strength Testing Results for Section S13 (GTR)**

**Simulations.** Section S13 was analyzed using the same linear elastic analysis discussed for Sections S5 and S6. However, since interface debonding was not observed only the fully bonded condition was simulated. In the simulation, presented in Figure 42, the maximum shear stress is located at the same location of the observed shearing in the cores and bond testing.

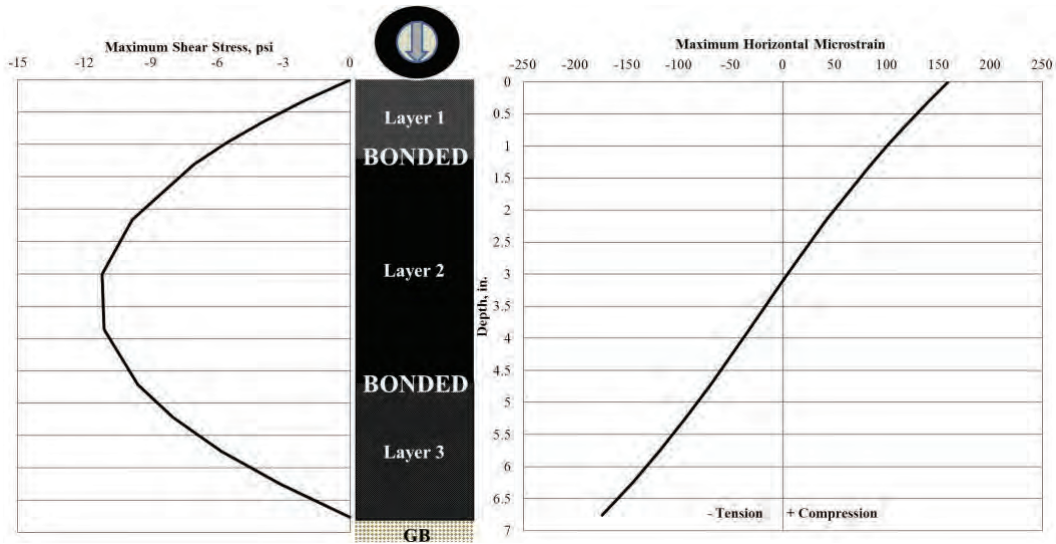


**Figure 42 WESLEA Simulation of Section S13 (GTR) in Fully Bonded Condition (1)**

*Summary*

For comparisons of performance among the Green Group experiment test sections, it is important to keep in mind that the experiment was designed to develop significant distresses within this research cycle. In the following discussion, the reconstructed Section S5 (High RAP) is also presented for better comparison.

The cracking performance for the GG experiment is summarized in Figure 43. Excluding the initial failure in S5, each of the sections performed better than the conventional pavement in Section N5. Section S6, using an SMA mix containing recycled shingles, a stiff intermediate layer containing a combination of RAS and RAP, and a fatigue resistant rich-bottom layer with 25% RAP and a PG 76-22 binder, withstood 39% more ESALs than N5 before reaching the cracking threshold. Section S13, using a GTR modified SMA surface, a GTR modified intermediate layer, and an Arizona-style gap-graded asphalt-rubber mix for the fatigue resistant bottom layer, withstood 17% more ESALs until the cracking threshold than N5.

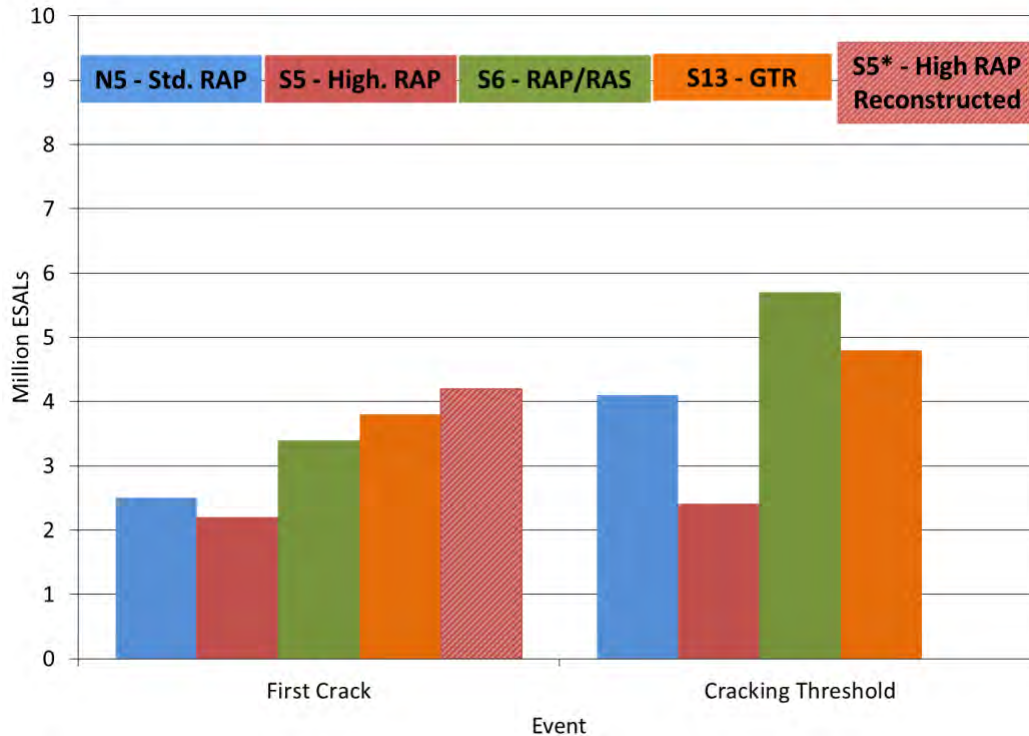
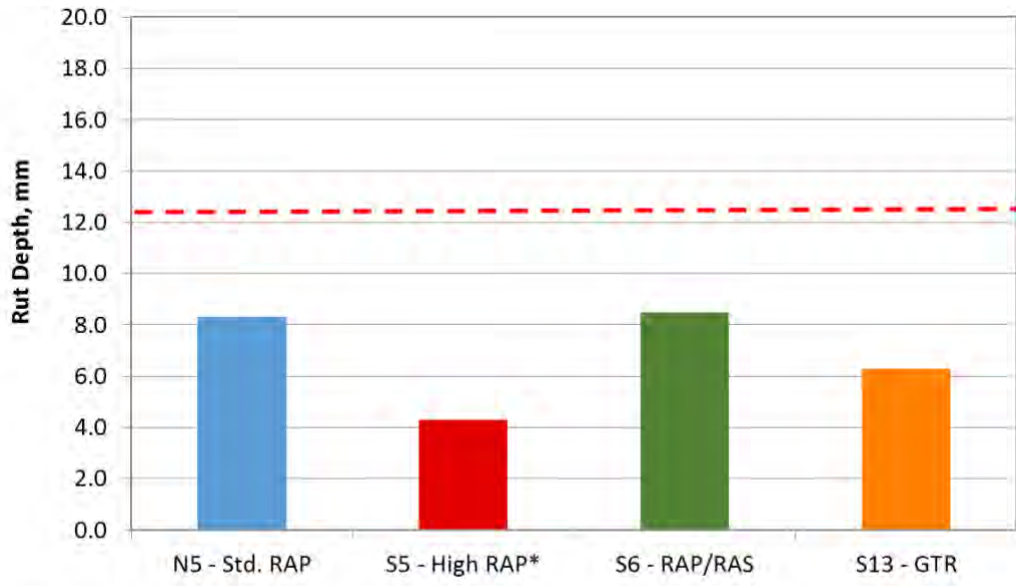


**Figure 43 Green Group Cracking Comparison**

The rutting and changes in roughness after 4 million ESALs are compared in Figures 44 and 45, respectively. For a pre-maintenance comparison, 4 million ESALs was selected because Section N5 (Standard RAP) reached the cracking threshold around 4 million ESALs and maintenance activities began to occur shortly thereafter. For these comparisons, the reconstructed Section S5 (High RAP) is presented. However, it must be kept in mind that this section was constructed and subjected to the start of traffic at a different time of year than the other sections.

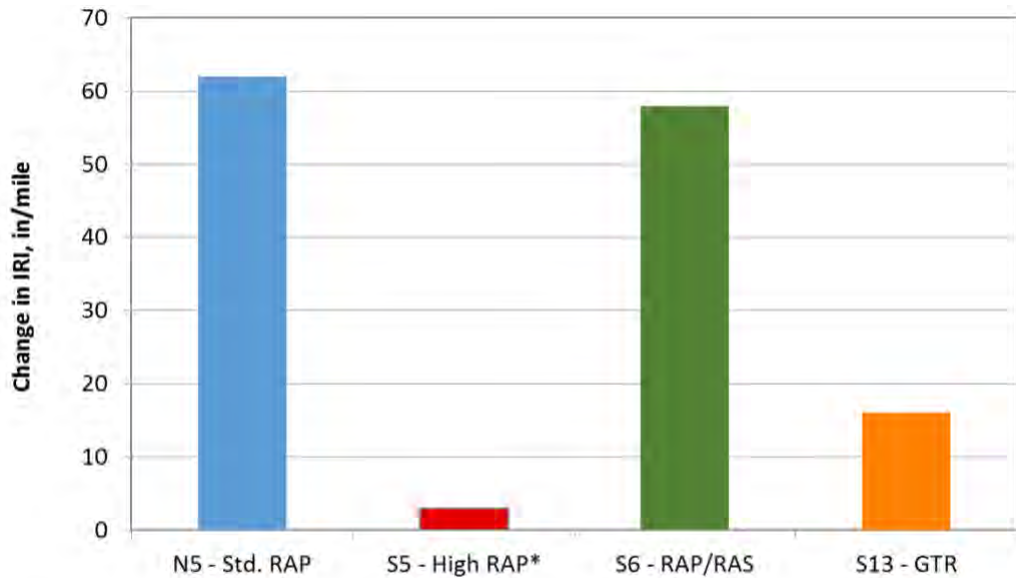
The rut depths at 4 million ESALs are below the rutting threshold of 12.5 mm, as indicated by the dashed line in Figure 44. Thus, the largest rut depths measured over the cycle occurred after cracking had originated in the sections. Section S6 (RAP/RAS) had similar rut depths to Section N5 (Standard RAP). Section S13 (GTR) had around 2.0 mm less rutting than N5 and the reconstructed Section S5 (High RAP) had around 4.0 mm less rutting than N5.



\*S5 - High RAP = Reconstructed

**Figure 44 Rut Depth After 4 Million ESALs**

The change in IRI over the same 4 million ESALs used for the rutting comparison is shown in Figure 45. The sections had different initial IRI levels; therefore, the change in IRI was used for this comparison. The largest changes in IRI were in Sections N5 (Standard RAP) and S6 (RAP/RAS). Although Section S13 (GTR) eventually had similar maximum IRI values as N5 and S6, S13 had a much smaller change in IRI. The reconstructed Section S5 (High RAP) had the smallest change, but this section was built and trafficked at a different time than the other sections.



\*S5 - High RAP = Reconstructed

**Figure 45 Change in IRI After 4 Million ESALs**

### *Conclusions and Lessons Learned*

The 2012 Green Group Experiment provided useful insights into pavements built to optimize recycled materials in asphalt mixes designed for engineering characteristics desired in specific layers of the pavement structure. The following conclusions can be drawn.

- Asphalt mixes designed and produced using recycled materials such as RAP, RAS, and GTR can provide enhanced characteristics that are beneficial for long lasting pavements.
  - Three SMA mixes were produced; one containing 25% RAP, a second containing 5% RAS, and a third containing a GTR modified binder. Each of these mixes had excellent rutting resistance in the field and laboratory tests. The Energy Ratio results indicated that the SMA mix with GTR modified binder was marginally susceptible to top-down cracking. Although none of the test sections had any signs of top-down cracking during the cycle, more traffic and time would be necessary to determine if the Energy Ratio provides a good indication of the durability for the surface layers.
  - High stiffness dense-graded mixtures were produced and constructed as intermediate layers to reduce tensile strains in the bottom of the asphalt pavement and vertical pressures in the base and subgrade. Despite the higher RAP content in the intermediate mix for S5, its  $E^*$  was similar to that of the conventional 35% RAP mix in N5. The S6 intermediate mix containing 25% RAP and 5% RAS did have a higher  $E^*$ , particularly at higher temperatures. At low frequencies and high temperatures, the  $E^*$  for the S13 intermediate mix containing 35% RAP and a GTR modified binder was higher than the N5 mix, but it was less stiff at low temperatures. More research is needed to optimize the stiffness and recycled materials content for high modulus layers.
  - Making asphalt base layers more fatigue resistant can be achieved by using recycled materials in combination with highly modified binders, a rich bottom mix design approach, or high asphalt rubber contents.
- It was not possible to isolate the impact of each mix variable on overall performance due to the variety of mixes used in each test section. However, this experiment demonstrated that there are multiple ways to utilize recycled materials to enhance the performance of asphalt pavements.
- Backcalculated moduli, and strain and pressure measurements were useful in indicating extent of pavement damage and structural effectiveness of maintenance activities.
- Application of the concepts used in this report in actual projects must include appropriate thickness designs for the actual traffic, environment, and soil support conditions. The pavement thicknesses used in this experiment were intentionally set too thin so that distresses would be evident within one cycle.
- After taking multiple corrective actions in the reconstruction process, Section S5 (High RAP) performed well after reconstruction. The interface debonding/ slippage failure observed in the original construction did not recur. The importance of sufficient bonding between pavement lifts should be emphasized. Further investigation into tack coats and mix compatibility should be conducted.

## References

1. Vrtis, M. C., D. Timm, and J. R. Willis. *Characterization of Resource Responsible Sections at the NCAT Test Track*. Presented at the 94th Annual Meeting of the Transportation Research Board, Washington, D.C., 2015.
2. Stonex, A., and J. M. Carusone. *Development of Mix Design Procedures for Gap-Graded Asphalt-Rubber Asphalt Concrete*. Final Report 524, FHWA-AZ-06-524, Arizona Department of Transportation, Phoenix, AZ, 2007.
3. Roque, R., B. Birgisson, C. Drakos, and B. Dietrich. Development and Field Evaluation of Energy-Based Criteria for Top-Down Cracking Performance of Hot Mix Asphalt. *Journal of the Association of Asphalt Paving Technologists*, 73, 2004, pp. 229-260.
4. Bonaquist, R. *NCHRP Report 691: Mix Design Practices for Warm Mix Asphalt*. Transportation Research Board of the National Academies, Washington, D.C., 2011.
5. West, R. C., J. Zhang, and J. Moore. *Evaluation of Bond Strength Between Pavement Layers*. NCAT Report 05-08. National Center for Asphalt Technology at Auburn University, Auburn, Ala., 2008.
6. West, R., D. Timm, R. Willis, B. Powell, N. Tran, D. Watson, M. Sakhaeifar, R. Brown, M. Robbins, A. Vargas-Nordcbeck, F. Leiva-Villacorta, X. Guo, and J. Nelson. *Phase IV NCAT Test Track Findings*. NCAT Report 12-10. National Center for Asphalt Technology at Auburn University, Auburn, Ala., 2012.

### 2.3. Virginia Department of Transportation CCPR and Stabilized Base Experiment

#### *Background and Objectives*

Cold central plant recycling (CCPR) is a process whereby the asphalt is milled from the roadway and brought to a centrally located recycling plant that incorporates recycling agents and additives into the material (1). The most common recycling agents and additives include foamed asphalt, emulsified asphalt, hydraulic cement, fly ash, and lime (2). This approach allows for material removal from the roadway so that the underlying foundation may be stabilized or replaced as needed. The reclaimed asphalt pavement (RAP) is used as a recycled layer with very little added virgin material. This process also allows for existing RAP stockpiles to be used in new construction or rehabilitation projects (1).

CCPR has not been widely used in rehabilitating asphalt pavements, especially on high volume roadways. To evaluate CCPR under accelerated traffic conditions, the Virginia Department of Transportation (VDOT) sponsored three test sections at the NCAT Test Track, complementing an existing field project using CCPR on I-81 in Virginia. The primary objectives were to characterize the field performance and to estimate the structural characteristics and contribution of the VDOT CCPR sections placed at the track.

#### *Test Sections*

The test sections in this experiment are shown in Figure 1, while the as-built properties are listed in Table 1. Each section featured a stone matrix asphalt (SMA) surface and Superpave dense-graded AC layers above the CCPR layer. The nominal maximum aggregate sizes (NMAS) are listed with the layer descriptions in Table 1. The CCPR was 100% RAP with 2% foamed performance grade (PG) 67-22 asphalt binder and 1% Type II hydraulic cement, as noted in Table 1. Sections N3 and N4 were constructed on top of a crushed granite aggregate base layer, while S12 was built on a cement-stabilized base layer. The base stabilization was done in-place using a reclaimer to simulate full-depth reclamation (FDR). Approximately 6 in. of crushed granite aggregate base and 2 in. of the subgrade were treated in place with 4% (by weight) Type II hydraulic cement. All three sections were constructed on the same subgrade native to the track and classified as an A-4 soil (3). Sections N3 and N4 were designed to evaluate the difference between 4 in. and 6 in. of AC over 5 in. of CCPR. Sections N4 and S12 were designed to determine the differences between 6 in. of aggregate base and 8 in. of cement stabilized base (CSB). It is important to note that Figure 1 represents the average as-built thickness of the entire test section which reflects natural variation due to standard construction practices at the track. The average represents measurements taken at 12 distinct locations within each section.

Figure 1 also shows the depth of instrumentation used in this investigation. Six horizontal asphalt strain gauges oriented in the longitudinal direction (parallel to traffic) were placed at the bottom of the CCPR layer to capture bending of the asphalt-bound layers. Six vertical strain gauges were installed to capture vertical deflection of the asphalt-bound layers. However, the vertical strain gauges were only functional for a short period of time (i.e., a few weeks), preventing the development of meaningful vertical strain data over time. Earth pressure cells were placed at the top of the base and top of the subgrade to capture vertical pressures transmitted through the

sections. Temperature probes were installed after paving at the middle of the composite AC/CCPR to measure mid-depth temperature during testing.

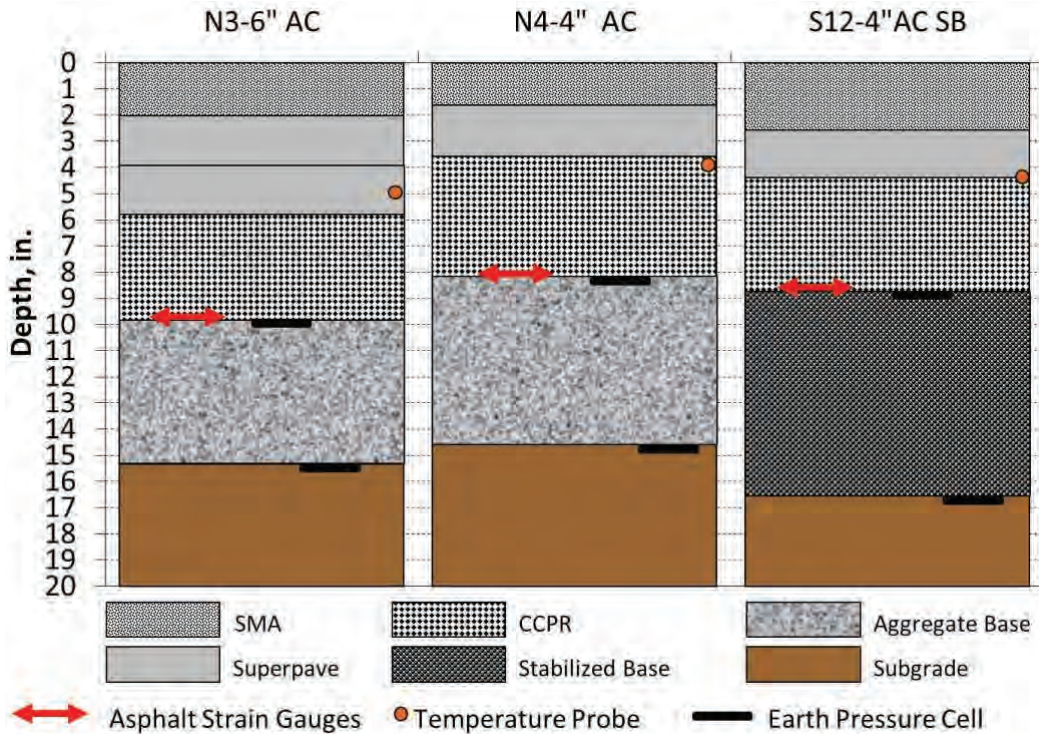


Figure 1 VDOT Experiment Average As-Built Thicknesses and Instrumentation Depth

Table 1 VDOT Experiment As-Built Layer Properties

Section	N3-6 in. AC	N4-4 in. AC	S12-4 in. AC SB
Layer Description	Lift 1-19 mm NMAS SMA with 12.5% RAP and PG 76-22 binder		
Binder Content, %	6.1	6.0	6.1
Air Voids, %	4.3	4.7	4.2
Layer Description	Lift 2-19 mm NMAS Superpave with 30% RAP and PG 67-22 binder		
Binder Content, %	4.6	4.6	4.7
Air Voids, %	7.1	7.4	6.7
Layer Description	Lift 3-19 mm NMAS Superpave with 30% RAP and PG 67-22 binder		
Binder Content, %	4.4	NA	NA
Air Voids, %	6.4	NA	NA
Layer Description	CCPR-100% RAP with 2% foamed PG 67-22 binder and 1% Type II hydraulic cement		
Layer Description	Crushed granite aggregate base (CGAB)	6 in. CGAB + 2 in. subgrade stabilized in-place with 4% Type II hydraulic cement	
Layer Description	Subgrade – AASHTO A-4 Soil		

*Performance*

Through the end of trafficking (October 2014), no cracking was observed in any of the three CCPR test sections. Figure 2 shows the rutting performance through the research cycle. The increasing rut depths noted between 3 and 4.5 million ESALs and between 8 and 9 million ESALs correspond to the increasing temperatures experienced during the summer months of trafficking. All sections

have exhibited excellent performance thus far, with a maximum rut depth of approximately 0.30 inches with very little practical differences between the three sections.

Pavement smoothness, expressed as the International Roughness Index (IRI), is shown in Figure 3. The data indicates relatively little change in smoothness over time through October 2014. Section S12, which included the stabilized base, had an initial roughness of nearly double the other sections. This was caused by a localized low spot approximately 40 to 60 feet into the section that was noted immediately after construction. However, the IRI has not changed appreciably over time, and S12 has performed well in terms of rutting and cracking.

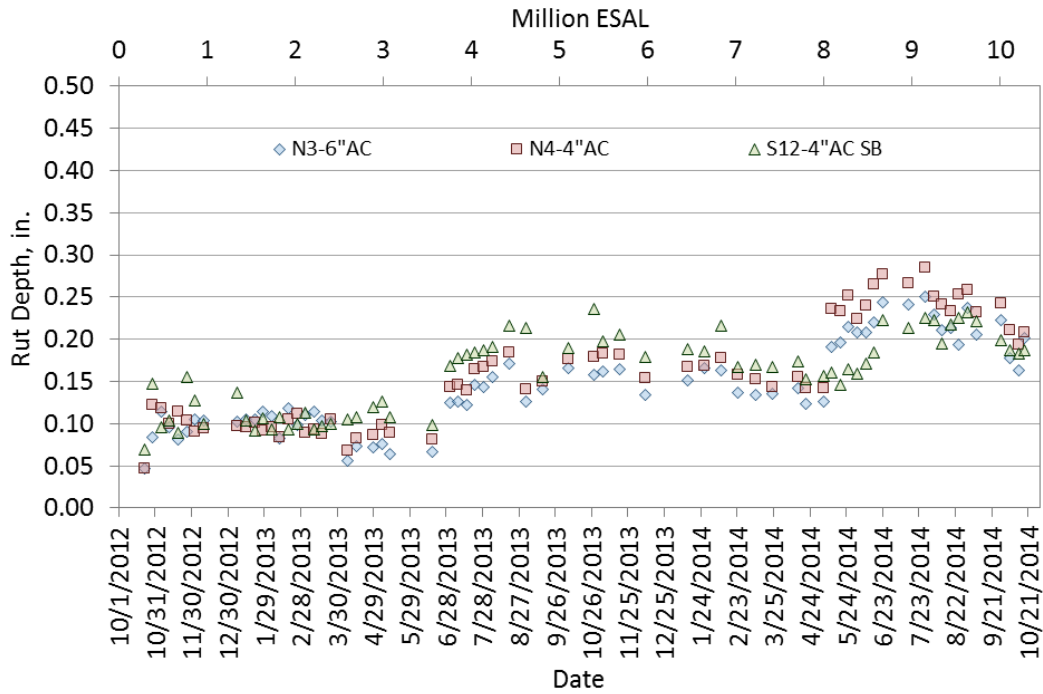


**Figure 2 Rutting Performance**

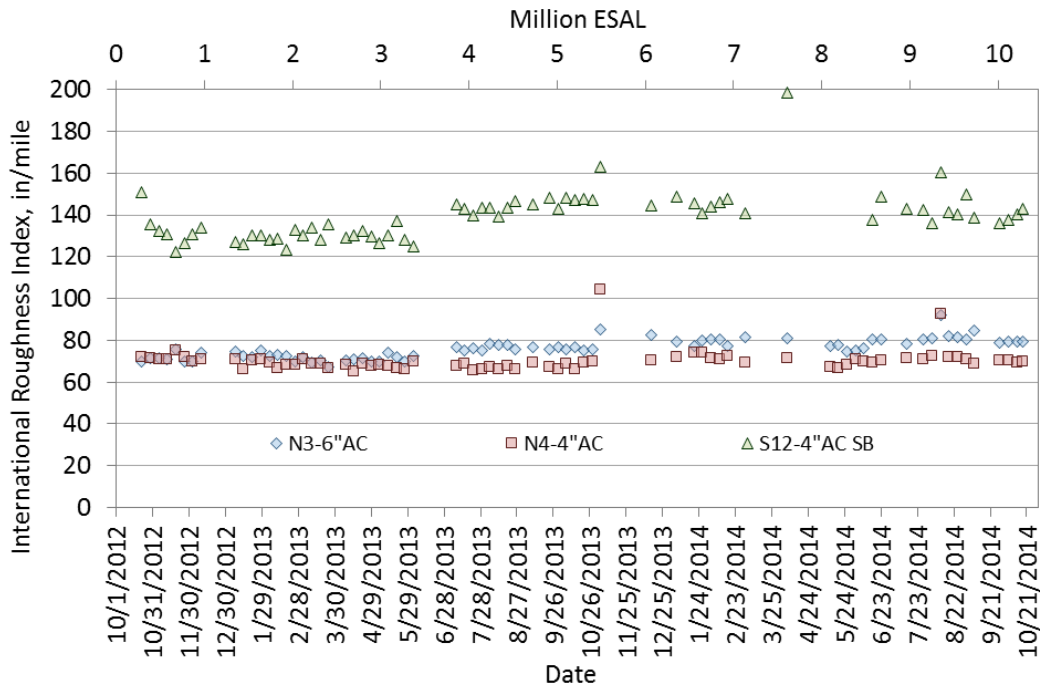


**Figure 3 Ride Quality**

*Backcalculated Moduli*

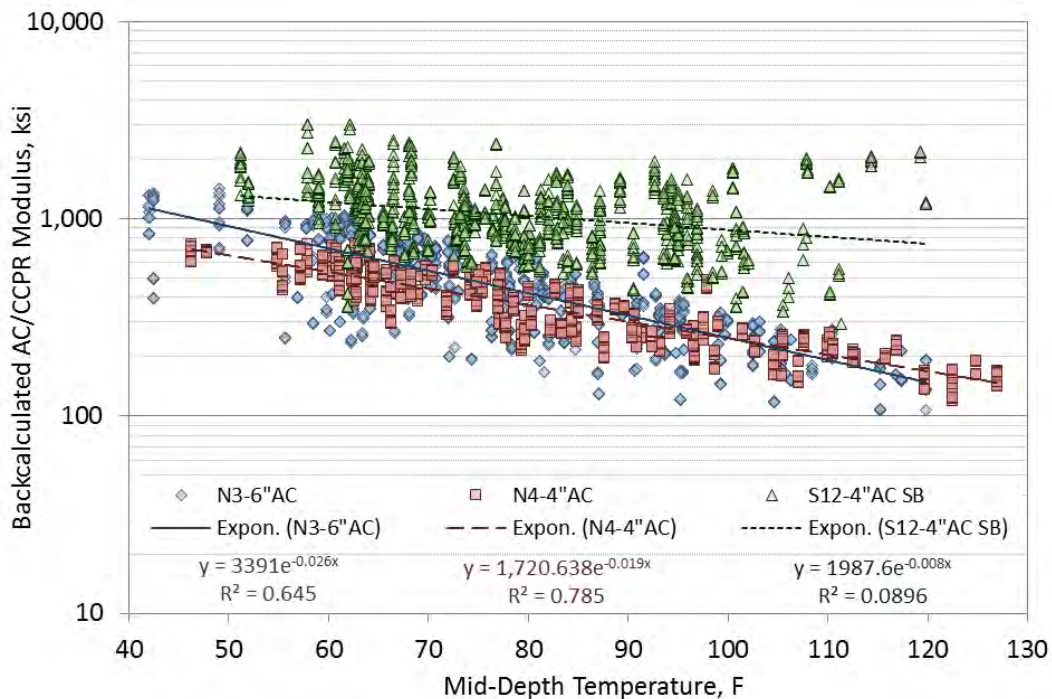
For backcalculation purposes, each pavement section was treated as a three-layer structure consisting of the AC/CCPR lifts as layer one, the aggregate base (N3 and N4) or stabilized base (S12) as layer two, and the subgrade as layer three. Previous research demonstrated that the CCPR would exhibit a behavior similar to that of AC (4), and therefore these layers were combined. Subsequent laboratory dynamic modulus testing of the CCPR by VDOT confirmed that the CCPR exhibited behavior consistent with AC materials and supported the combination of AC and CCPR for backcalculation (5).

Figure 4 shows the influence of mid-depth temperature on backcalculated AC/CCPR moduli. The sections having an unbound granular base layer (N3 and N4) show the strong influence of mid-depth temperature on the modulus, demonstrated by the exponential regression equations and corresponding coefficients of determination ( $R^2$ ). Very similar behavior has been reported previously for AC materials at the track (6). Therefore, it was further justified to consider the CCPR and AC materials as a single layer for backcalculation purposes. Interestingly, the thicker AC section (N3) appears to be slightly more temperature sensitive (i.e., steeper slope) than the thinner AC section (N4). This may be due to a higher percentage of RAP making up the backcalculated layer in N4. Previous studies at the track that compared a virgin AC section to a 50% RAP section found the RAP section to be less temperature sensitive, presumably due to the presence of more aged binder (7).

Section S12, having the cement stabilized base, shows a higher modulus and much less temperature sensitivity than the other two sections, as shown in Figure 4. The exponential regression coefficient is less than half that of the other two sections and the corresponding  $R^2$  is

relatively lower. Although it seemed reasonable to expect the modulus of S12 to resemble that of N4 due to the similar thickness of the AC/CCPR layer, it may be inferred that the increased modulus is an artifact of the backcalculation process. Essentially, the AC/CCPR was given a higher apparent modulus to adjust for smaller measured deflections on the stabilized base section. Furthermore, the lower temperature sensitivity observed for Section S12 may be attributed to the presence of the cement stabilized base.

Figure 5 shows the normalized AC/CCPR modulus over time. Linear trendlines were found for each data set. The sections having an aggregate base (N3 and N4) show virtually no change in modulus over time. The modulus for the stabilized base section (S12), however, clearly increased over time. It appears that the cement stabilized layer is curing over time, as expected (8). This should result in reduced pavement response measurements that will be explored in the next subsection.



**Figure 4 Backcalculated AC/CCPR Modulus vs. Temperature**

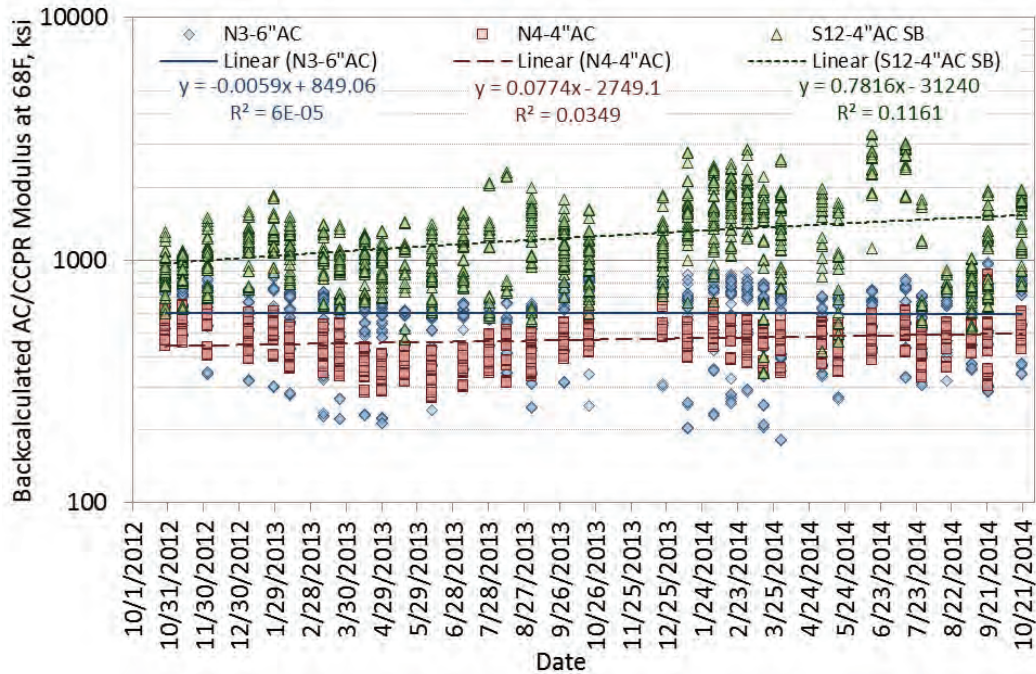


**Figure 5 Backcalculated AC/CCPR Modulus at 68°F vs. Date**

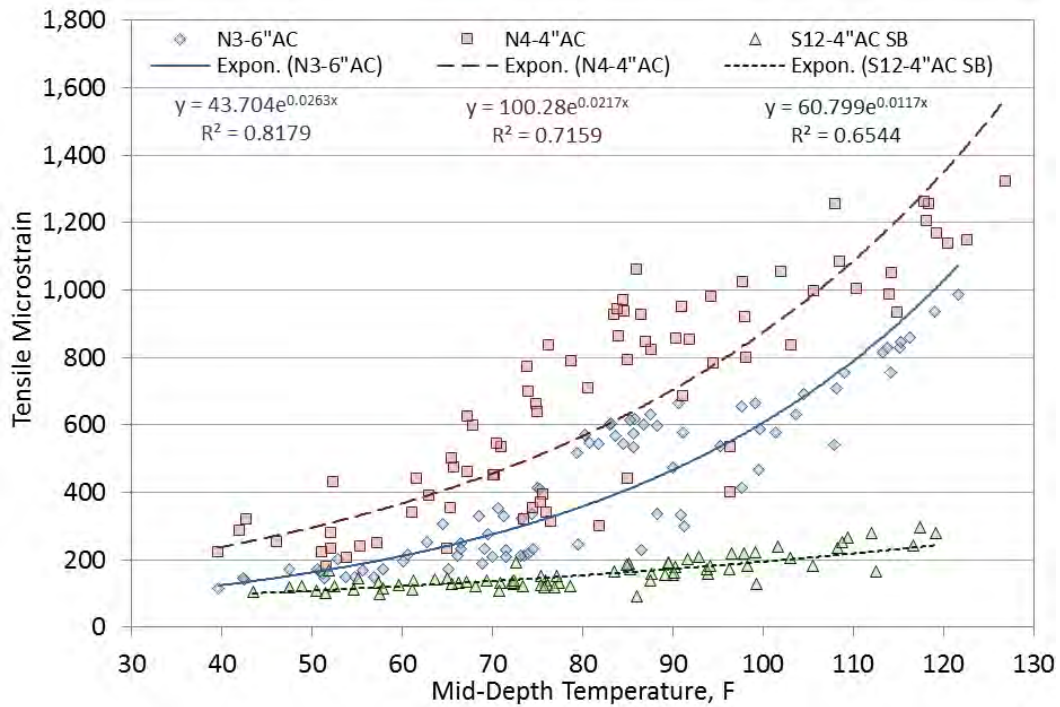
*Pavement Response*

Figure 6 shows the tensile strain response at the bottom of the CCPR layer versus temperature. Given the negative exponential relationship between backcalculated modulus and temperature presented above, the strain response was strongly correlated to temperature through exponential regression equations. As expected, the benefit of the additional 2 in. of AC in Section N3 (6 in. AC) as compared to Section N4 (4 in. AC) is clearly seen across the temperature spectrum. At 68°F, N3 had approximately 40% lower strain than N4. Both N3 and N4 exhibited similar temperature sensitivity as demonstrated by the very similar exponential coefficients in their respective regression equations.

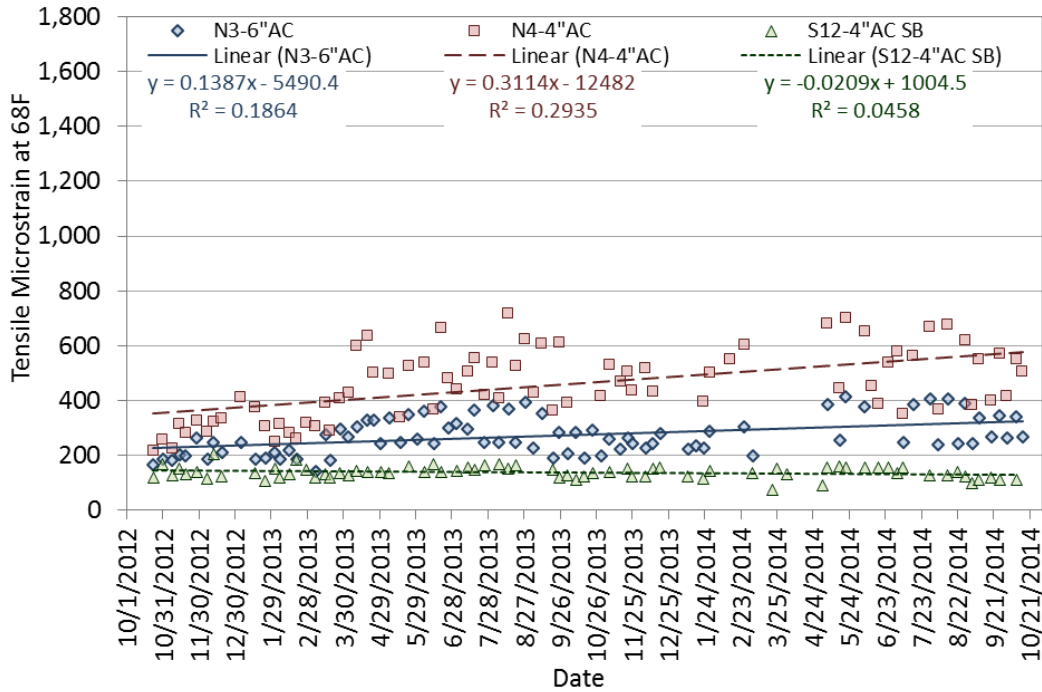
Section S12 experienced relatively lower strains than the other sections and demonstrated less sensitivity to temperature. Both characteristics are clearly shown in Figure 6. The exponential regression coefficient of S12 is approximately half that of the other sections. Similar observations were made regarding the backcalculated modulus regression equations. The strain magnitude is also significantly lower in S12 than the other two sections. The differences are less pronounced at colder temperatures but increase as temperatures increase. This is the combined effect of low temperature sensitivity and the stiff base layer producing lower strain levels. The tensile strain is also a function of the underlying supporting layer. In S12, this material is a cement-stabilized base layer, while it is an unbound granular material in N4. Therefore, it is reasonable to expect less strain in the section that has the stiffer underlying material, which limits, to an extent, the tensile strain in the CCPR layer.

Following the temperature normalization procedure described previously, the strain measurements were corrected to a reference temperature of 68°F. The normalized strains at the bottom of the CCPR layer with respect to date are presented in Figure 7, where linear trendlines

have been assigned to each data set. Both sections N3 (6 in. AC) and N4 (4 in. AC) show an increase in strain over time. The slope and relatively low  $R^2$  corresponding to N3 indicate relatively little change in strain over time. The slope of N4 is greater and has a corresponding higher  $R^2$  than N3, which may indicate some damage occurring in this section not yet detected by FWD testing. The small slope and low  $R^2$  corresponding to Section S12 (4 in. AC SB) indicate no appreciable change over time and a healthy pavement structure.



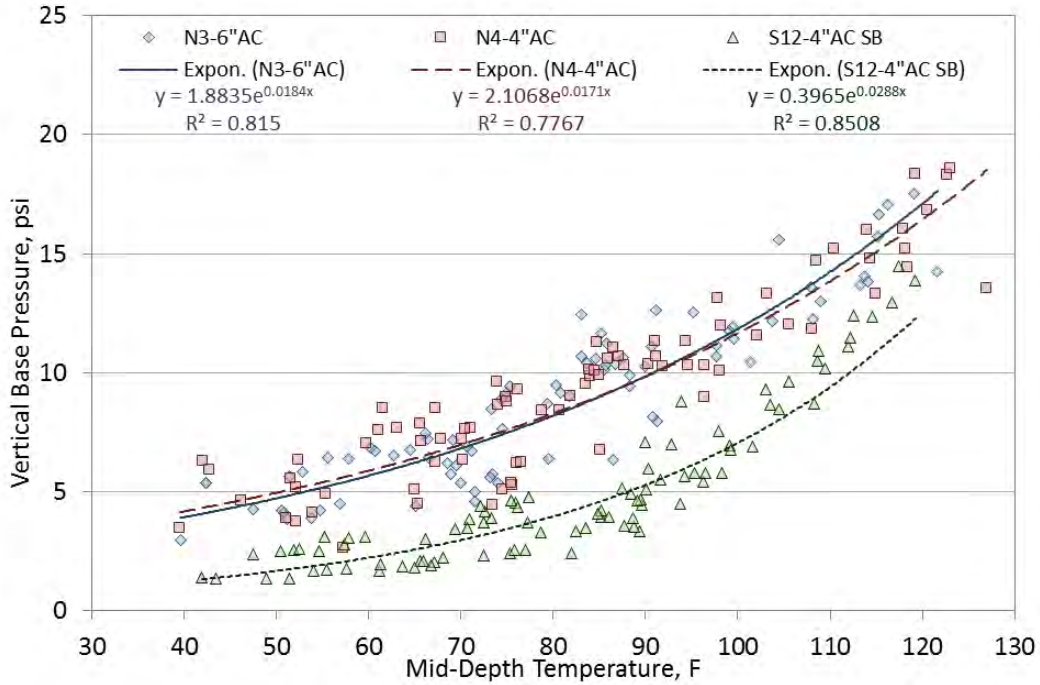
**Figure 6 Tensile Strain at the Bottom of the CCPR Layer vs. Temperature**



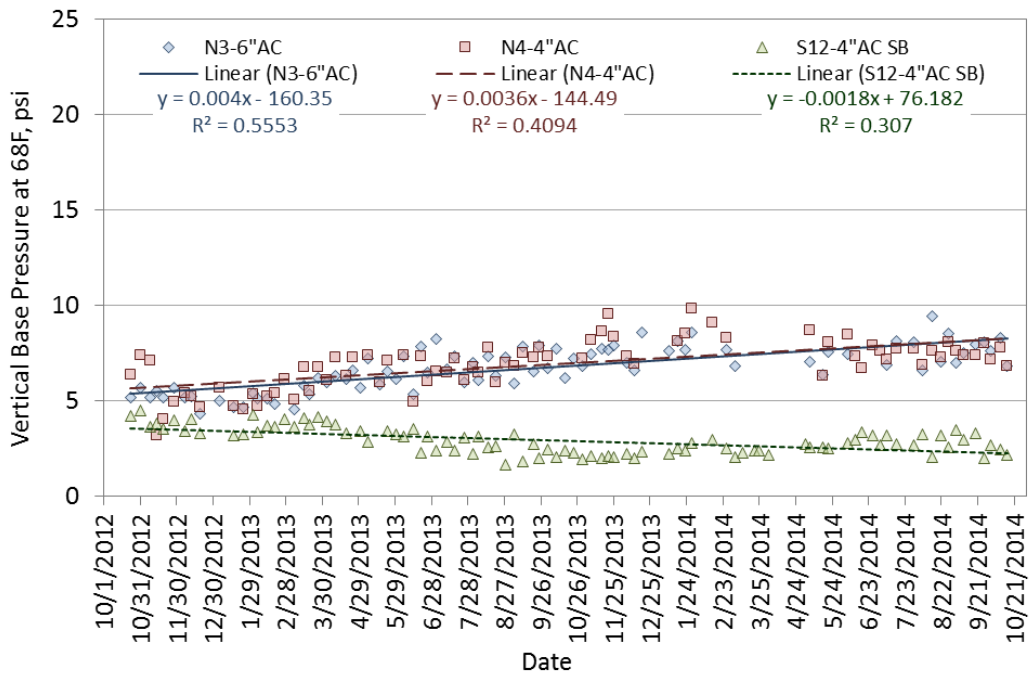
**Figure 7 Tensile Strain at the Bottom of the CCPR Layer at 68°F vs. Time/Traffic**

Figure 8 presents the pressure at the top of the base layer versus temperature, along with exponential regression equations for each section. Sections N3 (6 in. AC) and N4 (4 in. AC) show very similar behavior and strong correlation to temperature. The sensitivity and precision of this measurement was not sufficient to capture the expected reduction in base pressure from the additional AC thickness in N3. The measured base pressure for Section S12, on the stabilized base, is significantly lower than in the other two sections. The increased stiffness of the stabilized base layer may create unusual stress concentrations directly above the pressure plate. In that way, a larger portion of the stress induced by the load is absorbed by the stiffer layer, affecting the measurements and generating artificially low base pressures.

Figure 9 shows the base pressure normalized to 68°F versus time. As previously observed, sections N3 and N4 follow the same trend; both are increasing over time, which may indicate some distress development not yet seen at the pavement surface. Conversely, as S12 (4 in. AC SB) stiffens over time, there is a corresponding reduction in base pressure.



**Figure 8 Base Pressure vs. Temperature**



**Figure 9 Base Pressure at 68°F vs. Time/Traffic**

The subgrade pressure measurements more clearly show the differences between the sections. Figure 10 illustrates subgrade pressure measurements versus temperature. Sections N3 (6 in. AC) and N4 (4 in. AC) are clearly distinguishable and follow similar trends with respect to

temperature, though N3 has much greater measurement variability and corresponding lower  $R^2$ . The subgrade pressure in S12 (4 in. AC SB) is much lower and less responsive to temperature.

The temperature-normalized subgrade pressure measurements are plotted in Figure 11. Sections N3 (6 in. AC) and N4 (4 in. AC) show very little change in pressure over time and generally low  $R^2$ . Section S12 (4 in. AC SB) shows a decreasing trend, consistent with a curing process and a certain stiffening over time.

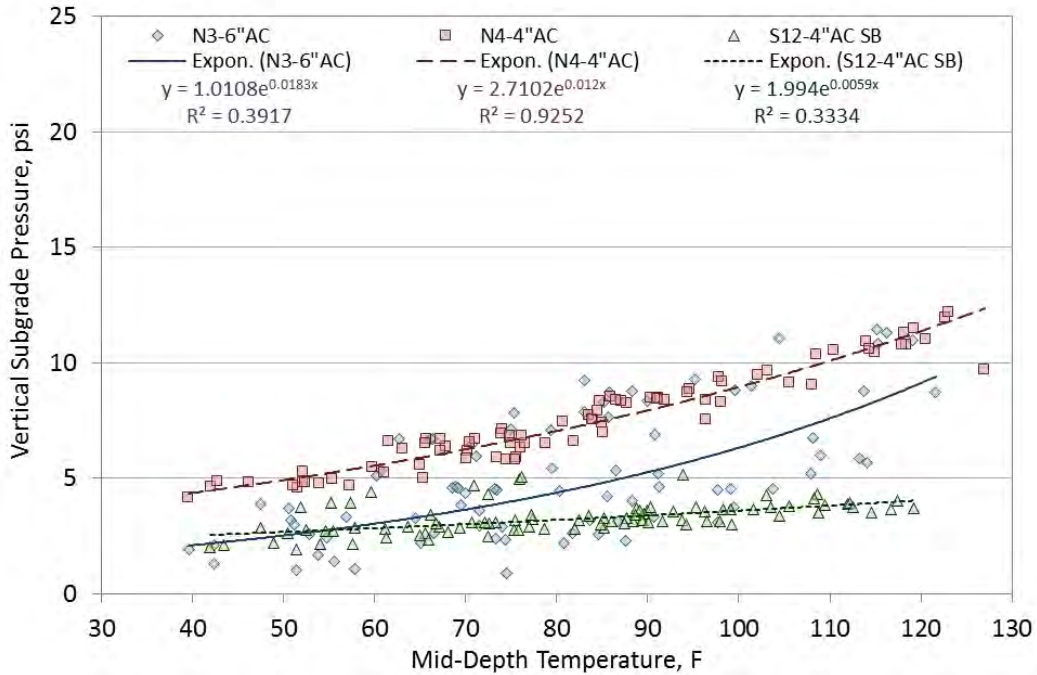


**Figure 10 Subgrade Pressure vs. Temperature**

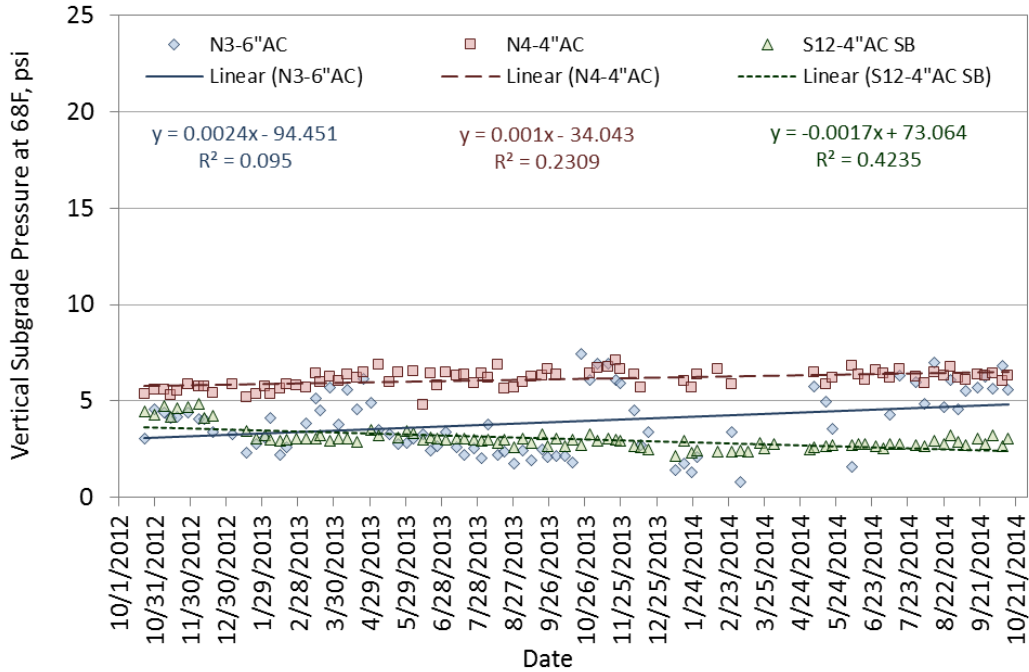


**Figure 11 Subgrade Pressure at 68°F vs. Time/Traffic**

#### *CCPR Structural Coefficient*

The structural performance and the functional characterization of sections N3 and N4 over the two-year research cycle were used to determine the structural contribution of the CCPR in terms of a layer coefficient. Only N3 and N4 were used for this part of the investigation since they did not contain the cement stabilized layer which would have confounded the analysis. According to the AASHTO Guide for Design of Pavement Structures, a direct correlation may be established between the structural layer coefficient and the measured elastic modulus of each layer (9). Based on such correlation, the structural layer coefficient may be used to empirically describe the structural contribution of a specific pavement layer under traffic loads.

A number of structural layer coefficients ranging between the layer coefficients of a granular base (0.06 – 0.14) and those of AC (0.35 – 0.54) have been recommended in the literature for CIR and CCPR layers recycled with foamed asphalt. Tia and Wood suggested using structural layer coefficients ranging from 0.25 to 0.40 for an artificially aged paving mixture recycled with foamed asphalt (10). Similarly, based on pavement deflection measurements in two road projects in Indiana, Van Wyk et al. (11) and Van Wijk and Wood (12) estimated the average layer coefficient of CIR with foamed asphalt between 0.26 and 0.37, with values as low as 0.10 and as high as 0.43. Marquis et al. determined the layer coefficient varied from 0.22 to 0.35 for three foamed asphalt recycling projects in Maine (13). Seebaly et al. recommended a layer coefficient of 0.26 for CIR layers in Nevada (14). Based on the results of full-scale accelerated pavement testing (APT) in Kansas, Romanoschi et al. recommended a structural layer coefficient of 0.18 for full-depth reclamation (FDR) using foamed asphalt (15). Loizos and Papavasiliou (16) and Loizos et al. (17) followed an analytical approach based on multilayer elastic analysis to estimate a structural layer coefficient at approximately 0.25 for CIR constructed on a major highway in Greece. More

recently, Diefenderfer and Apeageyi used deflection testing and laboratory measurements of the resilient modulus and indirect tensile strength of CCPR field cores to estimate a layer coefficient ranging from 0.36 to 0.48 (1). Furthermore, only two of the studies found in the literature specifically considered CCPR materials with foamed asphalt (1, 5), while most of the research addressed other in-place recycling techniques. Although it has been suggested that CCPR performs similarly to CIR in the field, it is necessary to determine the specific structural properties of CCPR (18).

The layer coefficient of the CCPR was determined using the correlation presented in Equation 1, originally reported by Schwartz and Khosravifar (19) and based on graphical correlations between the layer coefficient and the elastic modulus of AC developed at the AASHO Road Test.

$$a = 0.1665 \times \ln(E) - 1.7309 \quad (1)$$

where

- $a$  = Layer coefficient for AC; and
- $E$  = Elastic Modulus of the AC (ksi).

The approach considered the temperature-normalized modulus values obtained for the combined AC/CCPR layer on each testing date as the  $E$  parameter in Equation 1. Subsequently, using the layer coefficient ( $a$ ) computed from Equation 1, the structural number (SN) for the composite AC/CCPR layer was calculated according to Equation 2. The SN for the AC layer was then determined from Equation 3, with an AC layer coefficient of 0.54, as determined in a previous layer coefficient calibration performed at the track (20). The layer coefficient for the CCPR layer was calculated using Equation 4. It should be pointed out that using 0.54 for the hot mix AC layers is conservative relative to using 0.44, because more structural capacity is attributed to these layers and less to the CCPR. Had 0.44 been used for the AC layers, the CCPR structural coefficient would have been greater.

$$SN_{AC/CCPR} = D_{AC/CCPR} \times a \quad (2)$$

where

- $SN_{AC/CCPR}$  = AC layer coefficient determined for the first approach;
- $a$  = Layer coefficient of the AC/CCPR layer from Equation 1; and
- $D_{AC/CCPR}$  = AC/CCPR thickness (N3=9.84 in. and N4=8.17 in.).

$$SN_{AC} = 0.54 \times D_{AC} \quad (3)$$

where

- $SN_{AC}$  = Structural number for the AC layer; and
- $D_{AC}$  = AC thickness (N3=5.81 in. and N4=3.59 in.).

$$a_{CCPR} = \frac{(SN_{AC/CCPR} - SN_{AC})}{D_{CCPR}} \quad (4)$$

where

$a_{CCPR}$  = Layer coefficient for the CCPR; and  
 $D_{CCPR}$  = CCPR thickness (N3=4.03 in. and N4=4.58 in.).

An individual layer coefficient was determined for every testing date at every testing location by means of the normalized modulus determined previously. The results for both test sections are presented in Figure 12. As expected, the layer coefficients show certain variations with time, similar to that observed before with the backcalculated moduli. The insignificant slope of the linear trendlines and the low magnitude of their corresponding  $R^2$  indicate that the layer coefficients are not significantly increasing or decreasing over time and the average values may be used in the analysis. The average layer coefficients were determined as 0.39 for Section N3 and 0.36 for Section N4, with corresponding standard deviations of 0.13 and 0.06, respectively. These values are within the range described in the available literature and they adequately represent the structural capacity of the CCPR. Although a statistical analysis (t-test) revealed that these two values were different at a 95% confidence level ( $\alpha=0.05$ ,  $p\text{-value}=0.000$ ), it was reasoned that the difference was not necessarily significant for practical pavement design purposes.

Although the average layer coefficient was lower for Section N4, the lowest values corresponded to Section N3, approaching zero in some cases. This explained the greater standard deviation obtained for Section N3. Further investigation revealed that the lower values found for Section N3 corresponded to one specific random longitudinal location. As shown in Figure 13, most of the lower results in Section N3 could be attributed to random location 4. Location 4 was located in the middle of the instrumented area of the section, which could contribute to lower moduli and lower structural coefficients due to disturbances caused by gauge installation. If random location 4 is not considered in the analysis, the average layer coefficient for Section N3 is 0.43, with a corresponding standard deviation of 0.09. This relatively high layer coefficient approaches the value of 0.44 recommended by AASHTO for conventional AC (9). The testing location has a significant effect on the calculated layer coefficient for Section N3. However, this may also be attributed to natural variation in construction practices. Therefore, it was decided to consider the spatial variability in the analysis, and include location 4, as it would provide a layer coefficient more conservative from a structural design perspective.

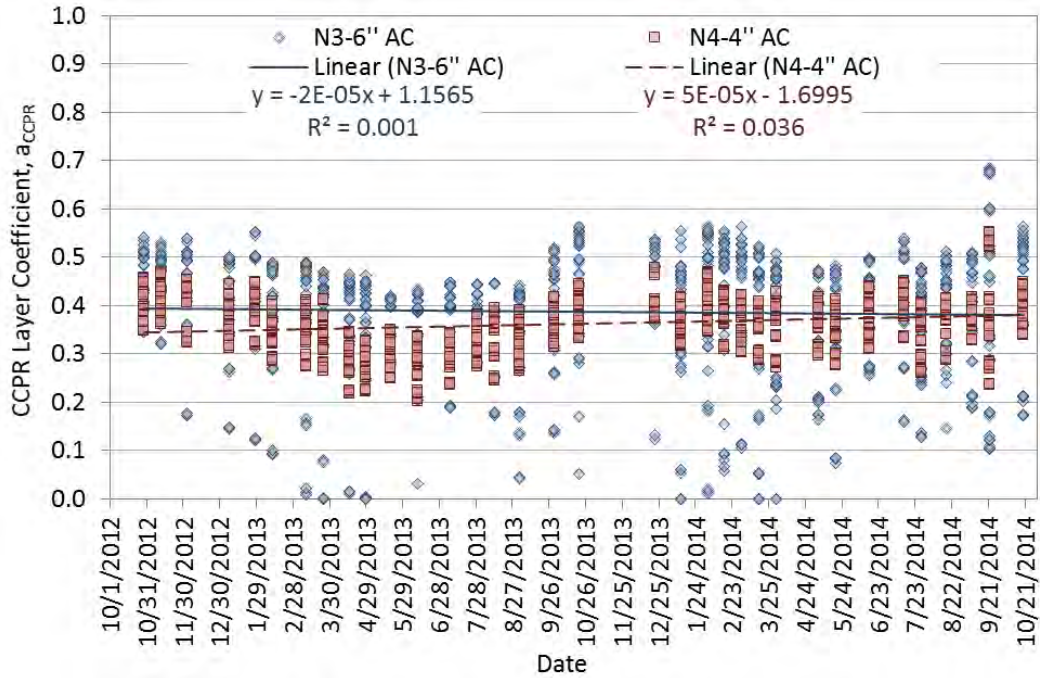


Figure 12 Structural Coefficient vs. Date/Traffic

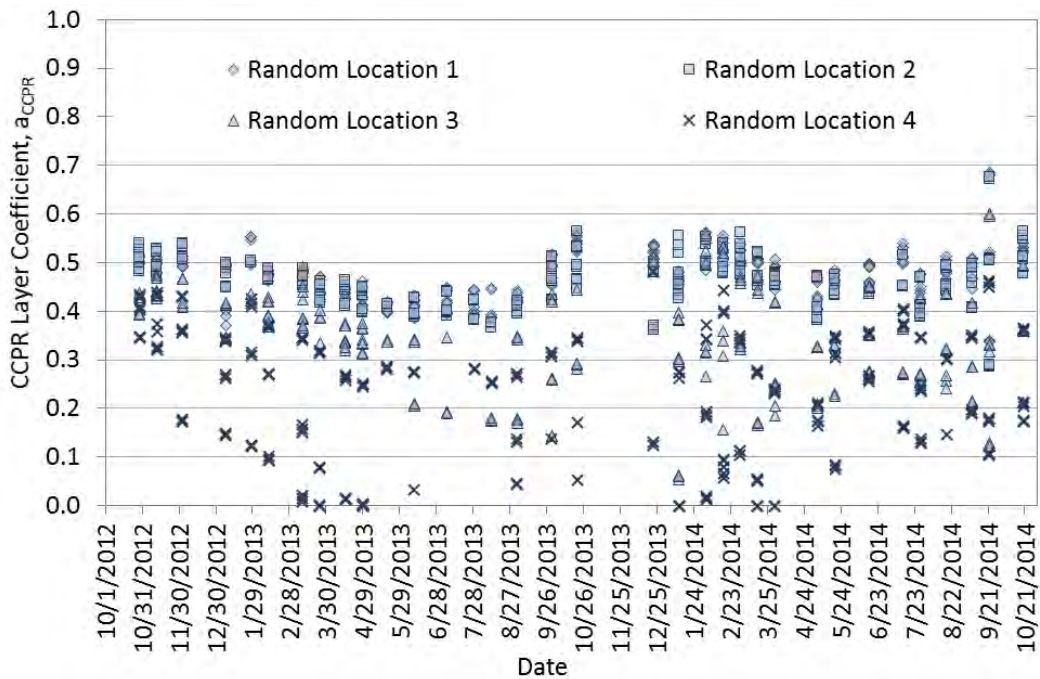


Figure 13 Structural Coefficient vs. Date/Traffic for Section N3

### *Summary and Conclusions*

This study was meant to investigate the field performance and structural characteristics of three CCPR sections at the NCAT Test Track under accelerated traffic loadings. Based upon the data presented above, the following conclusions and recommendations are made:

- All three CCPR sections have exhibited excellent performance over the research cycle. Very little difference was observed between sections in terms of rutting performance. Though S12 (4 in. AC SB) was originally built rougher than the other sections, all three had very little change in smoothness over time. Cracking has not yet been observed in any of the sections. There were no distinguishable surface-observable performance differences between the three pavements.
- The backcalculated AC/CCPR moduli in N3 (6 in. AC) and N4 (4 in. AC) respond to changes in temperature like conventional AC materials, which was also observed in a laboratory study of CCPR mixtures (5). Future mechanistic modeling should treat CCPR with similar production characteristics as a bituminous material.
- The backcalculated AC/CCPR moduli in S12 (4 in. AC SB) demonstrated much less temperature sensitivity and higher moduli than the other sections. It was believed to have resulted from the backcalculation process attributing some stabilized base properties to the AC/CCPR layer.
- Very little change in temperature-normalized modulus over time was found for N3 (4 in. AC) and N4 (6 in. AC). This indicates that the sections, in terms of modulus, do not appear to be curing or experiencing damage. Conversely, S12 (4 in. AC SB) showed an increase in temperature-normalized modulus over time, which was again thought to be related to the stabilized base layer curing over time. Future investigations should focus on laboratory evaluation of the cement stabilized material to determine its curing characteristics.
- Tensile strain was measured at the bottom of the CCPR in all three sections. These data further supported treating the CCPR as a bituminous material for mechanistic modeling and design purposes. Further monitoring of the sections for cracking is needed to evaluate where and when fatigue cracking develops. Investigation is also needed to develop fatigue transfer function coefficients to predict cracking of CCPR.
- The additional 2 in. of AC in N3 yielded lower strain levels than N4 across the entire temperature spectrum (40% lower at 68°F). The stabilized base in S12 yielded much lower strain magnitudes and less temperature sensitivity across the entire temperature spectrum. Strains normalized to 68°F showed that N4 (4 in. AC) was increasing over time, which may indicate some degradation of structural capacity not detected through FWD testing, while the other sections were relatively constant. Therefore, using 6 in. of AC or a stabilized base may be advantageous in controlling tensile strain in the pavement structure.
- The aggregate base pressure measurements did not capture any differences between N3 (6 in. AC) and N4 (4 in. AC). The measurements in S12 (4 in. AC SB) were significantly lower. In sections N3 and N4, base pressure at 68°F increased over time, while it decreased in S12 as the section stiffened. Therefore, in terms of base pressure only, it appears the additional 2 in. of AC does not impact the structural capacity, while the stabilized base appears to improve the structure over time.
- Subgrade pressure measurements did capture differences between the sections, with the highest reported in N4 (4 in. AC) and the lowest in S12 (4 in. AC SB). Very little change in

pressure at 68°F over time was noted in N3 and N4, though S12 again tended toward lower pressure over time.

- A mathematical procedure was used to estimate the layer coefficient for the CCPR from backcalculated modulus data. The resulting layer coefficients ranged from 0.36 to 0.39 at a reference temperature of 68°F. These values were also within the range reported in the literature for cold-recycling materials with foamed asphalt.
- Additional research is warranted to fully validate the layer coefficient of CCPR,  $a_{ccpr}$ . Continued traffic over the test sections may allow observing a change in serviceability which would allow an alternative approach to determining the magnitude of the layer coefficient. Furthermore, the obtained layer coefficients represent the local weather conditions observed at the track, and additional validation is required for additional climates or regions.

### References

1. Diefenderfer, B. K., and A. K. Apeageyi. *I-81 In-Place Pavement Recycling Project*. Report No. 15-R1. Virginia Center for Transportation Innovation and Research, Virginia Department of Transportation, Charlottesville, 2014.
2. *Basic Asphalt Recycling Manual*. Asphalt Recycling and Reclaiming Association (ARRA), Annapolis, MD, 2001.
3. Taylor, A. J., and D. H. Timm. *Mechanistic Characterization of Resilient Moduli for Unbound Pavement Layer Materials*. NCAT Report 09-06. National Center for Asphalt Technology at Auburn University, Auburn, Ala., 2009.
4. Kim, Y., H. D. Lee, and M. Heitzman. Dynamic Modulus and Repeated Load Tests of Cold-in-Place Recycling Mixtures Using Foamed Asphalt. *ASCE Journal of Materials in Civil Engineering*, Vol. 21, No. 6, 2009, pp. 279-285.
5. Diefenderfer, B. K., and S. D. Link. Temperature and Confinement Effects on the Stiffness of a Cold Central-Plant Recycled Mixture. Proceedings: *12<sup>th</sup> International Society for Asphalt Pavements Conference on Asphalt Pavements*, Raleigh, N.C., 2014.
6. West, R., D. Timm, R. Willis, B. Powell, N. Tran, D. Watson, M. Sakhaeifar, R. Brown, M. Robbins, A. Vargas-Nordcbeck, F. Leiva-Villacorta, X. Guo, and J. Nelson. *Phase IV NCAT Test Track Findings*. NCAT Report 12-10. National Center for Asphalt Technology at Auburn University, Auburn, Ala., 2012.
7. Vargas-Nordcbeck, A., and D. Timm. *Physical and Structural Characterization of Sustainable Asphalt Pavement Sections at the NCAT Test Track*. NCAT Report 13-02. National Center for Asphalt Technology at Auburn University, Auburn, Ala., 2013.
8. Diefenderfer, B. K., A. K. Apeageyi, A. A. Gallo, L. E. Dougald, and C. B. Weaver. In-Place Pavement Recycling on I-81 in Virginia. In *Transportation Research Record: Journal of the Transportation Research Board*, No. 2306, Transportation Research Board of the National Academies, Washington, D.C., 2012, pp. 17-24.
9. *AASHTO Guide for Design of Pavement Structures*. AASHTO, Washington, D.C., 1993.
10. Tia, M., and L. E. Wood. Use of Asphalt Emulsion and Foamed Asphalt in Cold-Recycled Asphalt Paving Mixtures. In *Transportation Research Record: Journal of the Transportation Research Board*, No. 898, Transportation Research Board of the National Academies, Washington, D.C., 1983, pp. 315-322.

11. Van Wyk, A., E. J. Yoder, and L. E. Wood. Determination of Structural Equivalency Factors of Recycled Layers by Using Field Data. In *Transportation Research Record: Journal of the Transportation Research Board*, No. 898, Transportation Research Board of the National Academies, Washington, D.C., 1983, pp. 122-132.
12. Van Wijk, A., and L. E. Wood. Use of Foamed Asphalt in Recycling of an Asphalt Pavement. In *Transportation Research Record: Journal of the Transportation Research Board*, No. 911, Transportation Research Board of the National Academies, Washington, D.C., 1983, pp. 96-103.
13. Marquis, B., D. Peabody, R. Mallick, and T. Soucie. *Determination of Structural Layer Coefficient for Roadway Recycling Using Foamed Asphalt*. Final Report, Project 26. Recycled Materials Resource Center, University of New Hampshire, Durham, 2003.
14. Seebaly, P. E., G. Bazi, E. Hitti, D. Weitzel, and S. Bemanian. Performance of Cold In-Place Recycling in Nevada. In *Transportation Research Record: Journal of the Transportation Research Board*, No. 1896, Transportation Research Board of the National Academies, Washington, D.C., 2004, pp. 162-169.
15. Romanoschi, S. A., M. Hussain, A. Gisi, and M. Heitzman. Accelerated Pavement Testing Evaluation of the Structural Contribution of Full-Depth Reclamation Material Stabilized with Foam Asphalt. In *Transportation Research Record: Journal of the Transportation Research Board*, No. 1896, Transportation Research Board of the National Academies, Washington, D.C., 2004, pp. 199-207.
16. Loizos, A., and V. Papavasiliou. Evaluation of Foamed Asphalt Cold-in-Place Pavement Recycling Using Nondestructive Techniques. *ASCE Journal of Transportation Engineering*, Vol. 132, No.12, 2006, pp. 970-978.
17. Loizos, A., V. Papavasiliou, and C. Plati. Early-Life Performance of Cold-in-Place Pavement Recycling with Foamed Asphalt Technique. In *Transportation Research Record: Journal of the Transportation Research Board*, No. 2005, Transportation Research Board of the National Academies, Washington, D.C., 2007, pp. 36-43.
18. Apeagyei, A. K., and B. K. Diefenderfer. Evaluation of Cold In-Place and Cold Central-Plant Recycling Methods Using Laboratory Testing of Field-Cored Specimens. *ASCE Journal of Materials in Civil Engineering*, Vol. 25, No.11, 2013, pp. 1712-1720.
19. Schwartz, C. W., and S. Khosravifar. *Design and Evaluation of Foamed Asphalt Base Materials*. Final Report, Project # SP909B4E. Maryland Department of Transportation, State Highway Administration, Baltimore, 2013.
20. Peters-Davis, K., and D. H. Timm. *Recalibration of the Asphalt Layer Coefficient*. NCAT Report No. 09-03. National Center for Asphalt Technology at Auburn University, Auburn, Ala., 2009.

## **2.4. Oklahoma Department of Transportation Perpetual Pavement Study**

### *Introduction*

Perpetual asphalt pavements are quickly becoming an option for developing a more sustainable pavement infrastructure. Intentionally designing the structure to prevent bottom-up fatigue cracking in the asphalt concrete (AC) and rutting in the granular and subgrade layers creates a long-life pavement that requires occasional surface rehabilitation. While the initial costs of the pavement section are typically higher than conventional designs, perpetual pavements have been outperforming conventional pavement structures, resulting in lower long-term life cycle costs and material consumption.

Two critical components of perpetual pavement design are limiting the horizontal tensile strain at the bottom of the AC and the vertical strain at the top of the subgrade to prevent bottom-up fatigue cracking and rutting, respectively. This is typically accomplished through mechanistic analysis of the pavement structure in the design phase to determine appropriate layer thicknesses based on the material properties of the asphalt mixtures.

Many of the original perpetual pavements in the U.S. were not designed as perpetual pavements but were eventually identified as perpetual. These pavements resulted from overdesign of the pavement structure due to the inherent conservatism built into the American Association of State Highway and Transportation Officials (AASHTO) Pavement Design Guides. As the demand for high performance and sustainable highway infrastructure continues to grow, there is a need to refine and optimize flexible perpetual pavement design.

To address this need, in 2006, the Oklahoma Department of Transportation (ODOT) designed a perpetual pavement experiment for the National Center for Asphalt Technology (NCAT) Test Track. The experiment was intended to examine the perpetual pavement concept, its viability, and potential economic benefits. The experiment featured two full-scale asphalt pavement test sections built in 2006 (1). Both sections were designed as perpetual with one on the thin side and the other slightly thicker. All other conditions (i.e., pavement foundation, climate, materials, and traffic) were held constant between the two sections. During that time, structural testing, performance evaluation, and necessary rehabilitation activities were undertaken. The information gathered over the past three research cycles serves to further the perpetual pavement concept and demonstrates the economic benefits of this option. Discussions of pavement design and N8's failure are documented elsewhere (1). Once N8 failed, it was no longer classified as a perpetual pavement.

### *Objectives and Scope*

The primary objective of this investigation was to document the structural and surface performance characteristics, and rehabilitation of the perpetual pavement experiment test sections at the NCAT Test Track. The secondary objective was to quantify the life cycle costs of each pavement option. The first objective was met by evaluating backcalculated asphalt concrete moduli from falling weight deflectometer (FWD) testing and utilizing weekly performance measurements. The performance measurements would then be tied to field performance. The second objective was accomplished by combining actual rehabilitation activities with cost data obtained from ODOT to provide real-world life cycle costs of the two pavement options.

### Test Sections

The two sections were built on the north tangent of the track, N8 and N9. The primary difference between the two sections was the inclusion of an additional intermediate PG 64-22 lift to increase the total AC thickness by 10 cm in Section N9 relative to N8 (Figure 1). Figure 1 also shows the depths of three instrument types embedded during construction. The purposes of these gauges is described elsewhere (2).

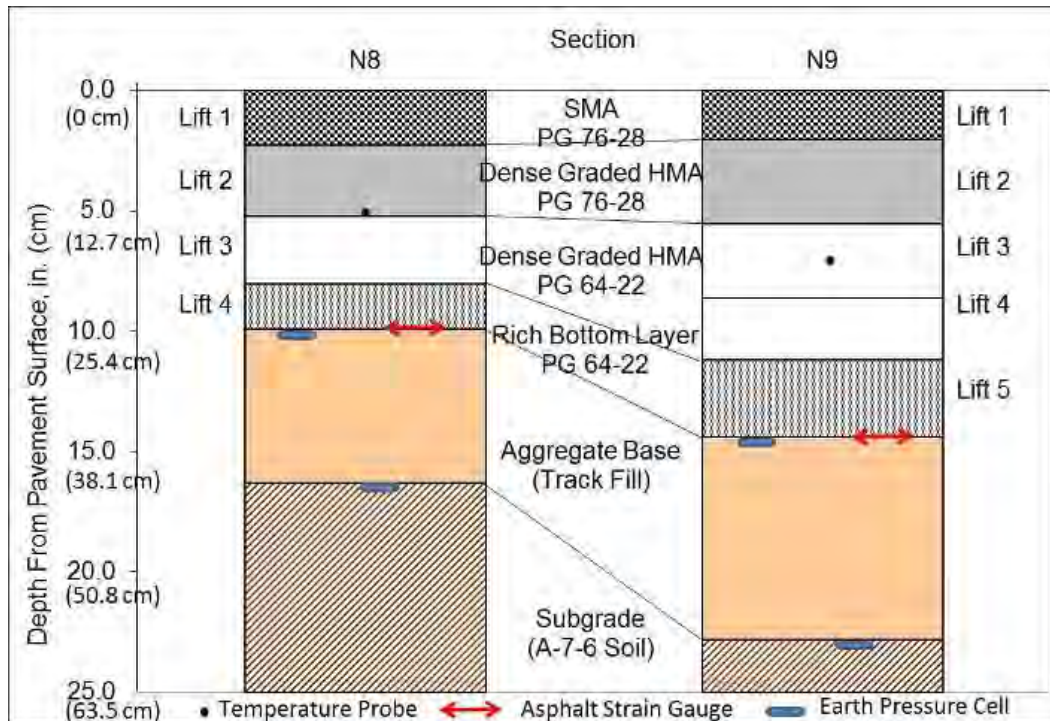


**Figure 1 Structural Cross Sections and Instrumentation (1)**

Table 1 lists the mixture properties measured during construction for each of the pavement lifts shown in Figure 1. The “QC” data represent measurements made as part of the construction quality control while the “As Built Air Voids” represent average in-place measurements from cores. Each section had a stone matrix asphalt (SMA) wearing course above intermediate layers of dense graded Superpave mixtures coupled with a rich-bottom layer designed with 2% air voids.

**Table 1 AC Mixture Properties (1)**

Section	Lift	Nominal Maximum Aggregate Size, mm	QC Asphalt Content, %	QC Air Voids, %	QC VMA, %	As Built Air Voids, %
N8	1	12.5	6.9	5.0	15.6	8.2
	2	19.0	5.2	2.8	10.4	6.4
	3	19.0	4.9	4.4	11.3	7.1
	4	12.5	7.1	2.1	12.6	2.8
N9	1	12.5	7.0	4.9	15.5	7.0
	2	19.0	5.1	3.0	10.5	7.1
	3	19.0	5.0	3.4	10.4	4.9
	4	19.0	4.6	3.8	10.4	6.1
	5	12.5	7.0	1.7	12.2	5.6

After construction, the sections were opened to traffic in November 2006. The fleet of triple-trailer trucks began operating 16 hours per day, five days per week to accumulate approximately 10 million ESALs from 2006 to 2008. An additional 10 million ESALs were applied in the following research cycle from 2009 to 2011 and again from 2012 until 2014. During that time, routine weekly performance measurements were made to include rut depth, ride quality, and visual inspection for cracking. Additionally, weekly strain and pressure measurements were taken and regular FWD testing was conducted several times per month. However, for the third research cycle, strain gauges were deemed unreliable or were off-line. Thus, additional strain data were not available for this work. The following sections describe each of these data sets and findings.

#### *Performance History*

During the initial round of testing from 2006 to 2008, it became apparent that N8 was not perpetual. It began to show signs of increased roughness after approximately 7 million ESALs with fatigue cracking reaching the surface of the pavement after 8.3 million ESALs. By the end of the first round of testing, it was determined that the cracking required remediation to continue into the following research cycle. At the same time, the perpetual section (N9) did not show any signs of distress or increased roughness.

Discussions with ODOT resulted in the decision to mill and inlay N8 with the same materials that were originally placed to address the cracking problem and restore the surface ride quality to begin the 2009 track cycle. Additionally, it was decided to include a geofabric interlayer with the conventional mill-and-inlay to evaluate the capability to prevent reflection cracking. Figure 2 shows the original and rehabilitated cross sections.

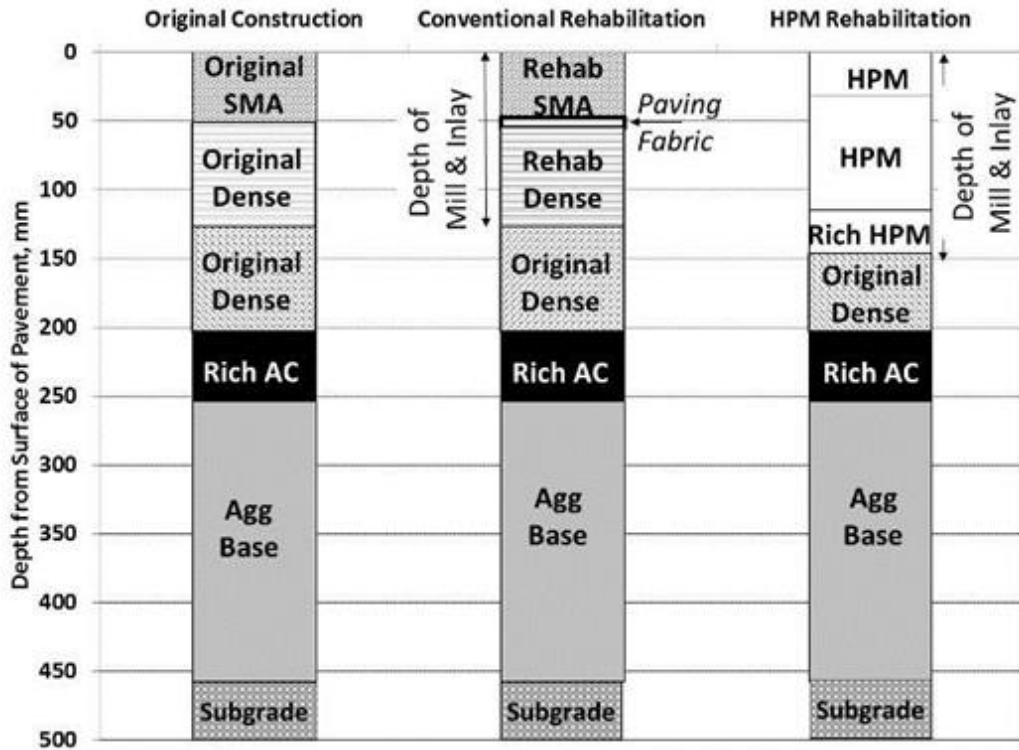


**Figure 2 N8 Cross Section History (3)**

As noted earlier, the mill and inlay with fabric to start the 2009 cycle initially improved the International Roughness Index (IRI). However, roughness quickly increased after an additional 2.5 million ESALs. After 3.5 million additional ESALs, there was significant distortion of the pavement surface as indicated by the extremely high IRI over 150 in/mile.

A quick fix was designed using GeoGrid but it failed quickly (Figure 2). The pavement distress in N8 at this point was sufficiently severe to warrant trucks diverting around the section for safety purposes. Further discussions with ODOT regarding rehabilitation resulted in the decision to do another mill-and-inlay, but this time to use a highly polymer-modified AC mixture (HPM) to withstand further cracking and restore the structural integrity of the section. Figure 2 also shows the final rehabilitation cross-section with the HPM. Further details regarding the HPM have been documented elsewhere (3).

The second rehabilitation using the HPM proved very effective in restoring the ride quality of Section N8 for the remainder of the 2009 cycle. Meanwhile, the perpetual pavement section (N9) endured the same traffic and environmental conditions with very little change in the ride quality and essentially no cracking over the first 20 million ESAL applications.

Though the primary form of distress in the non-perpetual section before the HPM rehabilitation was high roughness due to cracking, it is interesting to also compare the rutting performance of the two sections (Figure 3). The perpetual section clearly outperformed the non-perpetual with rut depths below 7 mm. Section N8 had rut depths approaching the traditional failure point of 12.5 mm before the HPM rehabilitation; however, after its rehabilitation, the rutting stabilized throughout the entire 2012 loading cycle ending with less than 7 mm of rutting.

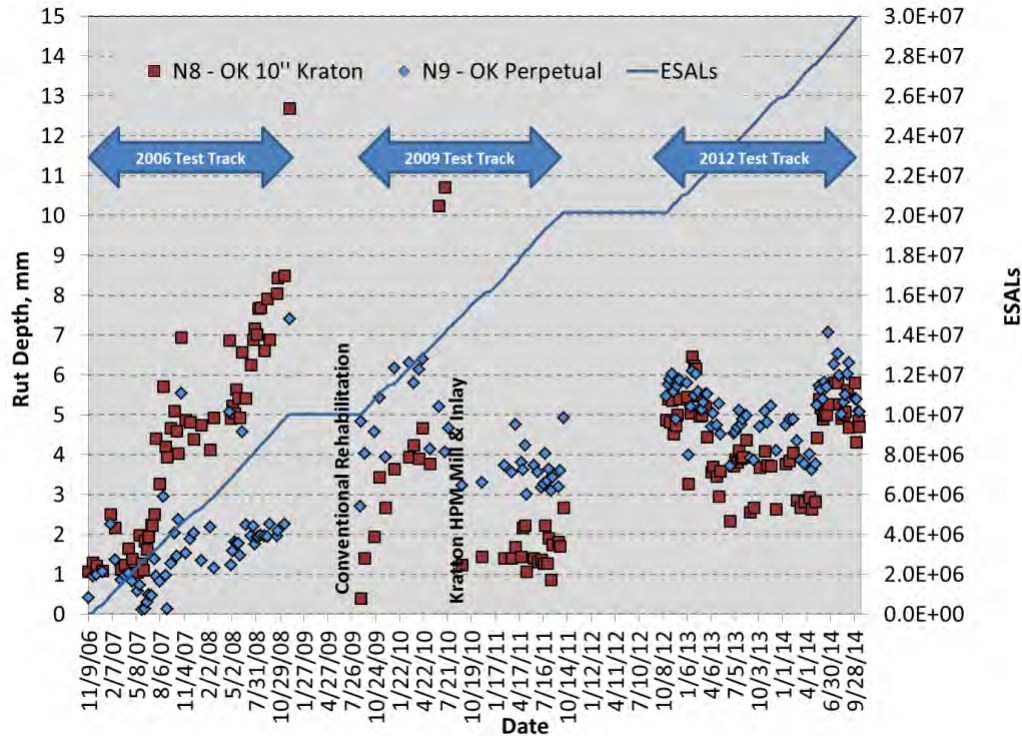


**Figure 3 Rutting Progression Versus ESALs**

The HPM rehabilitation also seemed to aid the ride quality and crack progression of Section N8. Figure 4 shows the IRI progression of the two test sections. As shown, the IRI before the HPM rehabilitation was approaching 300 in/mile; however, after the rehabilitation, the IRI steadily remained between 60 and 80 until near the end of the trafficking. At this point, an increase in cracking may have caused the increase in IRI. It is interesting to note almost no change in IRI occurred over the entire 2012 test cycle for the perpetual pavement.

Figure 5 shows the crack maps for the two sections. The HPM rehabilitation plot was generated in August 2014 while the perpetual pavement’s crack map was generated in October 2014. While the HPM rehabilitation was able to retard crack progression, reflective cracks were beginning to form in the HPM rehabilitation section. In the perpetual pavement section, however, the cracking was limited to the surface further validating the perpetual pavement experiment.

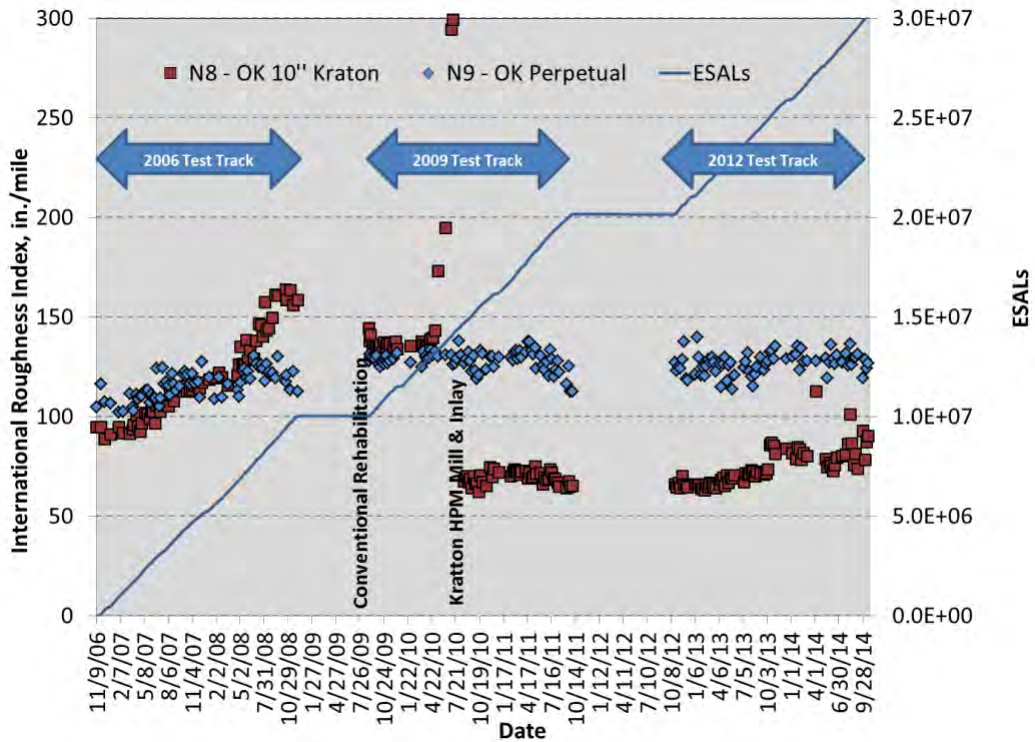


Figure 4 IRI Evaluation of Oklahoma Perpetual Pavement Sections

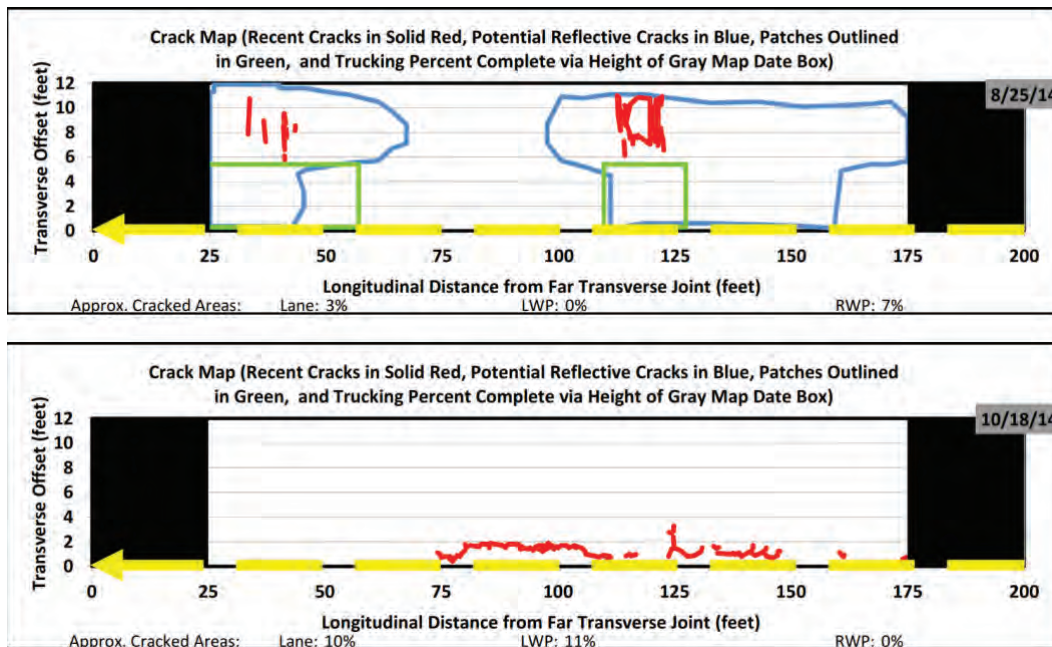
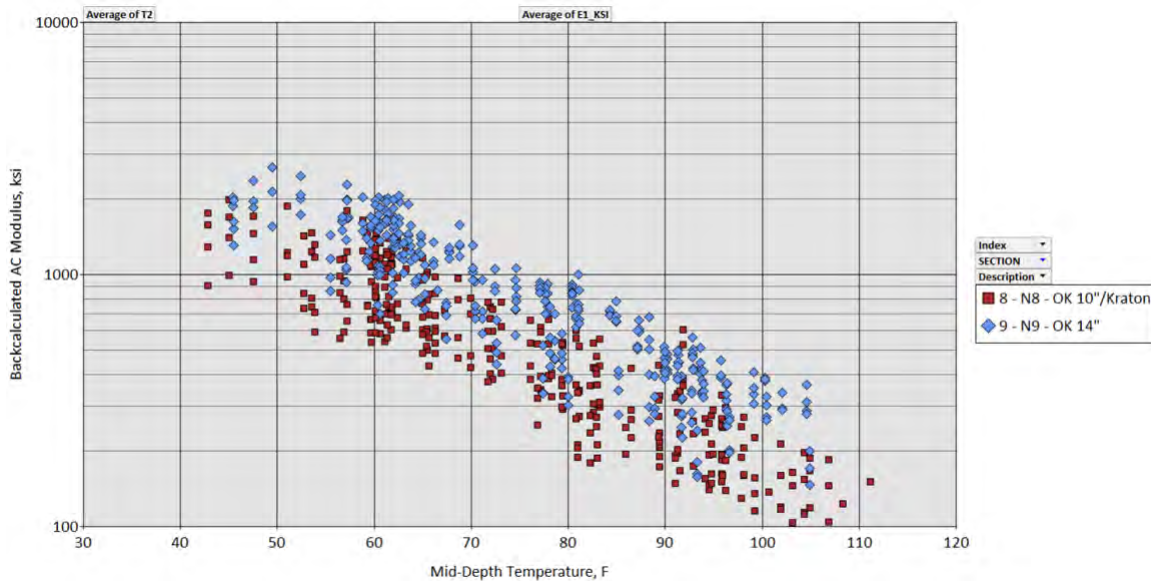


Figure 5 Cracking in Sections N8 (Top) and N9 (Bottom)

*Structural Response Characterization*

Since reliable strain data were not available, only modulus values were considered for the 2012 research cycle analyses. FWD testing conducted several times per month on each section was

used to generate deflection basin data for backcalculation in EVERCALC 5.0. Backcalculated AC moduli versus temperature are presented in Figure 6. Past research has shown that both sections had similar and relatively constant moduli through the 2006 cycle. However, at the start of the 2009 cycle, the non-perpetual section (N8) experienced somewhat lower and more scattered modulus values indicative of structural pavement damage. In the 2012 research cycle, the modulus of the non-perpetual section was lower than the perpetual section. A lower modulus coupled with a thinner pavement cross-section would result in higher strains and potentially accelerate damage from cracking.



**Figure 6 Backcalculated AC Modulus Versus Temperature**

The perpetual section (N9) clearly outperformed the non-perpetual section (N8) over the three test cycles. Though N8 seemed to have been brought up to the same performance and structural response level of N9 through the HPM rehabilitation, there is a major question regarding the cost of each pavement as discussed in the next section.

#### *Life-Cycle Cost Analysis*

The second objective of this research was to quantify the life cycle costs of each pavement. Based on the performance and rehabilitation histories previously discussed in this section of each pavement, a realistic real-world scenario was created that extrapolated the results to a 36 year performance period. Since the Test Track applies traffic in an accelerated manner, a longer time period was selected to be more realistic of typical pavement structures. However, this analysis was only conducted based on data from the 2006 and 2009 test cycles.

Table 2 summarizes the LCCA activities for each test section. ESAL calculations were used to estimate activity years for the analysis. Note that a shallow resurfacing was included for Section N9, though this was not done at the Test Track. It is generally accepted that a perpetual pavement will need some surface renewal over longer time periods. This was included to provide a fair comparison between the two pavement types.

**Table 2 LCCA Event Timing**

Section	Event	Year	Million ESALs	Description
N8	Initial construction	0	0	New 25-cm AC pavement
	1 <sup>st</sup> rehab	18	10	13-cm conventional mill and inlay with fabric
	2 <sup>nd</sup> rehab	24.3	13.5	15-cm mil and inlay with HPM mix
	End of Analysis	36	20	
N9	Initial construction	0	0	New 35-cm AC pavement
	1 <sup>st</sup> resurfacing*	18	10	5-cm conventional mill and inlay
	End of analysis	36	20	

\*Not done at Test Track, included only for hypothetical purposes

Actual cost data obtained from ODOT for the materials used to construct N8 and N9 were used in conjunction with the quantities for each section to create the cash flow diagrams pictured in Figure 7. Applying a 36-year real discount rate of 2% to each vector in the cash flow diagram resulted in the net present values (NPV) shown in Figure 8. Though the initial construction costs of the perpetual pavement were 32% higher, its life cycle costs were 26% lower due to significantly lower rehabilitation costs. It should be noted that the savings would be greater under live traffic conditions because of reduced work zone user costs that were not included in this analysis.

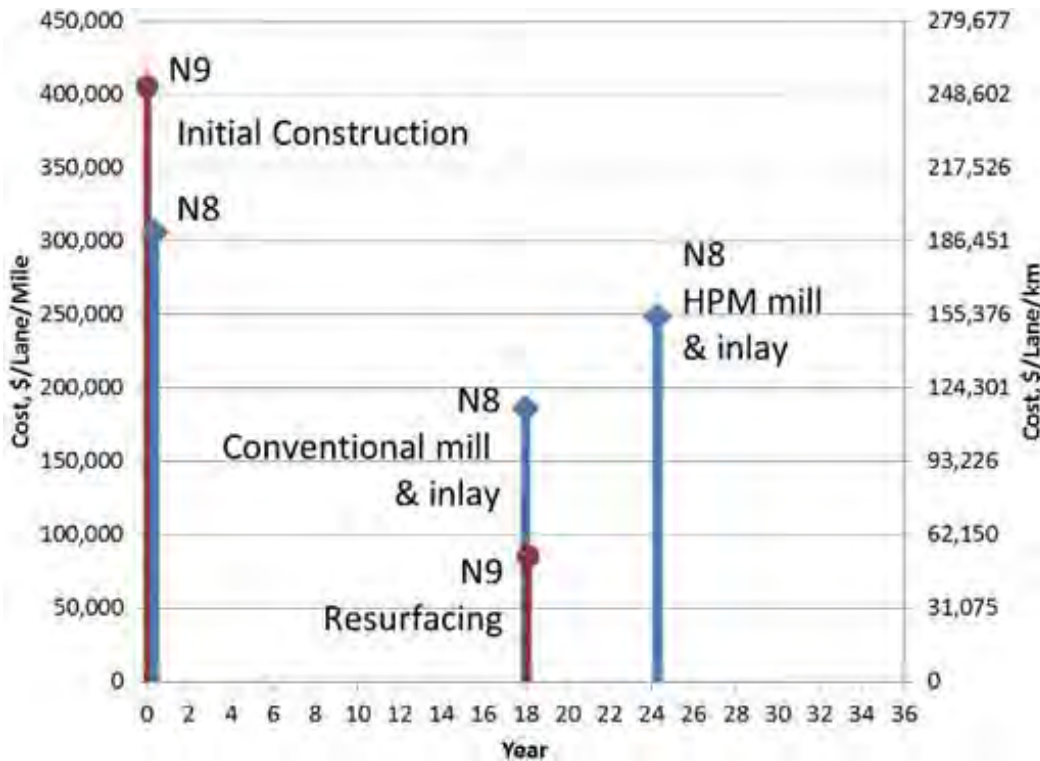


**Figure 7 LCCA Cash Flow Diagram**

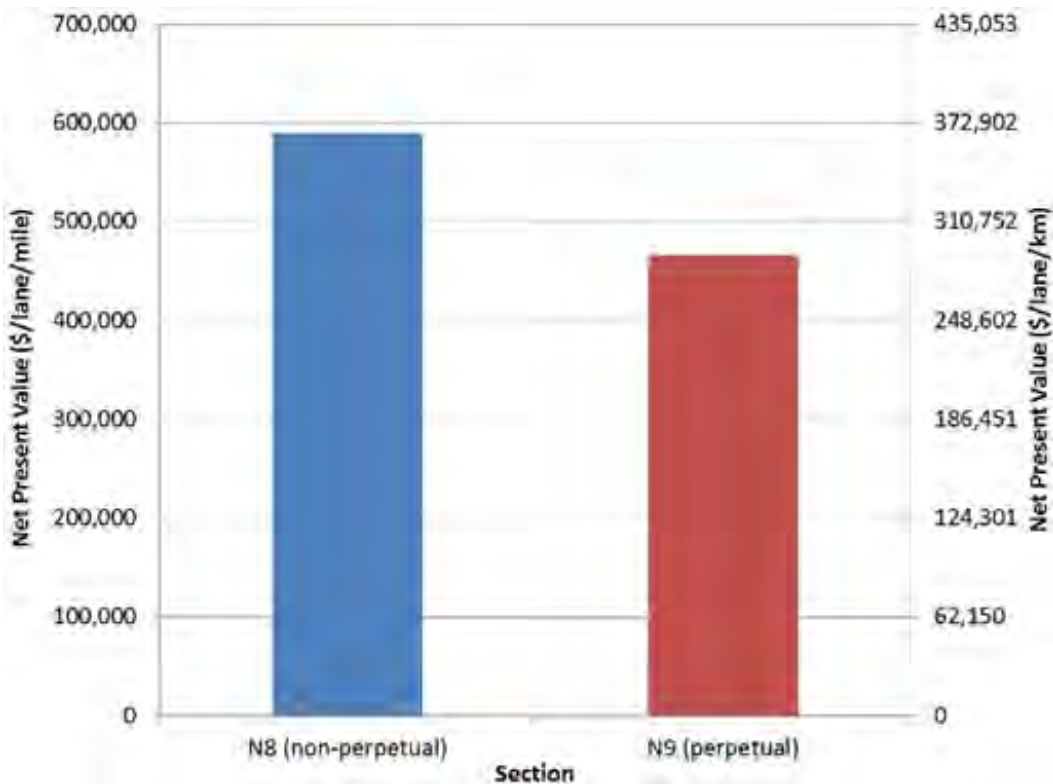


**Figure 8 LCCA Net Present Value**

*Summary*

This investigation focused on two full-scale pavement sections built in 2006 at the NCAT Test Track. The perpetual pavement was constructed with 10 cm additional AC thickness compared to the non-perpetual section. All other conditions between the two pavements were equivalent.

The perpetual pavement outperformed the other thin pavement that proved not to be perpetual. This was demonstrated through ride quality measurements, rut depth measurements, and cracking observations during the 30 million ESAL load applications. The non-perpetual section failed twice during the performance period and required an innovative repair using highly polymer-modified AC to continue performing. However, this pavement eventually began to crack as well after additional trafficking.

Past reports have shown measured pavement responses (strain and stress) in addition to backcalculated AC moduli demonstrate the structural value of the additional thickness in the perpetual pavement. The data also showed that the conventional mill-and-inlay with geofabrics and geogrid was not effective in restoring the structural integrity of the non-perpetual pavement. In fact, the HPM mill-and-inlay was needed to restore the structural capacity of the section. The perpetual pavement in this experiment was the more economical option and provided better performance.

## *References*

1. Timm, D. H., D. Gierhart, and J. R. Willis. Strain Regimes Measured in Two Full Scale Perpetual Pavements. *Proc., International Conference on Perpetual Pavement*, Columbus, Oh., 2009.
2. Timm, D. H. *Design, Construction, and Instrumentation of the 2006 Test Track Structural Study*. NCAT Report 09-01. National Center for Asphalt Technology at Auburn University, Auburn, Ala., 2009.
3. Timm, D. H., R. Powell, J. R. Willis, and R. Kluttz. *Pavement Rehabilitation Using High Polymer Asphalt Mix*. Presented at 91st Annual Meeting of the Transportation Research Board, Washington, D.C., 2012.

## 2.5. Kraton Polymers High Polymer Test Section

### Introduction

In 2009, Kraton Polymers US, LLC began sponsorship of a full-scale test section at the National Center for Asphalt Technology (NCAT) Test Track featuring their newly developed highly modified asphalt (HiMA). The HiMA mixtures were designed with 7.5% styrene-butadiene-styrene (SBS) polymer to have much improved fatigue and rutting resistance characteristics over conventional materials.

Using conventional materials, the Kraton section was built at the same time as a control section and opened to traffic as part of the 2009 Test Track research cycle. Figure 1 shows the structural designs for each section. The Kraton section was designed at 5.75 inches of asphalt concrete (AC) over 6 inches of granular base while the control section was designed with the same depth of aggregate base and 7 inches of AC.

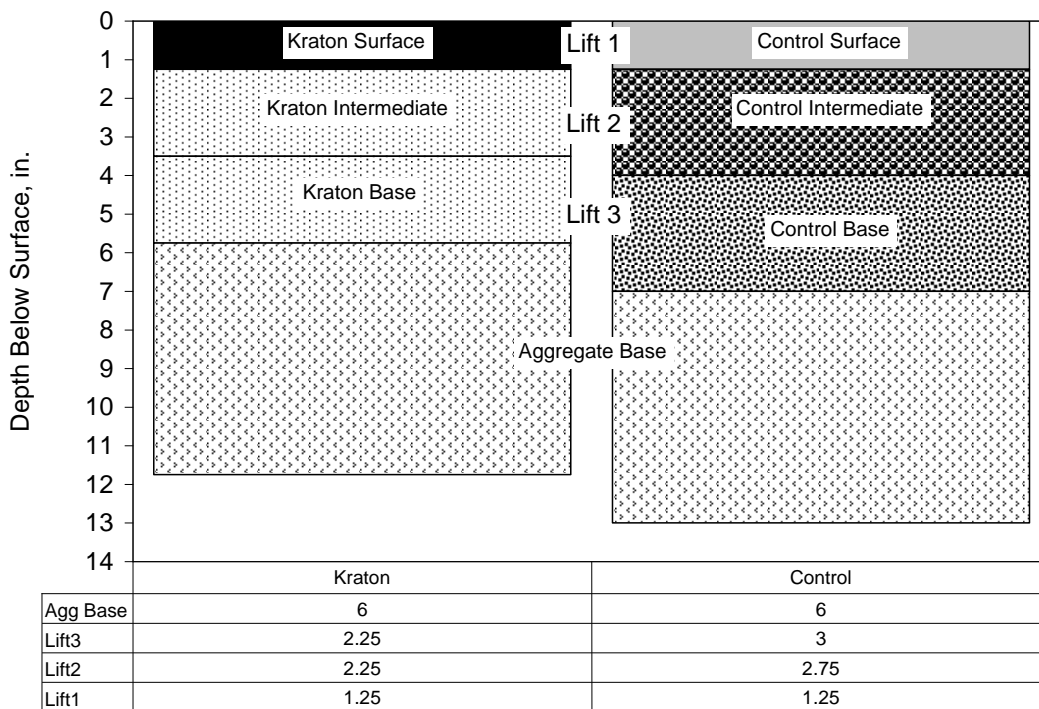


**Figure 1 Cross-Section Design: Materials and Lift Thicknesses**

The materials and mix design were previously documented by Timm et al. while only a summary is provided here (1). Two design gradations were used in this study. The surface layers utilized a 9.5 mm nominal maximum aggregate size (NMAS) while the intermediate and base mixtures used a 19 mm NMAS gradation. The aggregate gradations were a blend of granite, limestone, and sand using locally available materials. Distinct gradations were developed for each control mixture (surface, intermediate, and base) to achieve the necessary volumetric targets as the binder grade and nominal maximum aggregate size (NMAS) changed between layers. The Kraton gradations were very similar to the control mixtures. Table 1 provides a summary of the mix design parameters; further details are available in a previous report (1).

**Table 1 Mix Design Parameters**

Mixture Type	Control			Kraton	
	1	2	3	1	2 & 3
Lift (1=surface; 2=intermediate, 3=base)	1	2	3	1	2 & 3
Asphalt PG Grade	76-22	76-22	67-22	88-22	88-22
% Polymer Modification	2.8	2.8	0	7.5	7.5
Design Air Voids (VTM), %	4	4	4	4	4
Total Combined Binder (P <sub>b</sub> ), % wt	5.8	4.7	4.6	5.9	4.6
Effective Binder (P <sub>be</sub> ), %	5.1	4.1	4.1	5.3	4.2
Dust Proportion (DP)	1.1	0.9	1.1	1.1	0.9
Maximum Specific Gravity (G <sub>mm</sub> )	2.483	2.575	2.574	2.474	2.570
Voids in Mineral Aggregate (VMA), %	15.8	13.9	13.9	16.2	14.0
Voids Filled with Asphalt (VFA), %	75	71	71	75	72

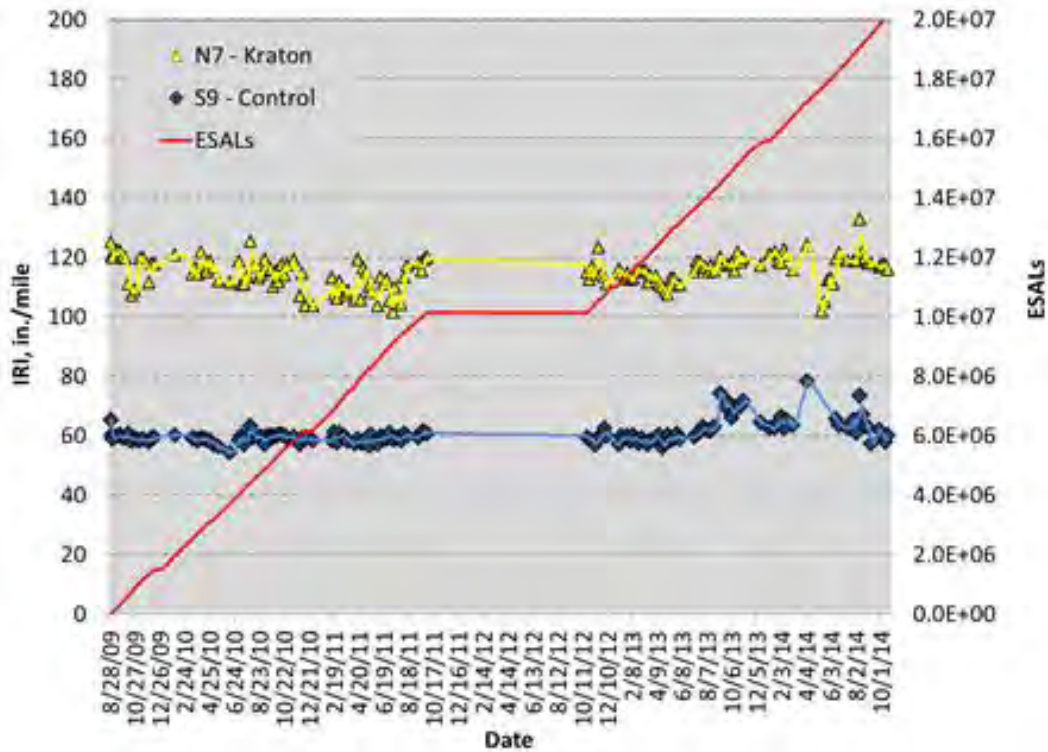
During construction, strain gauges, pressure plates, and temperature probes were installed in the section as previously described. The sections were opened to traffic on August 28, 2009. At that time, weekly pavement response and regular FWD testing began. Weekly performance monitoring in terms of rutting, ride quality, and visual inspection for cracking also commenced at that time. The first trafficking cycle ended on September 28, 2011 after the application of 10.14 million equivalent single axle loads (ESALs); however, since no damage had been accrued in the test section, Kraton decided to continue traffic on the test section to assess its performance. The control test section ultimately became part of another experiment during the second testing cycle. Past reports provide details regarding field and laboratory performance during the first research cycle (1, 2).

#### *Objective and Scope*

The objective of this study was to assess the continued field performance of Kraton's HiMA mixtures placed in Section N7. These mixtures were evaluated in terms of both field performance and structural capacity.

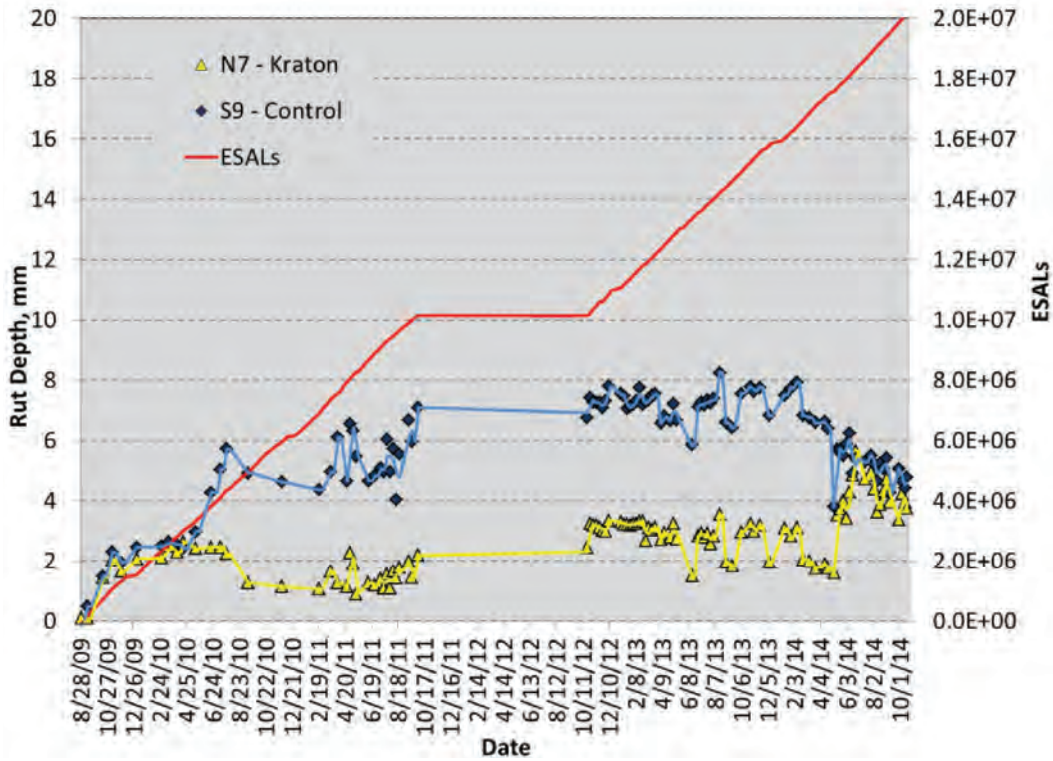
#### *Field Performance*

Section N7 was evaluated in terms of roughness, rutting, and cracking during the 2012 research cycle. Figure 2 shows the change in roughness over time for the HiMA section compared to the control (Section S9). Increases in roughness are commonly associated with pavement distresses; however, despite slight fluctuations in the smoothness of the pavement, the roughness of the HiMA section remained near 120 in/mile for 20 million ESALs of traffic. This was almost double the roughness of the control section. One should note that the pavement was built with a higher roughness, and the pavement's smoothness did not degrade over 20 million ESALs. There was also no degradation in the control mixture's IRI. The fluctuations in IRI values come from changing the profiler during the second cycle of testing.



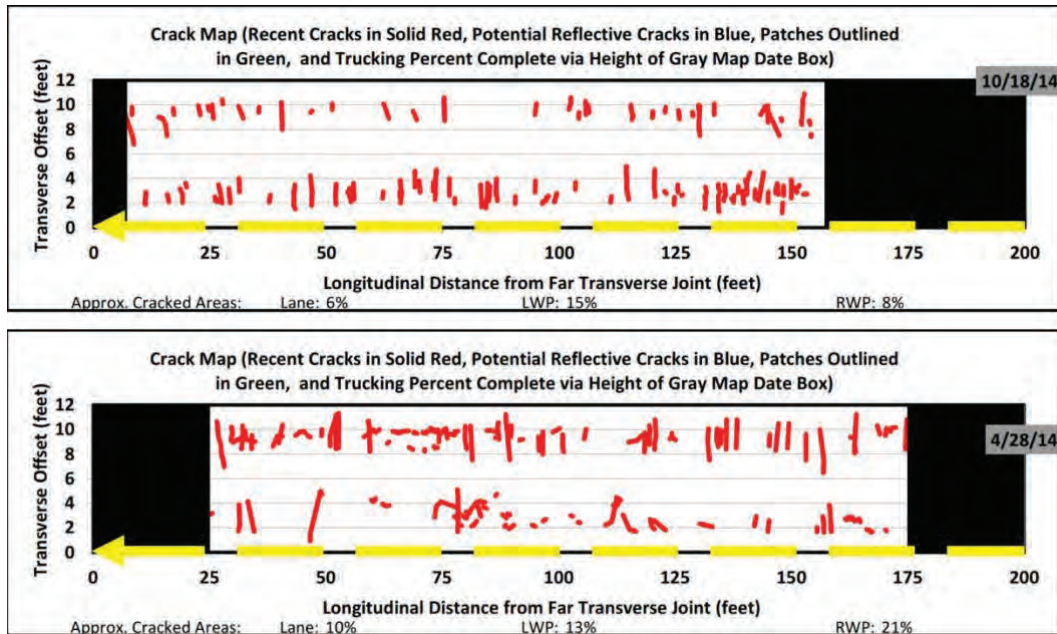
**Figure 2 Kraton HPM Roughness Versus Time**

Figure 3 compares the rut depths from the control section to the HiMA section versus time. It is important to remember that the HiMA section was 1.25 inches thinner than the control section; however, it still outperformed the control mixture in terms of rutting resistance. The rutting on the control section was reduced due to a pavement preservation treatment (100 feet of 4.75 mm thinlay and 100 feet of microsurfacing) that was applied; however, even after 20 million ESALs of traffic, the HiMA section had only rutted approximately 4 mm.



**Figure 3 Kraton HPM Rutting Versus Time**

The final assessment of field performance was mixture cracking (Figure 4). On April 28, 2014, the control test section had cracking in 10 percent of the lane area, 13 percent of the right wheelpath, and 21 percent of the left wheelpath. At the end of 20 million ESALs in October 2014, only 6 percent of the HiMA lane had cracked along with 8 and 15 percent of the right and left wheelpaths, respectively. Forensic coring showed that the HiMA section only had superficial surface cracking while the control test section had fatigue cracking.



**Figure 4 Crack Maps for HiMA in October 2014 (Top) and Control (Bottom) in April 2014**

### *Structural Capacity*

In the 2012 research cycle, there were not enough working gauges to continue collecting high speed strain and pressure measurements. The FWD program was continued to assess the mixture stiffness over time and versus temperature. Figure 5 shows the relationship between backcalculated asphalt modulus versus temperature for both the Kraton and the control test sections. Both test sections seem to follow similar trends; however, differences can be seen when comparing the temperature corrected asphalt moduli (Figure 6). When using a Tukey-Kramer comparison at a 5 percent level of significance, only the stiffness values from N7-2009 and S9-2012 are statistically similar. The other test sections have statistically stiffer moduli. This means that in the second cycle of testing, strains at the bottom of the HiMA section are expected to be reduced due to the stiffening of the test section. This, along with the high fatigue tolerance of the material, could explain the mixture's performance over 20 million ESALs.

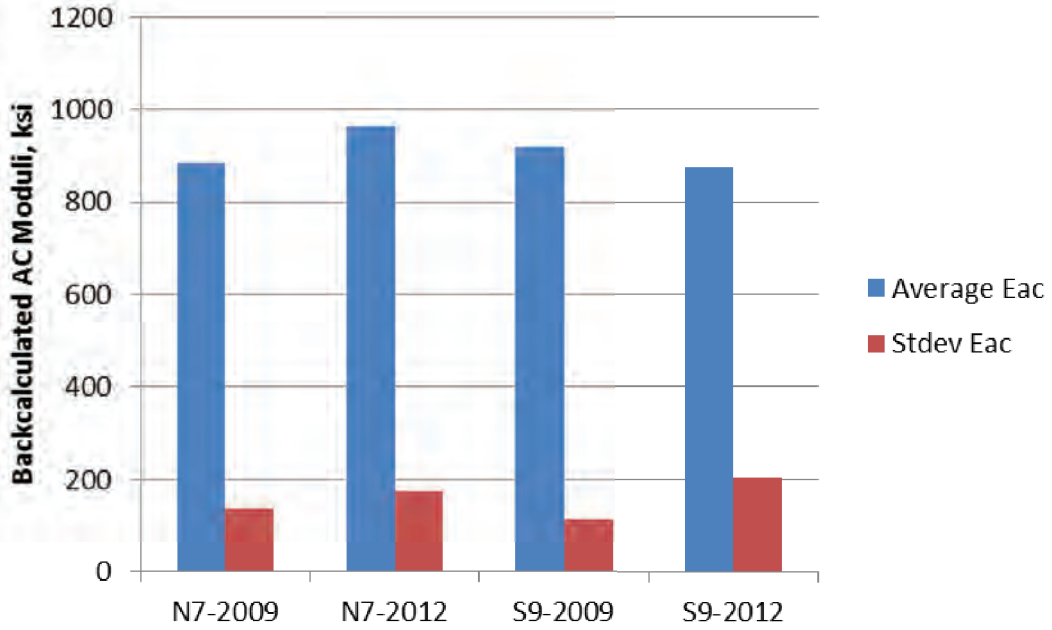


**Figure 5 AC Modulus Versus Temperature**

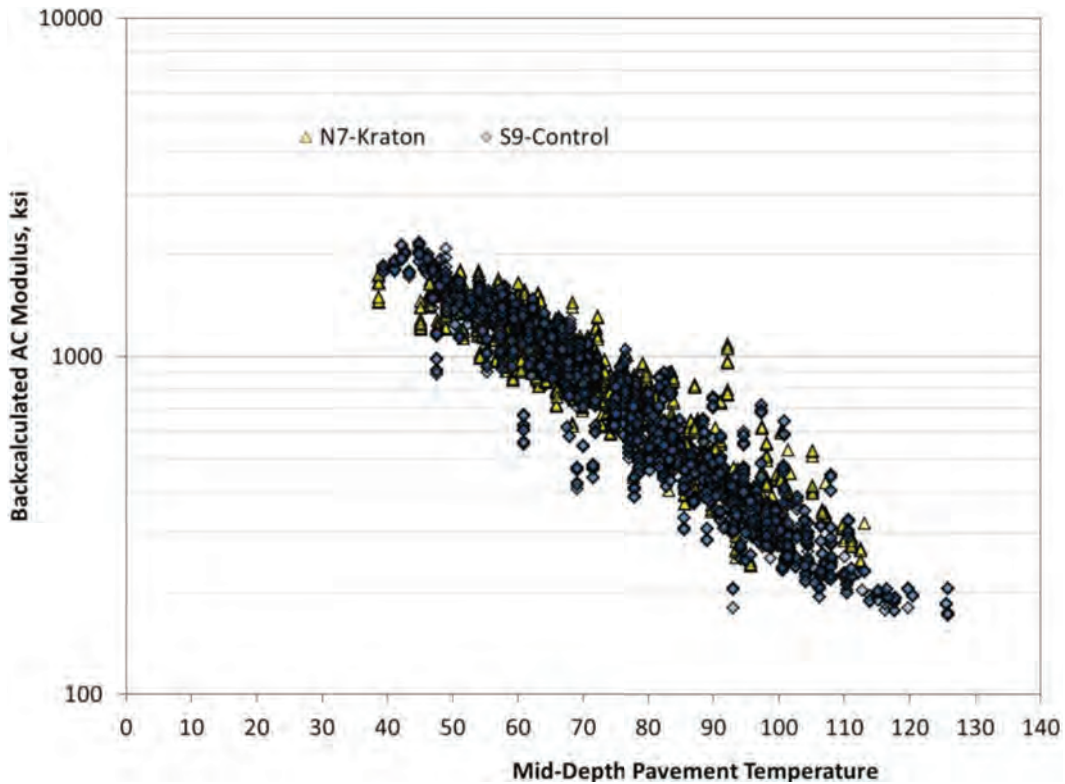


**Figure 6 Temperature Corrected AC Moduli**

*Summary*

The HiMA test section continued to outperform the control test section after 20 million ESALs of traffic. It should be noted that the test section had a higher initial IRI than the control but there

has been no degradation of smoothness since initial construction. Additionally, the recorded rutting and cracking is less in the HiMA section. The HiMA mixtures were both stiff and flexible, which allowed for better fatigue performance in the test section. These cracks were noted as superficial surface cracking.

#### *References*

1. Timm, D., M. Robbins, J. R. Willis, N. Tran, and A. Taylor. *Field and Laboratory Study of High Polymer Mixtures at the NCAT Test Track - Interim Report*. NCAT Report 12-08. National Center for Asphalt Technology at Auburn University, Auburn, Ala., 2012.
2. Timm, D., M. Robbins, J. R. Willis, N. Tran, and A. Taylor. *Field and Laboratory Study of High Polymer Mixtures at the NCAT Test Track - Final Report*. NCAT Report 13-03. National Center for Asphalt Technology at Auburn University, Auburn, Ala., 2013.

### 3. NON-STRUCTURAL EXPERIMENTS

Several sections on the 2012 track were placed for sponsors who want to improve the durability and performance of Porous Friction Courses (PFCs) either through modifications to mix design or tack applications. PFC test section objectives were as follows:

- Alabama – Improved Durability (E9A, E9B, E10)
- Florida – Comparative Tack Methods (N1A, N1B, N2)
- Oklahoma – Comparative Tack Methods (E1A, E1B)
- Tennessee – Use of Reclaimed Asphalt Shingles (S4—2003 vs. 2012)
- Virginia – Minimizing Road Noise (W10)
- Preservation Group – Effect of Fog Seal (S8A, S8B)

Two of the challenges with PFC mixtures are to extend service life and maintain functionality of the mixes for permeability. In a recent survey conducted by NCAT, 21 agencies responded that they currently use PFC mixes. The typical service life for PFC pavements in these states is about 8-10 years (Figure 1). These agencies listed raveling as the greatest cause of pavement distress, with clogging of the mix as the second highest concern (Figure 2).

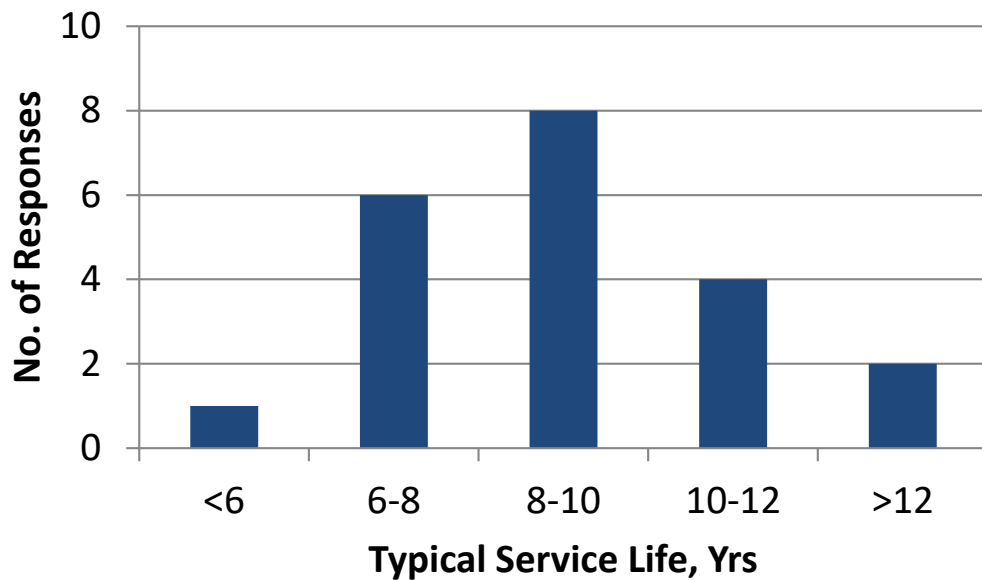
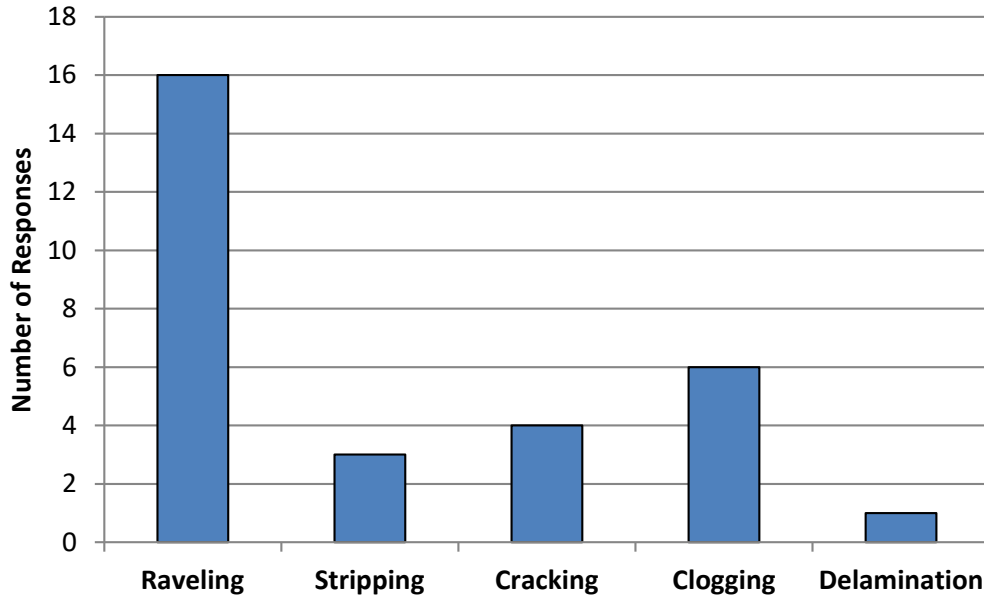
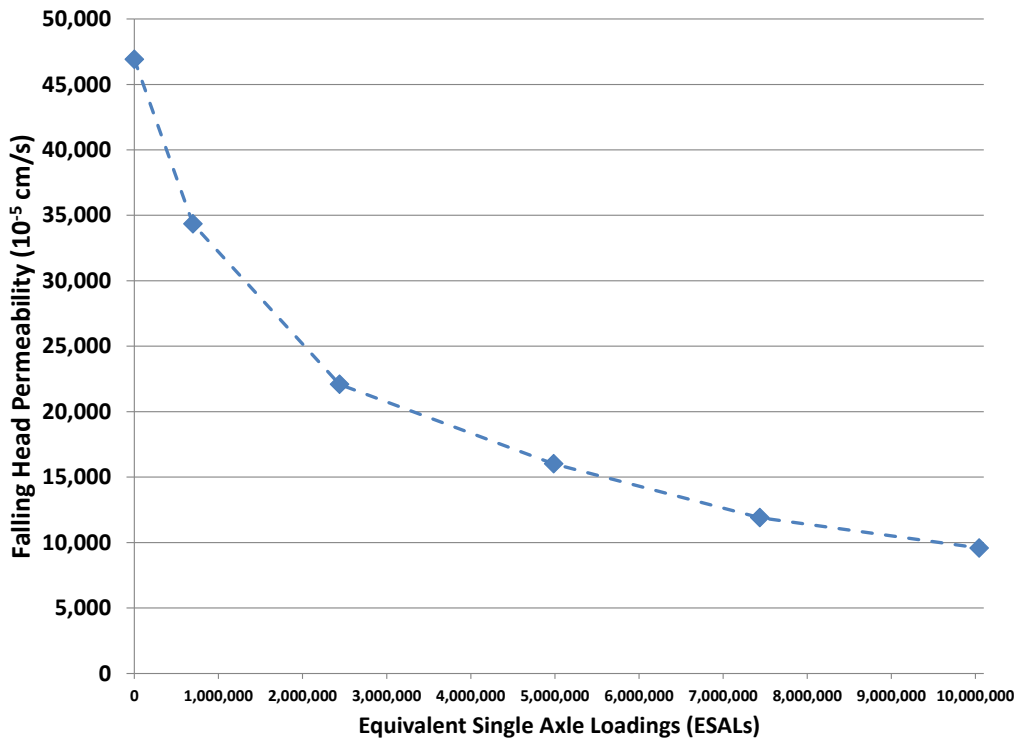


Figure 1 Typical Performance Life of PFC Mixtures



**Figure 2 Type of Distress Observed in PFC Pavements**

Field permeability testing at the NCAT Test Track during the 2012-2014 cycle shows that permeability values reduce considerably over time and with traffic loading. Figure 3 shows average field permeability for all PFC sections on the track combined and includes both 9.5 and 12.5 nominal maximum aggregate size (NMAS) mixtures.



**Figure 3 Reduction in Field Permeability Due to Time and Traffic**

Figure 3 shows that PFC mixes begin to reach a plateau, at which point they resist further densification or clogging (because the rate of change is decreasing). The plateau effect is readily apparent for the 9.5 mm mix in Oklahoma's section, E1 (Figure 4). This supports other research, which showed that PFC mixtures lose most of their porosity early in their service life, and beyond some point, the rate of clogging asymptotes (1). Although the mix has lost much of its initial drainage capacity, it is still somewhat functional even at its lowest permeability.

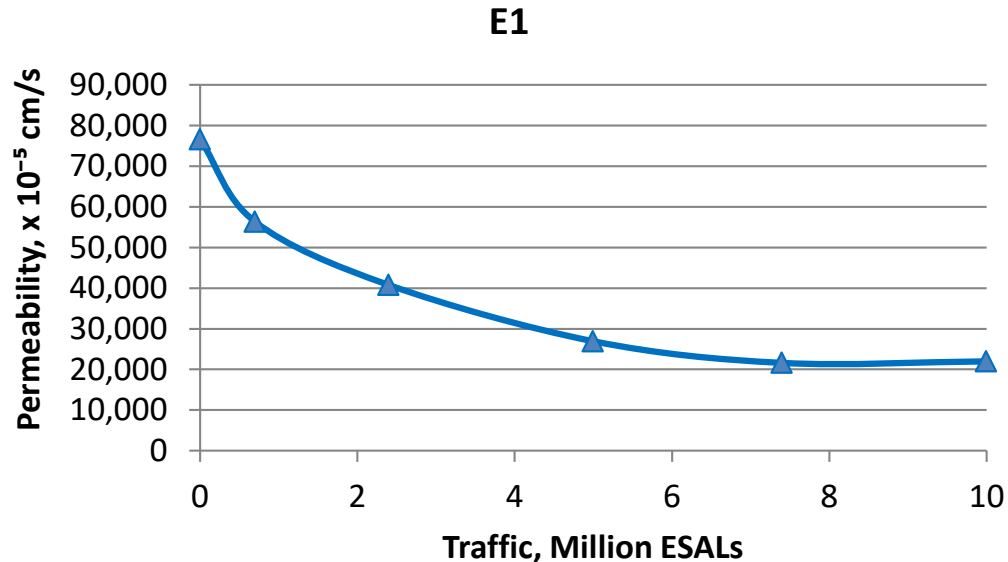


**Figure 4 Loss of Permeability Reaches a Plateau in E1**

Both Figures 3 and 4 indicate that approximately one-half of the loss in permeability occurred during the first two million ESALs. This is likely due to densification of the mix under loading rather than from clogging. The movement of aggregate particles early in the life of a PFC may be an explanation for premature raveling, as some of the internal bond from overlap of binder film thickness coating the particles is lost. Research has also shown that some of the reduction in permeability may be caused by binder creep (drain-down) which begins immediately after construction and continues especially during hot summer months as the binder softens (2). This results in a thinner asphalt film at the surface of the layer, which leads to accelerated aging and increases the raveling potential of aggregate particles near the surface. As the binder drains from the aggregate particle due to gravity flow, the binder begins to fill inter-connected air voids and reduces the flow of water.

Figure 5 shows that the in-place air voids immediately after construction were consistently higher (up to 6.7%) than the design air voids determined in the laboratory. Laboratory samples were compacted to 50 gyrations with a Superpave Gyratory Compactor (SGC). PFC mixtures are generally not compacted to a specified density in the field. The mix is rolled with a couple of passes using a smooth drum roller just to seat the aggregate particles into the tack coat. One expects the roadway density to approximate the laboratory density at which performance testing was conducted. It may be that traffic continues to densify PFC mixtures until they reach a "locking point", or stone-on-stone overlap beyond which crushing of aggregate particles begins to take

place. This reorientation, or movement, may result in loss of bond between some particles and may lead to some particles being raveled out almost immediately after construction.

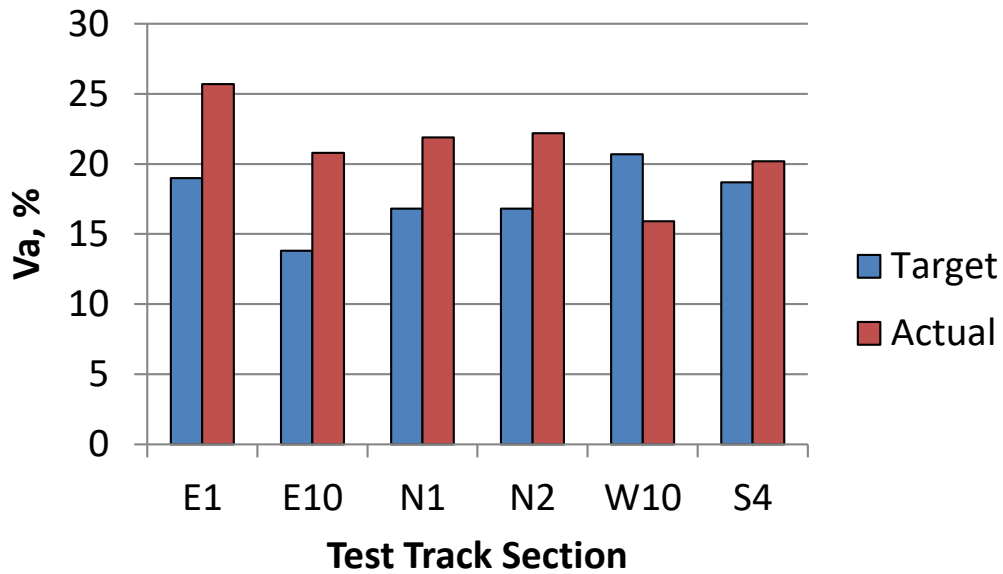


Figure 5 Mix Design vs. In-Place Air Voids

#### References

1. Hamzah, M. O., M. Hasan, and M. van de Ven. Permeability Loss in Porous Asphalt Due to Binder Creep. *Construction and Building Materials*, Vol. 30, No. 1, 2012, pp. 10-15.
2. Hamzah, M. O., N. Abdullah, J. Voskuilen, and G. Bochove. Laboratory Simulation of the Clogging Behaviour of Single-Layer and Two-Layer Porous Asphalt. *Road Materials and Pavement Design*, Vol. 14, No. 1, 2013, pp 107-125.

### 3.1. Virginia Department of Transportation Noise Experiment

#### Overview

Virginia sponsored two sections at the NCAT Test Track (W10, S1) for evaluating quiet pavements using a 12.5 mm NMAS PFC mix consisting of traprock aggregate common to Virginia with 10% RAP. Section W10 used PG 76-22 modified binder while the mix for Section S1 used 12% ground tire rubber (GTR).

#### Performance

Figure 1 shows that the sound intensity measured with the On-Board Sound Intensity (OBSI) system of microphones and data collection software were practically the same for both sections immediately after construction. The trend line diverges somewhat over time and traffic loading, however, with slightly more noise being generated in the GTR section.

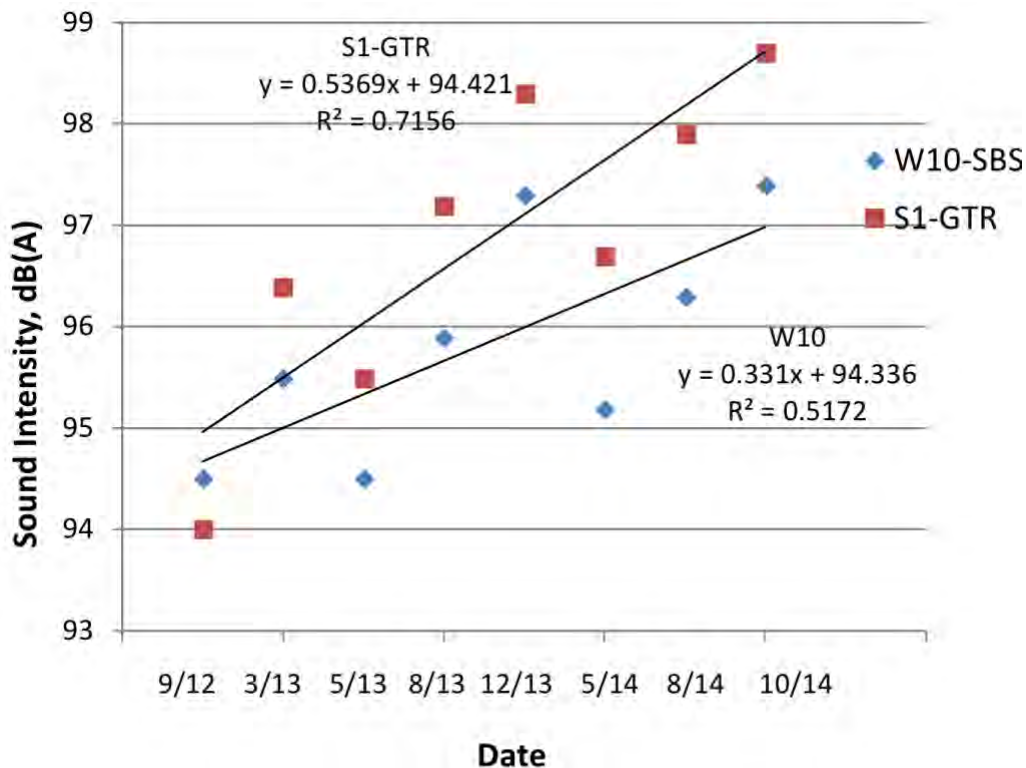
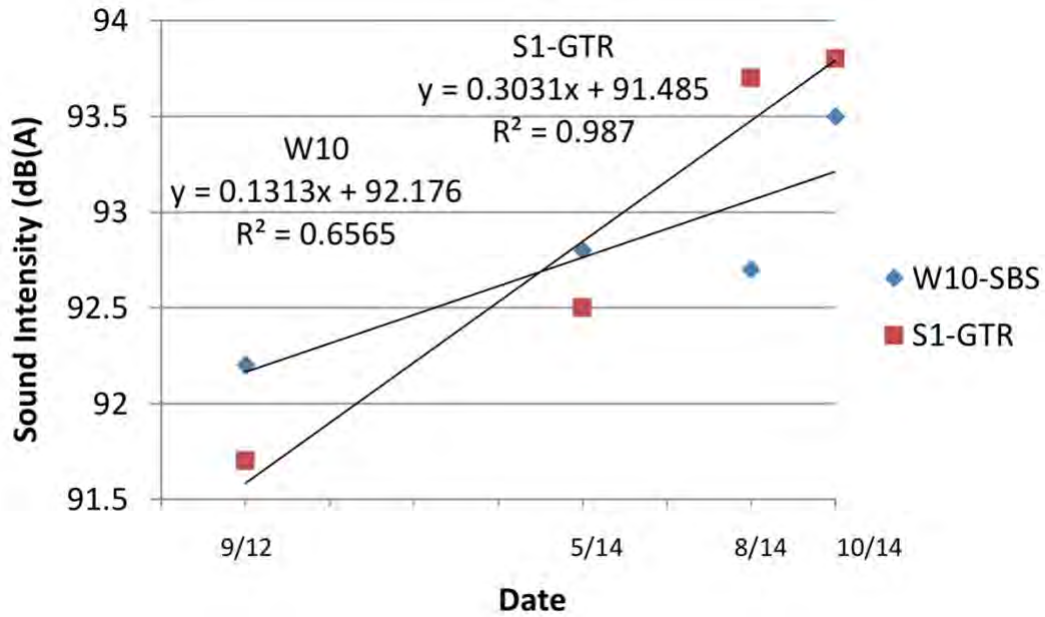


Figure 1 Section W10 & S1 OBSI Global Average Noise Measurements

Sound intensity was also measured using the close proximity (CPX) method. This method uses a special acoustical trailer developed by NCAT so that engine and drive train noise from the vehicle does not affect the sound intensity being measured. This will explain why the decibel levels measured with the CPX trailer are somewhat lower than for the OBSI measurements. The CPX results, Figure 2, show a trend similar to the OBSI results in that noise levels were higher in the GTR section at the end of 2014 although the sound intensity of the GTR section was initially slightly lower than Section W10.



**Figure 2 Section W10 & S1 CPX Global Average Noise Measurements**

Noise measurements were also taken with an impedance tube (ASTM C384-04 and ASTM E-1050). The impedance tube uses a noise source generator to send sound impulses to the pavement surface and has a set of microphones near the pavement to measure the amount of noise reflected (Figure 3). Calculations are made from that information as to how much noise was absorbed by the pavement. The device is somewhat limited since the “white noise” generated does not truly represent the same noise that is generated at the tire/pavement interface. However, it is much more mobile and convenient to transport than the other devices and results still sufficiently indicate differences caused by the pavement surface. Noise absorption results from the testing (Figure 4) show that the GTR mix absorbed more sound initially, but by the end of the 2012 cycle the trend line shows slightly less absorption than for the SBS section.



Figure 3 Impedance Tube

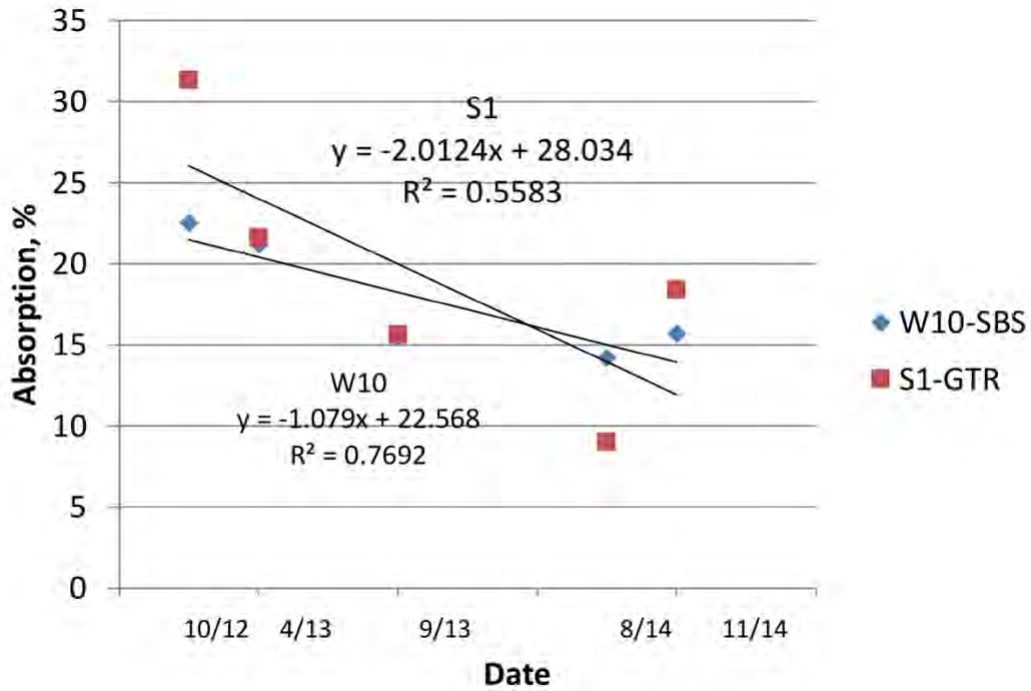
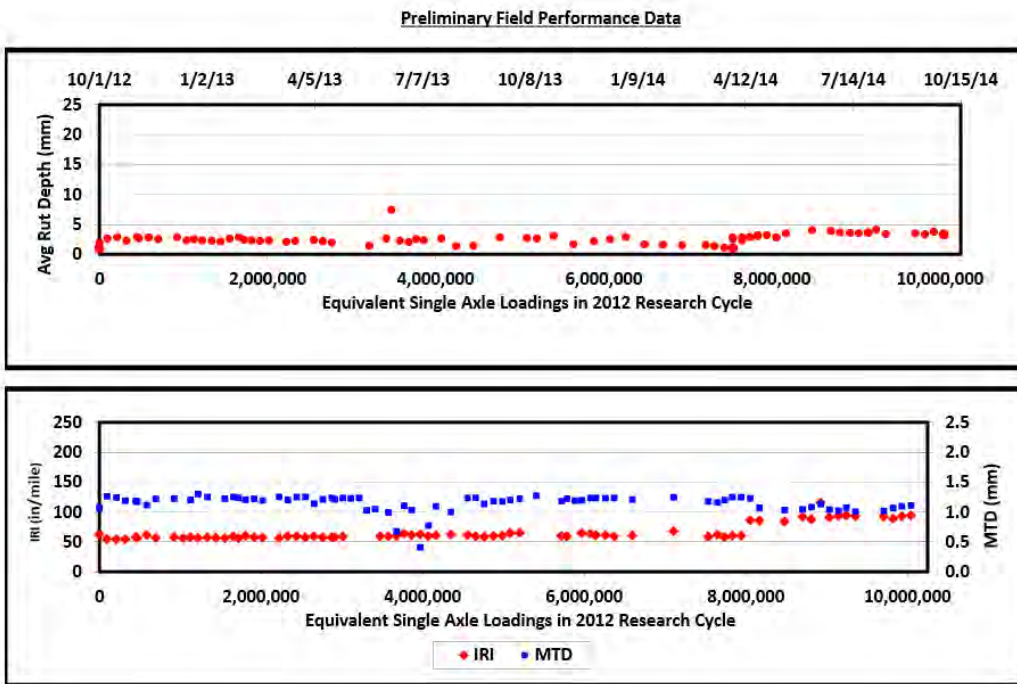
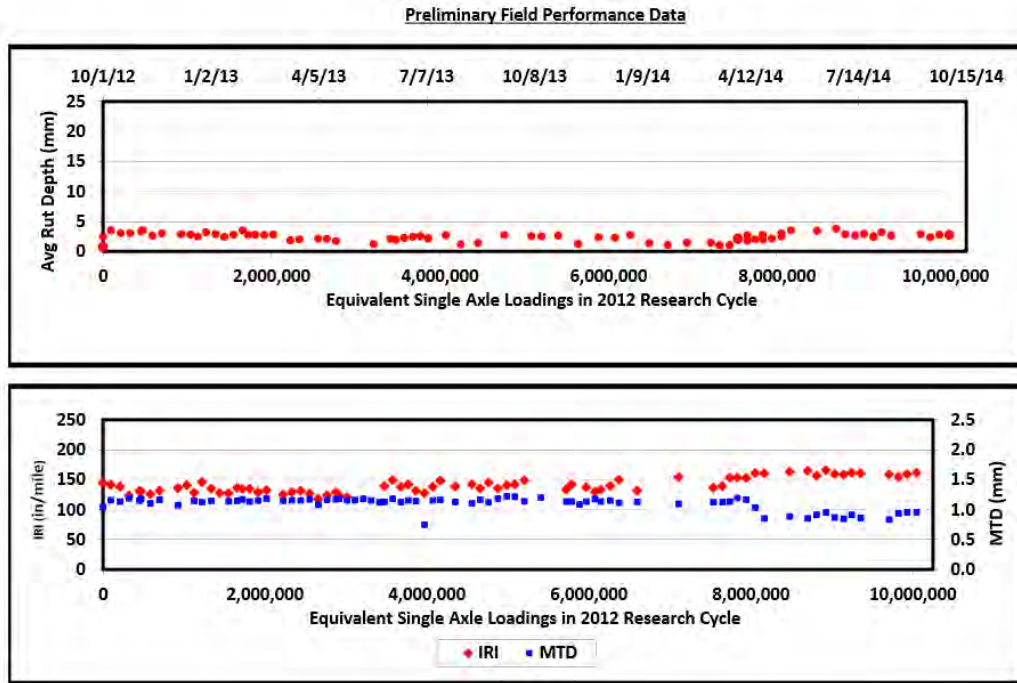


Figure 4 Noise Absorption (%) by Impedance Tube

Figures 5 and 6 show that performance is similar for both W10 and S1 in terms of rutting and mean texture depth (MTD). Smoothness of the pavement layers as determined by International Roughness Index (IRI) was considerably better for the GTR Section S1, but this may be related to

variability in construction and placement since the values were relatively constant throughout the two-year loading cycle.



### *Findings*

Sound intensity for the GTR asphalt modified sections were generally lower than the SBS section immediately after construction, but intensity became greater than the SBS section over time based on OBSI and CPX testing. Noise absorption was initially higher for the GTR section, but it decreased over time at a greater rate than the SBS section. Smoothness was better for the GTR section based on IRI results, but the differences may have been due to construction variability since the values were relatively constant for both mixes.

### 3.2. Alabama Department of Transportation OGFC Experiment

#### Background

Agencies are concerned with improving the durability of PFC mixtures so that raveling, the primary mode of distress, does not occur prematurely. The test used most often as a measure of durability or resistance to raveling is the Cantabro stone loss test. The test, developed originally for Marshall PFC specimens in Spain, subjects a sample of a known weight to 300 revolutions in a Los Angeles abrasion machine. Afterward, the largest mass is weighed and the amount of stone lost, or raveled, is recorded. European specifications typically limit Cantabro stone loss to a maximum of 20%.

Previous research at NCAT has shown that stone loss by the Cantabro procedure is almost always lower for SGC samples compacted to 50 gyrations than for Marshall specimens compacted to 50 blows as is done in European practice. The limited research shows that when stone loss from Marshall samples is compared to stone loss from SGC samples, a corresponding limit for unconditioned SGC samples should be about 15 percent maximum loss (Figure 1).

The 9.5 mm NMAS PFC placed in Section E9A easily met Cantabro requirements at each asphalt content increment during laboratory mix design testing. Figure 2 shows that Cantabro stone loss was reduced as asphalt content was increased. Figure 2 also shows that as asphalt increased, the percent air voids did not suffer significantly. This would indicate that increasing asphalt content can make PFC mixtures more resistant to raveling without greatly reducing air voids or potential permeability.

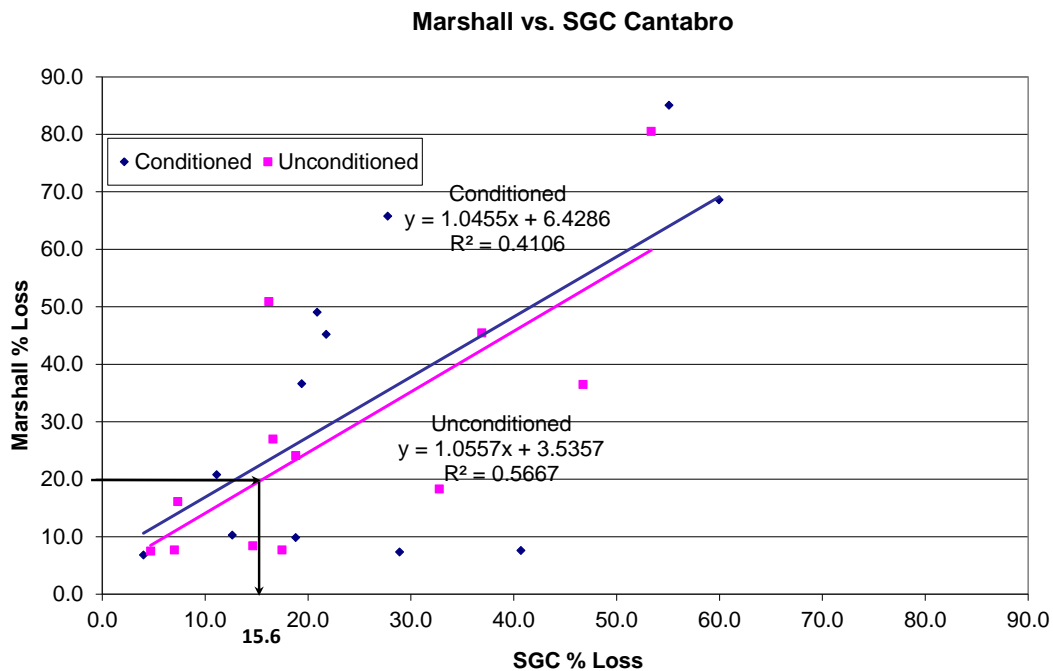
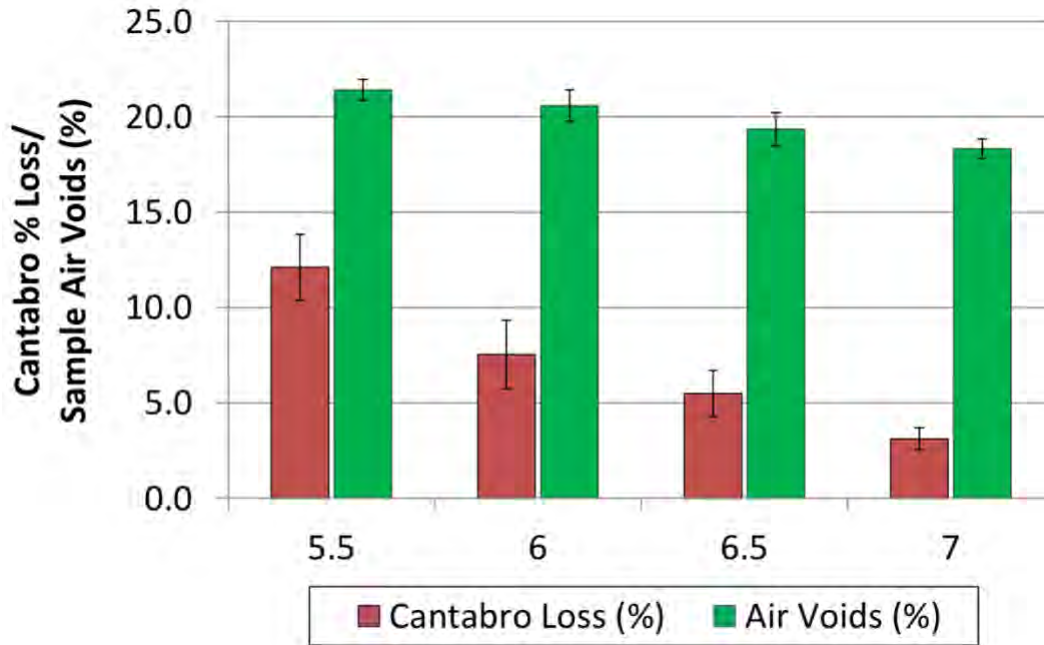


Figure 1 Comparison of Cantabro Stone Loss for Marshall vs Gyratory Samples



**Figure 2 Section E9A 9.5 mm PFC Mix Design Cantabro Stone Loss and Air Voids**

*Sections E9A, E9B, and E10*

For Section E9B and E10, ALDOT chose to use a 12.5 mm NMAS PFC mixture. Section E9B used the customary 0.3% cellulose fibers based on weight of binder to prevent drain-down of the thick asphalt binder film from aggregate particles. Cantabro stone loss for the mix placed in E9B was measured during the mix design at four asphalt contents (5.0%, 5.5%, 6.0%, and 6.5%) as given in Figure 3. At least 6.0% asphalt content was needed, based on the Cantabro results, to resist stone loss at the maximum of 15%. Two additional mixes were prepared at the optimum asphalt content of 6.0% with synthetic fibers at a dosage rate of 0.05% by weight of mix (1lb/ton of mix). One mix used the synthetic fiber alone as a stabilizer for the binder film to prevent drain-down. In the second mix, cellulose fiber was added as well to see whether the synthetic fiber alone would be able to eliminate drain-down and improve resistance to raveling or if both fibers would be beneficial. It is clear from Figure 3 that the addition of synthetic fibers improved resistance to raveling as measured by the Cantabro test. Figure 3 also shows that using cellulose fiber in addition to synthetic fiber was not necessary. Therefore, Section E9B was constructed with only the synthetic fiber stabilizer added to the mix.

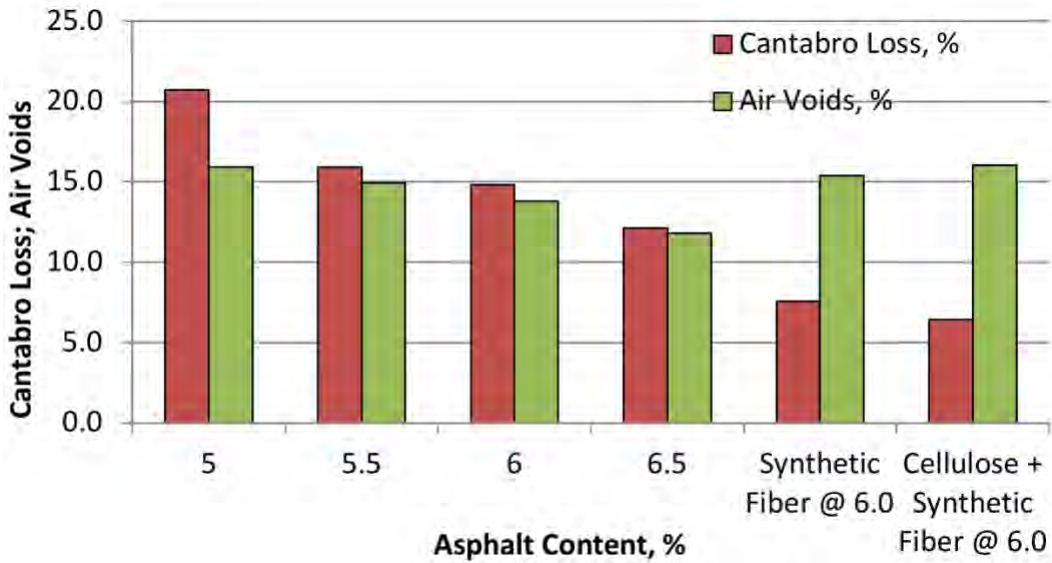


**Figure 3 Effect of Fiber with 12.5 mm NMAS PFC**

*Test Sections*

ALDOT Section E10 was constructed with the asphalt cement modified with ground tire rubber (GTR). A 12.5 mm NMAS mixture was used and 5.35% asphalt content was modified by adding 12% GTR by weight of asphalt binder to provide 6.0% total binder content. No fiber was added to the mix in order to determine whether GTR alone could prevent drain-down and provide resistance to raveling. The GTR was a minus No.30 mesh size and the virgin asphalt binder was PG 67-22. Cantabro results during mix design were within the 15% maximum loss values at 6.0% asphalt (Figure 4) so that was used as the target total binder content. The mix was placed 0.75 in. thick and in-place air voids immediately after construction were 20.8%.

A comparison of tensile strength results obtained during mix design for each of the ALDOT mixes is shown in Figure 5. Those results indicate that the GTR mix without fiber provided the highest tensile strength for 12.5 mm NMAS PFC mixes. The results also show that the 9.5 mm NMAS mixture had the highest strength of all.

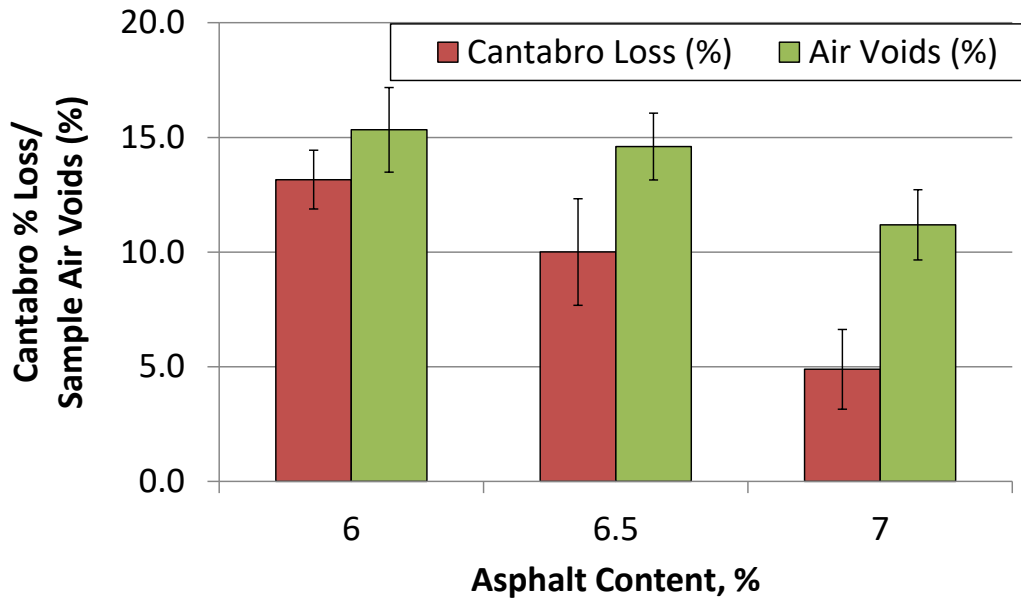


Figure 4 Cantabro Stone Loss for 12.5 mm NMAS PFC with 12% GTR

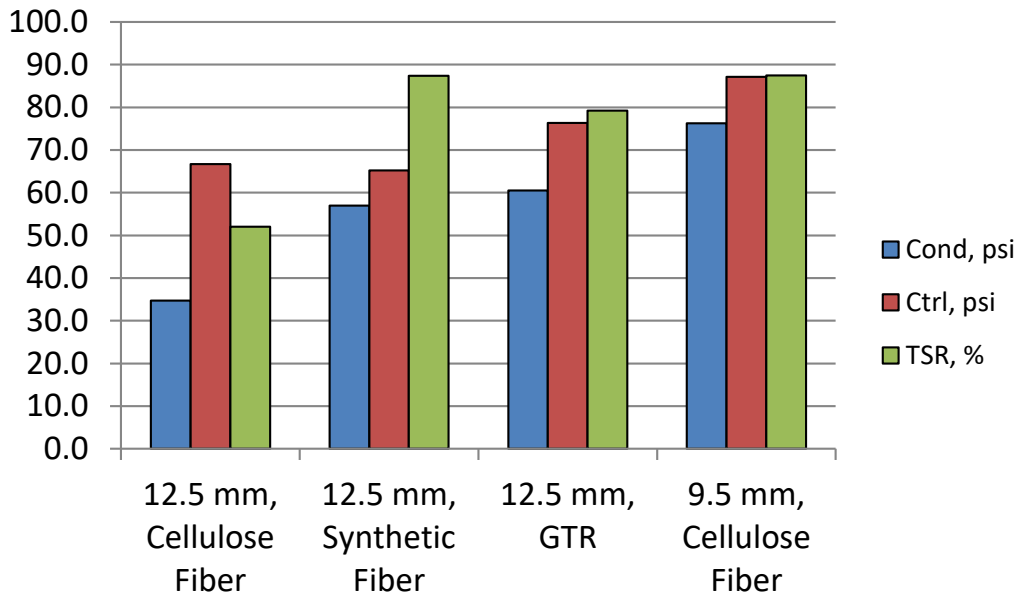


Figure 5 Comparison of Tensile Strength for ALDOT PFC

It appears that the 9.5 mm PFC may be more resistant to raveling than the 12.5 mm NMAS customarily used based on results from PFC mixes used in the ALDOT Sections. The 9.5 mm mix had lower stone loss based on the Cantabro test and had higher tensile strength. The 12.5 mm mixture modified with GTR also performed well in the laboratory for both resistance to stone loss and tensile strength. The synthetic stabilizer appeared to contribute some strength and resistance to raveling more so than conventional cellulose fibers.

None of the ALDOT sections experienced significant field rutting as rutting in all sections was less than 5 mm. Somewhat surprisingly the mean texture depth of the 9.5 mm section, E9A, was approximately the same as for the 12.5 mm sections of E9B and E10 (Figure 6). The 9.5 mm mix in E9A did experience an increase in roughness measured by IRI. The roughness for the 9.5 mm section was slightly higher throughout the test cycle but increased more over the last summer whereas roughness in the 12.5 mm sections did not change over the total test cycle.

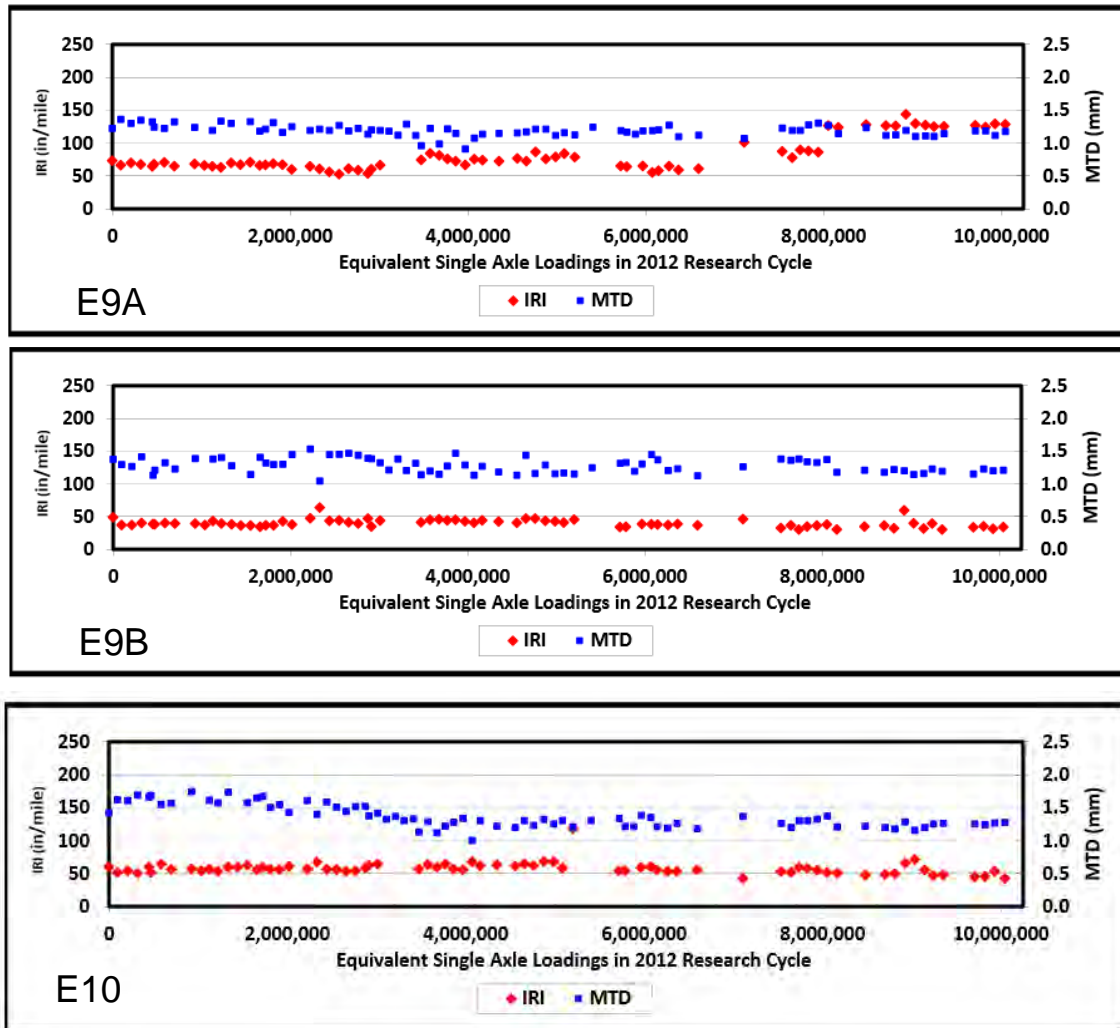


Figure 6 Performance Comparison of ALDOT Sections

*Findings*

- Increasing asphalt content can make PFC mixtures more resistant to raveling without greatly reducing air voids or potential permeability.
- The addition of synthetic fibers improved resistance to raveling as measured by the Cantabro test.
- The 12.5 mm PFC with GTR asphalt modifier had higher tensile strength than other 12.5 mm designed PFC mixes.

- The 9.5 mm PFC may be more durable than the 12.5 mm mix. The 9.5 mm PFC had higher tensile strength and less Cantabro stone loss than any of the 12.5 mm PFC mixtures.
- The 9.5 mm section experienced an increase in roughness over the last summer of the test cycle whereas the roughness of the 12.5 mm mixes was consistent throughout the cycle.

### 3.3. Tennessee Department of Transportation RAS Experiment

#### Comparison of OGFC from 2003 Cycle to OGFC with 3% RAS

Tennessee sponsored Section S4 in 2003 and placed a 12.5 mm OGFC using limestone aggregate and SBS modified PG 76-22 asphalt binder. The mix was placed directly on a milled surface at 1.3 inches thick. PG 67-22 was used for tack coat at an application rate of 0.03 gal/sy.

In 2012, Tennessee replaced the previous OGFC with another 12.5 mm limestone OGFC; in this case, the mix contained 3% post-consumer recycled asphalt shingles (RAS) based on total weight of aggregate. It was decided to omit the fiber stabilizer that is typically used in OGFC mix due to the anticipated binder stiffness from using RAS. Trackless tack was applied at a rate of 0.06 gal/sy residual asphalt. A comparison of the mix properties is provided in Table 1.

**Table 1: Comparison of S4 OGFC Mix Design Properties**

Gradation	2003 Track Cycle	2012 Track Cycle
3/4 in (19 mm)	100	100
1/2 in (12.5 mm)	95	96
3/8 in (9.5 mm)	78	72
No. 4 (4.75 mm)	19	14
No. 8 (2.36 mm)	5	5
No. 200 (0.075 mm)	1.6	2.0
AC, %	5.8	6.0
PG Grade	76-22	76-22
Asphalt Modifier	SBS	SBS/RAS

The OGFC mix with RAS had slightly more rutting (initial particle reorientation) than the 2003 mix and rut measurements were more variable for the RAS mix placed in 2012 (Figure 1). Some of the variability for months 18-22 (late summer of 2012) is due to measurement equipment changes, but the final rutting for both mixes was 3 mm, which is practically insignificant.

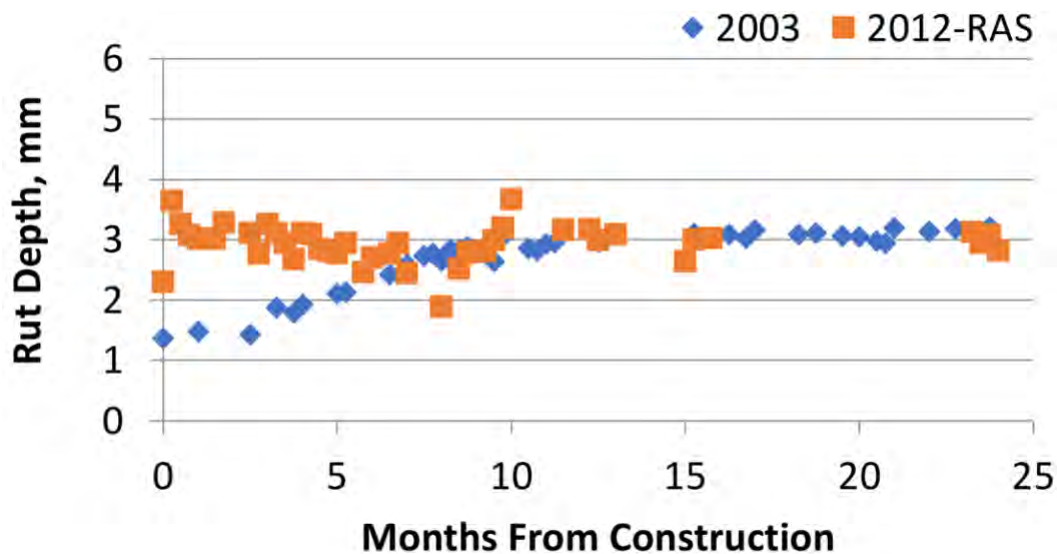


**Figure 1 Rutting Comparison of 2003 OGFC vs 2012 OGFC with RAS in Section S4**

A comparison of the Mean Texture Depth (MTD) for the OGFC mixes (Figure 2) shows that the RAS mix placed in 2012 had a MTD value approximately 0.2 mm less than the 2003 mix. Texture depth for both mixes decreased slightly throughout the two year cycle and indicates that the void structure may have started to gradually close up, but that raveling was not occurring. The texture of the 2012 RAS OGFC mixture is shown in Figure 3.

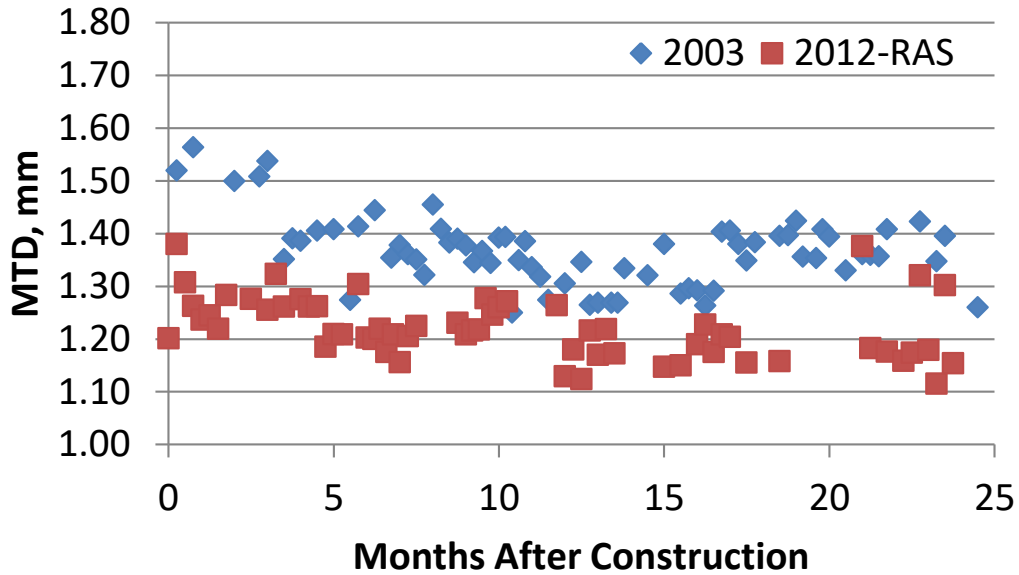
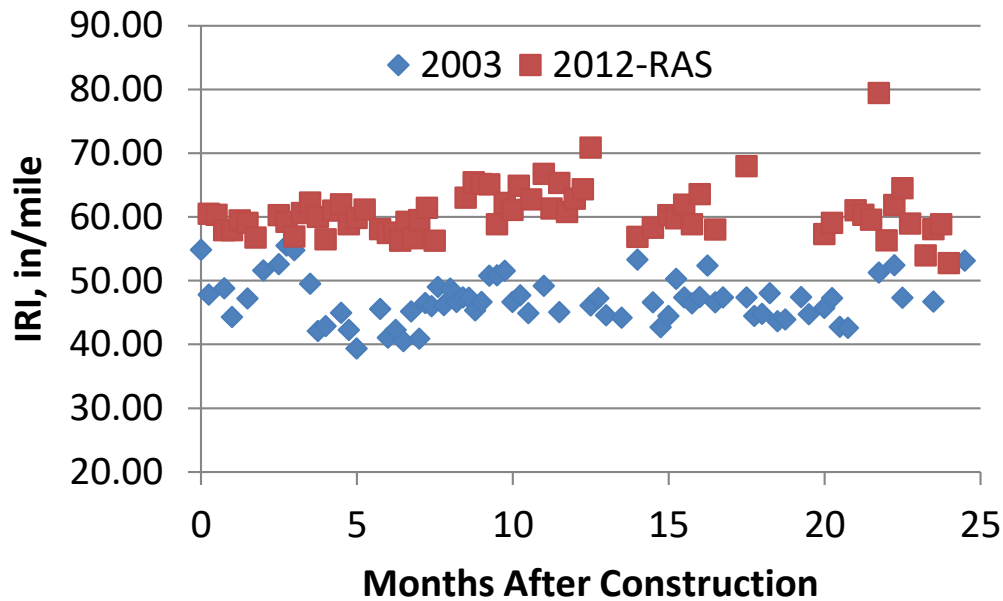


Figure 2 Comparison of MTD for TNDOT Section S4



Figure 3 Section S4 Surface Appearance After 10 Million ESALs (2012 Cycle)

Figure 4 shows that the RAS mixture was also slightly rougher than the 2003 mixture, but the measurements were consistent throughout the test cycle. This indicates that any difference in roughness is more likely due to differences in construction and placement than the effect of using RAS material.



**Figure 4 Roughness Measurements (IRI) for TNDOT Section S4**

*Findings*

- Rutting of both the 2003 OGFC and the 2012 OGFC with 3% RAS was about 3 mm after 10 million ESALs. There appeared to be more variability in the 2012 cycle measurements, but some of the variability was caused by a change in measurement equipment. The amount of rutting was practically insignificant.
- MTD results indicate that neither of the OGFC sections had begun to ravel after 10 million ESALs.
- The 2012 RAS mix was slightly rougher than the 2003 mix, but the measurements were consistent over the two-year cycle. It is believed the difference is due to changes in construction and placement equipment and procedures rather than any effect from the use of RAS.
- The OGFC with 3% RAS has performed as well as the previous OGFC mixture without RAS. There is only minor rutting and no raveling after 10 million ESALs of traffic loading.

### **3.4. Oklahoma Department of Transportation OGFSC Mix Design and Tack Method Study**

#### *Background*

Open-graded friction course, referred to in Oklahoma as open-graded friction surface course (OGFSC), has been used in the asphalt surface layer to provide safety and environmental benefits. With a high air void content, OGFSC allows water to quickly drain through the surface layer to an impervious intermediate layer below and out onto shoulders, which helps improve friction, minimize hydroplaning, and reduce tire spray. The high level of air voids in OGFSC can also reduce noise levels, as noise is attenuated in the voids.

The performance of OGFSC mixtures has improved significantly over the past decades with the use of high quality coarse aggregates, polymer-modified asphalt binders, stabilizing fibers, and hydrated lime (1, 2). However, OGFSC mixtures do not perform as well as other asphalt mixtures in terms of major distresses like raveling and cracking (3, 4). Past research studies have shown that the performance of OGFSC are dependent on several key factors, including the durability of the OGFSC mix, the interface bond between the OGFSC surface and the underlying layer, and the integrity of the underlying pavement structure (2, 3, 4, 5). To extend the service life of OGFSC mixtures in Oklahoma, the Oklahoma Department of Transportation (ODOT) sponsored a research study at the NCAT Test Track to improve both the durability and interface bond strength of OGFSC mixtures.

#### *Objective and Scope*

The objective of this ODOT study was to evaluate the field performance of an OGFSC mixture paved in Sections E1A and E1B using two different tack methods. The OGFSC mixture was designed by ODOT in accordance with an updated OGFSC mix design procedure. The OGFSC mix was placed in Sections E1A and E1B using a conventional paver. In Section E1A, a non-tracking hot-applied polymer tack (NTHAP) was applied using a conventional distributor truck at a higher spray rate of 0.15 gal/yd<sup>2</sup> (i.e., a residual rate of 0.15 gal/yd<sup>2</sup>). In Section E1B, an anionic non-tracking tack (NTSS-1HM) was also applied using a distributor truck but at a much lower spray rate of 0.08 gal/yd<sup>2</sup> (i.e., an equivalent residual rate of 0.05 gal/yd<sup>2</sup>). These sections were trafficked to 10 million ESALs for two years. Field performance of these sections, including surface functional characteristics and pavement distresses, was monitored on a weekly basis.

#### *Experimental Plan*

The original Section E1 (approximately 200 feet) was built in 2000 for the first research cycle of the Test Track. The pavement structure of this test section is comprised of 24 inches of asphalt over an aggregate base. To prepare for the ODOT study in 2012, approximately 0.75 inches of asphalt were milled from Section E1. The first half of Section E1 (hereafter referred to as Section E1A) was then tacked with the NTHAP material at a spray rate of 0.15 gal/yd<sup>2</sup> (i.e., a residual rate of 0.15 gal/yd<sup>2</sup>). The milled surface of the second half of Section E1 (referred to as Section E1B) was sprayed with the NTSS-1HM tack at a much lower spray rate of 0.08 gal/yd<sup>2</sup> (i.e., a equivalent residual rate of 0.05 gal/yd<sup>2</sup>). The OGFSC test mixture was then inlaid approximately 0.75 in. thick on the milled and tacked surfaces of Sections E1A and E1B on August 14, 2012.

All of the tack materials were supplied according to the requirements for non-tracking tack materials specified in Section 708.03 of the *ODOT 2012 Special Provision for Material Requirements for NT Tack Material*. Table 1 shows the specification requirements for the tack materials used.

**Table 1 ODOT Specifications for Tack Materials used in Sections E1A and E1B**

Properties	NTHAP (E1A)	NTSS-1HM (E1B)
Saybolt Furol Viscosity @ 77°F, sec. (T59)	N/A	15-100
Sieve test, % (T59)	N/A	≤ 0.3
Storage stability @ 1 day, % (T59)	N/A	≤ 1
Distillation test:		
Residue by distillation, % (T59)	N/A	≥ 50
Tests on residue from distillation		
Rotational Viscosity, 300°F, Pa•s (T316)	≤ 3	N/A
Penetration, 77°F, 100 g, 5 sec, 0.1 mm (T49)	≤ 25	≤ 20
Softening point, ring and ball, °F (D36)	≥ 158	≥ 149
Flash point, °F	≥ 500	N/A
Original DSR G*/sinδ, 180°F, 10 rad/sec., kPa (T315)	≥ 1.00	≥ 1.00
Solubility in TCE, % (T44)	N/A	≥ 97.5

The OGFSC mix placed in both of the sections was designed by ODOT based on a new aggregate gradation band. The new aggregate gradation band was generally similar to the current ODOT aggregate gradation band for OGFSC with a slight change for the percent passing on the No. 4 (4.75 mm) sieve. The aggregate mixture was a blend of virgin materials including 30% Dolese-Cooperton 3/8 in. Chips, 32% Dolese-Richards Spur 3/8 in. Chips, and 38% Martin-Marietta-Synder 'D' Rock. The asphalt binder specified in the mix design was a PG 76-28 modified with SBS. The optimum binder content was determined based on the pie plate drain-down method described in the South Carolina Department of Transportation (SCDOT) test procedure SC-T-91. During mix design, Cantabro tests were conducted according to ASTM D 7064. The Cantabro loss was 3% with a maximum limit of 20%. Table 2 summarizes the mix design and quality control (QC) testing information for the OGFSC mixture.

**Table 2 OGFSC Mix Design and QC Test Results**

Aggregate Gradation	% Passing			
	Design	QC	ODOT	Proposed
Sieve Size				
25 mm (1")	100	100	100	100
19 mm (3/4")	100	100	100	100
12.5 mm (1/2")	100	100	100	100
9.5 mm (3/8")	96	94	90-100	90-100
4.75 mm (#4)	25	19	25-45	10-35
2.36 mm (#8)	2	6	0-10	0-10
1.18 mm (#16)	1	5	-	-
0.60 mm (#30)	1	4	-	-
0.30 mm (#50)	1	3	-	-
0.15 mm (#100)	1	3	-	-
0.075 mm (#200)	1	2.4	0-5	0-5
<b>Volumetric Properties</b>				
Parameters	Design	QC	ODOT	Proposed
Binder Content (Pb), %	7.1	5.2	≥ 5.1	≥ 6.0
Eff. Binder Content (Pbe), %	6.7	4.8	-	-
Dust-to-Binder Ratio	0.1	0.5	-	-
Air Voids (Va), %	20	24.2	-	≥ 16.0
Voids in Mineral Agg (VMA), %	48	33	-	-
Voids Filled w/ Asphalt (VFA), %	61	27	-	-
Cellulose, %	0.3	0.3	-	0.2-0.5

During construction, loose mix was sampled at the Test Track for Cantabro testing. The Cantabro loss was 23% for the plant mix, which was much higher than the Cantabro loss measured during mix design. The high Cantabro loss may be partly due to the lower binder content in the plant mix and the higher air void content in the QC samples. A cause of the lower binder content in the plant mix may be due to an adjustment made during production to account for an increase in the water content in aggregate stockpiles due to a rain storm occurred on the night before the construction of the OGFSC layer.

After construction, field cores were cut to test the interlayer bond strength for both of the sections. Shear loading rate was 2.0 in./minute. The average bond strengths for Sections E1A and E1B were 107 and 117 psi, respectively. All of the cores did not break cleanly at the interface. For stiffer dense-graded mixes, the cores often break at the interface. However, for the OGFSC cores in this study, they broke mostly above the interface and into the OGFSC layers. This indicated that the interface bond strength exceeded the strength of the OGFSC layer.

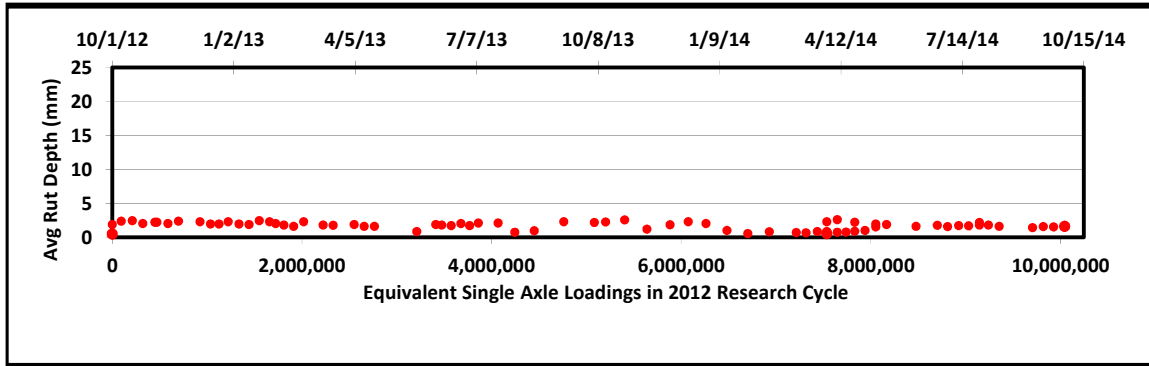
All of the test sections were trafficked to 10 million ESALs by a fleet of heavily loaded trucks from October 2012 through October 2014. During that time, condition survey of Sections E1A and E1B was conducted weekly on Mondays. Sections were inspected for signs of cracking, and multiple measurements of rutting and surface texture were made. In addition, field permeability tests were conducted on both the sections every three months in the first year and every six months in the second year. The field performance evaluation results are reported in the next section.

*Field Performance Evaluation Results*

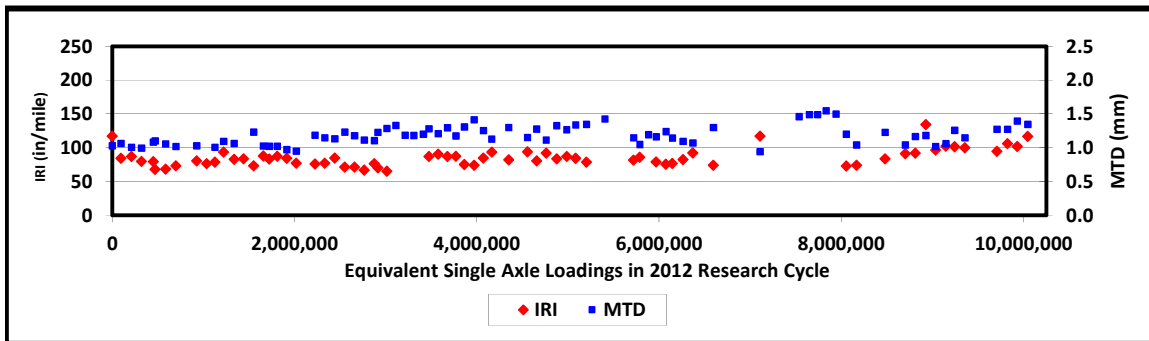
Figure 1 shows the surface condition of the two sections at the end of 2014. Figures 2 and 3 show the field performance measurements for the two test sections. Except for some raveling with widths of one to two inches along the longitudinal joint, both sections were still performing well at the close of the 2012 Test Track research cycle.



**Figure 3 Sections E1A and E1B at End of 2012 Research Cycle**

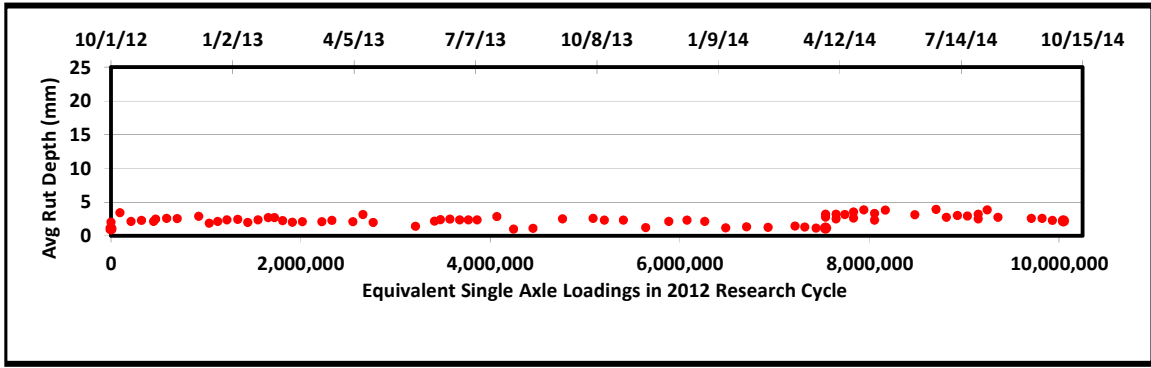


(a) Rutting

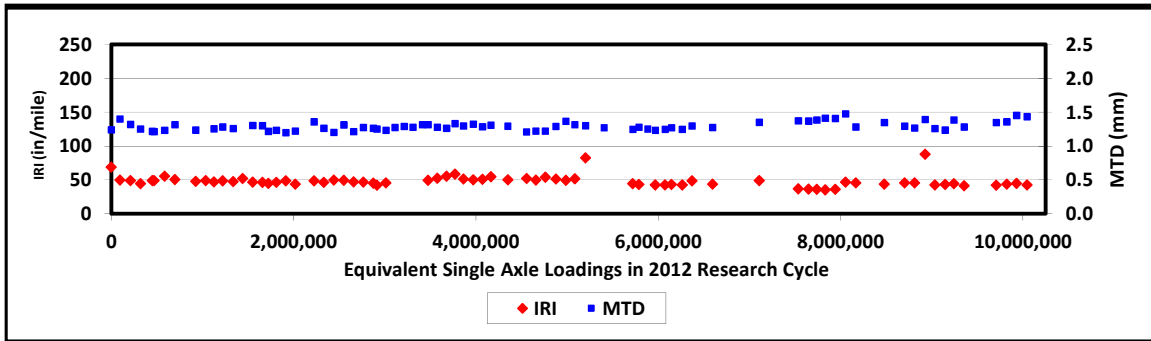


(b) Roughness and Surface Texture

**Figure 2 Rutting and Surface Texture Measurements for Section E1A**



(a) Rutting



(b) Roughness and Surface Texture

**Figure 3 Rutting and Surface Texture Measurements for Section E1B**

Figure 4 shows the field permeability test results for the OGFSC surface layers in Sections E1A and E1B. In the first six months with less than two million equivalent single axle loads (MESALs), the field permeability test results were lower for Section E1A with the NTHAP tack applied at the higher rate. However, the field permeability for Section E1B started decreasing at a higher rate at the beginning of the research cycle, and the field permeability test results for the two sections became almost the same after six months in service with approximately two MESALs at the Test Track. The field permeability test results for the two test sections continued to decrease at similar rates and stayed at approximately 200 m/day in the last six months (approximately last three MESALs) of the research cycle.

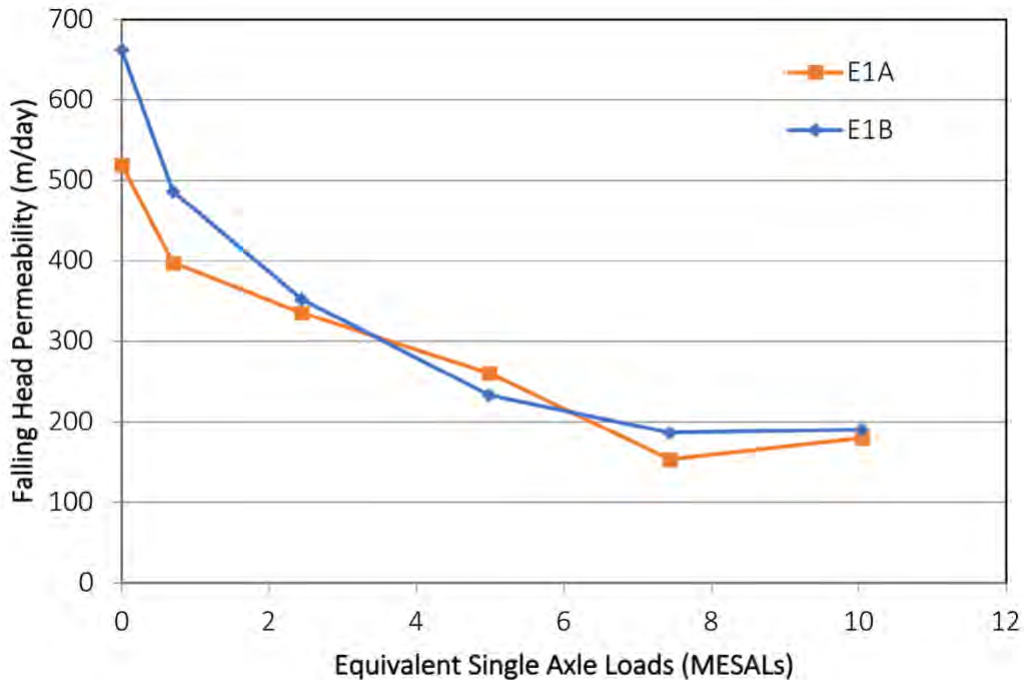


**Figure 4 Field Permeability Measurements for Sections E1A and E1B**

*Conclusions and Recommendations*

The objective of the OGFSC and tack coat study sponsored by the ODOT at the NCAT Test Track was to evaluate the field performance of an OGFSC surface paved in Sections E1A and E1B using two tack methods. The OGFSC mixture was designed in accordance with a proposed OGFSC mix design procedure. The proposed mix design procedure is generally similar to the current ODOT mix design procedure for OGFSC, except for two revisions. The first change is in the percent passing for the No. 4 (4.75 mm) sieve size from 25-45 to 10-35. The second change is that optimum binder content is now determined based on the pie plate drain-down method, similar to the South Carolina Department of Transportation (SCDOT) test procedure SC-T-91. A minimum of 0.3% cellulose fibers and a PG 76-28 were required as they were in the current OGFSC procedure.

The OGFSC mix was placed in Section E1A on a milled surface tacked with a non-tracking hot-applied polymer tack (NT-HAP) at a higher spray rate of 0.15 gal/yd<sup>2</sup> (i.e., a residual rate of 0.15 gal/yd<sup>2</sup>). In Section E1B, the OGFSC mix was also placed on a milled surface but tacked with an anionic non-tracking tack (NTSS-1HM) at a much lower spray rate of 0.08 gal/yd<sup>2</sup> (i.e., a equivalent residual rate of 0.05 gal/yd<sup>2</sup>).

Based on the laboratory testing results, the Cantabro loss for the plant mix was 23%, which was much higher than the 3% Cantabro loss measured during mix design. The higher Cantabro loss was due to the lower binder content in the plant mix and the higher air void content in the QC samples. The lower binder content in the plant mix may be caused by an adjustment made during production to account for extra water in aggregate stockpiles from a rain storm on the night before the construction of the OGFSC layer.

The average laboratory bond strength testing results were 107 and 117 psi for field cores extracted from Section E1A and E1B, respectively. The cores broke mostly above the interface and into the OGFSC layers. This indicated that interface bond strength exceeded mixture strength.

These sections were trafficked to 10 million ESALs from October 2012 through October 2014. Field performance of these sections, including surface functional characteristics and pavement distresses, was monitored on a weekly basis. Based on the field performance data, both sections were still performing well at the end of the 2012 Test Track research cycle in October 2014, except that the longitudinal joint had some raveling with widths of 1-2 inches. ODOT would have liked to continue traffic had funds been available.

A ¾ in. thick high friction OGFSC with NCAT gradation band will be laid with two tack coats applied on a micro-milled surface in Section N9 for evaluation in the 2015 research cycle. The first tack coat is an original PMCRS-1s tack, which will be applied at 0.20 gal/yd<sup>2</sup> using a spray paver. The second tack is an NTHAP tack applied at the same 0.15 gal/ yd<sup>2</sup> residual rate as used on Section E1A. The NTHAP tack will be overlapped 2 in. to see if longitudinal joint raveling can be mitigated.

### References

1. Mallick, R. B., P.S. Kandhal, L. A. Cooley, Jr., and D. E. Watson. *Design, Construction, and Performance of New Generation Open-Graded Friction Courses*. NCAT report No. 2000-01. National Center for Asphalt Technology, Auburn University, 2000.
2. Watson, D., K. Moore, K. Williams, L. Cooley Jr. Refinement of New-Generation Open-Graded Friction Course Mix Design. In *Transportation Research Record: Journal of the Transportation Research Board*, No. 1832, Transportation Research Board of the National Academies, Washington, D.C., 2003, pp. 78–85.
3. Birgisson, B., Roque, R., Varadhan, A., Thai, T., and Jaiswal, L. *Evaluation of Thick Open Graded and Bonded Friction Courses for Florida*. UF Report No. 4504-968-12, University of Florida, 2006.
4. Tran, N, D. Timm, B. Powell, G. Sholar, and R. Willis. Effectiveness of Heavier Tack Coat on Field Performance of Open-Graded Friction Course. In *Transportation Research Record: Journal of the Transportation Research Board*, No. 2372, Vol. 3 Transportation Research Board of the National Academies, Washington, D.C., 2013, pp. 1–8.
5. Chen, Y., G. Tebaldi, R. Roque, and G. Lopp. Effects of Interface Condition Characteristics on Open-Graded Friction Course Top-Down Cracking Performance. In *Road Materials and Pavement Design*, Vol. 13, Sup. 1, Taylor and Francis, 2012, pp. 56-75.

### 3.5. Florida Department of Transportation Tack Coat Effect on OGFC Performance Study

#### *Background*

Open-graded friction course (OGFC) has been used by transportation agencies as the final riding surface to provide safety and environmental benefits including improved friction, minimized hydroplaning, reduced splash and spray, and reduced noise level (1, 2). With advancements in material selection, mix design and construction, the performance of OGFC has been improved significantly over the last decades (3, 4). However, compared to a dense-graded asphalt mixture, OGFC is still more prone to pavement distresses, such as raveling and cracking, resulting in a shorter service life (5, 6).

The performance of an OGFC surface is influenced by several factors including the durability of the OGFC mixture, the integrity of the underlying pavement structure, and the bond strength at the interface of the OGFC surface and the underlying layer. To continue improving the longevity of OGFC mixtures used in Florida, the Florida Department of Transportation (FDOT) has sponsored several research projects. The following are three studies that focused on the interface bond between the OGFC and underlying layers.

The first FDOT study on the interface bond, which started in 2003 and completed in 2006, consisted of five test sections with a total length of 6.5 miles on US-27 in Highlands County, Florida (5). In the first four sections, two OGFC mixtures using limestone and granite were placed with a thick polymer-modified emulsion tack coat applied at a target application rate of 0.22 gal/yd<sup>2</sup> (residual rate of 0.14 gal/yd<sup>2</sup>) and with a conventional SS-1 tack coat applied at a target application rate of 0.05 gal/yd<sup>2</sup> (residual rate of 0.03 gal/yd<sup>2</sup>). The other test section was constructed using NovaChip® with the same polymer-modified emulsion tack coat applied at a target application rate of 0.22 gal/yd<sup>2</sup> (0.14 gal/yd<sup>2</sup>). The thick tack coat was placed using a spray paver that laid the thick tack coat just in front of OGFC, and the other tack coats were applied using a conventional tack distributor truck. Laboratory testing was conducted on plant mixtures and field cores to determine the mixture resistance to moisture damage, rutting, and cracking. Field testing was also conducted to evaluate the surface friction characteristics.

The second study was conducted in the laboratory on two-layer specimens made of OGFC and dense-graded mixes, respectively (7). The two layers were bonded with a conventional SS-1 tack coat and a thick polymer-modified tack layer. A new test (developed in that study) was conducted on the laboratory-prepared specimens to determine the effect of the thick polymer-modified tack coat on the OGFC resistance to top-down cracking. Results of the two studies indicated that using a thick polymer-modified tack coat helped improve the rutting and cracking resistance of OGFC without adversely affecting pavement surface friction and noise characteristics (5, 7).

Based on the findings of the previous two studies, the third study (hereafter referred to as the 2009 FDOT tack coat study) was conducted to validate the benefits of using a thicker tack coat on the field performance of OGFC. The study consisted of Sections N1 and N2, which were built identically on the NCAT Test Track in 2009 except for the tack coats used to bond the OGFC surfaces to the underlying dense-graded mix layers. Section N1 had a thicker polymer-modified tack coat applied at a target application rate of 0.21 gal/yd<sup>2</sup> (residual rate of 0.14 gal/yd<sup>2</sup>) using a spray paver (Figure 1), and Section N2 had a conventional tack applied at a regular target

application rate of 0.05 gal/yd<sup>2</sup> (residual rate of 0.03 gal/yd<sup>2</sup>) using a distributor truck. The sections were trafficked to 10 million equivalent single axle loads (ESALs) in two years. Field performance of the two sections was monitored on a weekly basis, including pavement stiffness, pavement structural response, surface functional characteristics, and pavement distresses. At the conclusion of the two-year trafficking cycle in 2011, the OGFC layer in Section N1 with a thicker tack coat performed better than the OGFC layer in Section N2 with a conventional tack coat based on the pavement structural response, rutting, cracking, and roughness measurements taken over the course of the study (8). Thus, the use of a thicker polymer-modified tack coat was recommended to improve the OGFC resistance to top-down cracking.



**Figure 1 Applying Thick Polymer-Modified Tack Coat Using Spray Paver**

When a spray paver with a distributor tank is utilized to apply a thick polymer-modified tack coat just in front of the OGFC mix, it may add additional costs to the OGFC construction and may limit its use in some paving projects due to the availability of the spray paver. Thus, a follow-up study (hereafter referred to as the 2012 FDOT tack coat study) was initiated to evaluate other tack methods using conventional pavers and distributor trucks that can potentially provide the same improvement for OGFC mixtures as the thick polymer-modified tack coat applied with the spray paver used in the 2009 FDOT tack coat study.

#### *Objective and Scope*

The objective of the 2012 FDOT tack coat study was to evaluate other tack methods that can potentially provide the same life extension for OGFC surface as the thick polymer-modified tack coat applied with a spray paver. Using conventional distributor trucks, three different non-tracking tack materials, including a cationic non-tracking tack (CRS-1HBC), a non-tracking hot-applied polymer tack (NT-HAP), and an anionic non-tracking tack (NTSS-1HM), were applied in N1A, N1B, and N2, respectively. The same OGFC mix from the 2009 FDOT tack coat study was placed using a conventional paver. As with the 2009 FDOT tack coat study, these sections were

trafficked to 10 million ESALs by a fleet of heavy trucks over the course of two years. Field performance of these sections, including surface functional characteristics and pavement distresses, was monitored on a weekly basis. This report summarizes the research activities and results of the 2012 FDOT tack coat study. The results were analyzed in conjunction with those of the 2009 FDOT tack coat study to draw conclusions based on the results of the two studies.

### *Experimental Plan*

The foundation of the two test sections in the 2009 study and the three test sections in the 2012 study was developed in 2006 to evaluate the Energy Ratio concept for determining the top-down cracking resistance of asphalt mixtures (9, 10).

To prepare for the 2009 FDOT tack coat study, approximately 5 inches of asphalt were milled from Sections N1 and N2, and then three new asphalt layers were inlaid in these sections. Similar to Sections N1 and N2 in 2009, Sections N1A, N1B and N2 were built in 2012 by removing the top 4.75 inches of existing pavements and replacing with three new asphalt layers.

As shown in Figure 2, the pavement cross-section was the same for all the test sections built in 2009 and 2012, which consisted of four asphalt layers (a 0.75-inch OGFC, two 2-inch dense-graded binder courses, and an existing 3-inch dense-graded base course) over 6-inch aggregate base on top of the track subgrade. The only differences in the five sections were the length of each section and the tack coat applied at the interface between the OGFC surface and the underlying dense-graded binder course. An anionic non-tracking tack (NTSS-1HM) was used at the interfaces between the dense-graded mix at a target application rate of 0.05 gal/yd<sup>2</sup> (residual rate of 0.03 gal/yd<sup>2</sup>).

The tack materials and their target application rates used in the two studies are summarized in Table 1. For the 2009 FDOT tack coat study, a polymer-modified tack coat (CRS-2P modified with *styrene-butadiene-styrene* (SBS) polymer) was applied in Section N1 at a higher application rate using a spray paver. An anionic non-tracking tack (NTSS-1HM) was applied at the application rate specified by FDOT using a distributor truck in Section N2. In the 2012 study, the same anionic non-tracking tack (NTSS-1HM) used in Section N2 in 2009 was applied at the same application rate in Section N2. The non-tracking hot-applied polymer tack (NT-HAP) was applied in Section N1B at a higher application rate. For section N1A, the cationic non-tracking tack (CRS-1HBC) was applied at an intermediate application rate.

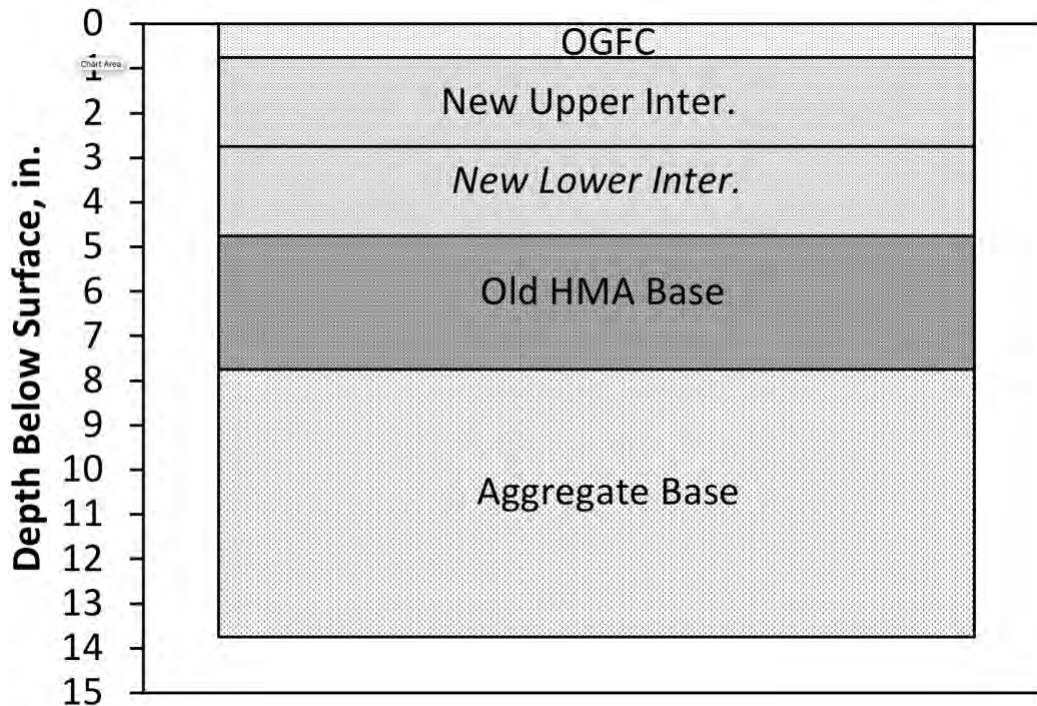


Figure 2 Pavement Cross-Section for N1 and N2 in 2009 and N1A, N1B, and N2 in 2012

Table 1 Tack Materials and Target Application Rates Used for OGFC Surface

Section	2009 FDOT Tack Coat Study		2012 FDOT Tack Coat Study		
	N1	N2	N1A	N1B	N2
Tack Material	CRS-2P	NTSS-1HM	CRS-1HBC	NT-HAP	NTSS-1HM
Spray Rate (gal/yd <sup>2</sup> )	0.21	0.05	0.10	0.15	0.05
Residual Rate (gal/yd <sup>2</sup> )	0.14	0.03	0.06	0.15	0.03

All of the tack materials, except the NT-HAP tack, were supplied according to the requirements for emulsified asphalts specified in the current FDOT Standard Specifications (11). The NT-HAP tack was supplied based on a proposed specification. Table 2 shows the specification requirements for all the tack materials used in both the 2009 and 2012 FDOT tack coat studies.

The optimum binder content of the OGFC mix placed in the surface layer was designed in 2009 in accordance with FDOT Procedure FM-5-588, which was developed based on the Federal Highway Administration (FHWA) pie plate drain-down procedure. The asphalt binder specified in the mix design was a PG 76-22 modified with SBS. The aggregate mixture was a blend of virgin granite aggregate, hydrated lime, and 15% reclaimed asphalt pavement (RAP). Table 3 summarizes the mix design information for the OGFC mixture. Detailed information about the mix design has been presented in a previous report (6). It should be noted that current FDOT specifications do not allow the use of RAP in OFGC mixtures and do not require durability testing, such as drain-down and Cantabro tests shown in Table 3.

**Table 2 FDOT Specifications for Tack Materials used in the Two Studies**

Properties	CRS-2P (N1, 2009)	NTSS-1HM (N2, 2009) (N2, 2012)	NT-HAP (N1B, 2012)	CRS-1HBC (N1A, 2012)
Viscosity @ 77°F, sec. (T59)	20-100	20-500	N/A	15-100
Sieve test, % (T59)	max 0.1	max 0.3	N/A	max 0.1
Storage stability @ 1 day, % (T59)	max 1	max 1	N/A	max 1
Distillation test:				
Residue by distillation, % (T59)	min 63	min 50	N/A	min 58
Oil distillate, % (T59)	min 2	max 1	N/A	max 1
Tests on residue from distillation				
Solubility in TCE, % (T44)	min 97.5	min 97.5	N/A	N/A
Elastic recovery, 50°F, 20-cm elongation, % (T301)	min 60	N/A		N/A
Penetration, 77°F, 100 g, 5 sec, 0.1 mm (T49)	60-150	max 20	max 25	40-90
Softening point, °F (D36)	N/A	min 149	min 158	min 120
DSR $G^* \sin \delta$ , 186.8°F, 10 rad/sec., kPa (T315)	N/A	min 1	min 1	N/A
Rotational Viscosity, 300°F, cP (T316)			max 3000	

**Table 3 OGFC Mix Design**

Aggregate Gradation		Draindown	
Sieve Size	% Passing	Test Temperature (°F / °C)	Draindown (%)
25 mm (1")	100	335 / 168 (Production)	0.01
19 mm (3/4")	100	362 / 183 (Production Plus 27°F)	0.01
12.5 mm (1/2")	95		
9.5 mm (3/8")	64		
4.75 mm (#4)	15		
2.36 mm (#8)	9		
1.18 mm (#16)	8		
0.60 mm (#30)	6		
0.30 mm (#50)	5		
0.15 mm (#100)	4		
0.075 mm (#200)	3.7		
Volumetric Properties		Moisture Susceptibility	
Parameters	Results	Parameters	Results
Binder Content (Pb), %	5.5	Conditioned tensile strength, psi	65.9
Eff. Binder Content (Pbe), %	4.9	Unconditioned tensile strength, psi	75
Dust-to-Binder Ratio	0.8	Tensile strength ratio	0.88
Air Voids (Va), %	16.8		
Voids in Mineral Agg (VMA), %	26.3		
Voids Filled w/ Asphalt (VFA), %	36		
		Cantabro Abrasion	
		Parameters	Results
		Test Temperature, °C	25
		Average Air Voids, %	17
		Percent Loss	17.9

Table 4 summarizes the as-built properties of the asphalt layers in the five sections built in 2009 and 2012. All of the test sections were trafficked to 10 million ESALs. Trafficking of the 2009 test sections started in August 2009 and was completed by the end of 2011. For the 2012 test sections, trafficking began in October 2012 and ended October 2014.

**Table 4 As-Built Asphalt Layer Properties**

Lift	1-Surface		2-Upper Intermediate		3-Lower Intermediate		4-Base
	2009	2012	2009	2012	2009	2012	2006
Year Built	2009	2012	2009	2012	2009	2012	2006
NMAS, mm	12.5	12.5	12.5	12.5	12.5	12.5	19
Modifier	SBS	SBS	NA	NA	NA	NA	NA
PG Grade	76-22	76-22	67-22	67-22	67-22	67-22	67-22
Asphalt, %	5.1	5.6	4.6	4.9	4.6	5.1	4.6
Air Voids, %	20.7	21.9	6.4	7.9	6.0	7.7	7.9
Plant Temp, °F <sup>a</sup>	335	335	325	330	315	335	315
Paver Temp, °F <sup>b</sup>	325		310		300		290
Comp. Temp, °F <sup>c</sup>	290		280		270		280

<sup>a</sup>Asphalt plant mixing temperature

<sup>b</sup>Surface temperature directly behind paver

<sup>c</sup>Surface temperature at which compaction began

### Results

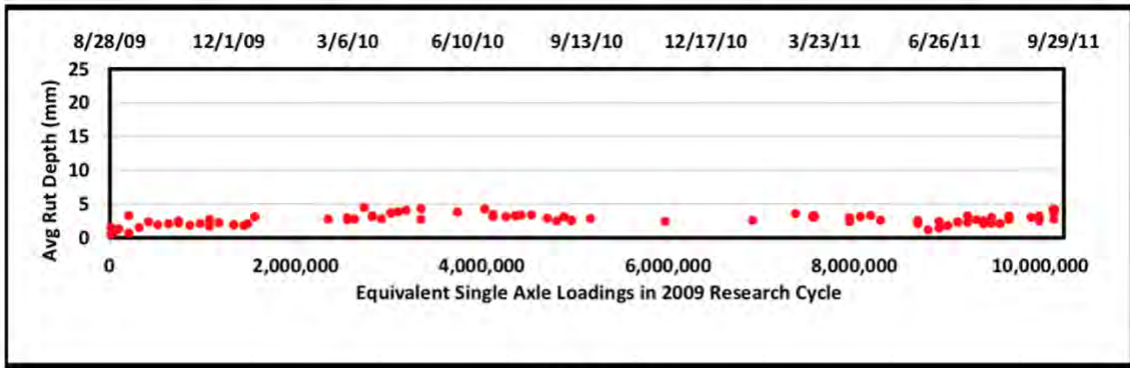
A condition survey of the five test sections was conducted on a weekly basis each Monday. Sections were inspected for signs of cracking, and multiple measurements of rutting and surface texture were made. Figures 3 through 7 show the field performance measurements for the five test sections (N1 and N2 in the 2009 FDOT tack coat study and N1A, N1B, and N2 in the 2012 FDOT tack coat study). Based on the field performance data, the following observations can be made:

- At the end of the 2009 FDOT tack coat study, Section N1 (CRS-2P) had a final rut depth of 4.1 mm, which was lower than the final rut depth of 6.7 mm measured in Section N2 (NTSS-1HM). The average rut depths measured in the two sections were relatively low. In the 2012 study, Section N1A (CRS-1HBC) had large patching areas and a higher total rut depth than Sections N1B (NT-HAP) and N2 (NTSS-1HM). The level of rutting in Sections N1A, N1B, and N2 in the 2012 study was similar to that of Section N2 in the 2009 study.
- In the 2009 study, surface cracks were seen in Section N2 (NTSS-1HM) after 2.2 million ESALs (February 2010) and in Section N1 (CRS-2P) after 4.1 million ESALs (June 2010). At the end of the 2009 research cycle (10 million ESALs), cracks were observed throughout Section N2 at a higher level of severity and with a greater area of severe cracking than in Section N1. Figure 8 shows surface cracks in Section N1 and N2 at the end of the 2009 research cycle. Cores cut from Section N2 showed top-down cracking propagated deeper into the underlying layers, which affected the structural performance of Section N2 (Tran et al. 2012).
- Cracks were also observed in the three test sections at the end of the 2012 research cycle (10 million ESALs), as shown in Figure 9. However, the cracked area was smaller in Section N1B (16% of the lane area) than in Section N2 (37% of the lane area) and in Section N1A (47% of the lane area).
- Since the level of crack severity in these sections was low or moderate, the rutting level in each test section significantly influenced the International Roughness Index (IRI). Due to the large patching areas, the changes in IRI in Section N1A (CRS-1HBC) were greater than those in the other sections. The four other sections had similar IRI and mean texture depth (MTD) measurements.

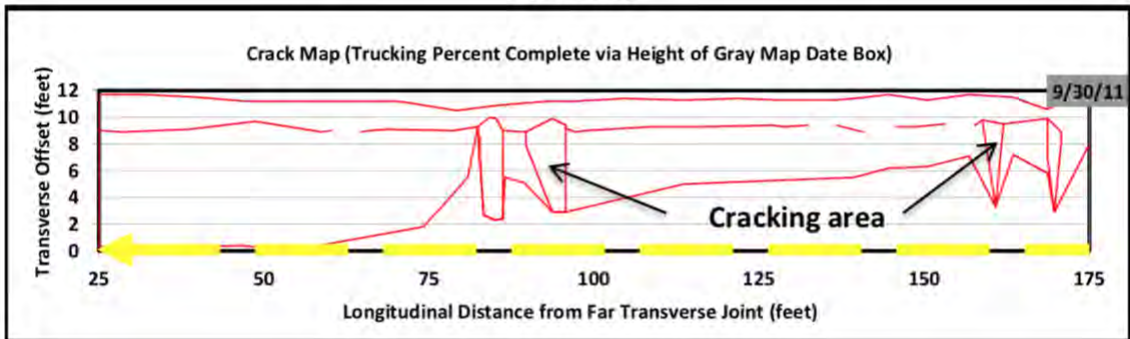
- When comparing the overall performance of the test sections in the two FDOT tack coat studies, Section N1 (CRS-2P) in the 2009 study showed similar field performance to that of Section N1B (NT-HAP) in the 2012 study. These two sections performed better than the other three sections. The field performance of Section N2 (NTSS-1HM) in the 2009 study was similar to that of Section N2 (NTSS-1HM) and Section N1A (CRS-1HBC) in the 2012 study.

Field permeability testing was also conducted on these test sections over the course of the 2009 and 2012 experiments, and the testing results are shown in Figure 10. Field permeability was similar for Sections N1 (CRS-2P) and N2 (NTSS-1HM) throughout the 2009 study. However, based on photos (Figure 11) taken during and after heavy rains, Section N2 (NTSS-1HM) with the lower tack coat rate appeared to provide better drainage than Section N1 (CRS-2P).

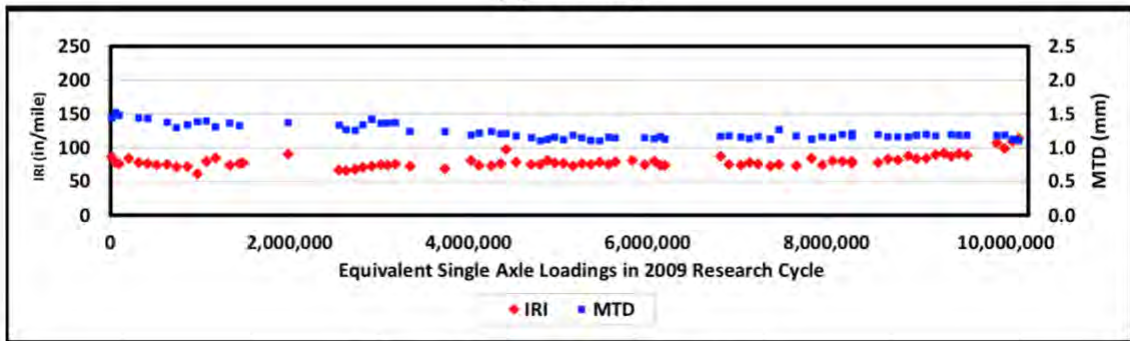
For the 2012 study, the results in Figure 10 showed that Section N2 (NTSS-1HM) with the lower tack rate had higher field permeability at the beginning. Towards the end of the 2012 research cycle, field permeability was similar for all the three sections. Based on the field permeability testing results and field observations, it was reasonable to suggest that a heavier tack rate would reduce field permeability of the OGFC surface.



(a) Rutting

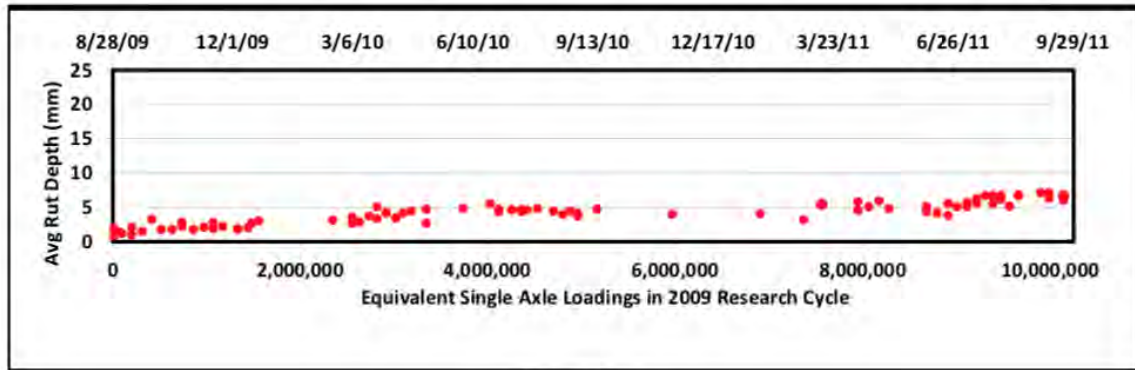


(b) Cracking

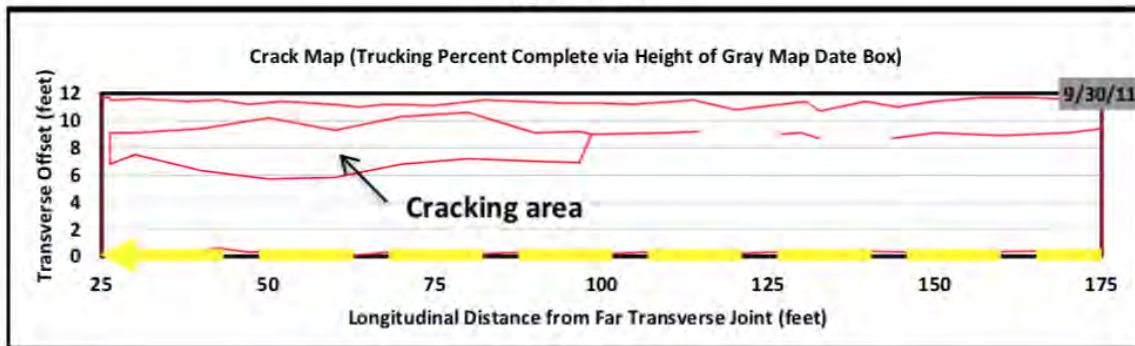


(c) Roughness and Surface Texture

Figure 3 Section N1 (CRS-2P) Rutting, Cracking and Surface Texture Measurements in 2009



(a) Rutting

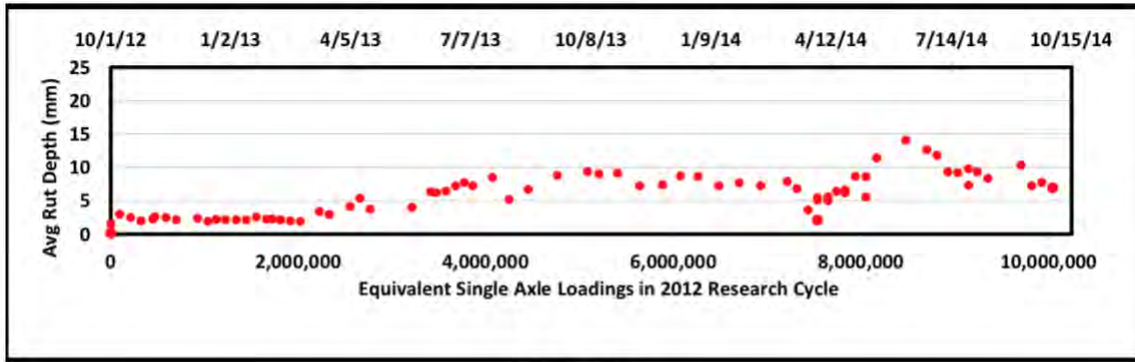


(b) Cracking

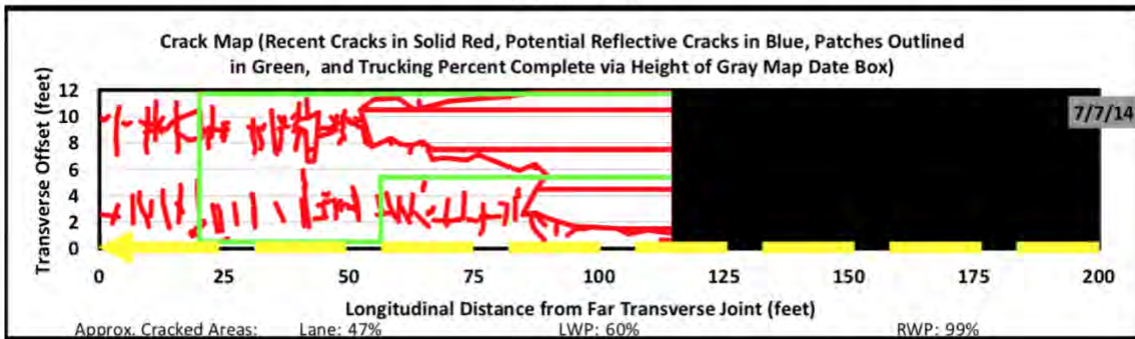


(c) Roughness and Surface Texture

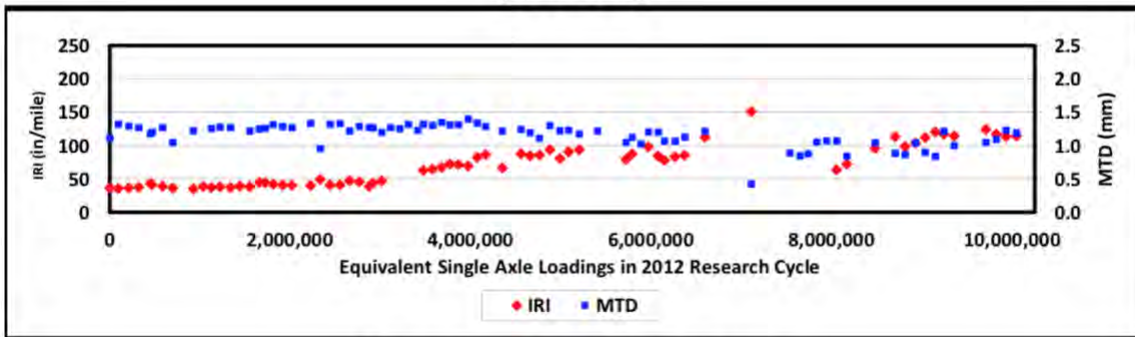
Figure 4 Section N2 (NTSS-1HM) Rutting, Cracking and Surface Texture Measurements in 2009



(a) Rutting

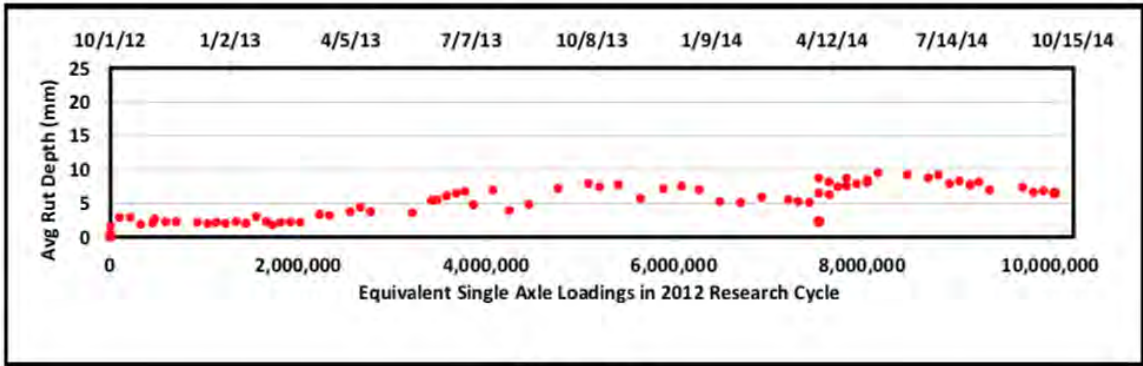


(b) Cracking

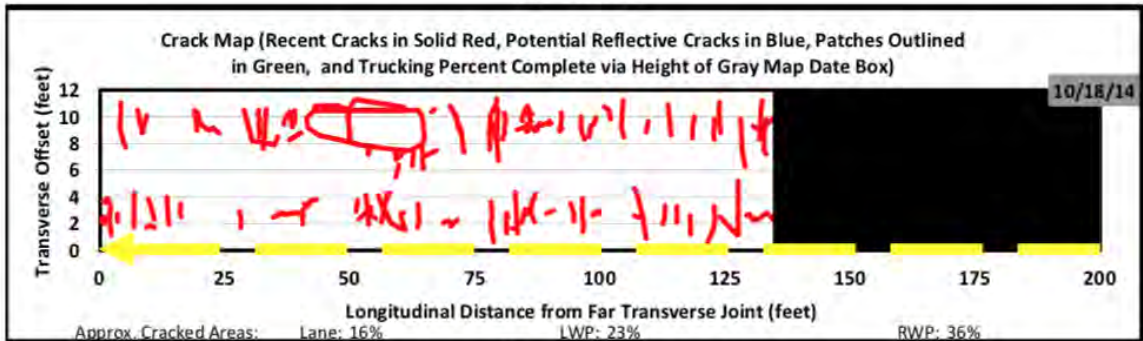


(c) Roughness and Surface Texture

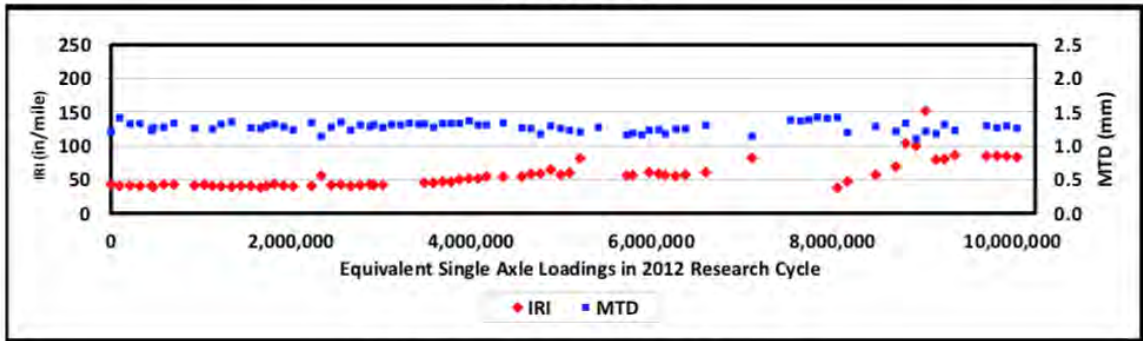
Figure 5 Section N1A (CRS-1HBC) Rutting, Cracking and Surface Texture Measurements in 2012



(a) Rutting

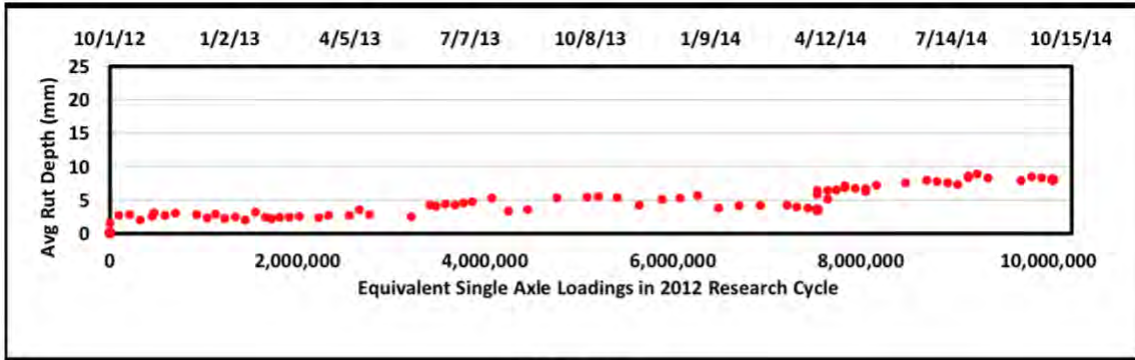


(b) Cracking

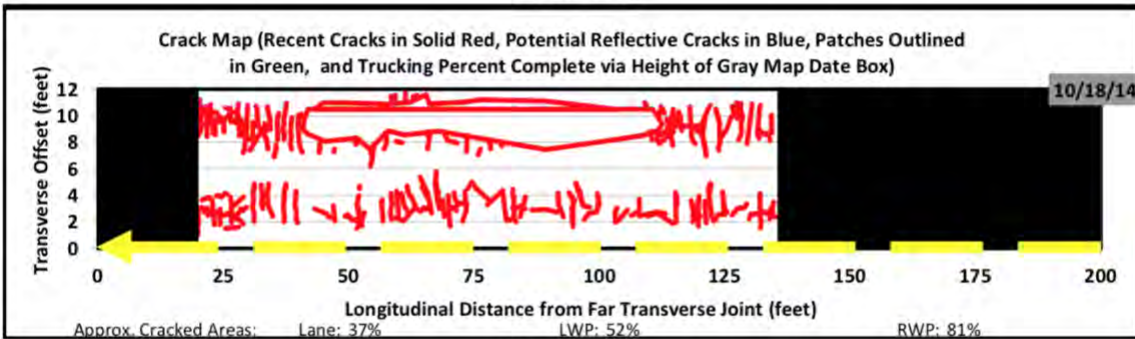


(c) Roughness and Surface Texture

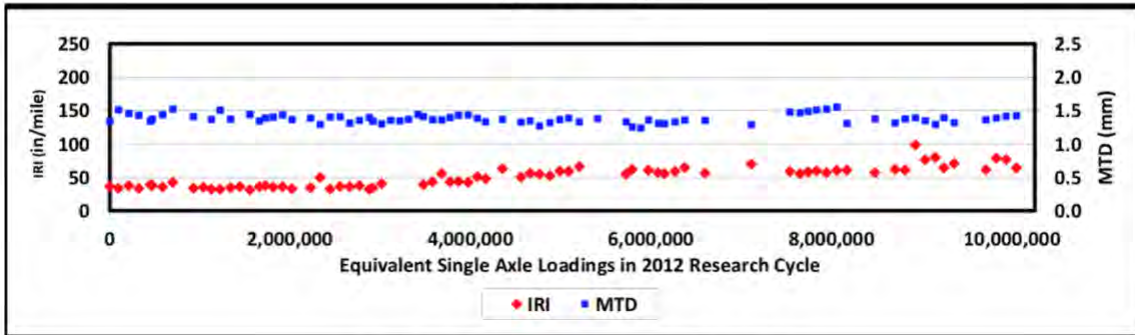
Figure 6 Section N1B (NT-HAP) Rutting, Cracking and Surface Texture Measurements in 2012



(a) Rutting



(b) Cracking



(c) Roughness and Surface Texture

Figure 7 Section N2 (NTSS-1HM) Rutting, Cracking and Surface Texture Measurements in 2012



(a) Section N1 (CRS-2P)



(b) Section N2 (NTSS-1HM)

**Figure 8 Cracking in Sections N1 and N2 at End of 2009 Research Cycle**



(a) Section N1A (CRS-1HBC) Overview and Close Up



(b) Section N1B (NT-HAP)



(c) Section N2 (NTSS-1HM)

**Figure 9 Cracks Seen in N1A, N1B and N2 at End of 2012 Research Cycle**

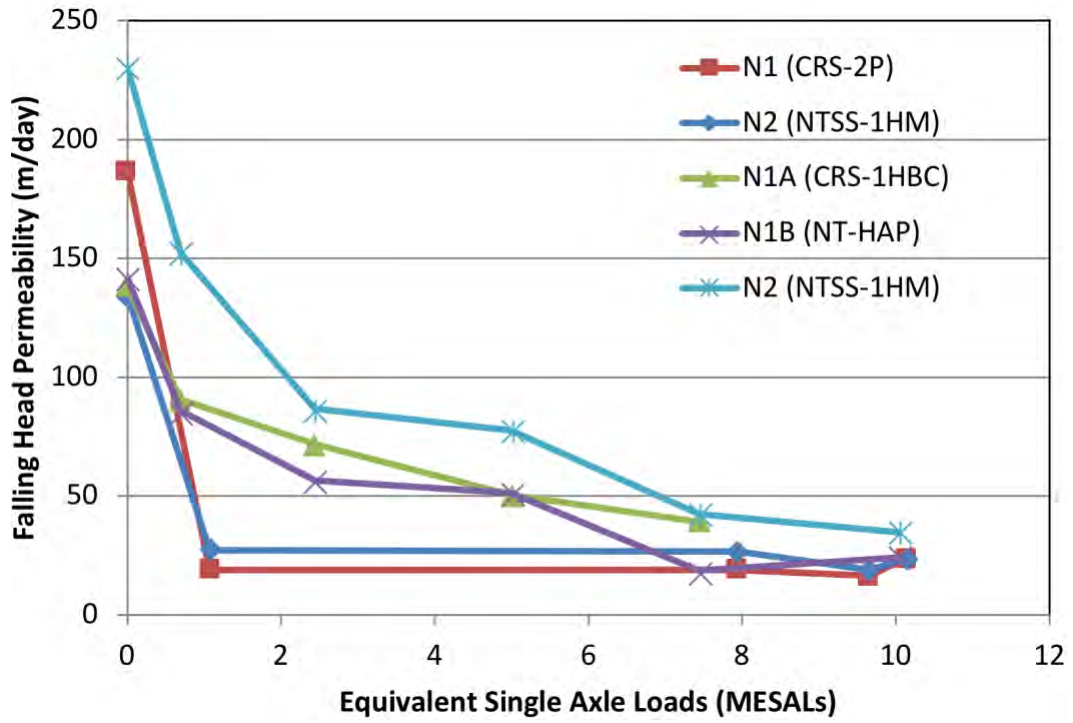


Figure 10 Field Permeability Testing Results



(a) During Heavy Rain



(b) After Heavy Rain

**Figure 11 Water Drained Faster in Section N2 (NTSS-1HM) than Section N1 (CRS-2P) in 2009 Study**

*Conclusions and Recommendations*

The objective of the 2009 and 2012 FDOT tack coat studies at the NCAT Test Track was to evaluate the comparative tack methods for improving the longevity of OGFC mixtures used in Florida. The study compared the field performance of the same OGFC surface placed using different tack methods on the same pavement structure. The OGFC mix was placed in Sections N1 and N2 in 2009 using a thick polymer modified tack (CRS-2P) and an anionic non-tracking tack (NTSS-1HM), respectively. The same OGFC mix was paved in Sections N1A, N1B, and N2 in 2012 using a cationic non-tracking tack (CRS-1HBC), a non-tracking hot applied polymer tack (NT-HAP), and the anionic

non-tracking tack (NTSS-1HM) used in 2009, respectively. The OGFC mix was placed in Section N1 in 2009 using a spray paver, and a conventional paver was used in the other sections. All sections were trafficked to 10 million ESALs for two years, during which the surface characteristics and pavement distresses were monitored on a weekly basis. Based on the field performance results, the following conclusions were offered:

- Based on laboratory test result, the OGFC mixture paved in the five sections met the FDOT requirements for an FC-5 mixture. The mix contained 15% RAP.
- Section N1 (CRS-2P) in the 2009 study appeared to have a lower final rut depth. However, the rutting level was practically similar in all the test sections except in Section N1A in the 2012 study, which had a large patching area.
- Sections N1 (CRS-2P) and N1B (NT-HAP) showed similar cracking performance. In addition, Sections N1A (CRS-1HBC) and N2 (NTSS-1HM) in both studies had similar cracking performance. However, the cracked areas in Sections N1 and N1B were smaller than those in the other three test sections.
- The International Roughness Index for Section N1 (CRS-2P) started higher but increased at a lower rate than in the other sections. The IRI level at the end of the evaluation period was similar for all test sections, except in Section N1A, which had a large patch. The patch affected both the rutting and IRI measurements of this section. The changes in the mean texture depth measurements were similar for all the test sections.
- Based on the field permeability testing results and field observations, a heavier tack rate would reduce field permeability or drainage of the OGFC surface during and after heavy rains.

In summary, Section N1 (CRS-2P) in the 2009 study showed similar field performance to that of Section N1B (NT-HAP) in the 2012 study. These two sections performed better than the other three sections, including Section N2 (NTSS-1HM) in the 2009 study, Section N2 (NTSS-1HM), and Section N1A (CRS-1HBC) in the 2012 study. It is recommended that a thicker tack coat be used to improve the performance of OGFC surfaces. Depending on the paving condition, the NT-HAP tack coat applied by a conventional distributor truck can be an alternative to the CRS-2P tack applied using a spray paver.

### References

1. Cooley, Jr. L. A., E. R. Brown and D. E. Watson. *Evaluation of OGFC Mixtures Containing Cellulose Fibers*. NCAT Report 00-05. National Center for Asphalt Technology at Auburn University, Auburn, Ala., 2000.
2. Hencken, J., T. Bennert, and A. Maher. *On-Board Sound Intensity (OBSI) Evaluation of Quiet Pavements Utilized in New Jersey*. Presented at 90<sup>th</sup> Annual Meeting of the Transportation Research Board, Washington, D.C., 2011.
3. Mallick, R. B., P. S. Kandhal, L. A. Cooley, Jr., and D. E. Watson. *Design, Construction, and Performance of New Generation Open-Graded Friction Courses*. NCAT Report 00-01. National Center for Asphalt Technology at Auburn University, Auburn, Ala., 2000.
4. Watson, D., K. Moore, K. Williams, and L. Cooley Jr. Refinement of New-Generation Open-Graded Friction Course Mix Design. In *Transportation Research Record: Journal of the*

- Transportation Research Board*, No. 1832, Transportation Research Board of the National Academies, Washington, D.C., 2003, pp. 78-85.
5. Birgisson, B., R. Roque, A. Varadhan, T. Thai, and L. Jaiswal. *Evaluation of Thick Open Graded and Bonded Friction Courses for Florida*. UF Report No. 4504-968-12. University of Florida, Gainesville, 2006.
  6. Tran, N., D. Watson, and N. Anwer. *Effect of Using Fog Seals without Sanding on Surface Friction and Durability of Open-Graded Friction Course*. Presented at 91<sup>st</sup> Annual Meeting of the Transportation Research Board, Washington, D.C., 2012.
  7. Chen, Y., G. Tebaldi, R. Roque, and G. Lopp. Effects of Interface Condition Characteristics on Open-Graded Friction Course Top-Down Cracking Performance. In *Road Materials and Pavement Design*, Vol. 13, Sup. 1, Taylor and Francis, 2012, pp. 56-75.
  8. Tran, N, D. Timm, B. Powell, G. Sholar, and R. Willis. Effectiveness of Heavier Tack Coat on Field Performance of Open-Graded Friction Course. In *Transportation Research Record: Journal of the Transportation Research Board*, No. 2372, Vol. 3, Transportation Research Board of the National Academies, Washington, D.C., 2013, pp. 1-8.
  9. Timm, D., G. Sholar, J. Kim, and J. Willis. Forensic Investigation and Validation of Energy Ratio Concept. In *Transportation Research Record: Journal of the Transportation Research Board*, No. 2127, Transportation Research Board of the National Academies, Washington, D.C., 2009, pp. 43-51.
  10. Willis R., D. Timm, B. West, B. Powell, M. Robbins, A. Taylor, A. Smit, N. Tran, M. Heitzman, and A. Bianchini. *Phase II NCAT Test Track Findings*. NCAT Report 09-08, National Center for Asphalt Technology at Auburn University, Auburn, Ala., 2009.
  11. Florida Department of Transportation. FDOT Standard Specifications for Road and Bridge Construction.  
[http://www.dot.state.fl.us/programmanagement/Implemented/SpecBooks/July2015/Files/715eBook\\_Revised.pdf](http://www.dot.state.fl.us/programmanagement/Implemented/SpecBooks/July2015/Files/715eBook_Revised.pdf). Accessed April 30, 2015.

### **3.6. Florida Department of Transportation Cracking Study**

#### *Introduction*

As many state agencies have successfully mitigated rutting as a primary cause of pavement deterioration, more emphasis has been placed on identifying properties of mixtures that may influence the overall durability of the pavement structure. One such distress that affects durability is top-down cracking, which has been documented worldwide. The Florida DOT (FDOT) and the University of Florida were some of the first to recognize the widespread nature of this distress with over 90% of cracking in the state of Florida categorized as top-down (1).

As the name implies, these cracks form at the top of the pavement structure and are load related, as they tend to originate in the wheelpath. However, Roque et al. note the complex interaction of load, thermal, and aging effects as contributing to top-down cracking (2). Equipment can also cause top down cracking. They further explain that after reviewing a wide variety of material characteristics, there is not one single mixture property that could reliably discern between acceptable and poor cracking performance (2).

#### *Objective and Scope*

The objective of this experiment was to determine which asphalt mixtures were more prone to surface cracking. A secondary objective of this work was to characterize the mixtures' properties in the laboratory to determine which cracking tests might most successfully predict cracking resistance. To complete this research, four mixtures were placed in 100-foot test strips in sections E7 and E8. The mixtures varied in terms of binder modification and recycled material content.

#### *Mix Design and Construction*

Four mixtures were designed at NCAT laboratory for this experiment. The first mix (E7A) was a virgin asphalt mixture using an asphalt binder modified by styrene-butadiene-styrene (SBS). The second mixture (E7B) used the same aggregate skeleton as E7A; however, instead of modifying the binder using SBS, the state chose to modify the binder using their experimental ground tire rubber (GTR) specification. E8A and E8B also used an SBS modified binder with the addition of recycled materials. E8A used reclaimed asphalt pavement (RAP) in the mix. The RAP-binder ratio for the mix was 29 percent. E8B incorporated RAP and a post-consumer or tear off recycled asphalt shingle (RAS) in the mixture. The RAP contributed 20 percent of the binder content in the mix while the RAS contributed an additional 21 percent beyond that of the RAP. Mixture gradations, base binder grades, volumetrics, and construction data for all four mixtures are provided in Table 1.

**Table 1 FDOT Cracking Mixture Characteristics**

Mix Design Parameters	E7A (SBS)	E7B (GTR)	E8A (RAP)	E8B (RAP + RAS)
Design Method	Superpave			
Compactive Effort	100 Gyration			
<b>Quality Control Data</b>				
Binder Grade in Tank	76-22	76-22	76-22	76-22
P <sub>1/2</sub> , %	98	97	98	99
P <sub>3/8</sub> , %	85	83	88	91
P <sub>#4</sub> , %	61	60	62	68
P <sub>#8</sub> , %	52	51	46	56
P <sub>#30</sub> , %	33	32	28	34
P <sub>#50</sub> , %	24	23	19	24
P <sub>#100</sub> , %	17	15	13	17
P <sub>#200</sub> , %	10.2	9.6	8.4	10.8
Total Binder Content, %	4.8	5.0	4.4	5.0
Effective Binder Content, %	4.4	4.6	3.9	4.6
% RAP (AC Content = 5.4% - Design)	0	0	25	20
% RAS (AC Content = 23.5% - Design)	0	0	0	5
RAP Binder Ratio	0	0	0.307	0.216
RAS Binder Ratio	0	0	0	0.235
Air Voids, %	3.0	2.6	3.2	2.6
Voids in Mineral Aggregate, %	13.6	13.6	12.5	13.5
Voids Filled with Asphalt, %	78	81	75	81
<b>Production/Construction Data</b>				
As-Built Lift Thickness, in	1.5	1.5	1.5	1.5
Type of Tack Coat	NTSS-1HM			
Undiluted Target Tack Rate, gal/sy	0.06			
Temperature at Plant, F	340	335	340	340
Average Mat Compaction, %	91.6	93.9	92.5	93.6

**Laboratory Testing**

While the field experiment was being conducted, materials (plant-produced loose mix and asphalt binder) that had been sampled during construction were taken back to the NCAT laboratory for evaluation. The binder was tested using both the performance grade (PG) and multiple stress creep recovery (MSCR) specifications. The mixtures were evaluated for rutting using the Hamburg Wheel Tracking Test and the Asphalt Pavement Analyzer. The Hamburg test also gives a measure of the moisture resistance of these mixes. The durability of the mixtures was assessed via the Florida energy ratio procedure and by the Overlay Tester.

**Binder Characterization.** The binders for the two asphalt mixtures in E7A and E7B were sampled from the tank at the plant and tested in the NCAT binder laboratory to determine the PG grade in accordance with AASHTO M 320. The tank binder used for Section E8 was the same binder in E7A; however, since RAS and/or RAP were used in the two mixtures in E8, the binder from the mixture had to be extracted and recovered before it could be tested. The blended asphalt binders were extracted and recovered using AASHTO T 164 Method A and ASTM D 5404 before AASHTO M 320 was conducted. The test results for these two procedures are shown in Tables 2 and 3.

Table 4 provides the test requirements from AASHTO MP 19. In addition to testing the mixtures, the PG properties of the RAP and RAS binders were determined.

Both sets of data show a significant increase in the stiffness of the E7A binder when RAS and/or RAP were added to the mix. The test section with RAP had a critical high temperature grade 13.5°C higher, and including RAS increased the critical binder high temperature another 7.9°C. Similar stiffness increases were seen for the critical low and intermediate temperatures. The RAP mixture had its critical low temperature reduced by one performance grade and the RAP/RAS mixture’s critical low temperature grade was reduced by three performance grades.

**Table 2 FDOT Cracking Study Performance Grades**

Test Section	Binder Modifier	Extracted	T <sub>crit</sub> , °C					True Grade	PG
			High Original	High RTFO	Int	Low S	Low m		
E7A	SBS	No	75.1	75.4	20.9	-27.5	-26.1	75.1 – 26.1	70 - 22
E8B	GTR	No	81.2	81.7	15.5	-31.5	-26.8	81.2 – 26.8	76 - 22
E7A	SBS	Yes	--	81.3	23.3	-28.3	-24.4	81.3 – 24.4	76 - 22
E8A	RAP	Yes	--	94.8	29.9	-22.5	-16.3	94.8 – 16.3	94 - 16
E8B	RAP/RAS	Yes	--	102.7	28	-25.6	-9.8	102.7 – 9.8	100 - 4
RAP	--	Yes	--	102.1	38.2	-15.9	-13.1	102.1 – 13.1	100 - 10
RAS	--	Yes	--	149.1	29.7	-31.6	-2.8	149.1 – 2.8	148 + 2

The increase in stiffness for the RAS and/or RAP test sections is noticed in the J<sub>nr</sub> values and the final AASHTO M 332 grade. The J<sub>nr</sub> values of E8A and E8B are much smaller than E7A, which suggests a more rut resistant binder. This is reflected in the final AASHTO M 332 grade. While the SBS modified binder was labeled as a “v” for very high trafficking, both mixtures with recycled binders and the GTR-modified binder were designated as “E” binders (extremely high traffic). It should also be noted that while AASHTO M 322 has a maximum of 75% for J<sub>nr</sub> Diff, low J<sub>nr</sub> values at 3.2 kPa make the percent difference meaningless.

**Table 3 FDOT Cracking Study MSCR Results at 64°C**

Section	Modifier	Extracted	Avg % Recovery		Avg J <sub>nr</sub> , kPa <sup>-1</sup>		Diff, % Recovery	Diff, % J <sub>nr</sub>	MP 19 Grade
			100 Pa	3200 Pa	100 Pa	3200 Pa			
E7A	SBS	No	53.70	43.08	0.4555	0.5863	19.8	28.7	V
E7B	GTR	No	50.34	35.82	0.2514	0.3431	28.9	36.5	E
E8A	RAP	Yes	62.71	62.72	0.043	0.042	0.017	-0.334	E
E8B	RAP/RAS	Yes	78.88	79.30	0.004	0.004	0.526	3.410	E

**Table 4 Requirements for Non-Recoverable Creep Compliance (AASHTO MP 19-10)**

Traffic Level	Max J <sub>nr3.2</sub> (kPa <sup>-1</sup> )	Max J <sub>nr</sub> diff (%)
Standard Traffic “S” Grade	4.0	75
Heavy Traffic “H” Grade	2.0	75
Very Heavy Traffic “V” Grade	1.0	75
Extremely Heavy Traffic “E” Grade	0.5	75

**Mixture Stiffness.** Dynamic modulus testing was conducted in accordance with AASHTO TP79 on the four previously described mixtures. This testing was performed using an IPC Global Asphalt

Mixture Performance Tester (AMPT). Dynamic modulus testing was performed for each of the mix designs listed previously. Specimens were produced in accordance with AASHTO PP 60. A Pine Instruments gyratory compactor was used to compact specimens to 150 mm in diameter and 175 mm in height. These samples were then cored using a 100 mm core drill and trimmed to 150 mm in height. The air voids for these cut specimens were  $7 \pm 0.5$  percent.

To provide the necessary information for M-E pavement analyses, the three samples of the four completed mix designs were tested using three temperatures (4, 20, and 45°C) and three frequencies (10, 1, and 0.1 Hz) in an unconfined state. The mixes were also tested at the 0.01 Hz frequency at the high test temperature. This testing produced a data set for generating master curves for the all four mixtures using the procedure outlined in AASHTO PP 61.

The test data were checked to ensure they met the data quality and within-lab repeatability requirements of AASHTO TP 79. Equations 1 and 2 were used to generate the master curve for each mix design. Equation 1 is the master curve equation, while Equation 2 shows how the reduced frequency is determined. The regression coefficients and shift factors, which are used to shift the modulus data at various test temperatures to the reference temperature of 20.0°C, are determined simultaneously during the optimization process using the *Mastersolver* Excel program.

$$\log |E^*| = \delta + \left[ \frac{\alpha}{1 + e^{\beta + \gamma \log f_r}} \right] \quad (1)$$

$$\log f_r = \log f + \log a(T) \quad (2)$$

where

- $|E^*|$  = dynamic modulus, psi;
- $f$  = loading frequency at the test temperature, Hz;
- $f_r$  = reduced frequency at the reference temperature, Hz;
- $\alpha, \delta, \beta, \gamma$  = regression coefficients; and
- $a(T)$  = temperature shift factor.

While the master curves are not indicators of performance, they are used in mechanistic pavement design and can give an indication of relative mixture stiffness. This is particularly useful for mixtures containing RAP or RAS where the degree of binder blending is unknown. For the four master curves (Figure 1), the mixture with the GTR modified binder was softer than the other three mixtures at all temperatures and frequencies. On the other hand, the two mixtures with recycled materials were stiffer than both of the virgin mixtures. One interesting trend is that the master curves for the RAP only and RAP/RAS mixtures crossed about halfway through the master curve, showing that the RAP/RAS mix was softer at the colder temperatures but stiffer at the hotter temperatures than the RAP only mixture.

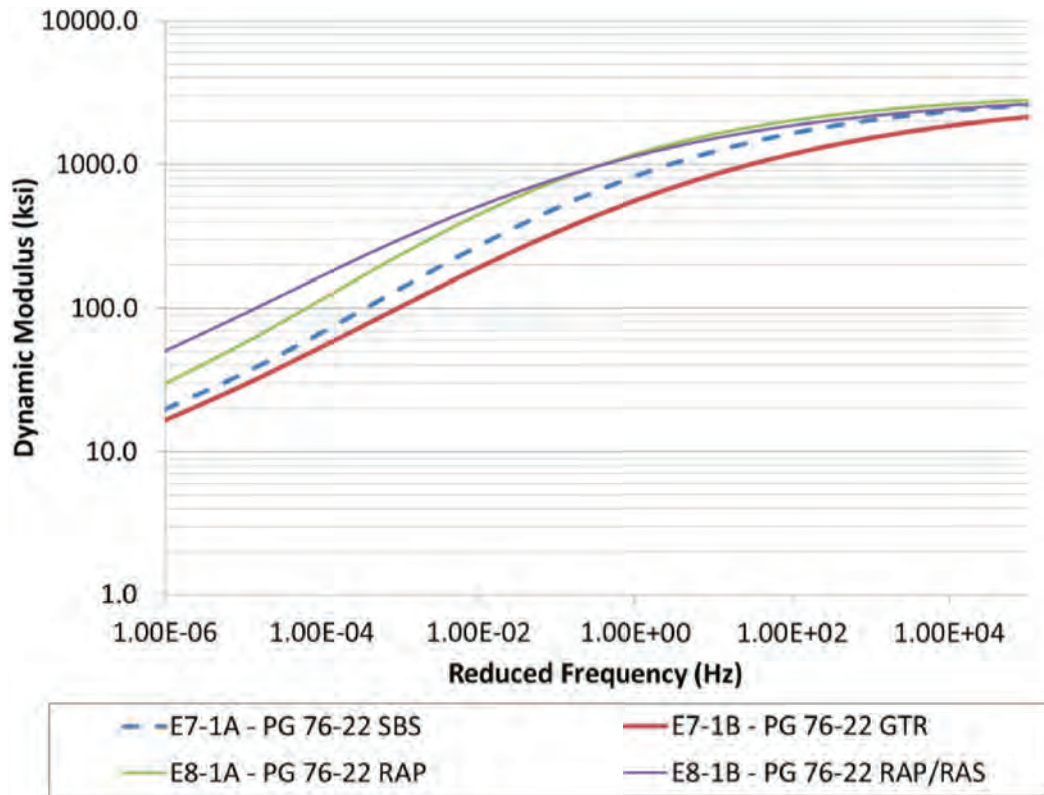


**Figure 1 FDOT Cracking Study Master Curves**

**Hamburg Wheel Tracking Test.** Hamburg wheel-track testing (Hamburg) was performed to determine the rutting and stripping susceptibility of the four FDOT mixtures. Testing was performed and samples were prepared in accordance with AASHTO T 324. For each mix, three replicates were tested. The specimens were originally compacted to a diameter of 150 mm and a height of 115 mm. These specimens were then trimmed so that two specimens, with a height between 38 mm and 50 mm, were cut from the top and bottom of each gyratory-compacted specimen. The air voids on these cut specimens were  $7 \pm 1$  percent.

The samples were tested under a  $158 \pm 1$  lb wheel load for 10,000 cycles (20,000 passes) while submerged in a water bath maintained at a temperature of  $50^{\circ}\text{C}$ . During testing, rut depths were measured by an LVDT, which recorded the relative vertical position of the load wheel after each load cycle. After testing, these data were used to determine the point at which stripping occurred in the mixture under loading and the relative rutting susceptibility of those mixtures. These data show the progression of rut depth with number of cycles. Two tangents are evident from this curve: the steady-state rutting portion of the curve and the portion of the curve after stripping. The intersection of these two curve tangents defines the stripping inflection point of the mixture.

The mixtures did not show any signs of stripping; therefore, it is not expected that any of the mixtures will be susceptible to moisture damage. Additionally, all four mixtures showed good resistance to rutting, as 12.5 mm is a common rutting threshold for this test. The mixture with the GTR binder had the most rutting numerically at 3.1 mm; however, an ANOVA ( $p\text{-value} = 0.731 > \alpha = 0.05$ ) showed no statistical differences between the performance of the four mixtures.

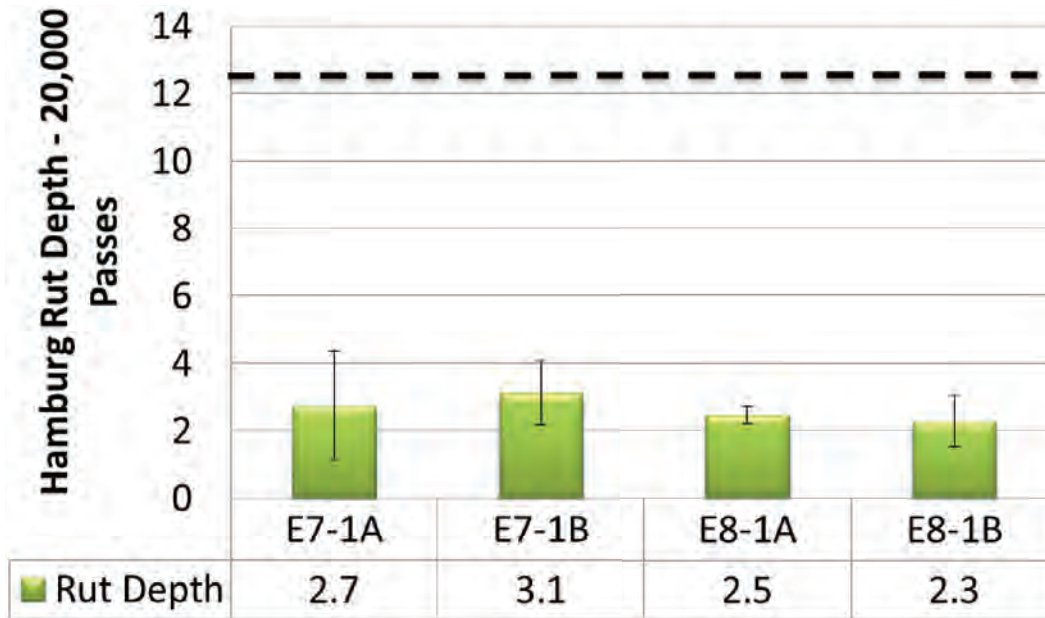


Figure 2 FDOT Cracking Study Hamburg Results

**Asphalt Pavement Analyzer.** The rutting susceptibility of asphalt mixtures is commonly assessed using the Asphalt Pavement Analyzer (APA). Therefore, the mixtures were also assessed for rutting susceptibility using AASHTO T 340. Tests were conducted at 64°C. Manual depth readings were taken at two locations on each sample after 25 loading cycles and at the conclusion of testing to determine the sample rut depth. Past research at NCAT suggests that mixtures with less than 5.5 mm of rutting in the APA should be able to withstand five million equivalent single axle loads (ESALs) without rutting more than 9.5 mm (3). As with the Hamburg Wheel Tracking Test, all four mixtures passed the 5.5 mm test threshold. The results of the four mixtures are provided in Table 5. Numerically, the GTR had the highest rut depths; however, since the APA is considered a “go/no go” test, the mixtures are all expected to resist rutting.

Table 5 FDOT Cracking Study APA Results

Mix ID	Average Manual APA Rut Depth (mm)	Average Automated APA Rut Depth (mm)	Standard Deviation Manual APA Rut Depth (mm)	Standard Deviation Automated APA Rut Depth (mm)
E7-1A	1.26	1.39	0.33	0.34
E7-1B	2.72	2.23	0.49	0.57
E8-1A	0.97	1.18	0.47	0.18
E8-1B	0.70	1.19	0.27	0.23

**Overlay Tester.** The Overlay Test (OT) was performed in accordance with Tex-248-F using the OT kit designed for the IPC Global AMPT. For this test, samples with a 150 mm diameter and 125 mm target height were produced using the Superpave gyratory compactor. Two test specimens from each gyratory sample were trimmed to the following dimensions: 150 mm long by 76 mm wide by 38 mm tall. Four replicates with air voids between 6 and 8 percent after trimming were tested at 25°C in controlled displacement mode. Loading occurs when a movable steel plate attached to the asphalt specimen slides away from the other plate, which remains fixed. Loading occurs at

a rate of one cycle every 10 seconds with a sawtooth waveform. The maximum load the specimen resists in controlled displacement mode is recorded for each cycle. The test continues until the sample fails. Failure is defined as 93% reduction in load magnitude from the first cycle. Tex248-F specifies a maximum opening displacement of 0.025 inches. There is no definitive pass/fail criterion for the OT, with minimum recommended cycles to failure at the above parameters ranging between 150 and 700 cycles to failure depending on the type of mixture tested (4, 5, 6).

Table 6 provides the OT results for the four mixtures. As can be seen, none of the mixtures performed well in this test highlighting the need for state specific parameters in performance tests to match field performance. Statistical analyses were not completed due to the low failure cycles for the mixtures. Inspection of the raw data actually showed that many of the specimens fractured on the first cycle. This was identified by extremely low peak loads on the first cycle (generally less than 100 lb) and examination of the load versus time data on the samples in question. When this was the case, the number of cycles until failure was noted as 1. Two of the four RAP mixture specimens fractured on the first cycle while all four RAP/RAS specimens fractured on the first cycle. While the current OT parameters may not be the most appropriate for assessing field performance, all of the mixtures showed signs of being excessively brittle in the OT, and the mixtures containing RAP and/or RAS are more brittle than the virgin mixes.

**Table 6 FLDOT Cracking Study Overlay Test Results**

Mix ID	Replicates	Average Peak Load (lb)	Average Cycles to Failure
SBS	4	556.8	30
GTR	4	377.7	18
RAP	4	280.8	9
RAP/RAS	4	38.8	1

**Energy Ratio.** The energy ratio test procedure was developed to assess an asphalt mixture’s resistance to top-down or surface cracking (2). This testing procedure has been used in past research cycles at the NCAT Test Track as a predictor of whether or not a mixture will be susceptible to top-down cracking (7). The energy ratio is determined using a combination of three tests: resilient modulus, creep compliance, and indirect tensile strength. These tests are described in greater detail below. These tests were performed at 10°C using an MTS® testing device. The tests were conducted on three specimens 150 mm diameter by approximately 38 mm thick, cut from gyratory compacted samples. The target air voids for the specimens was 7 ± 0.5 percent.

The resilient modulus was obtained by applying a repeated haversine waveform load in load control mode. The load was applied for 0.1 seconds and then followed by a 0.9 second rest. The resilient modulus was calculated using the values from the stress-strain curve. The creep compliance test was performed as described in AASHTO T 322-07; however, the temperature of the test was 10°C with a test duration of 1000 seconds. The power function properties of the creep compliance test were determined by curve-fitting the results obtained during constant load control mode. Finally, the tensile strength and dissipated creep strain energy (DCSE) at failure were determined from the stress-strain curve of the given mixture during the indirect tensile

strength test. Detailed testing procedures and data interpretation methods for the three testing protocols are described elsewhere (2, 7, 8).

The results from these tests were then used to evaluate each mixture’s surface cracking resistance using Equation 3. Data analysis was performed using a software package developed at the University of Florida. The details of the software operation are documented elsewhere (8). Table 7 lists the recommended thresholds for the energy ratio as a function of rate of traffic. A higher energy ratio provides more resistance to surface cracking. Additionally, a DSCE at failure of less than 0.75 kJ/m<sup>3</sup> has been used to identify excessively brittle mixes in the field (2). The energy ratio criteria in Table 7 are only recommended for mixtures with a DSCE at failure of between 0.75 and 2.50 kJ/m<sup>3</sup> (2).

$$ER = \frac{DSCE_f [7.294 \times 10^{-5} \times \sigma^{-3.1} (6.36 - S_t) + 2.46 \times 10^{-8}]}{m^{2.98} D_1} \quad (3)$$

where

- $\sigma$  = tensile stress at the bottom of the asphalt layer, 150 psi;
- $M_r$  = resilient modulus;
- $D_1, m$  = power function parameters;
- $S_t$  = tensile strength;
- $DSCE_f$  = dissipated stress creep energy at failure; and
- $ER$  = energy ratio.

**Table 7 Recommended Energy Ratio Criteria (2)**

Traffic: (ESALs/yr )	Minimum Energy Ratio
< 250,000	1
< 500,000	1.3
< 1,000,000	1.95

\*DSCE<sub>f</sub> must be greater than 0.75 or the mix is considered brittle.

Table 8 shows the energy ratio results for the four mixtures in the cracking study. When comparing these data, the RAP/RAS mixture had the highest energy ratio; however, one must also consider the DSCE<sub>f</sub>. Both the RAP and the RAP/RAS mixtures had DSCE<sub>f</sub> values less than 0.75, showing that the mixture would be brittle. The energy ratio for the SBS and the GTR mixtures showed that the mixtures should be able to handle trafficking less than 1,000,000 ESALs per year. These results indicate that the addition of a stiffer polymer-modified binder to the mixtures containing RAP and/or RAS was not beneficial to their fracture resistance.

**Table 8 FDOT Cracking Study Energy Ratio Results**

Mix	m-value	D <sub>1</sub>	S <sub>t</sub> (MPa)	M <sub>R</sub> (GPa)	FE (kJ/m <sup>3</sup> )	DCSE <sub>f</sub> (kJ/m <sup>3</sup> )	DCSE <sub>MIN</sub> (kJ/m <sup>3</sup> )	Failure Strain	Creep Compliance Rate	ER
SBS	0.399	3.03E-07	2.57	12.70	2.5	2.24	0.430	1,375	1.91E-09	5.21
GTR	0.358	4.15E-07	2.08	10.01	2.4	2.18	0.399	1,541	1.75E-09	5.47
RAP	0.265	2.66E-07	2.28	16.08	0.5	0.34	0.107	392	4.40E-10	3.15
RAP/RAS	0.253	1.11E-07	2.68	16.35	0.9	0.68	0.041	486	1.62E-10	16.54

### Field Cracking Performance

The final phase of the evaluation attempts to correlate the laboratory performance of these mixtures to their performance at the Test Track. Table 9 shows the percent cracking for each of the three sections from 0 to 10 million ESALs of traffic. As can be seen, the GTR mix was the first to crack; however, cracking progressed slowly in this mix. The RAP and the SBS mixtures were the second and third mixtures to crack. Due to combining 25% RAP with a stiffer polymer-modified binder, the cracking progressed quicker in this mixture than in the virgin SBS mixture. The last mix to crack was the RAP/RAS mix using a polymer modified binder; however, the rate of cracking was much greater once cracking initiated in the mix. All of the cracks in these sections were low severity cracks at the end of trafficking.

**Table 9 FDOT Cracking Study: Field Cracking**

Traffic, million ESALS	% Cracking			
	SBS	GTR	RAP	RAP/RAS
93,828	0	0	0	0
1,036,312	0	2.3	0	0
2,018,902	0.1	2.8	1	0
3,011,082	1.6	4.7	4.7	0
4,163,675	2.3	11.3	4.7	0
5,084,518	4.4	20.2	4.7	2.4
6,075,696	4.4	20.2	6.8	10.8
7,045,545	6.0	20.2	10.2	41.7
7,941,941	6.3	20.2	13.4	61.4
9,034,511	6.7	20.2	22.1	62.9
10,045,790	7.7	20.2	22.5	73.4

Pearson correlations were developed between the average laboratory mixture properties/results and the percent cracking in the field and are given in Table 10. The ER value was not included in this correlation due to the low  $DSCE_f$  values, which rendered the actual ER inconclusive for the RAP and RAP/RAS mixtures. R-values close to 1 and -1 show high degrees of correlation. R-values near zero are indicative of non-correlated variables. It is interesting to note that the correlation trends between the lab and field seem to become inverted when comparing the cracking results at 5 million ESALs and the results at 10 million ESALs. At 5 million ESALs, the laboratory resilient modulus showed the best correlation to field percent cracking, while the OT cycles to failure showed the poorest correlation. The  $DSCE_f$  and creep slope showed average correlation. The most interesting aspect of these correlations to cracking at 5 million ESALs is that the direction of the correlations runs counter to the expected trend (i.e. a higher fracture energy correlating to a higher percent cracking). At 10 million ESALs, the directions of the trends were reversed and fell more in line with expected trends. This trend reversal is likely driven by the delayed yet rapid, crack development in the RAP/RAS mixture as opposed to the more gradual crack development exhibited by the other sections. The OT cycles to failure showed the best correlation to field percent cracking at 10 million ESALs, while the  $DSCE_f$  showed the lowest correlation. However, all of the Pearson coefficients comparing the laboratory properties to the percent cracking at 10 million ESALs were above 0.57, indicating at worst, an average correlation.

**Table 10 Pearson Correlations – Laboratory and Field Measurements – FDOT Cracking Study**

	ESALs at 1 <sup>st</sup> Crack	% Cracking, 5 million ESALs	% Cracking, 10 million ESALs	OT N <sub>f</sub>	DSCE <sub>f</sub>	Mr	Creep Slope, m
ESALs at 1 <sup>st</sup> Crack	1.0						
% Cracking, 5 million ESALs	-0.588	1.0					
% Cracking, 10 million ESALs	0.964	-0.360	1.0				
OT, N <sub>f</sub>	-0.773	0.263	-0.853	1.0			
DSCE <sub>f</sub>	-0.603	0.572	-0.574	0.845	1.0		
Mr	0.720	-0.860	0.592	-0.686	-0.907	1.0	
Creep Slope, m	-0.715	0.419	-0.747	0.965	0.956	-0.819	1.0

### Conclusions

The results of this study support the following conclusions.

- After 10 million ESALs of traffic, the polymer-modified, GTR-modified, and 25% RAP mixtures had less than 22.5 percent cracking in their respective test sections. The RAP-RAS mixture using an SBS-modified binder had the highest cracking area despite being the last section to crack.
- The majority of the cracking in the test sections was low severity.
- Relative rankings in the Overlay Tester were similar to the final cracking measurements.
- Energy ratio testing was able to designate the RAP and RAP/RAS mixtures as brittle in the laboratory.
- The correlations between laboratory performance and field cracking area are completely different when the comparisons are made after 5 million ESALs of traffic and after 10 million ESALs of traffic. This trend reversal is likely driven by rapid crack development in the RAP/RAS mixture in the second half of the research cycle.
- The results from this study showed that polymer-modified binders should not be used in conjunction with RAP/RAS mixtures. These mixtures can become too stiff and thus, are susceptible to cracking.

### References

1. Wang, J., B. Birgisson, and R. Roque. Windows-Based Top-Down Cracking Design Tool for Florida Using Energy Ratio Concept. *Transportation Research Record: Journal of the Transportation Research Board*, No. 2037, Transportation Research Board of the National Academies, Washington, D.C., 2007, pp. 86-96.
2. Roque, R., B. Birgisson, C. Drakos, and B. Dietrich. Development and Field Evaluation of Energy-Based Criteria for Top-Down Cracking Performance of Hot Mix Asphalt. *Journal of the Association of Asphalt Paving Technologists*, Vol. 73, 2004, pp. 229-260.
3. Tran, N., R. West, R. Powell, and A. Kvasnack. Evaluation of AASHTO Rut Test Procedure Using the Asphalt Pavement Analyzer. *Journal of the Association of Asphalt Paving Technologists*, Vol. 78, 2009, pp. 1-24.

4. Sheehy, E. Case Study: High RAP Pilot Project. *Presentation from New Jersey Asphalt Paving Conference*. March 6, 2013. [https://cait.rutgers.edu/system/files/u10/High\\_RAP\\_NJDOT\\_--\\_Sheehy.pdf](https://cait.rutgers.edu/system/files/u10/High_RAP_NJDOT_--_Sheehy.pdf) Accessed August 20, 2014.
5. Chen, D. Field Experiences with RDD and Overlay Tester for Concrete Pavement Rehabilitation. *ASCE Journal of Transportation Engineering*, 2008, pp. 24-33.
6. Zhou, F., S. Hu, D. Chen, and T. Scullion. Overlay Tester: Simple Performance Test for Fatigue Cracking. *Transportation Research Record: Journal of the Transportation Research Board*, No. 2001, Transportation Research Board of the National Academies, Washington, D.C., 2007, pp. 1-8.
7. Timm, D. H., G. A. Sholar, J. Kim, and J. R. Willis. Forensic Investigation and Validation of Energy Ratio Concept. *Transportation Research Record: Journal of the Transportation Research Board*, No. 2127, Transportation Research Board of the National Academies, Washington, D.C., 2009, pp. 43-51.
8. R. Roque, W. G. Buttlar, B. E. Ruth, M. Tia, S. W. Dickison, and B. Reid. *Evaluation of SHRP Indirect Tension Tester to Mitigate Cracking in Asphalt Concrete Pavements and Overlays*. Final Report, FDOT B-9885, University of Florida, Gainesville, Fla., 1997.

### 3.7. Georgia Department of Transportation Surface Treatment vs. OGI Reflective Crack Prevention Experiment

#### Introduction

Georgia DOT (GDOT) has been exploring ways to help retard reflective cracking in pavements. A traditional approach has been to place a single surface treatment application of No. 7 stone before overlaying. The open texture of the surface treatment provides a disconnect plane between the existing surface and overlay so that underlying cracks are dissipated rather than reflected through to the surface. This approach has not been as effective as desired because of a relatively short life span before cracks are reflected.

#### Overview

GDOT decided to experiment with two alternative treatments for crack relief interlayer. First, the surface treatment was changed from a single layer of stone to what GDOT refers to as a double surface treatment with a sand seal surface. This treatment is constructed by placing No. 7 stone followed by No. 89 stone. A sand seal surface is then placed over the No. 89 stone before adding the asphalt layer. Secondly, GDOT developed an asphalt open-graded interlayer (OGI) and needed to conduct research to document its performance as compared to the surface treatment application. The mix is essentially a 12.5 mm NMAS PFC mixture (Table 1), but it is designed with lower asphalt content than a typical PFC surface mix. It also omits fiber stabilizer for economic reasons, and instead reduces mix temperature to 250°F ±20°F to resist drain-down.

**Table 1 OGI Mixture Properties**

Sieve	% Passing	Specification Range
3/4"	100	100
1/2"	96	80-100
3/8"	59	40-65
No. 4	14	10-25
No. 8	8	2-8
No. 200	2	1-4
<b>Mixture Properties</b>		
AC, %	4.5	4.0-5.0
Va, %	22.2	22±1
VMA, %	30.8	-
Film Thick.	23.2 μm	-

Deep saw cuts 1/8-inch-wide (width of saw blade) were made in the existing pavement (Figure 1) in order to create the effect of a cracked surface. The cuts were then filled with sand to keep the mixture from healing back together. The existing pavement was then covered with the double surface treatment and sand seal in Section N12 and with the OGI mixture in Section N13. A 9.5 mm NMAS surface mix was then placed over the interlayer treatments. Figures 2 and 3 show that the surface treatment section had slightly less cracking than the OGI section (1% vs 2% of total area) after more than 10 million ESALs, but the total amount of cracking was insignificant at the end of the 2012 test cycle.



**Figure 1 Deep Saw Cuts Simulating Pavement Cracks**

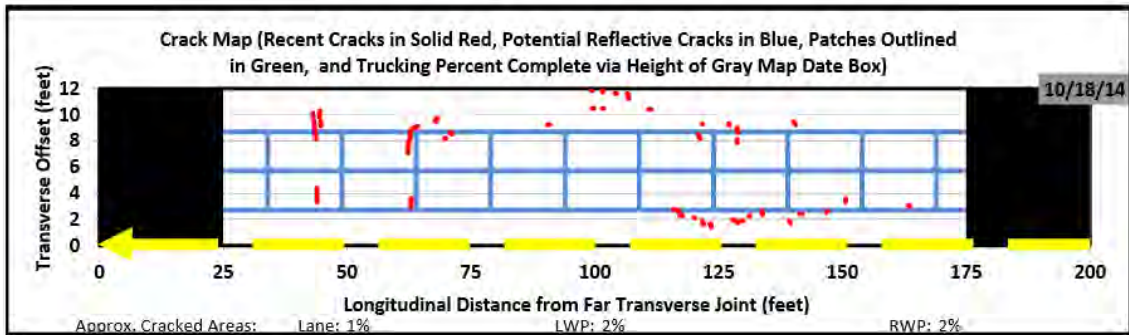


**Figure 2 Crack Map of N12 (Double Surface Treatment Interlayer)**

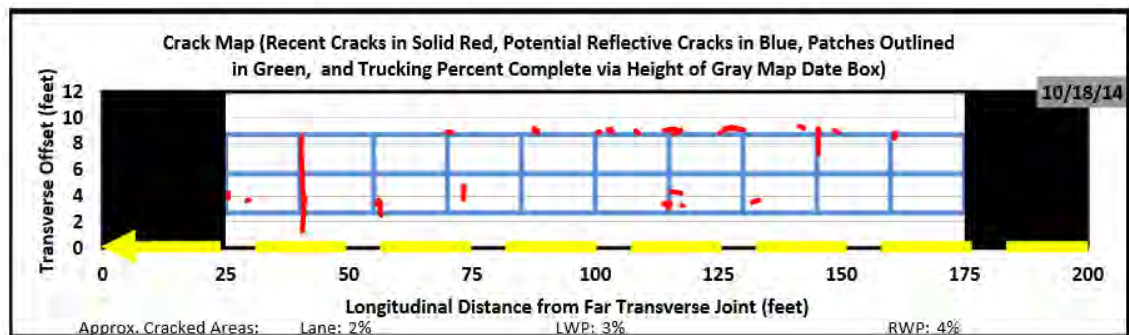


**Figure 3 Crack Map of N13 (OGI Interlayer)**

## Performance

The cracking that began to show up along the longitudinal joint of Section N12 is shown in Figure 2. This cracking is believed to indicate plastic movement of the mix since this cracking is outside the wheel path. This opinion appears to be supported by wire line rutting measurements revealing that N12 began to develop ruts in the wheel path (Figure 4). The rutting increased slightly over the summers of 2013 and 2014 (at about 4 million and 8 million ESALs). Most of the rutting shown after 8 million ESALs was due to a change in the equipment used to measure rutting; however, the final measurements shown in Figures 4 and 5 were wire-line measurements and are the most accurate. Based on the final measurement, rutting in Section N12 reached 11.5 mm after more than 10 million ESALs. Rutting on the OGI section was 5.3 mm (Figure 5), which is only about half that of N12.

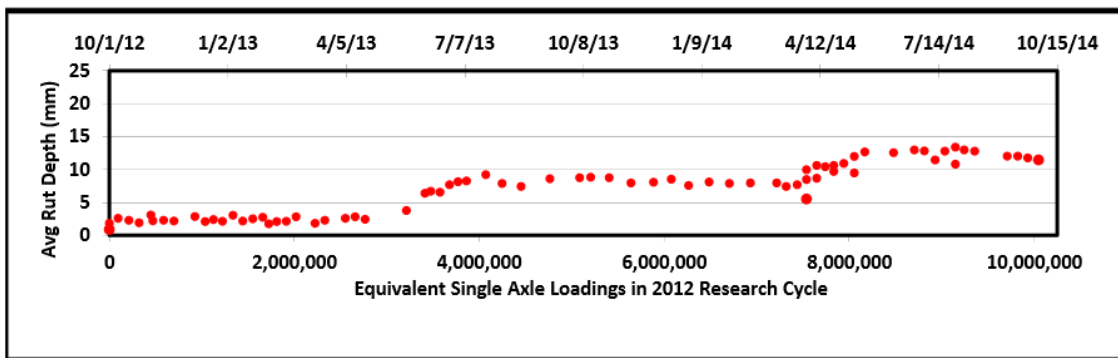


Figure 4 Rutting on Section N12 (Surface Treatment Interlayer)

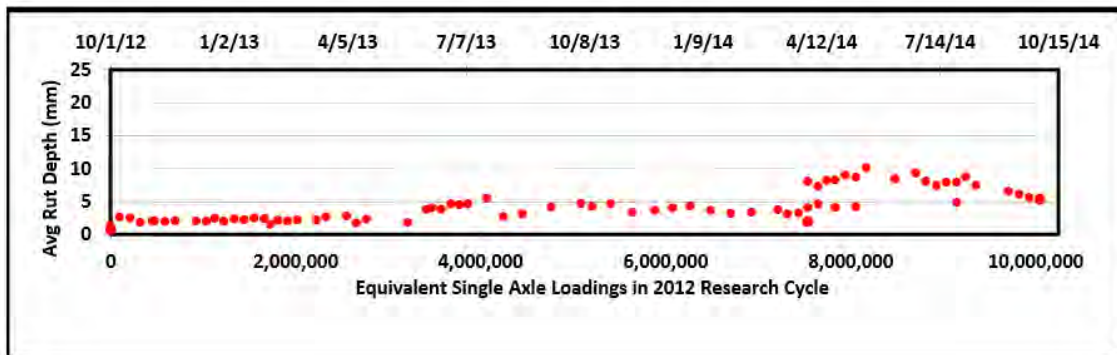


Figure 5 Rutting on Section N13 (OGI)

## Findings

- The total amount of cracking was practically insignificant at the end of the 2012 test cycle with no more than 2% of the total area.
- N12 (surface treatment section) had slightly more cracking outside the wheelpath, which may indicate that plastic flow was beginning to occur.
- N13 (OGI treatment) had 6.2 mm less rutting than N12. N12 has almost 0.5 inch (11.5 mm) rutting at the end of the 2012 research cycle.

- The OGI interlayer appears to be a better choice for a crack relief interlayer. It is more stable than the surface treatment section due to less rutting, and cracking for both sections was practically the same.

### 3.8. Mississippi Department of Transportation Evaluation of 45% RAP Mix Performance

#### Background

Mississippi DOT's high RAP test section (S2) was constructed in 2009 by milling four inches from the existing full-depth section and placing two lifts of a 9.5-mm NMAS mix containing 45% RAP. A summary of the mix design is shown in Table 1. The asphalt binder contributed by the two RAP sources was 41% of the total binder content. Quality control data for the binder and surface mixes sampled during production are shown in Table 2.

**Table 1 Mix Design Information for 45% RAP Mix**

Design Gyration	85	
Asphalt Binder	PG 67-22 (unmodified)	5.6%
Aggregate 1	Crystal Springs 1/2" gravel	20%
Aggregate 2	Crystal Springs 3/8" gravel	26%
Aggregate 3	Crystal Springs coarse sand	8%
RAP 1	S2 millings	15%
RAP 2	Newton RAP	30%
	Hydrated Lime	1%

**Table 2 Gradation and Volumetric Properties of 45% RAP Mix**

Sieve	Mix Design	Quality Control	
		Binder	Surface
3/4" (19.0 mm)	100	100	100
1/2" (12.5 mm)	97	98	98
3/8" (9.5 mm)	93	93	95
No. 4 (4.75 mm)	61	62	62
No. 8 (2.36 mm)	39	40	40
No. 16 (1.18 mm)	28	29	29
No. 30 (0.60 mm)	21	21	22
No. 50 (0.30 mm)	13	13	14
No. 100 (0.15 mm)	7	8	9
No. 200 (0.075 mm)	5.6	6.6	7.2
Asphalt Content (%)	5.6	5.3	5.2
Lab Air Voids (%)	4.0	4.0	5.0
VMA (%)	15.1	14.9	15.6
VFA (%)	74	73	68
In-Place Density (% of Gmm)		93.8	92.1

At the end of the 2009 Test Track cycle, after 10 million ESALs had been applied, the 45% RAP mix showed good performance with only 3.0 mm of rutting and low severity cracking (<6 mm wide) covering 3.4% of the total lane area, primarily between the wheelpaths. As shown in Figure 1, the cracking in the 45% RAP mix was in different locations than the 15% RAP mix MSDOT placed in Section S2 in 2006, so reflective cracking was not an issue. Cracking has been evident in Mississippi's previous test sections using gravel in Superpave mixes, so there could be an interaction effect related to aggregate characteristics. The total length of cracking at the end of the 2009 cycle was 61 feet, compared with 80 feet of cracking in the 2006 15% RAP mix. This

indicates that the 45% RAP mix performed equal to or better than the 15% RAP mix after 10 million ESALs. For the 2012 cycle, Section S2 was left in place for continued trafficking.

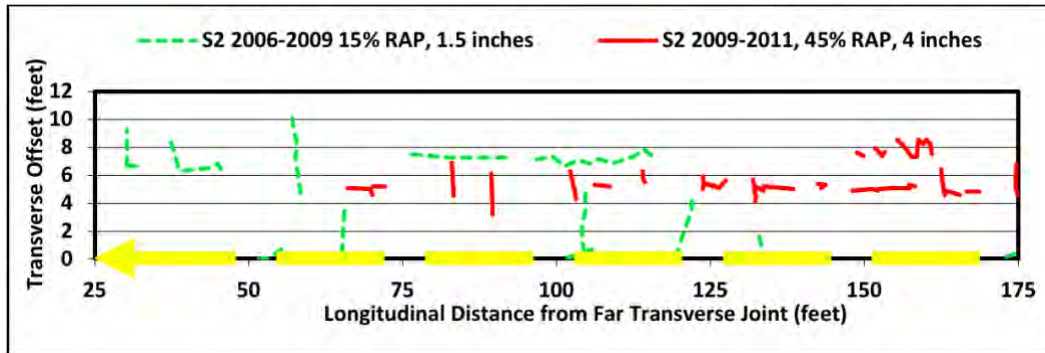


**Figure 1 Crack Map for Section S2 at End of 2006 and 2009 Cycles**

### *Objective*

The objective of this study was to evaluate the long-term performance of a 45% RAP mix containing Mississippi gravel and apply preservation treatments when a predetermined level of distress was reached.

### *Test Track Performance*

At the end of April 2014, after more than 17 million ESALs, preservation treatments were applied to Section S2 and it became part of the Pavement Preservation Experiment. As shown in Figure 2, S2 had longitudinal and transverse cracks but no interconnected fatigue cracking. Crack sealing was selected as the appropriate preservation treatment since there were no other distresses involved. Crack sealing helps retard crack growth and prevent further deterioration caused by water or debris entering the pavement structure. The section was divided into three 50-ft subsections (S2A, S2B, and S2C). In S2A, the cracks were sealed using the rout/fill method, while the blow/band method was used in S2B. S2C had a lesser amount of cracking and was left untreated for comparison.



**Figure 2 S2 45% RAP Mix After More Than 17 Million ESALs**

As shown in Figure 3, a router was used in S2A to prepare the cracks for treatment. Routing grinds the inner edges of the crack to create a good surface for adhesion of the sealant material. The cracks were cleaned of dust/debris and heated before being filled with crack sealant (Crafco Modified Asphalt Sealant – Roadsaver 211), as shown in Figure 4.



**Figure 3 Routing Cracks in Section S2A**



**Figure 4 Filling Cracks in Section S2A**

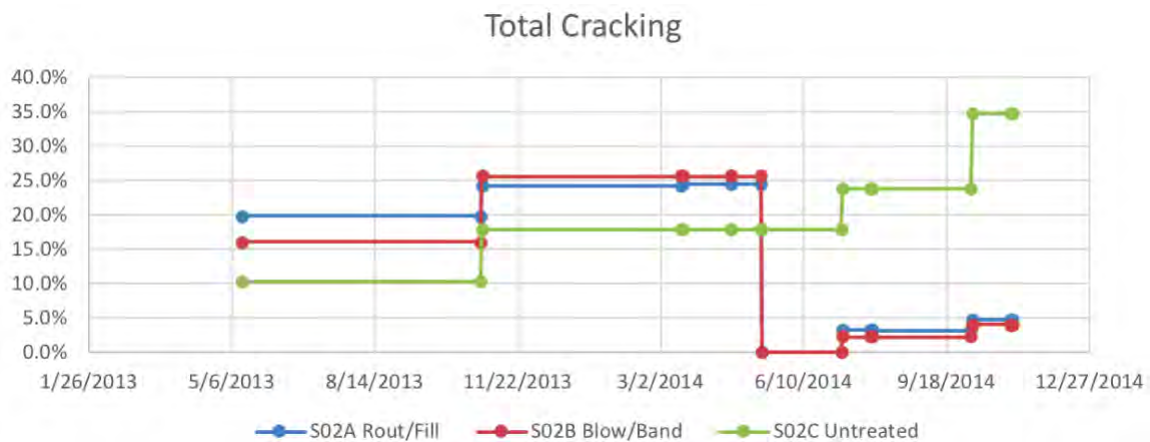
In S2B, the cracks were sealed using a different method. A heat lance was used to blow out dirt/debris from the crack, remove moisture, and heat the edges. The crack sealant was applied using a disc-shaped band attached to the nozzle so that excess sealant material was spread on the pavement surface along either side of the crack, as shown in Figure 5.



**Figure 5 Blow/Band Crack Sealing in Section S2B**

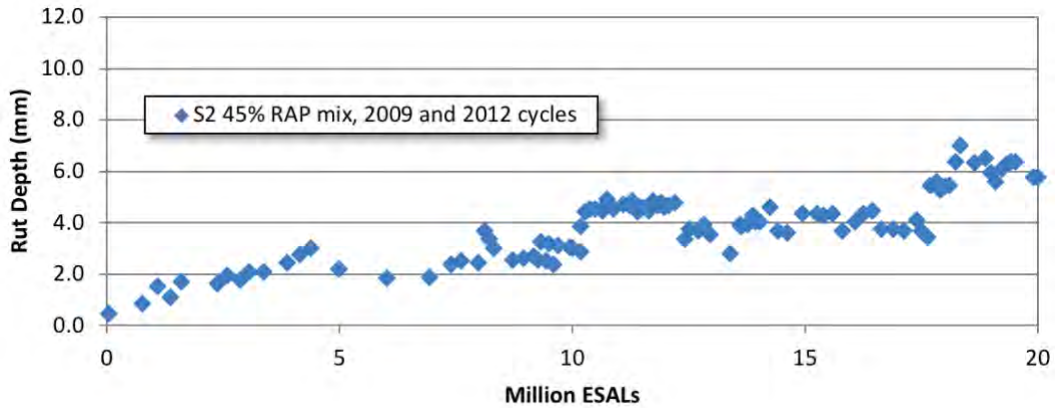
During the 2012 cycle, with the expansion of the Test Track to include the pavement preservation sections on Lee Road 159, NCAT researchers transitioned to a new method of quantifying cracking to allow for more frequent data collection. As in previous cycles, cracks were still identified by visual inspection and marked by hand. HD video footage of each section was then used to generate a panoramic photo, which was normalized to remove distortion due to perspective and digitized for analysis. Cracking results for the 2012 cycle are presented in graphical format as a percentage of area vs. time rather than the crack maps presented in previous cycles. Due to the time involved in developing and transitioning to the new method, the results are shown from the spring of 2013 rather than the fall of 2012 when trafficking began.

Figure 6 shows the progression of total cracking in the 45% RAP mix (Section S2) during the 2012 cycle. Total cracking is expressed as a percentage of the subsection area rather than a percentage of the entire section. When crack sealing occurred in late April 2014, total cracking was represented as zero in S2A and S2B. Cracks continued to form in all three subsections, but the increase in total cracking was significantly greater in S2C (untreated) than in S2A and S2B. During the remainder of the cycle (approximately 2.5 million ESALs), total cracking in S2C increased from 17.9% to 34.8%, while total cracking in S2A and S2B went from zero to 4.9% and 4.1%, respectively. This indicates that both the rout/fill and blow/band methods of crack sealing were effective in retarding crack development.



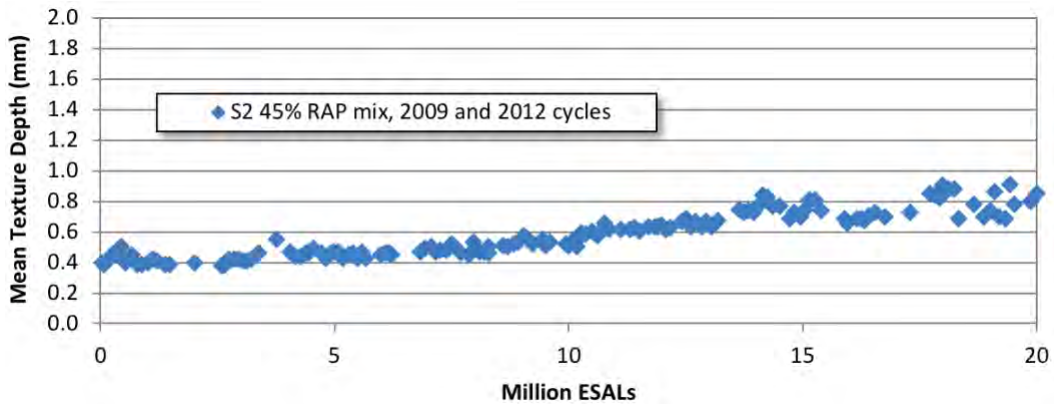
**Figure 6 Total Cracking for Section S2 During 2012 Cycle**

As shown in Figure 7, the 45% RAP mix performed very well with regard to rutting, with only 6 mm after 20 million ESALs were applied during the 2009 and 2012 cycles.



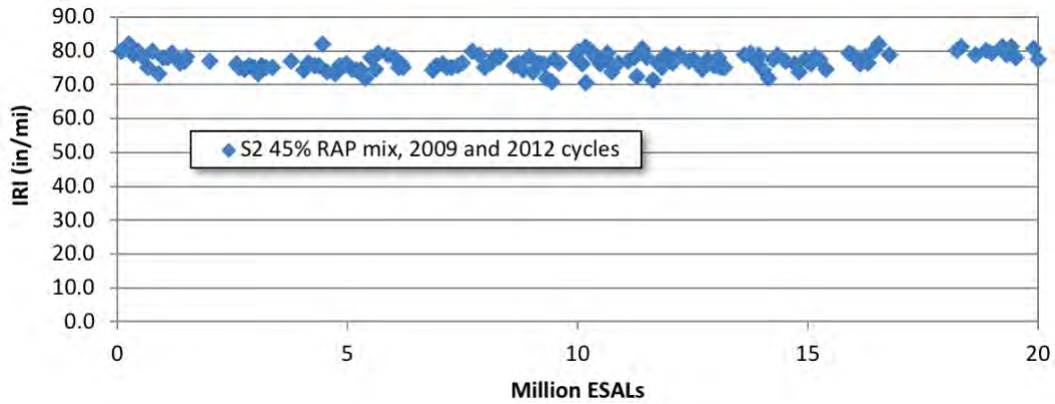
**Figure 7 Rutting Results for 45% RAP Mix During 2009 and 2012 Cycles**

Figure 8 shows the texture change of the 45% RAP mix through the 2009 and 2012 cycles. Macrotexture increased during the 2012 cycle as cracking progressed and crack sealing treatments were applied, yet the mean texture depth was still good at 0.8 mm after 20 million ESALs.



**Figure 8 Macrotexture Results for 45% RAP Mix During 2009 and 2012 Cycles**

Pavement roughness through the 2009 and 2012 cycles (quantified using IRI) is shown in Figure 9. The IRI data are very consistent, indicating that the pavement remained smooth despite crack propagation and crack sealing treatments.



**Figure 9 Roughness Results for 45% RAP Mix During 2009 and 2012 Cycles**

*Conclusions*

Section S2, a 45% RAP mix containing Mississippi gravel, received crack sealing treatments to address longitudinal and transverse cracking after more than 17 million ESALs. No interconnected fatigue cracking was present. Two crack sealing methods were used: rout/fill in S2A and blow/band in S2B. S2C was left untreated. From the time of treatment to the end of the 2012 cycle (an additional 2.5 million ESALs), total cracking in S2A and S2B went from zero to 4.9% and 4.1%, respectively, while total cracking in S2C increased from 17.9% to 34.8%. Thus, both crack sealing methods were effective in retarding crack growth and preventing further deterioration. The blow/band method of crack sealing shows slightly better performance than the rout/fill method as a stand-alone pavement preservation treatment. This could be attributed to the abrasive nature of the routing process, which may contribute to the formation of microcracks along the existing cracks. Rutting, roughness, and macrotexture results were good after 20 million ESALs.

### 3.9. Missouri Department of Transportation GTR Modified Surface Mixture Study

#### Introduction

As part of the 2009 NCAT Test Track cycle, the Missouri Department of Transportation sponsored two test sections to determine if ground tire rubber (GTR) would be an adequate substitute for styrene-butadiene-styrene SBS in asphalt mixtures without sacrificing mixture performance. The first mixture used a PG 67-22 asphalt that was terminally blended offsite at a terminal with 11% rubber (40 mesh ambient ground) by weight of the total binder. After modification, the binder was classified as a PG 76-22. The second mixture used a 2.5% SBS modified binder also classified as a PG 76-22. Both mixtures were Superpave 12.5 mm nominal maximum aggregate size (NMAS) and were constructed 1.75 inches thick. The underlying pavement structure for both sections included 23 inches of asphalt mix, a dense-graded aggregate base, and a firm subgrade soil. Table 1 summarizes the quality control gradations and mixture volumetric properties for each mix. The primary difference between the two mixtures was the asphalt content. The CR-modified asphalt mixture had a 0.6% higher binder content. This reduced the mixture's air voids to 3.3%.

**Table 1 Gradation and Mixture Quality Control Results**

Percent Passing – Gradation		
Sieve Size	GTR	SBS
3/4"	100	100
1/2"	97	96
3/8"	89	86
#4	59	55
#8	37	34
#16	22	21
#30	13	13
#50	9	9
#100	7	7
#200	5.6	5.4
Mix Information		
Binder Modifier	GTR	SBS
Design Gyration	100	100
Binder Grade	76-22	76-22
Binder Content, %	6.0	5.4
Effective Binder Content, %	5.1	4.5
Voids in Mineral Aggregate, %	15.0	14.8
Air Voids, %	3.5	4.5
Dust Proportion	1.1	1.2

A total of approximately 10 million equivalent single axle loads (ESALs) were applied to both sections from August 28, 2009 through September 28, 2011. At the end of this cycle, neither section showed any signs of cracking and the rutting for both was less than 5 mm. Additional information regarding laboratory and field performance of these sections has been documented elsewhere (1). Due to its good performance, the sponsor decided to continue trafficking on this section during the track's fifth testing cycle to assess its long-term performance.

### Objective

The objective of this study was to assess the long-term performance of a test section with a surface mixture containing a GTR modified binder. This section was built in 2009 (Section S7) and has endured two cycles of trafficking, which corresponds to 20 million ESALs. The polymer-modified test section was not sponsored in the 2012 Test Track cycle.

### Field Performance

The section was evaluated weekly in terms of rutting, cracking, and roughness (in terms of the International Roughness Index [IRI]). At the end of the 2012 cycle, with an additional 10 million ESALs of traffic, the rutting remained approximately the same at 5 mm. The section did not show any signs of cracking. In terms of IRI, a value of approximately 50 in/mile was reported at the end of the 2009 cycle. At the end of the 2012 cycle, this number had increased to approximately 70 in/mile. The texture reported at the end of the previous cycle was 0.5 mm; this value increased to 0.7 mm at the end of the 2012 cycle. Figure 1 shows the performance of this section for the second cycle of trafficking.

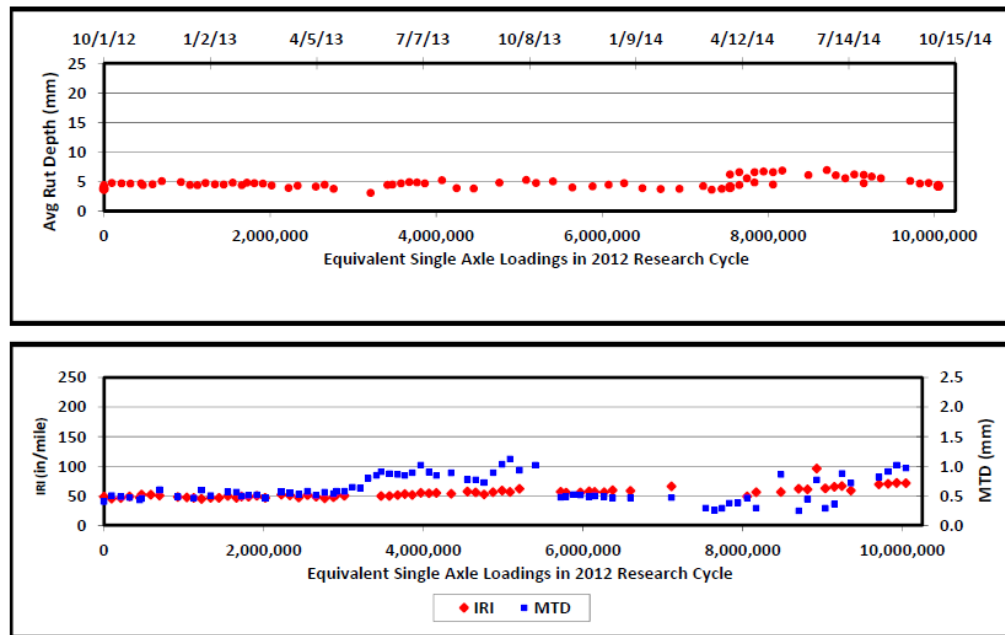


Figure 1 Section S7 Performance

### Conclusions

Section S7 was originally built during the 2009 test track cycle as a GTR modified asphalt mixture and has performed well after 20 million ESALs. No signs of cracking were observed and no additional rutting has occurred over the last two years of traffic. Roughness increased to 70 in/mi, which is still considered good performance. Texture has increased slightly, but no signs of raveling have been reported. Based on the results of this study, it is expected that mixtures with GTR modified binders used as in this dense graded mixture will perform well, and it appears to be an adequate substitute for SBS modified mixtures.

## *References*

1. West, R., D. Timm, R. Willis, B. Powell, N. Tran, M. Sakhaeifar, R. Brown, M. Robbins, A. Vargas-Nordbeck, F. Leiva Villacorta, X. Guo, and J. Nelson. *Phase IV NCAT Pavement Test Track Findings*. NCAT Report 12-10, National Center for Asphalt Technology at Auburn University, Auburn, Ala., 2012.

### 3.10. Federal Highway Administration HFST Alternative Aggregates Study

#### *Introduction*

High friction surface treatments (HFSTs) are used to improve roadway surface conditions in locations with high crash rates. An HFST is a thin surface layer consisting of an angular aggregate, predominantly No. 8 and No. 12 size particles, bound to the pavement surface by a specially formulated epoxy. A uniform application of epoxy is placed on the pavement surface and the aggregate is dropped into the epoxy. HFST specifications commonly recommend crushed calcined bauxite aggregate, which is an imported and costly product.

#### *Objective and Scope*

NCAT performed a series of studies to examine the performance of seven alternative friction aggregates from sources in the United States to determine if they provided similar friction performance. The alternative aggregates are listed in Table 1.

The research program was divided into three studies: Lab-1, Field, and Lab-2. The Lab-1 Study evaluated HFST test slabs with bauxite and seven alternative aggregates under accelerated laboratory polishing and testing procedures. The Field Study evaluated the friction performance of HFST surfaces in Test Track Sections W8 and W9 using the same eight aggregates. The Lab-2 Study evaluated the influence of particle size on HFST friction performance and examined the feasibility of using other laboratory aggregate tests to qualify friction aggregates in HFST specifications. Findings of the Field Study are presented here. A detailed report of the entire three-phase study, NCAT Report 15-04, is available on the NCAT website.

**Table 1 HFST Study Aggregate Types and Sources**

<b>Aggregate Type</b>	<b>Aggregate Source</b>
Granite	Wisconsin
Bauxite (Calcined Bauxite)	China
Flint (Chert, Chat)	Picher, Oklahoma
Basalt	Washington
Silica (Silica Sand)	Ohio
Slag (Steel Slag)	Mechanicsburg, Pennsylvania
Emery (Alumina-Ferrous Oxide)	Halsey, Oregon
Taconite	Minnesota

#### *Construction and Testing*

An HFST contractor installed a full lane-width test section for each of the eight aggregates. Granite was placed 85-ft long (due to available aggregate supply), and bauxite and flint were placed 100-ft long. Basalt, silica sand, steel slag, emery and taconite were each placed 15-ft long. All sections were placed in a single day using the same epoxy binding agent and same placement procedures. Figure 1 shows an aerial view of Sections W8 and W9, and Table 2 provides a list of the sections in the order they were placed.

All eight sections were conditioned by truck traffic during the last six months of the 2009 research cycle, an equivalent of approximately 350,000 18-wheel tractor-trailer units (2.5 million ESALs).

An additional 1,000,000 tractor-trailer units (8.0 million ESALs) were applied to the three longer sections during the first 18 months of the 2012 research cycle.

The same dynamic friction tester (DFT) and circular texture meter (CTM) devices were used to measure friction and texture of the field sections. Friction was also measured with the full-scale locked-wheel skid trailer on the three longer sections. The planned test frequency was monthly for the locked-wheel skid trailer, DFT, and CTM. Actual testing frequency varied with equipment and staff availability as well as weather conditions. Replicate measurements were made with all test devices and data quality was evaluated for outliers. The NCAT Service Center performed the DFT and CTM testing, and the Alabama DOT performed the locked-wheel skid trailer testing.



**Figure 1 View of HFST Sections W8 and W9 on Test Track**

**Table 2 NCAT Test Track HFST Sub-Section Locations**

Sub-Section ID	HFST Aggregate	Subsection Length (Ft)
W8a	Granite	85
W8b	Bauxite	100
W9a	Flint	100
W9b	Basalt	15
W9c	Silica	15
W9d	Slag	15
W9e	Emery	15
W9f	Taconite	15

*Data Analysis*

Data analysis examined the changes in HFST friction and texture to establish terminal values. As shown in Figure 2, all of the sections except for basalt and taconite showed 0.20 to 0.30 mm lower mean profile depth (MPD) texture values after one to two months of traffic. Most of the sections continued to gradually decrease an additional 0.10 to 0.20 mm MPD through six months

of traffic conditioning. The six-month terminal texture values ranged from 1.10 to 1.50 mm MPD for all sections except the steel slag, which dropped below 0.90 mm.

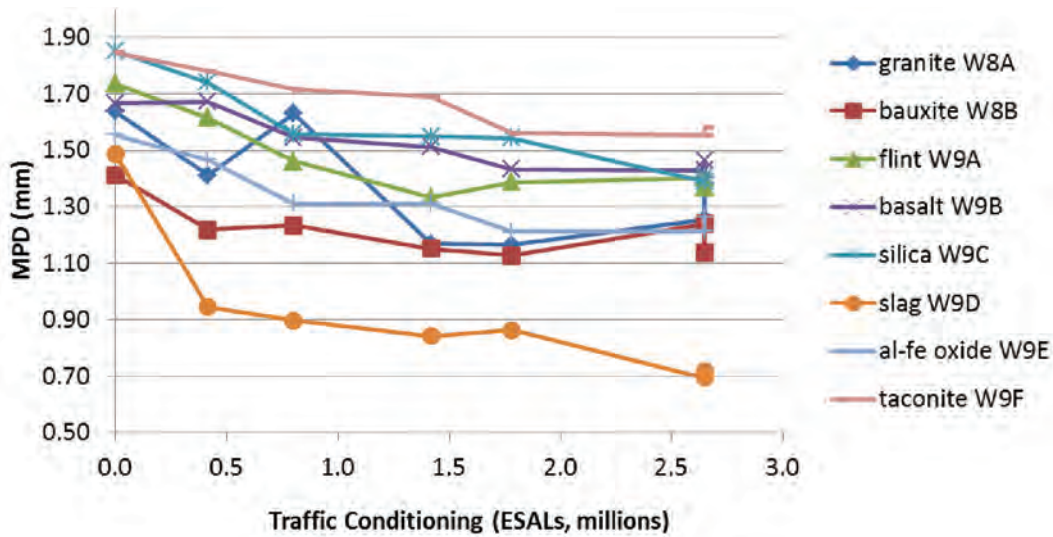


**Figure 2 Left Wheel Path Surface Texture Values Measured by CTM**

Figure 3 shows that after one month of traffic, the wheel path DFT friction values for all of the HFST test sections had a general reduction of 0.15 in surface friction. The most probable explanation for the reduction in measured friction within the first month is the traffic abrasion wearing down the sharp edges of the crushed faces on the surface of the aggregate particles. Most of the HFST test sections maintained their relative ranking of surface friction throughout the six-month conditioning period. Bauxite and taconite had the highest DFT(40)  $F_n$  terminal values (0.78 and 0.60, respectively), while slag and granite had the lowest terminal values (0.48 and 0.42, respectively) over this period. Figure 4 shows the three sections that received an additional 18 months of traffic conditioning. There was no change in the ranking of friction performance.

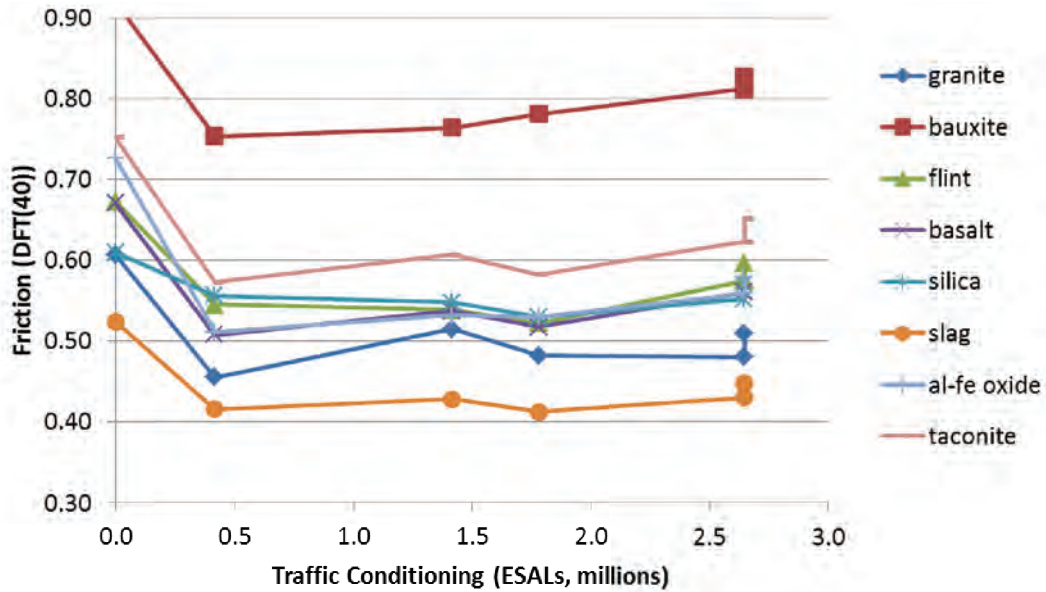


**Figure 3. Left Wheel Path DFT(40) Fn Values After 2.6M ESALs**

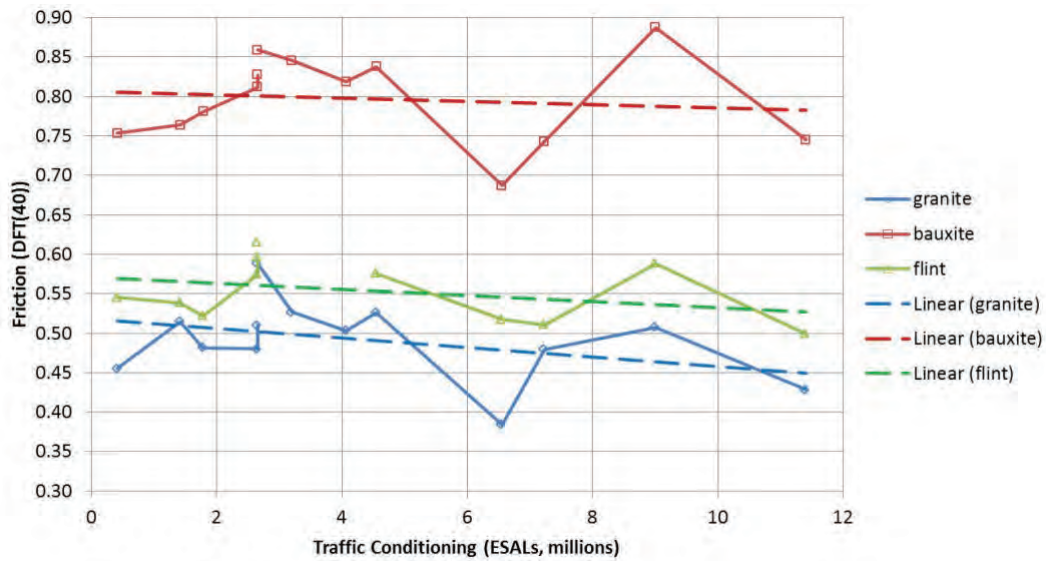


**Figure 4 Left Wheel Path DFT(40) Results After 10M ESALs**

Locked-wheel skid trailer data for the three longer sections was only reliable for the extended 18 months during the 2012 research cycle. As displayed in Figure 5, the trend lines generated by the data sets showed bauxite friction dropped from SN40R of 70 to 63, flint dropped from 54 to 43, and granite dropped from 54 to 40. The results clearly show that the bauxite HFST test section maintained higher friction levels over the 24 months of accelerated truck traffic conditioning at the track.

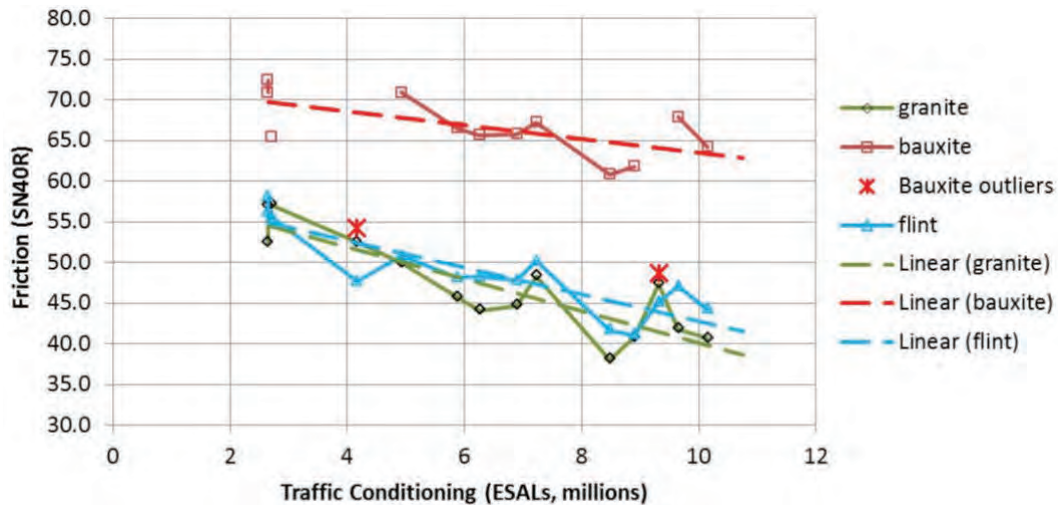


**Figure 5 Left Wheel Path Field Skid Trailer Testing Summary**

*Findings*

In summary, this study found that HFST using calcined bauxite maintained better friction values than comparable HFSTs with all of the alternative U. S. source aggregates. Most of the alternative aggregate surfaces provided better friction than conventional dense-graded asphalt surfaces.

Further research is needed to separately measure the influence of macro-texture and micro-texture on crash rate potential. In this study, standard friction testing with a locked-wheel skid trailer was used as an objective measure to correlate/predict crash rate potential (i.e., higher pavement surface friction has shown to reduce crash rates). The pavement surface properties of macro-texture and micro-texture each influence the crash rate potential. However, the relative degree to which macro-texture and micro-texture influence the crash rate potential is not documented, particularly at critical locations where HFST are typically placed. This further research may establish that common (high quality, good micro-texture) friction aggregates used in the U.S. combined with high HFST macro-texture could reduce crash rates comparable to HFST with bauxite.

NCAT acknowledges the generous donations from material suppliers and POLY-CARB, Inc from the HFST industry. NCAT Assistant Research Engineer Pamela Turner and Auburn University Civil Engineering graduate student Mary Greer were major contributors to the data analysis and reporting.

## 4. EXECUTIVE SUMMARY

This report summarizes the research activities and key findings of the studies that were conducted as part of the 2012 Test Track. Compared with previous research cycles, the 2012 Test Track featured a more complex range of experiments conducted on new and existing pavement sections. These experiments can be divided into four focus areas. The first focus area is on the use of recycled materials in asphalt pavements. These included the 2009 Group Experiment, 2012 Green Group Experiment, Cold-Central Plant Recycling and Stabilized Base Experiment, and mix evaluation sections containing GTR, RAS, or high RAP. The second major focus of the 2012 cycle was on the performance of porous friction courses (PFCs). Eight new PFC test sections and one section with a PFC surface built in the previous cycle were evaluated. The third major focus of the 2012 cycle was placed on pavement preservation. The fourth major focus was on the perpetual pavement design concept and premium mixes using high polymer binders. In the following sections, key findings of each study are synthesized.

### 4.1. Structural Experiments

Structural studies, which have been conducted at the Test Track since 2003, feature test sections constructed with embedded instrumentation to monitor pavement response. Instrumentation within each section typically includes an array of 12 asphalt strain gauges to capture strain at the bottom of the structural asphalt layers, two earth pressure cells to measure vertical stress at the interface between the asphalt base layer and the aggregate base, and temperature probes installed outside the edge stripe to measure temperature at different depths within the pavement structure. Strain and pressure data are collected weekly, and FWD testing is conducted several times per month throughout the two-year research cycle. Pavement distress surveys include weekly manual crack mapping as well as measurements of rutting and ride quality (IRI) with an ARAN van. The rutting threshold was set at 12.5 mm, the cracking threshold was set at 25% of lane area, and the ride quality threshold was set at 170 in/mile.

#### *2009 Group Experiment*

Six sections were built as part of the Group Experiment in 2009 to compare structural responses and field performance under heavy trafficking. Each section was designed with 7 inches of asphalt over 6 inches of graded aggregate base. The HMA control section (S9) contained all-virgin materials. Section S8 was identical to S9, except that the surface layer was OGFC. Two sections were built with full-depth WMA, including S10 with the water-injection foaming method and S11 with Evotherm warm mix additive. Two sections were built with 50% RAP in each layer, including N10 with all the mixes being produced as HMA and N11 with all the mixes being produced as WMA using foamed asphalt. All sections were left in place for continued evaluation during the 2012 Test Track. In April 2014, after more than 17 million ESALs, several of the sections reached the cracking threshold and became part of the Pavement Preservation Experiment.

Performance of each section exceeded design expectations since fatigue failure was expected prior to 10 million ESALs based on the 1993 AASHTO Design Guide and the MEPDG. Each section performed well with respect to rutting, ranging from approximately 3.5 mm to 10.6 mm. The WMA sections had slightly higher rut depths than the control, and the 50% RAP sections had the least rutting. Field performance validated the criteria used for APA and FN testing. Fatigue

cracking ranged from 1% to more than 25% of lane area after 17 million ESALs, and fatigue cracking was consistent with measured high strain levels. The 50% RAP sections exhibited the least amount of cracking. The Bending Beam Fatigue Test, Simplified Viscoelastic Continuum Damage test, and a modified version of the Overlay Test were used to evaluate the bottom layer mixes, but only the modified Overlay Test correlated well with observed field performance.

Based on backcalculated effective structural numbers from FWD testing, a structural coefficient of 0.15 was estimated for the OGFC layer. Neither of the WMA technologies appeared to affect pavement response versus temperature relative to the control, but the moduli of the WMA sections were 7-10% lower than the control. Reduced pavement responses to load and environmental changes were observed in the 50% RAP sections, with 7-31% lower critical tensile strains and 14-55% lower subgrade pressures than the control. Backcalculated moduli of the 50% RAP sections were 16-43% higher than the control. This increased stiffness makes high-RAP mixes well suited for use as high-modulus base layers in perpetual pavement designs.

### *2012 Green Group Experiment*

Alabama DOT, Alabama Department of Environmental Management, North Carolina DOT, South Carolina DOT, and Tennessee DOT sponsored the 2012 Green Group Experiment to enable structural and performance characterization of sustainable pavement materials under heavy traffic conditions. All four sections were designed with 6 inches of asphalt—thin enough that distresses would develop within the two-year research cycle based on previous experience at the Test Track. Each section featured a high-modulus intermediate layer and strain-tolerant base layer. All of the mixes were produced using WMA technologies. Section N5 (Standard RAP) contained RAP contents typical of current maximum specifications (20% RAP in surface and 35% RAP in lower layers). The main differences between Section N5 and the others were the use of higher RAP contents in Section S5 (High RAP), the addition of RAS in Section S6 (RAP/RAS), and the use of GTR-modified binders in Section S13 (GTR).

Laboratory testing of each plant-produced mix included resistance to moisture damage (AASHTO T283). Surface mixes were also evaluated for rutting resistance (APA and FN testing) and resistance to top-down cracking (energy ratio). Intermediate layers were tested for dynamic modulus, and base layers were evaluated for fatigue resistance (bending beam fatigue and simplified viscoelastic continuum damage testing).

The control section built with conventional asphalt mixes reached the cracking threshold (25% of total area) after approximately 4 million ESALs, requiring a patch in the right wheel path. Rehabilitation (a two-inch mill and fill) occurred at approximately 7 million ESALs, but rut depths and IRI steadily increased thereafter. Cores showed that bottom-up fatigue cracking was the primary distress mechanism.

The section featuring high RAP contents failed after less than 2.5 million ESALs due to interface debonding between the intermediate and base layers. Fatigue testing and linear elastic analysis using WESLEA illustrated that the low strain tolerance of the intermediate lift combined with the high strain levels it experienced after debonding resulted in the rapid deterioration of the section after the first crack appeared. The section was reconstructed with the same mixes and structure but a higher tack coat rate and performed well by withstanding more than 4 million ESALs before

cracking started. The interface debonding failure did not recur. The early failure of this section illustrates the importance of adequate bonding between pavement layers.

The section featuring RAS in the surface layer and a combination of RAP and RAS in the stiff intermediate layer reached the cracking threshold after approximately 5.7 million ESALs and was rehabilitated at about 7 million ESALs. Rehabilitation consisted of milling 1.75 inches and replacing with a highly polymer modified mix. Surface conditions were initially improved, but pre-maintenance distress levels were quickly surpassed. Cores taken from distressed areas showed irregularities along the interface between the intermediate and base layer. Linear elastic analysis showed that maximum strain would occur at that interface if it was slipped and no longer fully bonded.

The section featuring ground tire rubber modified mixtures reached the cracking threshold at about 4.7 million ESALs. The top 1.75 inches were milled and replaced at approximately 7.3 million ESALs, but distresses recurred rapidly. Bond strength testing was conducted on cores taken prior to rehabilitation. Shearing was evident within the intermediate layer itself, and linear elastic analysis of the fully bonded condition confirmed that the maximum shear stress would be in the same location where shearing was observed in the cores and bond testing.

Compared to the control section with conventional mix designs, which reached the cracking threshold at 4 million ESALs, the section containing RAS in the surface and intermediate layers withstood 39% more ESALs, and the section featuring GTR modified mixes withstood 17% more ESALs before the cracking threshold was reached. The reconstructed control section withstood more than 4 million ESALs before the first crack appeared. At 4 million ESALs, rut depths for the reconstructed section and the other three sections were all well below the rutting threshold of 12.5 mm.

For each section, modulus, strain, and pressure measurements were used to help determine the extent of pavement damage as well as the structural effectiveness of maintenance and rehabilitation activities. Although isolating the impact of each mix variable on performance was not possible due to the variety of mixes in each section, the Green Group Experiment illustrated multiple ways to use recycled materials for enhancing pavement performance.

Each of the SMA surface mixes (25% RAP, 5% RAS, and GTR) had excellent rutting resistance in the laboratory and field. Energy ratio results indicated that the SMA with RAS was susceptible to top-down cracking and that the SMA with GTR was marginally susceptible as well. None of the sections showed evidence of top-down cracking during the two-year research cycle, so more traffic/time would be needed to determine durability ranking in the field.

High-stiffness dense-graded mixes were placed as intermediate layers to reduce tensile strains at the bottom of the asphalt structure and vertical stresses in the unbound layers. Dynamic modulus ( $E^*$ ) was similar for the intermediate mixes containing 35% and 50% RAP. The  $E^*$  was higher for the intermediate mixture containing 25% RAP and 5% RAS, especially at higher temperatures.  $E^*$  for the intermediate mix with 35% RAP and GTR was lower than the control mix (with 35% RAP) at low temperatures but higher at high temperatures. Optimizing the stiffness and recycled material contents for intermediate layers requires more research.

Based on laboratory fatigue testing, fatigue resistant asphalt base layers can be achieved by combining recycled materials with highly modified binders, high asphalt rubber contents, or a rich bottom mix design approach.

#### *Virginia Department of Transportation CCPR and Stabilized Base Experiment*

Cold central plant recycling (CCPR)—a method of combining RAP with foamed or emulsified asphalt and additives in a central recycling plant without the application of heat—has been used for rehabilitating low- and medium-volume roadways. To determine the viability of this technology for high volume roadways, VDOT sponsored three test sections, complementing an existing project on I-81 in Virginia, to evaluate field performance of CCPR material and characterize its structural contribution. Sections N3 and N4 were designed to evaluate the difference between 6 and 4 inches of asphalt built on top of the same underlying layers, including 5 inches of CCPR material and 6 inches of aggregate base. Sections N4 and S12 were designed to evaluate the difference between underlying base material (6 inches of aggregate base vs. 8 inches of cement-stabilized base (CSB)) in supporting the same upper layers, including 4 inches of HMA and 5 inches of CCPR material.

After 10 million ESALs, all three sections (N3, N4 and S12) performed well with no cracking, minimal rutting, and no appreciable change in ride quality. Structural evaluations showed that CCPR material responds to temperature changes like conventional mix, which makes it appropriate to model CCPR material as a bituminous material in mechanistic design. Compared to N3 and N4, the backcalculated AC/CCPR moduli in S12 had less temperature sensitivity and higher moduli, probably due to the backcalculation process attributing some of the CSB properties to the AC/CCPR layer. S12 also showed an increase in temperature-normalized modulus over time probably due to the CSB curing.

N3, with an additional 2 inches of AC, had lower strain levels than N4, and the CSB in S12 yielded much lower strain magnitudes and less temperature sensitivity. Strains normalized to 68°F showed that N4 had an increasing trend over time, while N3 and S12 were relatively constant. Thus, using 6 inches of AC or a stabilized base may help control tensile strain.

The estimated layer coefficients for CCPR material ranged from 0.36 to 0.39 based on backcalculated modulus data for N3 and N4. Continued traffic might produce an observed change in serviceability, which would allow an alternative means of determining the layer coefficient.

#### *Oklahoma Department of Transportation Perpetual Pavement Study*

In 2006, ODOT constructed Sections N8 and N9 to evaluate the perpetual pavement concept. The perpetual Section N9 had a total asphalt thickness 4 inches greater than Section N8, which proved to be non-perpetual. Field performance and structural characteristics were documented over the course of three track cycles, which included two rehabilitations for Section N8. Life cycle costs were also quantified for each pavement option based on actual ODOT cost data.

Throughout the application of 30 million ESALs, N9 outperformed N8 in measurements of ride quality, rutting, and cracking. N8 failed near the end of the first testing cycle and was rehabilitated using a conventional mill-and-inlay with geofabric interlayer, which proved to be ineffective in restoring structural integrity. A second rehabilitation incorporating highly polymer-

modified asphalt was required halfway through the second testing cycle, and it eventually began to crack as well. LCCA showed that despite a 32% higher initial cost, the perpetual pavement had 26% lower life cycle cost than the non-perpetual option due to significantly lower rehabilitation costs. The perpetual pavement provided better performance and was the most economical option.

#### *Kraton Polymers High Polymer Test Section*

Section N7 was placed in 2009, featuring Kraton Polymers' highly modified asphalt (HiMA) with 7.5% styrene-butadiene-styrene (SBS) by weight of binder for enhanced fatigue and rutting resistance. N7 was designed with 5.75 inches of asphalt over 6 inches of aggregate base, compared to a control section (S9) with 7 inches of conventional asphalt over the same aggregate base. At the end of the 2009 track cycle, no damage was present in Section N7, so it was left in place for continued evaluation. After two testing cycles (20 million ESALs), Section N7 continued to outperform the control, with less cracking and only 4 mm of rutting. While the control section experienced fatigue cracking, forensic cores revealed that the HiMA section only had superficial surface cracking. The HiMA mixtures were both stiff and ductile, allowing for better fatigue performance with an 18% thinner AC cross-section.

#### **4.2. Non-Structural Experiments**

Non-structural studies evaluate mix performance through weekly pavement distress surveys for cracking, rutting, and ride quality. These sections do not include instrumentation for monitoring pavement response.

Several sections during the 2012 Test Track cycle were constructed for sponsors seeking to improve performance and durability of porous friction courses (PFCs) through modifications to mix design or tack application. PFC challenges include extending service life and maintaining functionality of the layers' permeability. Average permeability values for all 2012 PFCs decreased by approximately 50% during the first two million ESALs. Permeability reached a plateau, however, after which point the PFCs resisted further densification or clogging. Although much of the initial drainage capacity was lost, the PFCs were still somewhat functional at their lowest permeability level. The as-constructed in-place air voids of the 2012 PFC sections were consistently higher than design air voids. As traffic densifies PFC mixes, the movement of aggregate particles could result in loss of bond between some particles, which could explain premature raveling sometimes seen in PFCs. Although the ASTM procedure for OGFC mix design (ASTM D7064-08) includes the Cantabro abrasion test as an option on both unaged and aged specimens, very few agencies require this step as a means to assess the effects of aging on raveling potential.

#### *Virginia Department of Transportation Noise Experiment*

VDOT sponsored two sections to evaluate mixes for quiet pavements. Both were 12.5 mm NMAS PFC mixes with typical Virginia traprock and 10% RAP; Section W10 used SBS-modified PG 76-22 while Section S1 used 12% GTR. Sound intensity was measured using the On-Board Sound Intensity (OBSI) system and the Close Proximity (CPX) method. Based on OBSI and CPX testing, sound intensity was initially lower for the GTR section but became greater than the SBS section over time. Noise absorption was measured using an impedance tube. Initially, noise absorption

was higher for the GTR section, but it decreased at a greater rate than the SBS section over time. IRI values were better for the GTR section, but the difference in smoothness was likely due to construction variability as the IRI values for both sections were relatively constant over time.

#### *Alabama Department of Transportation OGFC Experiment*

ALDOT evaluated three PFC mixes in Sections E9A, E9B, and E10 with a goal of improving durability and preventing premature raveling. Section E9A was paved with a 9.5 mm NMAF PFC, while Sections E9B and E10 were paved with 12.5 mm NMAF mixes. The E9A mix contained 0.3% cellulose fiber to prevent drain-down. The E9B mix was initially designed using cellulose fibers but was constructed using 0.05% synthetic fiber after additional laboratory testing showed that the synthetic fibers appeared to contribute some strength and resistance to raveling. The E10 mix incorporated 12% GTR by weight of binder and was constructed without fibers to determine if GTR alone could prevent drain-down and resist raveling. The three mixes were verified during the mix design process to pass the maximum Cantabro loss of 15% in order to have acceptable resistance to raveling as recommended by previous NCAT research.

Based on Cantabro testing of lab-produced mixes, increasing the asphalt content of PFC mixes can increase resistance to raveling without greatly reducing air voids or potential permeability. The 9.5 mm PFC had lower Cantabro stone loss and higher tensile strength than either of the 12.5 mm mixes. The 12.5 mm PFC with GTR performed well in the laboratory for both Cantabro loss and tensile strength.

Through two years of trafficking, none of the ALDOT PFC sections had any raveling or a significant amount of rutting. Interestingly, the mean texture depth of the 9.5 mm section (E9A) was approximately the same as the 12.5 mm sections (E9B and E10). The 9.5 mm section experienced an increase in roughness during the last summer of the test cycle, whereas roughness in the 12.5 mm sections was consistent throughout the cycle.

#### *Tennessee Department of Transportation RAS Experiment*

Tennessee DOT sponsored a test section to determine the effect of RAS in an OGFC. In 2003, a conventional 12.5 mm limestone OGFC containing SBS-modified PG 76-22 was placed on section S4. In 2012, it was replaced with a similar OGFC containing 3% post-consumer RAS. Due to the anticipated stiffness of the binder with added RAS, stabilizing fibers were omitted from the mix. To date, the OGFC mix with 3% RAS has performed as well as the conventional OGFC; each had minimal rutting and no raveling after 10 million ESALs.

#### *Oklahoma Department of Transportation OGFSC Mix Design and Tack Method Study*

To improve durability and interface bond strength of OGFSC mixtures, ODOT sponsored a study to evaluate the field performance of different tack methods and a new OGFSC mix design procedure. In Section E1A, a non-tracking hot-applied polymer tack (NTHAP) was applied at a spray rate of 0.15 gal/yd<sup>2</sup> (0.15 gal/yd<sup>2</sup> residual); in Section E1B, non-tracking tack (NTSS-1HM) was applied at a lower spray rate of 0.08 gal/yd<sup>2</sup> (0.05 gal/yd<sup>2</sup> residual). The OGFSC mix was placed at 0.75 inch thick and included two proposed mix design changes: optimum asphalt content was determined using the pie plate drain down method, and percent passing the No. 4 sieve was reduced from 25-45% to 10-35%. Based on bond strength testing of cores, the interface

bond strength exceeded the mixture strength for both E1A and E1B. Cantabro loss was much higher for the plant mix (23%) than during mix design (3%), but this was attributed to the plant mix having higher air void content and lower binder content (due to a change during production to account for aggregate stockpile moisture). Both sections performed well after 10 million ESALs, except for some raveling (1-2 inches wide) along the longitudinal joint.

#### *Florida Department of Transportation Tack Coat Effect on OGFC Performance Study*

FDOT sponsored tack coat studies in the 2009 and 2012 Test Track research cycles to evaluate comparative tack methods for improving the longevity of OGFC mixes. In 2009, FDOT found that a thick polymer-modified tack coat (CRS-2P) applied with a spray paver improved OGFC performance. In 2012, FDOT evaluated other tack materials and application methods using conventional equipment that can potentially provide equivalent performance. Three different tack materials, including a cationic non-tracking tack (CRS-1HBC) at a rate of 0.10 gal/yd<sup>2</sup> (0.06 gal/yd<sup>2</sup> residual), a non-tracking hot-applied polymer tack (NT-HAP) at a rate of 0.15 gal/yd<sup>2</sup> (0.15 gal/yd<sup>2</sup> residual), and an anionic non-tracking tack (NTSS-1HM) at a rate of 0.05 gal/yd<sup>2</sup> (0.03 gal/yd<sup>2</sup> residual), were applied using distributor trucks in Sections N1A, N1B, and N2, respectively. The same OGFC mix from the 2009 study, which used PG 76-22 and 15% RAP, was placed 0.75 inch thick in each section using a conventional paver.

After 10 million ESALs were applied during the 2-year research cycle, Section N1B had less cracking (16% of lane area) than Section N1A (47% of lane area) or Section N2 (37% of lane area). The cracking performance of N1B (NT-HAP) was similar to that of the 2009 section placed with a spray paver. Section N1A required a large patch and had increased rutting and IRI levels, but rutting in Sections N1B and N2 was not significant and similar to the rutting in the 2009 section. Final IRI levels and changes in mean texture depth were similar for Section N1B, Section N2, and the 2009 section. Based on field permeability testing and field observations, a heavier tack rate (such as Section N1B and the 2009 section) does reduce permeability and drainage during and after heavy rains. The field performance of Section N1B was similar to that of the 2009 section placed with a spray paver, and these two sections performed better than N1A and N2. Based on the results of these studies, a thicker tack coat is recommended to improve OGFC performance. NT-HAP applied with a conventional distributor can be considered an alternative to CRS-2P applied with a spray paver, depending on paving conditions.

#### *Florida Department of Transportation Cracking Study*

FDOT sponsored Sections E7 and E8 to determine how binders and recycled materials affect top-down cracking in dense-graded mixtures and which laboratory tests best predict cracking resistance. Four mixes were placed in 100-foot test subsections: E7A was an all-virgin mix using SBS-modified binder; E7B had the same aggregate gradation as E7A but used GTR-modified binder; E8A used a mix containing 25% RAP and SBS-modified binder; and E8B used a mix containing 20% RAP, 5% RAS, and SBS-modified binder. Laboratory testing included binder characterization (PG and MSCR specifications), dynamic modulus, Hamburg Wheel Tracking Test, Asphalt Pavement Analyzer, Overlay Tester (OT), and the Florida energy ratio (ER) procedure, which incorporates resilient modulus, creep compliance, and indirect tensile strength. Field performance throughout the two-year testing cycle was correlated with OT and ER test results.

After 10 million ESALs, most of the cracking in all four sections was low severity. The SBS, GTR, and RAP sections each had less than 22.5% cracking. Although the mix containing RAP and RAS was the last to have any observed cracking, when it did start it progressed quickly and ended the cycle with the highest cracking area (73.4%). All four mixes failed very quickly in the OT, but relative OT rankings were similar to the final field cracking measurements. ER testing identified both the RAP and RAP/RAS mixes as brittle. Correlations between lab and field results are completely different when the comparisons are made after 5 million ESALs and after 10 million ESALs. This trend reversal is probably driven by the rapid, but delayed, crack development in the RAP and RAS section as opposed to the more gradual crack propagation in the other sections.

Although the RAP and RAS mix had the highest energy ratio, its  $DSCE_f$  value was less than 0.75, indicating that the mix would be brittle. OT results also indicated excessively brittle behavior, as all four RAP and RAS specimens failed on the first cycle. These laboratory results, combined with the field performance of Section E8B, indicate that polymer-modified binders should not be used with RAP and RAS mixes to avoid cracking susceptibility.

#### *Georgia Department of Transportation Surface Treatment vs. OGI Reflective Crack Prevention Experiment*

Georgia DOT has traditionally used a single surface treatment to retard reflective cracking, but a more effective approach is needed. Two alternatives were evaluated: a double surface treatment with a sand seal top layer (Section N12) and an open-graded interlayer (OGI) (Section N13). The OGI (Section N13) was similar to a 12.5 mm NMAS PFC but with lower asphalt content and no fibers (the mix temperature was lowered to prevent drain-down). To simulate cracking, deep saw cuts were made in the existing pavement and filled with sand to avoid self-healing. After applying the experimental crack relief interlayers, a 9.5 mm NMAS dense-graded surface mix was placed on both sections. After more than 10 million ESALs, total cracking in both sections was insignificant. However, N12 had 11.5 mm rutting (almost 0.5 inch), while N13 had only 5.3 mm. Thus, the OGI is more stable and appears to be a better choice for a crack relief interlayer.

#### *Mississippi Department of Transportation Evaluation of 45% RAP Mix Performance*

Mississippi DOT's high RAP test section (S2) was constructed in 2009 by milling four inches from the existing full-depth section of 15% RAP mix and placing two lifts of a 9.5-mm NMAS mix containing 45% RAP and Mississippi gravel. At the end of the 2009 Test Track cycle, after 10 million ESALs had been applied, the 45% RAP mix showed good performance with only 3.0 mm of rutting and low severity cracking covering 3.4% of the total lane area. The cracking in the 45% RAP mix was in different locations than the original 15% RAP mix MSDOT placed in Section S2 in 2006, so reflective cracking was not an issue. The total length of cracking at the end of the 2009 cycle was 61 feet, compared with 80 feet of cracking in the 2006 15% RAP mix. This indicates that the 45% RAP mix performed equal to or better than the 15% RAP mix after 10 million ESALs. For the 2012 cycle, Section S2 was left in place for continued trafficking to evaluate the long-term performance of the 45% RAP mix.

At the end of April 2014, after more than 17 million ESALs, preservation treatments were applied to Section S2 and it became part of the Pavement Preservation Experiment. The section had longitudinal and transverse cracks but no interconnected fatigue cracking. Crack sealing was

selected as the appropriate preservation treatment since there were no other distresses involved. The section was divided into three 50-ft subsections (S2A, S2B, and S2C). In S2A, the cracks were sealed using the rout/fill method, while the blow/band method was used in S2B. S2C had a lesser amount of cracking and was left untreated for comparison.

When crack sealing occurred in late April 2014, total cracking was represented as zero in S2A and S2B. Cracks continued to form in all three subsections, but the increase in total cracking was significantly greater in S2C (untreated) than in S2A and S2B. During the remainder of the cycle (approximately 2.5 million ESALs), total cracking in S2C increased from 17.9% to 34.8%, while total cracking in S2A and S2B went from zero to 4.9% and 4.1%, respectively. This indicates that both the rout/fill and blow/band methods of crack sealing were effective in retarding crack development. The blow/band method of crack sealing showed slightly better performance than the rout/fill method as a stand-alone pavement preservation treatment.

The 45% RAP mix performed very well with regard to rutting, with only 6 mm after 20 million ESALs. Macrottexture increased during the 2012 cycle as cracking progressed and crack sealing treatments were applied, yet the mean texture depth was still good at 0.8 mm after 20 million ESALs. Pavement roughness through the 2009 and 2012 cycles, quantified using IRI, were very consistent, indicating that the pavement remained smooth despite crack propagation and crack sealing treatments.

#### *Missouri Department of Transportation GTR Modified Surface Mixture Study*

During the 2009 Test Track research cycle, Missouri DOT sponsored two sections to compare GTR- and SBS-modified dense-graded surface mixes. Both mixes were 12.5 mm NMAS and were placed 1.75 inches thick over a substantial underlying pavement structure. The GTR section used PG 67-22 binder modified with 11% ambient GTR in the 30-40 mesh size. Both sections performed well at the end of the 2009 research cycle. The GTR section (S7) was kept in place during the 2012 research cycle to continue evaluating its long-term performance. Modified Asphalt Solutions, the GTR-modified binder supplier, sponsored this traffic continuation study.

At the end of two trafficking cycles, corresponding to 20 million ESALs, no cracking was evident in the section. Rutting was approximately the same (5 mm) as after 10 million ESALs. Section S7 also showed good performance with regard to roughness, as the IRI increased only slightly from 50 in/mile at the end of the 2009 cycle to 70 in/mile at the end of the 2012 cycle. Mean texture depth also increased slightly from 0.5 mm to 0.7 mm, but with no signs of raveling. Thus, the GTR section showed excellent long-term performance over the course of two testing cycles (20 million ESALs).

#### *Federal Highway Administration HFST Alternative Aggregates Study*

The FHWA sponsored a study to evaluate alternative aggregates in high friction surface treatments (HFSTs), which are typically used in areas with high crash rates to improve roadway surface conditions. HFST specifications currently require calcined bauxite, an imported aggregate. Sections W8 and W9 included eight HFST subsections incorporating calcined bauxite and seven less costly domestically-sourced friction aggregate alternatives (granite, flint, taconite, emery, basalt, steel slag, and silica). Approximately 2.5 million ESALs were applied to all eight subsections during the last 6 months of the 2009 research cycle, and an additional 8 million ESALs

were applied to the longest subsections (calcined bauxite, granite, and flint) during the first 18 months of the 2012 research cycle.

Based on the results of dynamic friction testing (DFT) and circular texture meter (CTM) testing for all subsections, as well as locked-wheel skid trailer testing of the three longest subsections, the HFST using calcined bauxite maintained better friction values than the other HFSTs using alternative aggregates. However, most of the alternative aggregate HFSTs provided better friction values than dense-graded asphalt mixes.